GPC

COLUMN REGENERATION SERVICE

μSTYRAGEL™ TOYO SODA ULTRA STYRAGEL™
SHODEX μBONDAGEL™ μSPHEROGEL™

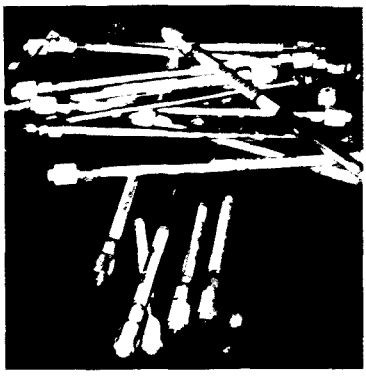

All of these GPC columns give excellent performance. However, when they fail for various reasons (many of which are beyond your control) you must replace them at great expense. The GPC gels themselves NEVER WEAR OUT and may be used over and over as often as necessary!

ASI can clean and repack any 10 micron GPC packing to ***exceed*** new column specifications. All columns are unconditionally guaranteed for ***in use*** performance. Regardless of responsibility, if an ASI repacked column fails ***for any reason*** within the warranty period it will be repaired at no additional cost.

Compare the performance, warranty and price and you will see that ASI offers a truly remarkable value.

REPACKED BY ASI			REPLACEMENT COST			
PERFORMANCE	WARRANTY	PRICE	COLUMN TYPE	PERFORMANCE	WARRANTY	PRICE
›20,000 p/m	120 days	$250	WATERS ASSOC. μSTYRAGEL™	9000-12000 p/m	?	$595.
›30,000	90	$350	WATERS ASSOC. ULTRASTYRAGEL™	›46,000	?	$675
›20,000	120	$250./500.	TOYO SODA (TSK)	20,000	?	$630./1(
›20,000	120	$250./500.	SHODEX	20,000	30 DAYS	$750./1(
›20,000	120	$250	BECKMAN μSPHEROGEL™	20,000	30?	$620.
›15,000	90	$175	WATERS ASSOC. μBONDAGEL™	?	?	$405/49

asi ANALYTICAL SCIENCES INCORPORATED

SUITE B-24, AIRPORT PARK • 1400 COLEMAN AVENUE • SANTA CLARA, CALIF. 95050 • (408) 779-0131

. . . . THE WORLD'S FINEST LIQUID CHROMATOGRAPHY COLUMNS

Circle Reader Service Card No. 101

JOURNAL OF LIQUID CHROMATOGRAPHY

Editor: DR. JACK CAZES Editorial Secretary: ELEANOR CAZES
P. O. Box 1440-SMS
Fairfield, Connecticut 06430

JOURNAL OF LIQUID CHROMATOGRAPHY

JOURNAL OF LIQUID CHROMATOGRAPHY

October 1983

Aims and Scope. The journal publishes papers involving the application of liquid chromatography to the solution of problems in all areas of science and technology, both analytical and preparative, as well as papers that deal specifically with liquid chromatography as a science within itself. Included will be thin-layer chromatography and all modes of liquid chromatography.

Indexing and Abstracting Services. Articles published in *Journal of Liquid Chromatography* are selectively indexed or abstracted in:

• Analytical Abstracts • ASCA • BioSciences Information Service of Biological Abstracts (BIOSIS) • Chemical Abstracts • Current Awareness in Biological Sciences • Current Contents/Life Sciences • Current Contents/Physical and Chemical Sciences • Engineering Index • Excerpta Medica • Journal of Abstracts of the All-Union Institute of Scientific and Technical Information of the USSR • Physikalische Berichte • Science Citation Index

Manuscript Preparation and Submission. See the last page of this issue.

Subscription Information. *Journal of Liquid Chromatography* is published in fourteen numbers and two supplements in January, February, March (3 numbers), April, May, June (2 numbers), July, August, September (2 numbers), October, November, and December by Marcel Dekker, Inc., 270 Madison Avenue, New York, New York 10016. The subscription rate for Volume 6 (1983), containing fourteen numbers and two supplements, is $298.00 per volume (prepaid). The special discounted rate for individual professionals and students is $149.00* per volume. To secure this special rate, your order must be prepaid by personal check or may be charged to MasterCard or VISA. Add $36.80 for surface postage outside the United States. For airmail to Europe, add $72.32; to Asia, add $91.52.

Mailing Address. *Please mail payment with order to:* Marcel Dekker Journals, P. O. Box 11305, Church Street Station, New York, New York 10249.

Contributions to this journal are published free of charge. Second-class mailing permit pending at New York, New York and at additional mailing offices.

***THIS REFLECTS A 50% DISCOUNT GIVEN TO INDIVIDUAL SUBSCRIBERS.**

Shodex® GPC KF-800

SHOWA DENKO

A New Series of Packed Columns

Developed by Showa Denko K.K., the packed columns of the Shodex® GPC KF-800 series enable high speed and high resolution chromatography with 70,000 theoretical plates per meter.

We recommend the new series to you for high performance separation of oligomers and organic substances by molecular size.

Separation of standard polystyrenes and benzene

Column: KF-802, 300 mm
Mobile phase: THF; 1 ml / min
Samples:
1. Polystyrene, Mw: 42,800
2. Polystyrene, Mw: 2,800
3. Polystyrene, Mw: 300
4. Benzene

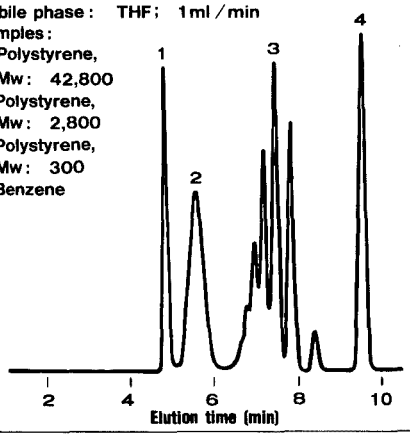

Separation of phthalates and benzene

Column: KF-801, 300 mm
Mobile phase: THF; 2 ml / min
Samples:
1. DOP
2. DBP
3. DEP
4. DMP
5. Benzene

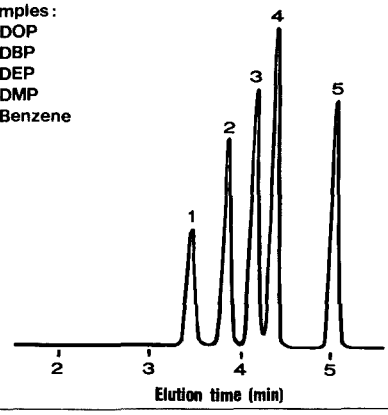

Nomenclature	Specifications			
	Theoretical plates	Exclusion limit (Polystyrene)	Size	In-column eluent
GPC KF-801	16,000 minimum	1.5×10^3	8mmϕ × 300mm	THF
KF-802	〃	5×10^3	〃	〃
KF-802.5	〃	2×10^4	〃	〃
KF-803	〃	7×10^4	〃	〃
KF-800P	Protective column for KF-801 to KF-803		4.6mmϕ × 10mm	〃

A number of other high-quality Shodex® devices are also available. They include Shodex® GPC A-800(THF), AC-800($CHCl_3$) and AD-800(DMF) series, packed columns for GPC with water used as mobile phase and for partition and adsorption chromatography and a refractive index detector.

Contact us for further information.

SHOWA DENKO K.K.
Instrument Products Department
13-9, Shiba Daimon 1-chome, Minato-ku, Tokyo 105, Japan
Telephone : (03) 432-5111 Telex : J26232
Cable : SECIC TOKYO

SHOWA DENKO AMERICA, INC.
280 Park Avenue
West Building, 27 th Floor
New York, N. Y. 10017, U. S. A
Telephone : (212) 687 0773
TLX : 423898
TWX : 710-581-2987

LIQUID CHROMATOGRAPHY/ELECTROCHEMISTRY PART 2*

Edited by

RONALD E. SHOUP
Research Laboratories
Bioanalytical Systems Inc.
1205 Kent Avenue
West Lafayette, Indiana 47906

and

R. W. FREI
The Free University of Amsterdam
Department of Analytical Chemistry
Amsterdam, The Netherlands

This is a special issue of *Journal of Liquid Chromatography*, Volume 6, Number 12, 1983. *Part 1 was published in Volume 6, Number 10, 1983.

MARCEL DEKKER, INC. New York and Basel

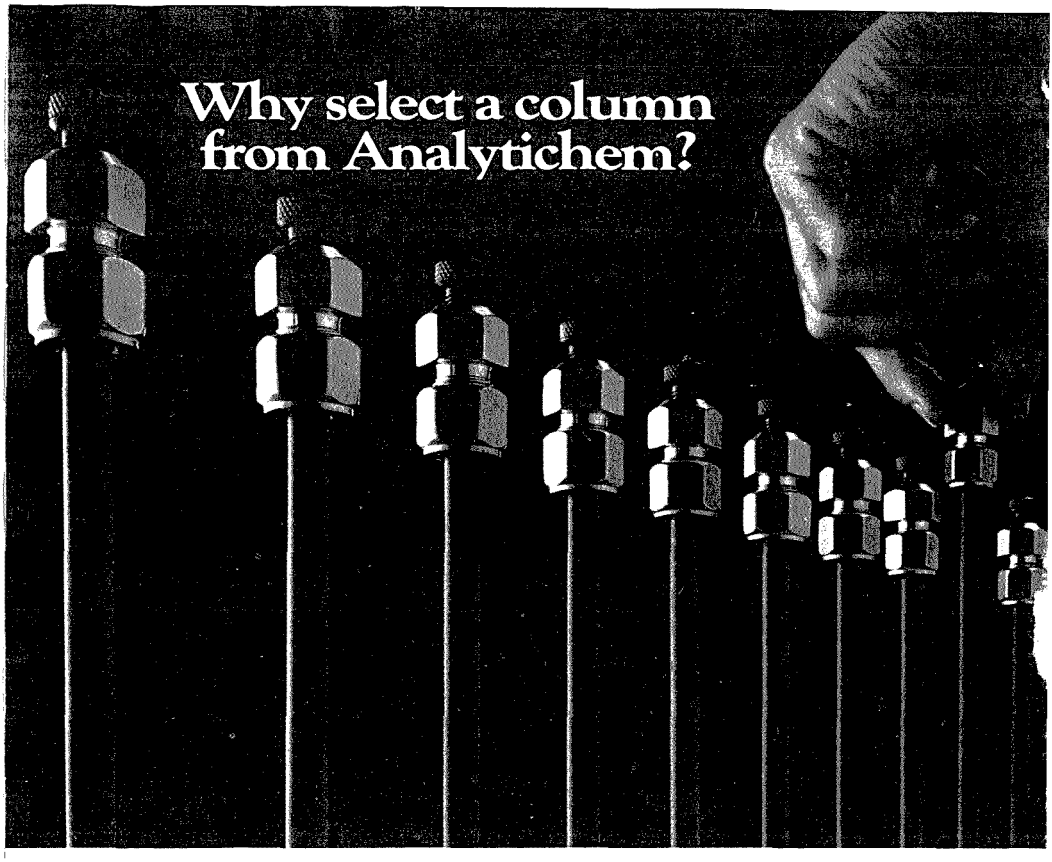

Because the greater the selection the greater the selectivity.

The new line of HPLC columns from Analytichem provides selectivity unequalled by anyone. The reason is simple. Analytichem offers a wider selection of phases than anyone.* Now you can choose the phase that is precisely suited to your particular application. These new columns, packed with our unique Sepralyte™ 5μm spherical media, set an unprecedented standard of chromatographic efficiency... regardless of the phase you select.

The performance of each new Analytichem column is fully guaranteed and backed by the industry's strongest customer service and technical support teams. Our technical advisors have the training and hands-on experience to assist you in solving virtually any separation problem. Next time you're considering HPLC columns, be selective. Call Analytichem. You'll find the columns you need and the service you deserve.

Analytichem International
24201 Frampton Ave., Harbor City, CA 90710, USA, (800) 421-2825, In California (213) 539-6490
TELEX 664832 ANACHEM HRBO

JOURNAL OF LIQUID CHROMATOGRAPHY

Volume 6, Number 12, 1983

Special Issue on Liquid Chromatography/Electrochemistry. Part II

CONTENTS

Liquid Chromatography / Electrochemistry

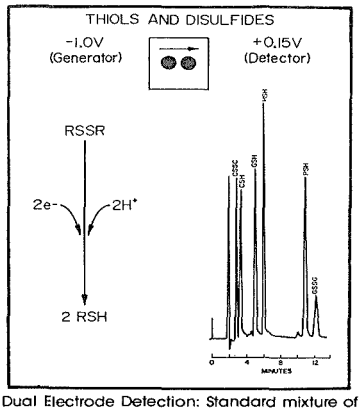

Dual Electrode Detection: Standard mixture of Cystine, Cysteine, Glutathione, Homocysteine, Penicillamine, Glutathione Disulfide

In 1974 BAS introduced the first commercial LCEC system. With over 5000 units installed and the largest research team to support them, it's not surprising that our nearest competitors are several generations behind us. Our thin-layer transducers lead the way with a wide selection of electrode materials in a variety of interchangeable configurations. The latest member of the family is the new LC4B/17 dual electrode amperometry package. Parallel and series amperometry can enhance selectivity, detection limits, speed and gradient compatibility. Let us show you how it's done, no one else can.

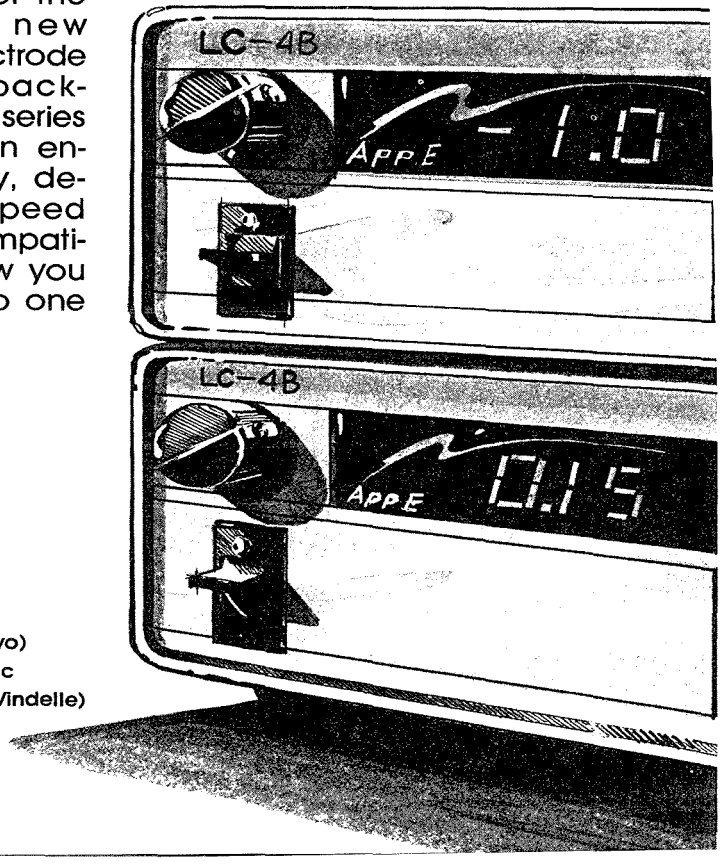

BAS

Purdue Research Park,
2701 Kent Avenue,
West Lafayette, IN. 47906
317-463-4527 TLX 276141

JAPAN: Tokai Irika Co. (Tokyo)
CANADA: Mandel Scientific
FRANCE: Biochrom s.a.r.l. (Vindelle)

JOURNAL OF LIQUID CHROMATOGRAPHY, 6(12), 2141-2156 (1983)

LIQUID CHROMATOGRAPHY WITH ELECTROCHEMICAL DETECTION OF PHENOL AND NADH FOR ENZYME IMMUNOASSAY

Kenneth R. Wehmeyer, Matthew J. Doyle, D. Scott Wright, H. Mitchell Eggers, H. Brian Halsall and William R. Heineman*

Department of Chemistry, University of Cincinnati
Cincinnati, Ohio 45221

ABSTRACT

Enzyme immunoassays based on chromatographic separation and amperometric detection of an enzyme generated product have been investigated. These assays combine the selectivity of the antigen/antibody reaction with the high sensitivity of thin layer amperometry. The feasibility of utilizing LCEC as a detection scheme was demonstrated using the Syva EMIT® kit for phenytoin. NADH production by glucose-6-phosphate dehydrogenase was monitored following a homogeneous procedure. Heterogeneous assays were developed for alkaline phosphatase labeled species which were based upon LCEC determination of phenol. Assays were designed for a common serum glycoprotein (orosomucoid) and a clinically important drug (digoxin). Detection limits approach the pg/mL level and as such may prove fruitful in the quantitation of numerous antigens of clinical interest.

INTRODUCTION

Immunoassay is a widely used analytical technique, especially for the analysis of biological samples in clinical laboratories (1,2). One form of immunoassay is based on the competition between an antigen (the species to be determined) and labeled

 0148-3919/83/0612-2141$3.50/0

antigen for a limited amount of highly specific antibody-binding sites. The predominant immunoassay technique is radioimmunoassay in which the label is a radioactive isotope that is detected by various disintegration counting techniques.

Numerous other labels have been explored for use in immunoassay, and a few of these are now used routinely (3,4). For example, an enzyme label that catalyzes the production of nicotinamide adenine dinucleotide (NADH), which is detected spectrophotometrically, is widely used (5,6). The low detection limit of fluorescence has also stimulated the development of immunoassays based on fluorescent labels (7,8).

We and other research groups have investigated the potential of electrochemical techniques for analytical detection in immunoassay (9-13). One strategy that we have pursued involves the use of an enzyme label for catalyzing the production of an electroactive species. Liquid chromatography with electrochemical detection (LCEC) has proved to be an effective analytical technique for use with such enzyme immunoassays. We describe here the application of LCEC to the detection of phenol and NADH which are catalytically generated by enzyme-labeled antigens.

MATERIALS AND METHODS

Heterogeneous Enzyme Immunoassay

Polystyrene cuvettes were purchased from Gilford Instruments, Cleveland, OH 44135. Alkaline phosphatase Type VII, orosomucoid (OMD), antibody to OMD and digoxin were obtained from Sigma Chemical Co., St. Louis, MO 67138. Orosomucoid was coupled to alkaline phosphatase by a known procedure (14). The digoxin alkaline phosphatase conjugate was obtained from Immunotech Corp., Cambridge, MA 02139. Phenyl phosphate was purchased from Calbiochem-Behring Corp., La Jolla, CA 92037. Digoxin antisera was a gift from the Center for Disease Control, Atlanta, GA.

The buffers used in the heterogeneous assay were phosphate buffered saline with Tween 20 (PBS-Tween): 4.08 g KH_2PO_4, 8.37 g K_2HPO_4, 500 µL Tween 20, dilute to 1.0 L and adjust the pH to 7.4 with 5.5 M NaOH; 0.05 M sodium carbonate: 2.93 g $NaHCO_3$, 1.59 g Na_2CO_3, dilute to 1.0 L (pH=9.6); and 0.1 M potassium phosphate: 6.16 g KH_2PO_4, 9.59 g $KHPO_4$, dilute to 1.0 L (pH=7.0). Antibody coating solutions of 10 µg/mL for the digoxin assay and 1.0 µg/mL for the OMD assay were made by dissolving the appropriate amount of antibody in 0.05 M carbonate buffer containing 0.02% sodium azide. Antigen-enzyme conjugate dilutions of 1/125 and 1/100 were used for the digoxin and OMD alkaline phosphatase conjugates respec tively. PBS-Tween was used to dilute the enzyme conjugates. Standard solutions of digoxin (50 pg/mL - 5.0 ng/mL) and OMD (1.0 ng/mL - 200 ng/mL) were prepared in human serum and PBS-Tween, respectively. The enzyme substrate solution employed in this study was made by dissolving 0.20 g phenyl phosphate and 0.30 g $MgCl_2 \cdot 6H_2O$ in 100 mL of carbonate buffer.

Electrochemical analyses were performed with flow-amperometric equipment from Bioanalytical Systems Inc. (BAS), W. Lafayette, IN 47906. The amperometer was a BAS Model LC 3. The electrochemical cell was a 2.0 mil thin-layer cell with a carbon paste working electrode, Ag/AgCl reference electrode and either a glassy carbon or stainless steel auxiliary electrode. All electrochemical analyses were performed at +870 mV using 0.1 M phosphate buffer (with 0% to 4.0% MeOH) as the eluent and a flow rate of 1.2 mL/min. A 12 cm by 4 mm Knauer column (Unimetrics, Anaheim, CA 92801) was dry packed with LC-4 37-44 µm pellicular C-18 packing material and placed between the pump and injection valve to presaturate the mobile phase. A 5 cm by 2 mm precolumn was slurry packed with 10 µm irregularly shaped RSiL C-18 material (Alltech Associates, Deerfield, IL 60004) and was used for the separation of phenol from the assay buffer. A Milton Roy pump (Model 29-290) and a 20-µL injection loop were used.

For the heterogeneous assay cuvettes were coated with specific antibody through passive adsorption by incubation with antibody coating solutions for 12 hrs. The coating solution was then aspirated and the cuvettes were washed 3X with PBS-Tween, allowing the PBS-Tween to stand in the cuvettes for 10 min during each wash. The antigen solution (375 µL for digoxin, 400 µL for OMD) and the antigen-enzyme conjugate dilution solution (25 µL for the digoxin conjugate, 100 µL for the OMD conjugate) were added to the cuvettes and incubated for 6 hrs (digoxin) and 12 hrs (OMD). The contents of the cuvettes were then aspirated and the cuvettes washed consecutively with 1X PBS-Tween, 1X PBS-Tween (5 min), and 2X carbonate buffer. The enzyme substrate solution was then added to each cuvette and incubated for 25 min and 60 min for digoxin and OMD, respectively. For the digoxin assay the enzyme reaction was stopped by the addition of 25 µL of 5.5 M NaOH to each cuvette. Directly before injection 25 µL of 5.5 M HCl was added to each solution. For the OMD assay the enzyme reaction was stopped by simply removing the substrate solution from the cuvette with a pipet.

Homogeneous Immunoassay

EMIT® phenytoin assay kits were purchased from Syva Co., Palo Alto, CA 94304. NADH (N8129) was a product of Sigma Chemical Company. Phosphate buffer (0.1 M, pH=6.5) was made from K_2HPO_4 and KH_2PO_4. Syva Model 1500 pipetter-diluter was used for sample handling procedures.

Electrochemical analyses were conducted using BAS flow-amperometric equipment. Conditions were similar to those reported in the previous section except that the working electrode was glassy carbon (+750 mV vs Ag/AgCl) and the analytical column was a 25 cm X 4.6 mm Knauer column dry packed with LC-4 (37-44 µm) ODS phase packing material. Periodically, the working electrode was polished with alumina, then conditioned and pretreated before use

by cycling the electrode between +1.5 V and -1.5 V at a scan rate of 100 mV/s for 20 min. A potential of +1.5 V was applied for 2 min, followed by 2 min at -1.5 V. This was repeated twice. Each day the background current was allowed to decay to a constant value before starting analyses.

For the homogeneous assay the EMIT® assay components were diluted according to the manufacturer's instructions except that before injection the reaction mixture was further diluted 121-fold with phosphate buffer at 2, 5, 8, or 11 min after mixing. This was carried out to prevent fouling of the electrode surface by adsorbed NAD^+. This dilution step also effectively stops the enzymatic generation of NADH. The diluted solutions (20 μL) were injected into the LC at 3, 6, 9, and 12 min, respectively.

RESULTS AND DISCUSSION

Heterogeneous Enzyme Immunoassay

Heterogeneous enzyme immunoassays are used routinely for the clinical determination of small quantities (ng/mL-pg/mL) of biologically important compounds in serum and urine. In a competitive assay format an enzyme labeled antigen and an unlabeled antigen compete for a limited number of antibody binding sites, which are attached to a solid support (Equation 1). After the

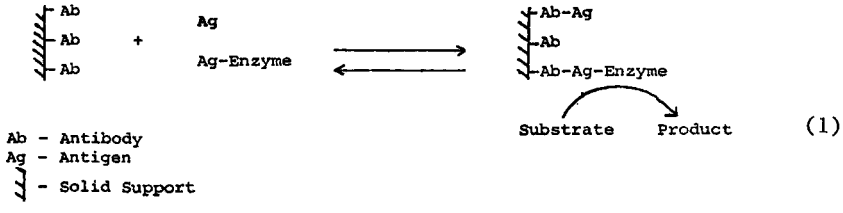

(1)

reaction in Eqn. 1 has reached equilibrium, the labeled and unlabeled antigen bound to the solid phase antibody are separated from the material free in solution. The amount of bound

labeled antigen is then determined by allowing the enzyme to react with its substrate for a given length of time. Enzyme generated product is then detected by an appropriate analytical method. In the competitive format the amount of bound labeled antigen will be inversely related to the amount of unlabeled antigen present. A standard curve is constructed using known concentrations of antigen, and the concentration of antigen in an unknown sample is found by reference to this standard curve.

Competitive heterogeneous immunoassay methodology has been developed utilizing alkaline phosphatase (AP) as the labeling enzyme. AP catalyzes the conversion of an electroinactive substrate (phenylphosphate) to an electroactive product (phenol), as shown in Equation 2.

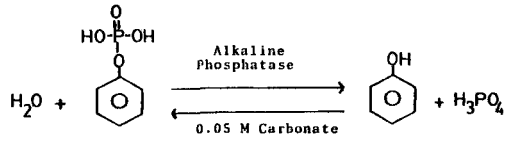

(2)

A cyclic voltammogram for phenol at a carbon paste electrode (CP-OE) is shown in Figure 1. The irreversible 1-electron oxida-

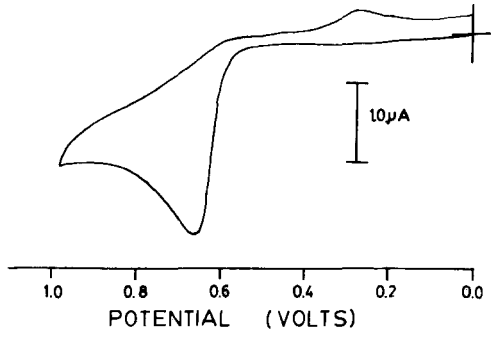

FIGURE 1. Cyclic voltammogram of 1.5×10^{-4} M phenol in 0.05 M carbonate buffer (pH = 9.6); carbon paste working electrode, Ag/AgCl reference electrode, scan rate = 10 mV/s.

tion wave of phenol was observed at +670 mV vs Ag/AgCl in a 0.1 M carbonate supporting electrolyte. Repetitive scans indicated that electropolymerization of the phenolic radical resulted in fouling of the electrode surface.

LCEC methodology was utilized to avoid fouling and increase sensitivity. A CP-OE working electrode was employed in a thin layer configuration. A 5 cm by 2 mm precolumn packed with 10 μm C-18 was used to retain phenol from the assay buffer (Figure 2). The hydrodynamic voltammogram for the determination of phenol is depicted in Figure 3. Maximum current response was obtained at potentials greater than +850 mV, and a potential of +870 mV was chosen for subsequent studies. The LCEC detection of phenol has a linear dynamic range from 9.0 X 10^{-9} M to 9.6 X 10^{-6} M (slope = 0.57 nA/nmol, y-intercept = -0.30 nA, r = 0.999).

The immunoassay reaction was carried out, and the bound material was separated from "free" by simply aspirating the

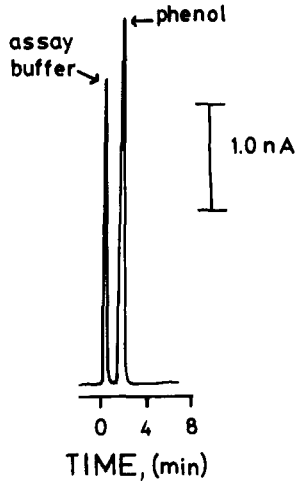

FIGURE 2. LCEC chromatogram of a 20 μL injection of 5.3X10^{-7} M phenol in 0.05 M carbonate buffer. Flow rate; 1.2 mL/min; eluent, 0.1 M phosphate buffer (pH = 7.0).

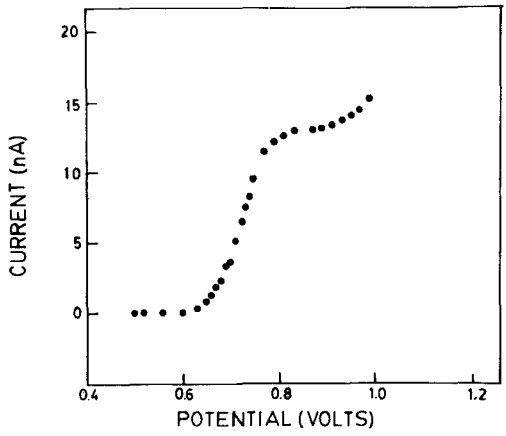

FIGURE 3. Hydrodynamic voltammogram for a $7.0X10^{-7}$ M phenol solution. See conditions for Figure 2.

assay solution. The amount of enzyme labeled antigen bound to the solid phase antibody was then determined by adding enzyme substrate to the cuvette and detecting the phenol generated after a given time interval.

The effect of varying concentrations of digoxin and OMD on the amount of their enzyme labeled analogues bound by the solid phase antibody are shown in Figure 4 and Figure 5. As the concentration of digoxin or OMD was increased the amount of the corresponding enzyme labeled material bound by the solid phase antibody decreased via the equilibrium reaction of Eqn. 1. The decrease in the amount of bound labeled antigen resulted in a decline in the amount of enzymatically generated phenol. The quantitative detection of phenol, following the heterogeneous LCEC procedure, provides the basis for the analytical determination of digoxin and OMD.

Homogeneous Enzyme Immunoassay

Enzyme immunoassays with electrochemical detection are being developed with glucose-6-phosphate dehydrogenase as the enzyme

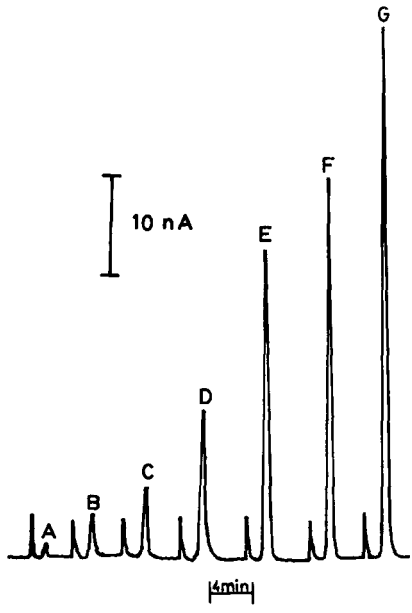

FIGURE 4. LCEC analysis of a series of digoxin standard solutions in serum. Concentration of digoxin in serum: A = 2.0 ng/mL, B = 1.0 ng/mL, C = 0.5 ng/mL, D = 0.25 ng/mL, E = 0.10 ng/mL, F = 0.05 ng/mL and G = 0.0 ng/mL.

label. These assays depend on the competition of an antigen (Ag) and an enzyme labeled antigen (Ag-E) for a limited amount of specific antibody (Ab) as shown in Equation 3. The free Ag-E catalyzes

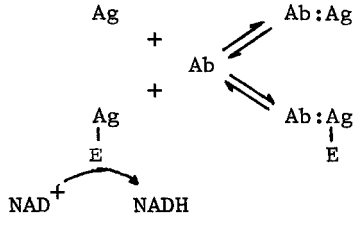

(3)

the reduction of NAD^+ to NADH, whereas the catalytic activity of the bound (Ab-Ag-E) label is substantially diminished. Consequent-

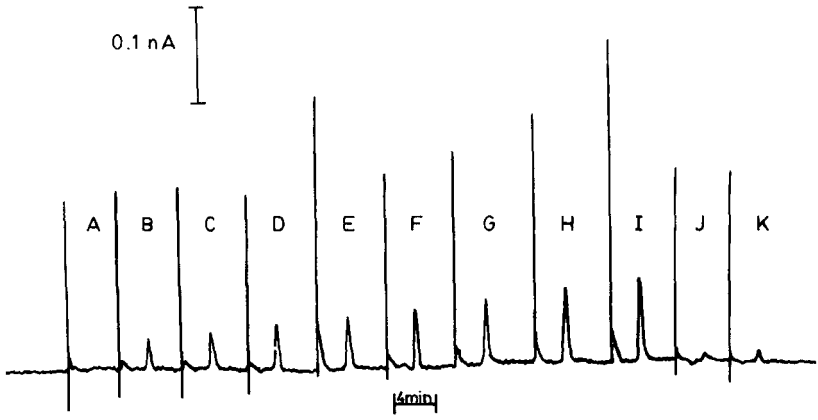

FIGURE 5. LCEC analysis of a series of OMD standard solutions: A) 0.05 M carbonate buffer, B) 200 ng/mL, C) 100 ng/mL, D) 60 ng/mL, E) 10 ng/mL, F) 5 ng/mL, G) 2.5 ng/mL, H) 1.0 ng/mL and I) 0.75 ng/mL. The addition of AP alone (J) or OMD-AP in cuvettes coated with non-specific IgG (K) showed little activity and hence minimal non-specific adsorption.

ly, a greater concentration of Ag in the sample or standard results in a greater concentration of free Ag-E, following competitive equilibration with a limited amount of Ab. This in turn results in more rapid production of NADH. There is a commercially available kit for drug analysis, EMIT® (15), based on the spectrophotometric determination of the rate of NADH production.

An alternative method of detecting NADH is by electrochemical oxidation. Figure 6 shows a cyclic voltammogram of NADH at a glassy carbon electrode. An oxidation wave with a peak potential of +0.85 V was observed. Reduction of the electrogenerated NAD^+ occurred at -1.2 V, making the system electrochemically irreversible. Curve A in Figure 7 shows a hydrodynamic voltammogram for NADH oxidation obtained by flow injection analysis (FIA). It is apparent from this curve that optimum sensitivity for FIA is obtained by maintaining the potential more positive than +0.8 V.

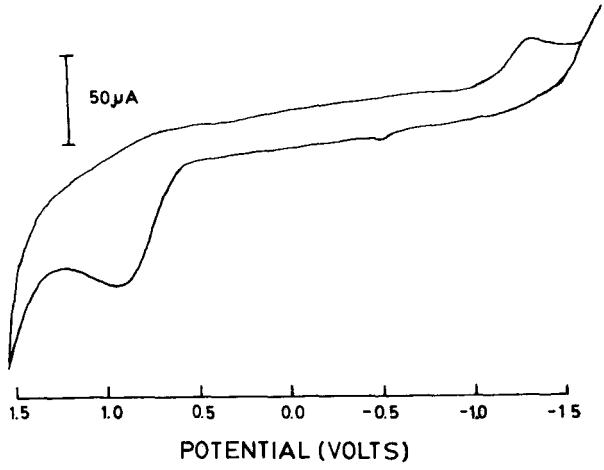

FIGURE 6. Cyclic voltammogram of $8.2X10^{-3}$ M NADH in 0.1 M phosphate buffer (pH = 6.5); glassy carbon working electrode, Ag/AgCl reference electrode, scan rate = 10 mV/s.

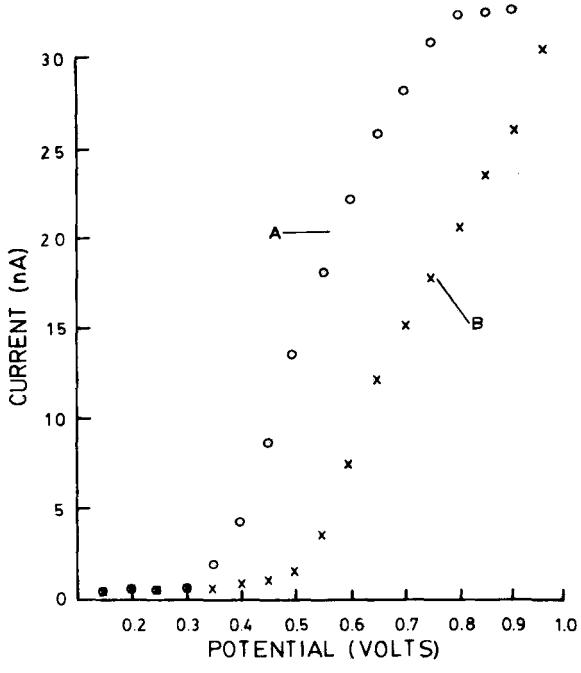

FIGURE 7. Hydrodynamic voltammograms for A) NADH and B) antibody by flow injection analysis.

Reproducible peak heights were obtained with repeated injections of NADH so long as the concentration of NADH was maintained at 10^{-6} M or below. Repetitive injections of higher concentrations resulted in continuously diminishing peak heights due to electrode fouling by adsorbed product(s) of NADH oxidation. Thus, adjusting conditions so that NADH concentrations are maintained below 10^{-5} M was essential to the successful amperometric detection of NADH at glassy carbon.

A standard curve for the FIA detection of NADH showed a linear response for peak current vs. concentration of NADH over the range 9.0×10^{-7} M to 1.8×10^{-6} M (slope = 0.63 μA/μmol, y-intercept = 0.28 nA, r = 0.999). The detection limit for this system was 1×10^{-7} M. Eleven repeated injections of a 8.7×10^{-6} M standard gave reproducible peak currents with a CV of 1.5%.

Although NADH can be determined with simple flow injection analysis, the use of a reversed-phase C-18 column was found to be necessary to implement the immunoassay scheme for several reasons. First, slight retention of NADH to separate it from the current response accompanying the void volume enabled lower detection limits to be achieved. Second, Ab was electroactive at the optimum potential for NADH determination. Curve B in Figure 7 depicts a hydrodynamic voltammogram for Ab. Third, Ab and protein components in serum samples were found to gradually foul the electrode surface by adsorption, resulting in diminished peak currents for NADH. This behavior is illustrated in Figure 8. Repetitive injections of NADH were performed first followed by repetitive injections of Ab. A systematic decrease in the Ab peak was observed and is attributed to electrode fouling by adsorbed Ab. Subsequent injection of the same amount of NADH as originally injected gave the substantially diminished peak currents shown in Figure 8. The insertion of a C-18 column overcame these difficulties by retarding the NADH peak about 30 s from the void volume peak (1.5 min). The LC column also irreversibly retained

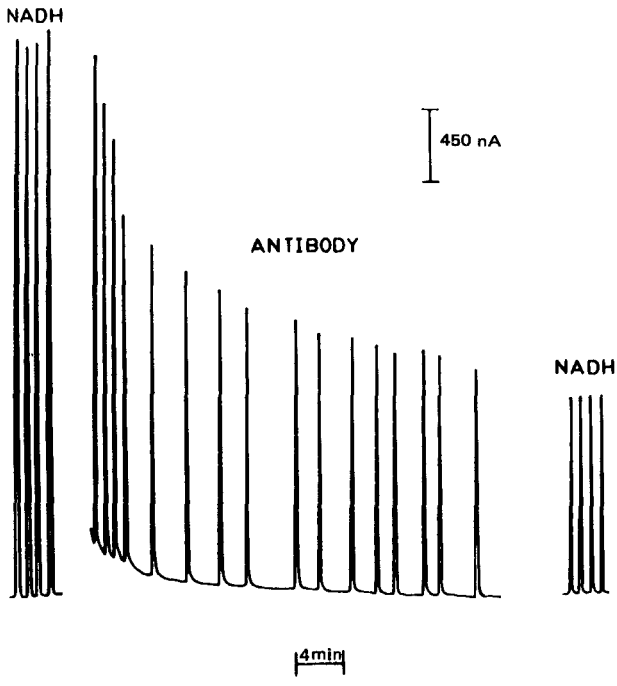

FIGURE 8. Flow injection analysis performed sequentially on aliquots of a NADH solution, an antibody solution and then the same NADH solution.

Ab and prevented electrode-fouling by serum proteins. In general, a C-18 column would last for about 80 - 100 injections during immunoassays. A protein-saturated column was immediately detectable by a decrease in the peak current for the enzymatic reaction. Columns could be regenerated by flushing with methanol or ethanol.

LCEC using a C-18 column and a thin-layer cell containing a glassy carbon working electrode (maintained at 0.75 V) was found to be an effective means of determining NADH, and hence phenytoin, based on the EMIT® assay. Phenytoin standards are mixed with the various assay reagents according to the assay protocol. The rate

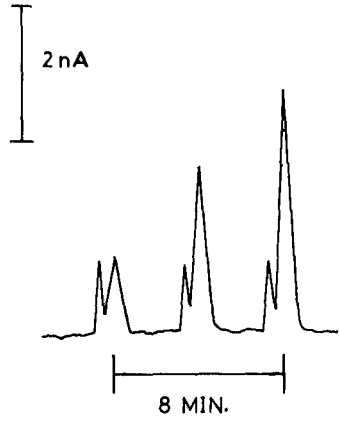

FIGURE 9. Current response for a 30 µg/mL phenytoin standard injected at 3, 6 and 9 min after mixing. The first smaller peak in each case is from the Tris-HCl buffer, and the second peak is NADH.

of NADH production for each standard is determined by injecting aliquots of the assay mixture at various times into the LCEC. Chromatograms showing the rate of NADH production with time for a 30 µg/mL phenytoin standard are shown in Figure 9. The rate of NADH production, for a given standard, can be evaluated by measuring the slope of a peak height (nA) vs time (min) plot. After computing the rates for each phenytoin standard, a calibration plot can be generated for unknown sample analysis (10).

ACKNOWLEDGMENTS

K.R.W. would like to acknowledge the support received as the Law Fellowship recipient sponsored by the Chemistry Department of the University of Cincinnati and the University Research Council for a summer fellowship. K.R.W. also would like to acknowledge Dr. Julius Zodda for his assistance and Dr. Douglas Faust for the generous gift of the digoxin antisera.

M.J.D. would like to acknowledge support as an ACS Analytical Division Research Fellow sponsored by the ACS Division of Analytical Chemistry and as a Twitchel/Schubert/Lowenstein Scholar sponsored by the Chemistry Department of the University of Cincinnati.

D.S.W. would like to acknowledge support received as a Research Fellow sponsored by the University of Cincinnati's Biomedical Research Fellowship Program.

This work was supported by NSF grants CHE-8217045 and CHE79-11872 and NIH grant AI-16753.

REFERENCES

1. Masbacher, C.J. Now and Future RIA, Res. Dev. July, 20 (1977).

2. Ebersole, R.C. and Chait, E.M. Clinical Analysis, Anal. Chem. 53, 682A (1981).

3. Nakamura, R.M. and Ditio, W.A. Nonradioisotopic Immunoassays for Therapeutic Drug Monitoring, Lab. Medicine, 11, 807 (1980).

4. Schall, R.F. and Tenoso, H.J. Alternatives to Radioimmunoassay: Labels and Methods, Clin. Chem., 27, 1157 (1981).

5. Voller, A.; Bartlett, A.; Bidwell, D.E. Enzyme Immunoassays with Special Reference to ELISA Techniques, J. Clin. Pathology, 31, 507 (1978).

6. Scharpe, S.L.; Cooreman, W.M.; Bloome, W.J.; Laekman, G.M. Quantitative Enzyme Immunoassay: Current Status, Clin. Chem., 22, 733 (1976).

7. O'Donnell, G.M. and Suffin, S.C. Fluorescence Immunoassays, Anal. Chem., 51, 33A (1979).

8. Lidofsky, S.D.; Imasaka, T.; Zare, R.N. Laser Fluorescence Immunoassay of Insulin, Anal. Chem., 51, 1602 (1979).

9. Wehmeyer, K.R.; Halsall, H.B.; Heineman, W.R. Electrochemical Investigation of Hapten-Antibody Interactions by Differential Pulse Polarography, Clin. Chem., 28, 1968 (1982).

10. Eggers, H.M.; Halsall, H.B.; Heineman, W.R. Enzyme Immunoassay with Flow-Amperometric Detection of NADH, Clin. Chem., 28, 1848 (1982).

11. Doyle, M.J.; Halsall, H.B.; Heineman, W.R. Heterogeneous Immunoassay for Serum Proteins by Differential Pulse Anodic Stripping Voltammetry, Anal. Chem., 54, 2318 (1982).

12. Weber, S.G. and Purdy, W.C. Homogeneous Voltammetric Immunoassay: A Preliminary Study, Anal. Lett., 12(B1), 1 (1979).

13. Yuan, C.; Kaun, S.S.; Guilbault, G.G. Immunoelectrochemical Assay for Creatine Kinase Isoenzyme MB, Anal. Chem., 53, 190 (1981).

14. Avrameas, S. Coupling of Enzymes to Proteins with Glutaraldehyde, Immunochem., 6, 43 (1969).

15. Bastiani, R.J. The EMIT System: A Commercially Successful Innovation, Antibiotics, Chemother., 26, 89 (1979).

JOURNAL OF LIQUID CHROMATOGRAPHY, 6(12), 2157-2172 (1983)

CARBON COMPOSITE ELECTRODES FOR LIQUID CHROMATOGRAPHY/ELECTROCHEMISTRY: OPTIMIZING DETECTOR PERFORMANCE BY TAILORING THE ELECTRODE COMPOSITION

Dennis E. Tallman* and Duane E. Weisshaar**

Department of Chemistry
North Dakota State University
Fargo, ND 58105

ABSTRACT

Results obtained in this laboratory and elsewhere suggest that carbon composite electrodes may possess a signal-to-noise (S/N) advantage compared to continuous electrodes such as glassy carbon when used for detection of analytes in flowing streams. One such composite electrode which appears particularly attractive in this regard is the Kel-F-graphite (Kelgraf) electrode, compression molded from Kel-F and powdered graphite and containing 5 to 30% graphite by weight. Studies of the electrode surface by scanning electron microscopy and X-ray photoelectron spectroscopy in conjunction with electrochemical investigations employing chronoamperometry, cyclic voltammetry, and capacitance measurements have led us to view the electrode surface as an ensemble of microelectrodes, the dimensions of which can be varied by changes in particle size and/or ratio of Kel-F to graphite in the composite. The S/N advantage of the composite electrode apparently arises from a signal (current) enhanced by radial diffusion of analyte to the individual microelectrodes, resulting in a response greater than that obtained from a continuous electrode of equal active area. Since detector noise is generally assumed proportional to the active area of the electrode, S/N enhancement results.

For composite electrodes employed in a thin-layer channel design LC detector, the observed variations in the S/N ratio with changes in (1) composite composition (%C), (2) particle

---

* Author to whom correspondence should be addressed.
** Present address, Department of Chemistry, The Ohio State University, Columbus, OH 43210.

0148-3919/83/0612-2157$3.50/0

size of Kel-F used in fabrication of the composite, and (3) area of composite exposed in the flow channel are discussed within the context of the microelectrode ensemble model. It is further demonstrated that the ability of the electrode to resist fouling can be modified by variation in composite composition.

INTRODUCTION

A variety of electrode materials have been incorporated into the design and construction of flow-through electrochemical (EC) detectors, including many forms of carbon (1-6). For liquid chromatography with electrochemical detection (LCEC), the detector electrode material should be compatible with a variety of solvents and organic modifiers, useful over a large potential range, and easy to fabricate or machine into the desired configuration at reasonable cost. Carbon is an attractive electrode material which meets most of these criteria. Indeed, numerous EC detectors have incorporated working electrodes made of various forms of solid carbon or graphite, including glassy carbon (2,7), highly oriented pyrolytic graphite (8), low-temperature isotropic carbon (9), reticulated vitreous carbon (4,10,11), and carbon cloth (6,12). Many other detectors have employed carbon or graphite particles either in packed beds (13) or mixed with a binder such as Nujol (1), silicone rubber (14,15), ceresin wax (16), polypropylene (17), polyethylene (3), Teflon (18), or Kel-F (5,19,20,21). This latter group of electrodes in which carbon particles are mixed with a binder shall be referred to as composite electrodes, the most popular of which is undoubtedly the carbon paste electrode (1).

The Kel-F-graphite (Kelgraf) composite electrode developed in our laboratory (19) possesses several advantages compared to either solid carbon (e.g., glassy carbon) or other composite electrodes (5,19,20). Fabrication of the Kelgraf electrode consists of mixing Kel-F (polychlorotrifluoroethylene) particles and powdered graphite in the desired weight proportion (typically 5-30% graphite) and compression molding the mixture in a steel die using a heated laboratory press (the type used in preparing KBr pellets for IR analysis) (19,22). The resulting composite (Kelgraf) is essentially a conducting

plastic which retains many of the properties of Kel-F itself. As a result, Kelgraf is more easily fabricated or machined into the desired configuration than are solid carbon materials and, unlike most carbon paste electrodes, is virtually impervious to the organic solvents and modifiers encountered in liquid chromatography.

In surveying the LCEC literature, one perceives that EC detectors employing composite electrodes rather consistently produce higher signal-to-noise (S/N) ratios than do detectors employing continuous electrodes such as glassy carbon (23). Admittedly, rigorous comparisons under controlled conditions of the S/N behavior of various electrode materials are lacking and such studies are being initiated in this laboratory. Nonetheless, composite electrodes used in flowing stream detectors appear to us to possess an inherent S/N advantage.

In an earlier report the S/N behavior of the Kelgraf electrode was shown to depend on the composite composition (5) and it was proposed that the lateral diffusion regime around small isolated active sites on the composite surface leads to steady-state current response on liquid chromatographic flow time scales, resulting in partial flow noise immunity (5). It was further suggested that variations in composite composition produced corresponding variations in active and inactive site sizes which were responsible for the observed S/N dependence (5). However, experimental data verifying a link between electrode composition and active and inactive site sizes were not available at that time.

More recent studies confirm that the Kelgraf composite electrode (and most likely other composites as well) behaves as an ensemble of microelectrodes, the dimensions of which can indeed be adjusted by variations in composite composition and/or particle size of Kel-F used in the fabrication (22). Radial diffusion at individual microelectrodes results in an enhanced analytical signal compared to a continuous electrode of equivalent <u>active</u> area (22). Since noise is generally taken to be proportional to active electrode area (7,17), a composition-dependent S/N advantage is predicted.

In this report, the observed variations in the S/N ratio of a thin-layer channel-type EC detector with changes in composite electrode composition (% graphite), particle size of Kel-F used

in fabrication of the composite electrode, and area of composite electrode exposed in the flow channel are discussed within the context of the microelectrode ensemble model. It is further demonstrated that the ability of the electrode to resist fouling can be modified by variation in composite composition.

MATERIALS

The p-methoxyphenol (Eastman) and resorcinol (Baker) were crystalline materials with no visible discoloration and were used as received. Reagent grade $NaH_2PO_4 \cdot 3H_2O$ (Baker) was dried at 100°C for 24 hr. to remove the water of hydration and was used without further purification. The water used for the preparation of LC eluents was purified as described previously (5) and the HPLC grade acetonitrile (Burdick and Jackson) was used as received.

The powdered graphite ("F" purity, Ultracarbon Corp., Bay City, MI) used in fabrication of the electrodes had a particle size of <1 μm. The Kel-F-81^R (3M Corp., St. Paul, MN) had a particle size after sieving of ca. 150-450 μm. The 19-00 wax (polychlorotrifluoroethylene, i.e., Kel-F, Halocarbon Products Corp., Hackensack, NJ) had a particle size after sieving of <75 μm.

METHODS

The HPLC system and the electrochemical detector utilizing the Kelgraf electrode have been described in detail elsewhere (5,20).

Electrodes

Disk electrodes for the EC detector were fabricated as described previously (19,22). Three series of electrodes of 5, 10, 15, 20, and 25% carbon were fabricated. The first series used Kel-F-81 as the binder and were fabricated without degassing the composite mixture before compression molding (19). For the higher carbon compositions this resulted in voids

on the surface (visible under ca. 50X magnification) and throughout the composite which had a detrimental effect on the performance of the electrode (see discussion below). These electrodes, hereafter referred to as 3M-A electrodes, were fabricated with an insulating Kel-F sheath surrounding a center core of Kelgraf. The geometric area of conducting Kelgraf exposed in the flow channel varied somewhat from electrode to electrode, but it was ca. 20 mm^2 for all electrodes in the 3M-A series.

The second series of electrodes was also fabricated with Kel-F-81, but in this case the degassing step (22) was employed. In this series no voids were visible on the surface of any of the electrodes. The entire electrode disk was made of Kelgraf (no sheath) so the geometric area exposed in the flow channel was defined by the area of the channel itself (61 mm^2). These electrodes will be referred to as 3M-B electrodes. This series also included a 30% electrode.

The third series of electrodes was fabricated by the same procedure as the 3M-B series (22) except that the 19-00 wax was employed as the binder instead of the Kel-F-81. These electrodes will be referred to as HC electrodes. A 30% electrode was not fabricated for this series and the 5% HC electrode had such a high resistance (>1kΩ) that it was not used in this study.

RESULTS AND DISCUSSION

In trace analysis employing LCEC, one performance characteristic which is of considerable importance is the detection limit, defined here as the amount of injected analyte which produces a signal-to-noise (peak-to-peak) ratio of two. In principle, detection limits can be improved (lowered) by enhancing the signal (current) obtained from a given amount of analyte and/or reducing the system noise. Assuming the detector electrode is maintained at a potential such that the current is mass transfer limited, then signal enhancement can be achieved by increasing the flux of analyte to the electrode surface. If flow through the detector is laminar and if migration is negligible, then analyte is transported to the electrode by

convective diffusion. The limiting current at a conventional channel type electrode is then given by (17)

$$I = 1.467\ nFCW_e\ [\frac{DL}{b}]^{2/3}\ [\frac{\bar{U}}{W_c}]^{1/3} \qquad (1)$$

where W_e and L are the width and length, respectively, of the continuous electrode, b is the channel thickness, $\bar{U}$ is the average volume flow rate, W_c is the width of the channel, C is the concentration of analyte in the bulk solution, D is the diffusion coefficient, and n and F have their usual electrochemical definitions. Equation 1 indicates that flux to the electrode, and hence analytical current, can be increased by decreasing the channel height (thickness of the solution layer adjacent to the electrode) and/or increasing the volume flow rate. Both of these approaches, however, have practical limits. For example, planarity of electrode and cell surfaces limit the smallness of b and chromatographic considerations (resolution, backpressure, etc.) as well as the desire to maintain laminar flow through the detector restrict the range of $\bar{U}$. It should also be noted that an increase in L does not produce a proportional increase in signal (eq 1), a result of the depletion effect which is manifested by an increase in diffusion layer thickness at downstream portions of the electrode. In fact, increasing L may lead to a degradation in the S/N ratio (see discussion below).

Reducing detector noise can also lead to improved detection limits. Although several different types of EC detector noise can be identified, a general theoretical treatment of such noise does not yet exist. Neglecting environmental noise which can be effectively minimized if necessary by appropriate shielding, there appear to be three major sources of noise in an EC detector: electronic noise due principally to voltage fluctuations in the control amplifier of the potentiostat (7); chemical noise attributed to incomplete wetting of the electrode surface which causes variations in eluent flow path across the electrode and also to the porosity of the electrode material and to localized turbulance due to surface roughness (5,7); and flow noise (pump noise) synchronized with the stroke of a piston-type LC pump (24). Both electronic and chemical

noise appear to be random and proportional to electrode area (7,17) and when such noise dominates, increasing electrode area (by increasing L for example) can actually degrade the S/N ratio. Indeed, a reduction in the electrode area has been suggested for reducing noise and increasing the S/N ratio (17). Flow noise due to variations in $\bar{U}$ should exhibit the same dependence on the electrode area as the signal (eq 1), and changes in the area of a continuous electrode should have little effect on the S/N ratio when flow noise dominates. Decreasing electrode area to increase S/N and thus improve detection limit has an obvious limit. Greater amplification of the small currents would be required and eventually noise in the current follower and subsequent amplification system would become limiting.

Work in our laboratory suggests that composite electrodes may possess an inherent S/N advantage compared to continuous electrodes such as glassy carbon. To a first approximation, a composite electrode may be viewed as an array of microelectrodes as depicted in Figure 1. The dimensions of the microelectrodes and of the insulating regions separating the microelectrodes can be controlled by the size of graphite particles, the weight percent graphite, and in the case of Kel-F binder, the particle size of the binder used in fab-

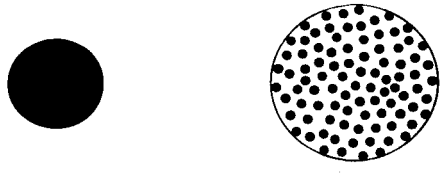

Continuous Electrode (glassy carbon) **Microelectrode Ensemble (carbon composite)**

Ag = Qg **Ac < Qc**

Figure 1. Comparison of a continuous electrode (e.g., glassy carbon) and an ensemble of microelectrodes (e.g., Kelgraf Composite) having the same active area. Ag and Ac represent the active areas of the glassy carbon and composite electrodes, respectively, with Ag = Ac. Qg and Qc represent the geometric areas of the glassy carbon and composite electrodes, respectively, with Qc > Qg.

rication of the composite (22). With the Kelgraf electrode, each active region or microelectrode on the surface is actually an aggregate of small carbon particles (22), and such is probably the case with many other composites as well. However, one feature of the Kelgraf electrode which distinguishes it from other composites is the relatively low carbon content of the composite, typically ca. 15%, resulting in a proportionately low active area (corresponding to conducting graphite on the surface) relative to the geometric area (22).

Radial diffusion contributes significantly to the current obtained with electrodes of very small diameter (25). With an ensemble of microelectrodes (e.g., a composite electrode), one would expect to obtain a time dependent enhancement of the current relative to that obtained from a continuous electrode of equal active area. Indeed, we have demonstrated by means of chronoamperometry that the apparent area of a Kelgraf electrode varies from the true active area at very short measurement times (a few milliseconds) to something approaching geometric at longer measurement times (a few seconds) (22). As mentioned earlier, one way of enhancing the analytical signal of an EC detector is to enhance the flux of analyte to the electrode surface. In effect, reconfiguring a continuous electrode (e.g., glassy carbon) into an ensemble of microelectrodes (e.g., Kelgraf composite) as depicted in Figure 1 results in an enhancement of flux, and thus signal, a consequence of radial diffusion. Since this is accomplished without an increase in active area and, hence, random noise, a S/N enhancement is predicted. A further enhancement of the S/N ratio can be obtained with the composite electrode (relative to the continuous electrode) if flow noise is the dominant type of noise. The composite electrode tends to be more immune to flow fluctuations than a continuous electrode, a result of the tendency of the microelectrodes to achieve steady state current response during the pump refill stroke (5). This has also been demonstrated for a channel-type EC detector employing a carbon fiber array electrode (26).

To estimate the degree of S/N enhancement which might be obtainable, we have applied a modification of the model of Matsuda et. al (27) for partially blocked electrodes to the calculation of the chronoamperometric response of Kelgraf com-

posite electrodes (22). For residence times of 0.2-0.4 s for analyte adjacent to the electrode surface of our detector (5), an enhancement in S/N of ca. 2-3 is predicted for composites similar to the 15% 3M-A and 3M-B electrodes and ca. 5 for composites similar to the 15% HC electrodes, assuming noise is proportional to active area (22). These results also assume that the relative enhancement of flux resulting from radial diffusion is independent of convection, an approximation to be sure.

Since the active and inactive site dimensions of the Kelgraf composite electrode can be varied (22), it should be possible to optimize the S/N ratio of these detector electrodes. As the carbon content of the composite increases, the surface of composite electrodes approaches that of a continuous carbon electrode, neglecting specific effects of the binder (28), and the S/N advantage diminishes. For this reason, composite electrodes with relatively high carbon content may not be as advantageous as those with lower carbon content. Indeed, a carbon paste electrode (ca. 60% C) displays a S/N of approximately one-half that of a 25% 3M-A Kelgraf electrode (29). On the other hand, as carbon content (hence, active area) decreases, the resistance of the electrode increases, leading to increasing electronic noise (30) which, when coupled with the higher gain necessary to measure the smaller current, should lead to a deterioration of S/N.

Figure 2 illustrates the dependence of the sensitivity (signal normalized with respect to concentration)-to-noise ratio on composition for the three series of Kelgraf electrodes employed in a channel-type flow-through EC detector. In each case, the S/N decreases as graphite content increases beyond 15%. Visible voids on the surface of the 20% and 24% 3M-A electrodes (see experimental section) probably account for the exceptionally low S/N for those electrodes, since such voids appear to increase noise (7). Table I displays the observed signal and noise for each electrode where it is noted that, although active electrode area decreases proportionately with %C (22), the signal does not decrease proportionately with %C. We believe this to be due to the smaller sizes of the microelectrodes at lower %C (22) and a current enhancement resulting from increased radial diffusion at these smaller

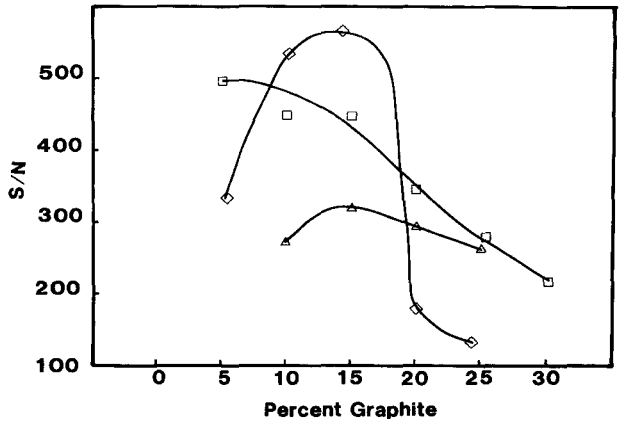

Figure 2. Variation in the S/N ratio with percent graphite for the three series of electrodes. ◇ = 3M-A electrodes; □ = 3M-B electrodes; △ = HC electrodes.

active sites. Similarly, the consistently larger signals obtained from the HC electrodes (Table I) compared to the 3M-B electrodes (equal areas exposed in the flow channel) result from the smaller active site sizes of the HC electrodes (22).

The variation of noise with composite composition is also very interesting. Unless noted otherwise, the noise (Table I) was random, presumably consisting of electronic and chemical contributions. As noted earlier, such noise is believed proportional to active area of the electrode (7). With the 3M-A electrodes, random noise decreased with decreasing active area (% carbon) until flow noise became dominant, at which point noise was insensitive to further changes in composite composition. At lower carbon content, the average dimensions of the inactive region between microelectrodes is relatively independent of composition (5,22). Since separation of microelectrodes is an important factor governing flow noise immunity (5,26), the observed dependence of noise on composition for the 3M-A electrodes can be rationalized.

The noise observed with the 3M-B electrodes was random throughout the range of compositions studied, which we attribute to the larger geometric area (ca. 3X) exposed in the flow channel with the 3M-B electrodes compared with the 3M-A elec-

Table I

Signal and Noise as a Function of Electrode Composition

Electrode Series	Composition (%C)	Signal[a] (nA/μM)	Peak-to-Peak Noise (pA)	S/N
3M-A[b]	24.3	20	150	130
	20.0	18	100	180
	14.3	17	30[d]	570
	10.2	16	30[d]	530
	5.4	10	30[d]	330
3M-B[c]	30.0	76	350	220
	25.3	70	250	280
	20.0	69	200	350
	15.0	67	150	450
	10.0	56	125	450
	5.0	50	100	500
HC[c]	25.0	79	300[d]	260
	20.0	88	300[d]	290
	15.0	81	250[d]	320
	9.9	68	250[d]	270

[a] p-Methoxyphenol. Signals normalized with respect to concentration but not with respect to geometric electrode area.

[b] Column: μ-Bondpak C_{18} (5 μm); E_{app} = 1.15V vs. Ag/AgCl/3.5M KCl; 0.05M phosphate buffer, pH 4.2, 25/75 (v/v) acetonitrile/water, 1.1 mL/min.; geometric electrode area ca. 20 mm^2.

[c] Column: Ultrasphere C_8 (5 μm); E_{app} = 1.25V vs. Ag/AgCl/3.5 M KCl; 0.05M phosphate buffer, pH 4.2, 40/60 (v/v) acetonitrile/water, 1.1 mL/min.; geometric electrode area 61 mm^2.

[d] Predominantly pump noise.

trodes. Thus random noise could not be reduced to a sufficiently low level to permit observation of a flow noise limit as in the case of the 3M-A electrodes. Figure 3 displays the dependence of random noise on electrode composition for the 3M-B electrodes. Random noise does indeed decrease monotonically with area (% carbon) though the dependence is not strictly linear as suggested for continuous electrodes (7). The departure from linearity may reflect the influence of other composite characteristics on the random noise, such characteristics as composite resistance and granularity. It is interesting to note that for this electrode series throughout which the

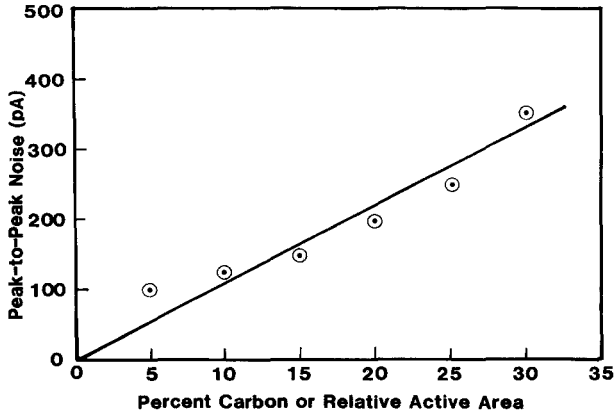

Figure 3. Dependence of random noise on percent graphite (or relative active area) for the 3M-B series of electrodes. The solid line is for reference only and has no theoretical significance.

dominant noise is random, the enhancement in S/N by a factor of two to three in going from higher carbon content (more closely approximating a continuous electrode) to lower carbon content is consistent with our earlier estimate of predicted enhancement for these electrodes.

The noise of the HC electrodes was dominated by flow noise (Table I) for all compositions investigated. Consequently, the S/N ratio exhibited much less dependence on composition than did the other series of electrodes (Fig. 2). Scanning electron microscopy and chronoamperometry indicate that the average active and inactive site dimensions of the HC electrodes are five to ten times smaller than those of the 3M-A or 3M-B electrodes (22), reflected in the enhanced signal of the HC electrodes compared with the 3M-B electrodes (Table I). The smaller and more closely spaced active sites result in an apparent electrode area which, on the detector time scale, more closely approaches the geometric area (22), resulting in the larger signal, but also rendering the electrode more susceptible to the effects of flow fluctuations. In the absence of flow fluctuations, it would be reasonable to expect the HC electrodes to exhibit random noise similar to that of the 3M-B electrodes

(equal active areas) and, thus, exhibit a greater S/N ratio than observed with the 3M-B electrodes.

The foregoing discussion suggests the possibility of tailoring a composite electrode for a particular flow detector application so as to maximize the S/N ratio. For applications involving pulsation-free flow, an electrode similar to the 15% HC electrode (consisting of small, closely spaced microelectrodes) is predicted to result in the highest S/N. For chromatographic applications in which flow fluctuations are typically present, a 10-15% 3M electrode (consisting of somewhat larger, more widely spaced microelectrodes) exhibits better flow noise immunity and yields the highest S/N. As observed with continuous electrodes (17), reducing the geometric area of the composite electrode exposed in the flow channel can lead to further improvement in the S/N (3M-B vs. 3M-A .lectrodes, Fig. 2).

Though similar results could be obtained by tailoring the diameter and spacing of carbon fibers in an array electrode (26), the composite electrodes are considerably simpler to fabricate (19,22). For example, the detection limit for dopamine extrapolated from the results of Wightman et al. (26) for the carbon fiber array electrode (ca. 12 pg versus ca. 50 pg on glassy carbon, S/N = 2 at 1 V vs. SCE) is comparable to the detection limits reported for other phenols (ca. 3-14 pg) on a 15% 3M Kelgraf electrode (5). However, the carbon fiber array required over ten hours to fabricate compared to ca. one hour for a Kelgraf electrode. The more precise control of the size and placement of the microelectrodes in the carbon fiber array would certainly be an advantage for comparing experimental results with theoretical predictions of models describing convective-diffusion at ensembles of microelectrodes.

Finally, we have observed that the composition of a Kelgraf electrode has a rather profound effect on the ability of the electrode to resist fouling. With 5% 3M-B and 10% HC electrodes, the signal observed for repetitive 20 μL injections of 100 μM resorcinol (notorious for fouling electrodes) decreased with each injection such that after 50 injections the signal had decreased by 50%. Resurfacing these electrodes restored the original sensitivity. However, with 15% 3M-B and 20% HC electrodes, the signal from repetitive injections did

not decrease, and 100 injections of 100 μM resorcinol on these two electrodes yielded peak heights with a standard deviation of 2-3%. Indeed, we have used a 15% 3M-A electrode routinely for phenol determinations for over six months without resurfacing or deterioration of response (5). The reason for this composition dependence of electrode fouling is not yet clear. Perhaps it is related to the overall wetability of the composite which increases with increasing carbon content (31). With smaller microelectrodes (lower %C), the binder (Kel-F) surrounding each microelectrode may have a more pronounced influence on the nominal polarity compatibility of solutes and solvent with the microelectrode which in turn influences the tendency of products of the electrode reaction to adsorb onto the surface. Whatever the reason, adjusting the composition of composite electrodes for optimum performance should include consideration of fouling tendencies. It is convenient that the 15% 3M electrodes which display nearly optimum S/N behavior for LCEC applications also exhibit excellent resistance to fouling.

Since double layer charging current is a function of active area while Faradaic current is a function of apparent area (22), a composite electrode may possess an enhanced Faradaic current-to-charging current ratio (compared to a continuous electrode) in detector schemes involving pulsing of the electrode potential. Efforts are continuing in our laboratory to explore and exploit this and other possible advantages of composite electrodes as applied to LCEC.

ACKNOWLEDGMENTS

The authors thank William Cassanos of Halocarbon Products Corp. for supplying the Halocarbon 19-00 wax and Darryl Anderson of 3M Corp. for providing the Kel-F-81 used in this work. This work was supported by the U.S. Department of the Interior, Office of Water Research and Technology (Grant B-055).

REFERENCES

1. Kissinger, P.T., Refshauge, C., Dreiling, R. and Adams, R.N., Anal. Lett. 6, 465, 1973.

2. Bollet, C., Oliva, P. and Caude, M., J. Chromatogr. 149, 625, 1978.

3. Armentrout, D.N., McLean, J.D. and Long, M.W., Anal. Chem. 51, 1039, 1979.

4. Strohl, A.N. and Curran, D.J., Anal. Chem. 51, 1050, 1979.

5. Weisshaar, D.E., Tallman, D.E. and Anderson, J.L., Anal. Chem. 53, 1809, 1981.

6. Takata, Y. and Muto, G., Anal. Chem. 45, 1864, 1973.

7. Lankelma, J. and Poppe, H., J. Chromatogr. 125, 375, 1976.

8. Wightman, R.M., Paik, E.C., Borman, S. and Dayton, M.A., Anal. Chem. 50, 1410, 1978.

9. Hepler, B.R., Weber, S.G. and Purdy, W.C., Anal. Chim. Acta 41, 102, 1978.

10. Strohl, A.N. and Curran, D.J., Anal. Chem. 51, 1045, 1979.

11. Blaedel, W.J. and Wang, J., Anal. Chem. 51, 799, 1979.

12. Girard, J.E., Anal. Chem. 51, 836, 1979.

13. Blaedel, W.J. and Strohl, J.H., Anal. Chem. 36, 1245, 1964.

14. Pungor, E. and Szepesvary, E., Anal. Chim. Acta 43, 289, 1968.

15. Nagy, G., Feher, Zs. and Pungor, E., Anal. Chim. Acta 52, 47, 1970.

16. Fenn, R.J., Siggia, S. and Curran, D.J., Anal. Chem. 50, 1067, 1978.

17. Weber, S.G. and Purdy, W.C., Anal. Chim. Acta 100, 531, 1978.

18. Klatt, L.N., Connell, D.R., Adams, R.E., Honigberg, I.L. and Price, J.C., Anal. Chem. 47, 2470, 1975.

19. Anderson, J.E., Tallman, D.E., Chesney, D.J. and Anderson, J.L., Anal. Chem. 50, 1051, 1978.

20. Chesney, D.J., Anderson, J.L., Weisshaar, D.E. and Tallman, D.E., Anal. Chim. Acta 124, 321, 1981.

21. Anderson, J.L., Weisshaar, D.E. and Tallman, D.E., Anal. Chem. 53, 906, 1981.

22. Weisshaar, D.E. and Tallman, D.E., Anal. Chem. 55, 1146, 1983.

23. King, W.P., Joseph, K.T. and Kissinger, P.T., J. Assoc. Off. Anal. Chem. 63, 137, 1980.

24. Swartzfager, D.G., Anal. Chem. 48, 2189, 1976.

25. Dayton, M.A., Brown, J.C., Stutts, K.J. and Wightman, R.M., Anal. Chem. 52, 946, 1980.

26. Caudill, W.L., Howell, J.O. and Wightman, R.M., Anal. Chem. 54, 2532, 1982.

27. Gueshi, T., Tokuda, K. and Matsuda, H., J. Electroanal. Chem. 89, 247, 1978.

28. Rice, M.E., Galus, Z. and Adams, R.N., J. Electroanal. Chem. 143, 89, 1983.

29. Weisshaar, D.E., Ph.D. Dissertation, North Dakota State University, 1982.

30. Weber, S.G., "The Signal-to-Noise Ratio Problem in Electrochemical Detectors Used in Liquid Chromatography", Presented at FACSS, 1982, Philadelphia, PA.

31. Anderson, J.E., Ph.D. Dissertation, North Dakota State University, 1979.

JOURNAL OF LIQUID CHROMATOGRAPHY, 6(12), 2173-2194 (1983)

DUAL ELECTRODE LIQUID CHROMATOGRAPHY-ELECTROCHEMICAL DETECTION (LCEC) FOR PLATINUM-DERIVED CANCER CHEMOTHERAPY AGENTS

X-D. Ding and I.S. Krull*

Institute of Chemical Analysis
Northeastern University
360 Huntington Avenue
Boston, Massachusetts 02115 USA

ABSTRACT

Trace methods of analysis and speciation have now been developed for a number of platinum derived anti-cancer chemotherapeutic agents, drugs such as: cis-dichloro diammine platinum (CDDP),cis-diammine-1,1-cyclobutane dicarboxylate platinum (CBDCA), and cis-dichloro-trans-dihydroxy diisopropylamine platinum (CHIP). It is possible to utilize parallel dual electrode operations for all three of these Pt derivatives, with overall improved analyte specificity and identification. At the same time, these approaches provide calibration plots of detector sensitivity as a function of the particular working electrode potentials in use via dual electrode LCEC. These response ratios as a function of the applied potentials then become quite unique for individual Pt compounds. By suitably selecting the operating electrode potentials in parallel operation, it is possible to alter the detectability of individual Pt analytes and to drastically vary the resultant LCEC chromatograms. The overall analyte selectivity possible via dual electrode LCEC surpasses that thus far possible via LC-polarographic reduction or single electrode LCEC operations. Glassy carbon as well as gold/mercury electrodes can readily be used for some of these Pt derivatives. These overall trace methods of analysis and speciation for the Pt anti-cancer agents have also been applied to plasma samples spiked with known levels of each drug. It is also possible to utilize these single or dual electrode approaches for the analysis of each of these Pt derivatives in cancer patients undergoing chemotherapy treatment.

*Author to whom correspondence and reprint requests should be addressed.

0148-3919/83/0612-2173$3.50/0

INTRODUCTION

A relatively large number of platinum derivatives have exhibited varying degrees of anti-tumor activity, and several of these have reached clinical trials within the past decade or two (1, 2). Synthetic efforts continue to produce more advantageous Pt derived cancerostatic/chemotherapeutic agents, which would hopefully then find their way into the clinical setting. To some extent, pharmacokinetics, pharmacology, and clinical studies have been hampered by a general lack of sensitive and truly specific methods of trace analysis for any of the Pt derivatives and their metabolites or breakdown products (3). Sternson and colleagues have described a number of HPLC based methods for a variety of these Pt derivatives, including the use of graphite furnace atomic absorption spectroscopy (GFAA), ultraviolet detection (UV), and most recently, dropping mercury electrode polarographic reduction (DME) (1, 4-6). Recently, Krull et al. have described the utilization of single electrode liquid chromatography-electrochemical detection (LCEC) for the trace analysis and speciation of three distinct platinum derived chemotherapeutic agents (3). Figure 1 indicates the structures of these three compounds, which are the same derivatives of interest in this current dual electrode LCEC study. These three platinum compounds are: cis-dichloro diammine platinum (II)(CDDP, cis-Pt), cis-diammine-1,1-cyclobutane dicarboxylate platinum (II)(CBDCA), and cis-dichloro-trans-dihydroxy diisopropylamine platinum (VI)(CHIP). Ideally, any trace analysis and speciation method should offer a number of advantages, including: 1) parts-per-billion (ppb) or sub-ppb detection limits; 2) high degree of analyte specificity leading to unambiguous compound identification; 3) minimum amount of sample preparation compatible with analytical instrumentation; 4) ease of instrumental operation; 5) high reproducibility of analysis and high precision for repeat analyses on same sample; and 6) inexpensive overall instrumentation, materials, supplies, support items. Although most analytical laboratories today possess at least one complete HPLC system, relatively few of these same labs have the ability and/or inclination to interface this with GFAA in order to perform Pt compound speciation analyses (5). At the same time, those laboratories with HPLC have rarely utilized the dropping mercury electrode (DME) polarographic detector in order to perform reductive LC-DME type studies (4). Although some Pt derivatives are UV absorbing, HPLC-UV cannot provide suitably low detection limits for routine application in clinical or research settings (4-6). Of the more commonly used HPLC detectors, including UV, FL (fluorescence), RI (refractive index), and EC (electrochemical), perhaps only EC meets all of the above suggested criteria for a trace method of analysis and speciation for these and other Pt derivatives (7, 8).

Although single electrode LCEC, utilizing the thin-layer flow cell, has been available for about the past decade, it is only within the past few years that dual electrode LCEC has gained popularity and interest (9-12).

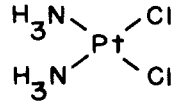

cis-DICHLORO DIAMMINE
PLATINUM (II) (CDDP) (cis-Pt)

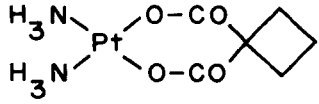

cis-DIAMMINE-1, 1-CYCLOBUTANE
DICARBOXYLATE PLATINUM (II) (CBDCA)

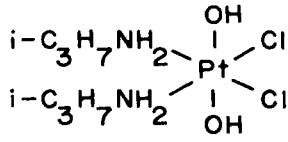

cis-DICHLORO-trans-DIHYDROXY
DIISOPROPYLAMINE PLATINUM (IV) (CHIP)

Figure 1. Cis-Platinum derivatives detected via liquid chromatography-electrochemical detection approaches (LCEC).

Although coulometric dual electrode type detectors for HPLC are now commercially available, it would appear that almost all of the basic research, system optimization, and applications have involved the amperometric type dual electrode approach (13). In view of the rather significant advantages that single electrode LCEC approaches have now been shown to possess for Pt compound analyses, it seemed natural to develop and demonstrate any additional analytical capabilities that dual electrode LCEC might provide (3). All three of the Pt derived anti-cancer agents indicated in Figure 1 have now been studied via these newer approaches, in order to improve detection limits and overall compound/analyte specificity. At the same time, these studies have been applied to these same drugs in human plasma samples. The current report summarizes all of this information.

EXPERIMENTAL

Reagents

Cisplatin (CDDP) was obtained from a number of sources: 1) pure CDDP from Strem Chemicals, Inc. (Newburyport, Mass.); 2) cis-Platinol from The Massachusetts General Hospital/Harvard Medical School, formulated and marketed by Bristol Laboratories, Inc. (Syracuse, New York); and 3) pure CDDP from Johnson-Matthey, Inc. (West Chester, Penna.). HPLC mobile phase water and that used for sample solution preparations was HPLC grade from Fisher Scientific Co. (Medford, Mass.). HPLC grade methanol (MeOH) used for the mobile phase was obtained from MCB Manufacturing Chemists, Inc. (Cincinatti, Ohio), as their Omnisolv brand solvent. Hexadecyltrimethylammonium bromide (HTAB), used as the ion-pairing reagent in the HPLC mobile phase, was obtained from Eastman Kodak Co. (Rochester, N.Y.). Sodium acetate for the HPLC buffer was obtained from J.T. Baker Chemical Co. (Phillipsburg, N.J.) as their trihydrate crystal of HPLC grade purity.

Apparatus

The cyclic voltammogram of CDDP was obtained on a Bioanalytical Systems (BAS) Model CV-1B unit (Bioanalytical Systems, Inc., West Lafayette, Ind.), using a supporting electrolyte of 50 mm, pH 3.5 phosphate buffer plus 10% MeOH, at a scan rate of 200 mV/sec, with a glassy carbon working electrode and an Ag/AgCl reference electrode (4). The CVs were obtained by plotting applied working potential vs current generated, in the conventional manner.

The HPLC instrumentation consisted of the following items: 1) a Laboratory Data Control (LDC) Model 709 pulse dampened solvent delivery system (Laboratory Data Control, Riviera Beach, Florida); 2) a Rheodyne Model 7010 syringe loaded HPLC injection valve (20ul loop attached) (Rheodyne Corp., Berkeley, Calif.); 3) an Alltech reversed phase, C_{18}, 10 um, 25-cm x 4.6-mm i.d., stainless steel HPLC analytical column (Alltech Associates, Inc., Deerfield, Ill.), or a Biophase, C_{18}, 10 um, 25-cm x 4.6-mm i.d., HPLC analytical column (Bioanalytical Systems, Inc.); 4) a Bioanalytical Systems (BAS) Model LC-4B amperometric detector for electrochemical detection (Bioanalytical Systems, Inc.); 5) a BAS dual electrode LCEC cell with two Au/Hg or two glassy carbon working electrodes and a Ag/AgCl reference electrode ($[Cl^-]$ = 3.0 M) (Bioanalytical Systems, Inc.); and 6) a Honeywell dual pen strip chart recorder, 10 mV (Honeywell Corp., Minneapolis, Minn.). All HPLC injections were performed with a 25 ul or 50 ul flat-tipped micro-syringe made by Hamilton Corp. (Reno, Nev.). The nitrogen gas used for degassing the HPLC mobile phase in reductive LCEC work was obtained from Yankee Oxygen, Inc. (Boston, Mass.).

Methods

The optimum potentials eventually used in these LCEC studies were determined either by an initial cyclic voltammetry (CV) study, as with CDDP

(3), or by linear hydrodynamic voltammetry, using either flow injection or LCEC approaches. Those oxidative or reductive potentials, with a given working electrode surface, which provided for the maximum current response (peak heights) for a given amount of analyte injected, with minimum electrode fouling after prolonged use, were then used for the final LCEC determinations. An actual CV for CDDP has been presented elsewhere, using a glassy carbon working electrode, as above (3).

Most of the HPLC separations described below involved a mobile phase consisting of 0.01M sodium acetate buffer at pH 4.60 and 0.15 mM hexadecyltrimethylammonium bromide (HTAB), all at a flow rate of 1.0 ml/min. Specific pH values for the various mobile phases are indicated below (Results and Discussion). In some cases, capacity factors were adjusted by the addition of methanol (MeOH) in a fixed ratio to the above aqueous phase. Specific electrochemical detector working potentials are indicated for the individual experiments described below. In the reductive operating mode, oxygen was continuously removed from the HPLC mobile phase by degassing under nitrogen, as recommended by the supplier of the EC detectors (10-12). Sample solutions used for injections in either the oxidative or reductive modes were not initially degassed, due to the small volumes often available and the satisfactory HPLC resolution of the oxygen peak from the analytes. This is the reason for the often large oxygen peak evident in many of the reductive LCEC chromatograms. Retention times of the Pt derivatives were measured directly from the final chromatograms or with an electrical timer off-line. Quantitation and minimum detection limits (MDLs) were determined using peak heights rather than peak areas, with a signal-to-noise ratio of at least 3:1 for MDL determinations. Plasma was obtained from pooled, whole blood by centrifuging fresh blood samples at 2,000 rpm for about 10 mins, and then carefully separating the plasma from the separated red blood cells. This plasma was then immediately used for the analytical work-up and LCEC studies with individual Pt drugs or mixtures thereof. LCEC analyses of stability solutions or blood/plasma samples were done at least in duplicate, alongside multiple injections of freshly prepared standards, separated by at least one injection of blank mobile phase, infusion solution, blood, or plasma alone.

The final analysis of CDDP from plasma involved the spiking of plasma at known concentration levels, a simple filtration of this solution, and then direct injection onto the LCEC system. In the case of CHIP from plasma, these solutions were initially diluted with an equal volume of MeOH, centrifuged, filtered, and then injected onto the LCEC. The analysis for CBDCA in these dual electrode studies did not involve the derivatization to CDDP described earlier in the single electrode approaches (3). Rather, CBDCA was analyzed directly in these current studies, and its determination in human plasma was not studied via dual electrode methods. Recoveries of all three derivatives from whole blood required an initial separation of the plasma from the whole cells, followed by a sample work-up as described above. Another approach for whole blood analysis involved the addition of an equal volume of acetonitrile (ACN), shaking for a

few minutes to lyse the cells present, centrifugation at 2,000 rpm for about 5-10 mins to remove solid matter, filtration of the supernatant aqueous:ACN portion, and final injection onto LCEC.

In the analysis for CDDP from actual cancer patient blood samples, it was shown that the presence of both ethylenediamine tetraacetic acid (EDTA) and heparin, added to the patient blood at the hospital to stabilize and prevent clotting, did not interfere in the final LCEC analysis for the Pt drug of interest. Once the patient blood was treated as above, it was then spun down at 1,500 rpm for 5-10 mins, and the plasma was separated from the heavier red blood cells. To 5 ml of this plasma was then added 0.5 ml of 5.0 M saline solution (NaCl), both solutions were thoroughly mixed, and this final sample was placed on Dry-Ice for shipment from the hospital to the analytical laboratory at the University. Analysis of CDDP infusion solutions simply involved an addition of 0.5 ml of the 5.0 M saline solution to 5.0 ml of the infusate, mixing, and storage as above. When received at the University, trichloroacetic acid (TCA) in a 10% aqueous solution was added to the plasma in a 1/1 (v/v) ratio, and this mixture was vigorously shaken in order to precipitate all proteins present. This solution was then spun down in a centrifuge at 2,000 rpm for about 10 mins, and the supernatant was removed and filtered through a BAS sample filtration kit (micro filter) with centrifugation (Bioanalytical Systems, Inc.). The filtered liquid was then used for direct LCEC injections. Overall percent recoveries of CDDP spiked to human (non-patient) plasma at the 20 ppm level using the above methods were 89.0 ± 1.3% (average ± standard deviation) (n=3).

Optimization of the basic LCEC operating conditions involved aqueous solutions of the Pt derivatives prepared in HPLC grade water or saline solutions. These were simply filtered and then injected onto the LCEC. All sample filtrations were performed with a 0.45 um sample filtration kit for HPLC (Waters Assocs., Inc., Millipore Corp., Bedford, Mass.). HPLC mobile phases prior to degassing were filtered through a 0.45 um solvent filtration kit for HPLC (Waters/Millipore Corp.).

The methods of performing reductive LCEC analyses with dual electrode detection, using either glassy carbon or gold/mercury surfaces, were essentially those suggested by the manufacturer of the electrochemical detector for LC (Bioanalytical Systems, Inc.), in their various technical publications. Additional technical information and guidance is available in certain recent scientific/technical publications (10-12). The parallel dual electrode LCEC methods used in these studies have been based, in part, on earlier literature reports and/or scientific presentations (9-12). Application of such techniques and instrumentation to this class of Pt derived anti-cancer agents is described here for the first time (3).

RESULTS AND DISCUSSION

The results described here for the trace analysis and speciation of three important Pt anti-cancer agents, Figure 1, have entirely utilized dual

electrode detection in HPLC (LCEC). All of the results presented here have utilized dual electrodes oriented in the parallel adjacent mode, although the use of both parallel and series has been advocated elsewhere in the literature (10-12). At least in our own experience, dual electrode LCEC is more reproducible and internally consistent, intra- and inter-day, in the parallel adjacent orientation. Most dual electrode work thus far reported has utilized the glassy carbon type electrodes, with much less being described for the gold/mercury type. It has been our experience that the glassy carbon surfaces can be made more reproducible from day-to-day than the gold/mercury type, and that the former are perhaps more amenable to series operation than the latter. In any case, since this work has been directed towards improving the overall specificity (speciation) of the analysis for Pt derivatives, the parallel adjacent mode is ideally suited for such goals. Improved detection limits may sometimes be obtained via the series orientation, but since our initial single electrode results provided satisfactory minimum detection limits (MDLs) for these compounds (10 ppb for CDDP), there was no need to further improve them via the dual electrode techniques available with series operation (3). Whereas the earlier LCEC results utilized only the gold/mercury electrode surface for reductive operations, it has now proven possible to utilize the glassy carbon type for both oxidation and reduction of certain Pt derivatives, as well as the Au/Hg electrodes. A dual electrode cell with a single glassy carbon and a single Au/Hg surface might provide additional capabilities over those already available for these studies. The final, overall LCEC approaches described below have now been shown more than adequate, qualitatively and quantitatively, for the direct analysis of residual, intact CDDP in patient infusion solutions and blood plasma samples, the latter obtained at the end of a 2 hr infusion period.

Parallel Dual Electrode LCEC Calibration Plot Ratios for Improved Specificity. Application of Overall LCEC Dual Electrode Methods to Actual Samples.

The utilization of dual electrode LCEC in the parallel mode can provide significantly improved analyte identification (speciation) by plotting the EC detector response (peak height/peak area) vs concentration injected as a function of the working potential of each electrode (10, 12). We have now applied these methods for improved LCEC analyte identification with both the glassy carbon and Au/Hg type dual electrodes, utilizing a wide variety of applied working potentials (vs Ag/AgCl). These are, in essence, two calibration plots for each Pt derivative, wherein each calibration plot varies according to the working potential applied. The overall data at each concentration point on such plots can then be ratioed, similar to wavelength ratioing in multiple wavelength UV detection in HPLC. In addition, the EC detector responses obtained at the two different potentials can be subtracted, in order to provide another data point specific for that particular analyte. Both the ratio of EC detector responses and the differences of these same two EC detector responses can then be utilized to confirm or deny the presence of a suspected

analyte in a complex sample matrix (10, 12). These dual electrode LCEC approaches are best utilized for a suspected analyte in a sample matrix wherein the known standard is analyzed under the same LCEC conditions on the same working day. Working curves at the dual potentials of interest must be obtained for both the suspected standard and the analyte in the sample matrix at the same time or thereabouts. Identical EC detector ratios or differences in EC detector responses for the known standard and the suspected analyte can then provide significant qualitative confirmation to the overall LCEC analysis. It is very important to recognize at the start that dual electrode EC responses will vary from day-to-day, and that working calibration curves obtained on one day cannot be accurately or reliably utilized to confirm the presence of that analyte in a sample analyzed on another day. However, this is no different, in practice or principle, from the well accepted practice of determining calibration plots for standards on the same day as the samples are being analyzed via any detection method in HPLC, GC, or direct instrumental analysis. Instrumental response variability is a very common occurrence, whether one works with separation-detection or direct-detection methods of analysis and instrumentation.

Figure 2 illustrates a set of calibration plots (linear) obtained for CDDP using glassy carbon dual electrode LCEC at working potentials of +1.05 V and + 1.00 V, over the concentration range of 5-40 ppm. The HPLC conditions utilized here involved a reversed phase C_{18} column with a mobile phase of 0.01 M acetate buffer, pH 4.60, plus 0.15 mM hexadecyltrimethyl-ammonium bromide (HTAB), at a flow rate of 1.0 ml/min. Figure 3 is the same study performed under the identical conditions as in Figure 2, but on another day, with somewhat different results obtained. Clearly, different surfaces on one or both of the glassy carbon or gold/mercury electrodes would provide different EC detector responses from day-to-day. This is the same as the observation that UV lamp intensities for an HPLC-UV detector will and often do vary from day-to-day as well. We have now obtained a large number of similar dual electrode response ratios for both glassy carbon and Au/Hg surfaces, for CDDP, CBDCA, and CHIP, as a function of applied, operating potentials. The final ratios of these detector responses have been summarized in Table 1, using HPLC conditions as indicated above (Experimental Section) or below in various Figures. All of these results using glassy carbon electrodes were obtained on the same working day, as were those utilizing the Au/Hg surfaces, but these were two different days.

Our previous efforts in utilizing single electrode LCEC with these same Pt drugs made no attempt to speciate for one or more of these drugs when all three were present in the same injection solution (3). In cases where more than a single Pt derivative is used simultaneously in cancer chemotherapy, this could be of interest. Ideally, an analyst would like to be able to vary the selectivity possible via dual electrode LCEC, for one or more Pt derivatives, and obtain final conditions selective for one, two, or more such compounds. It

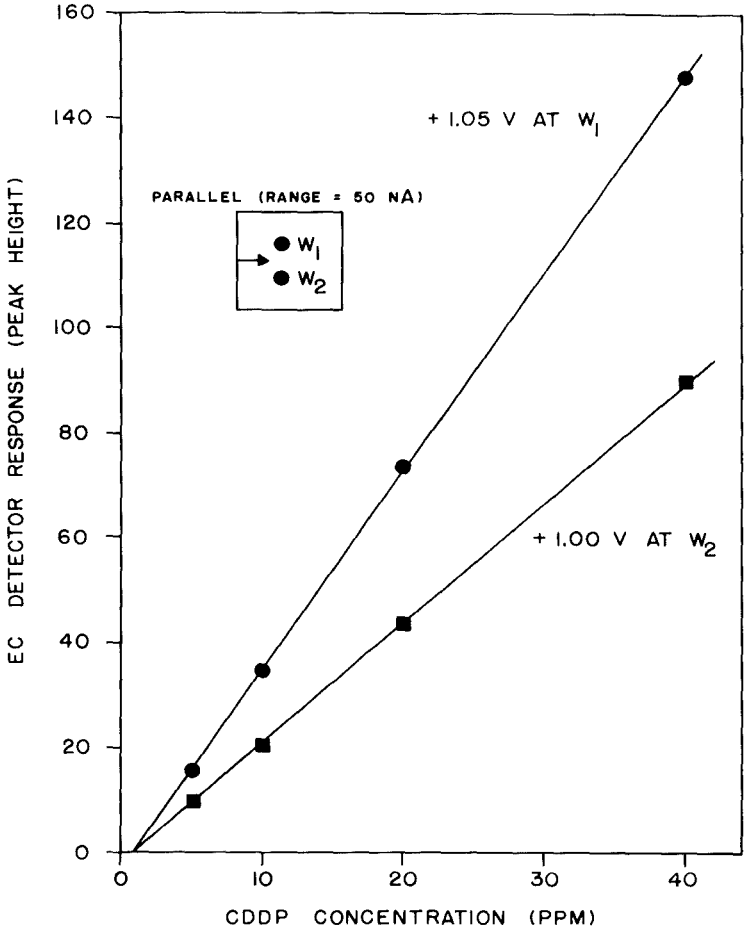

Figure 2. Plot of [CDDP] vs oxidative EC peak heights at two different working potentials with dual glassy carbon electrodes in parallel orientation to HPLC effluent.

should be entirely feasible to vary the LCEC detector parameters appropriately, and thereby have one of the three compounds present appear on the LCEC chromatogram, change the EC conditions somewhat, make another one appear and the first disappear or remain apparent, etc. Of course, in the final HPLC eluent, all three analytes of interest would always be present, but the dual

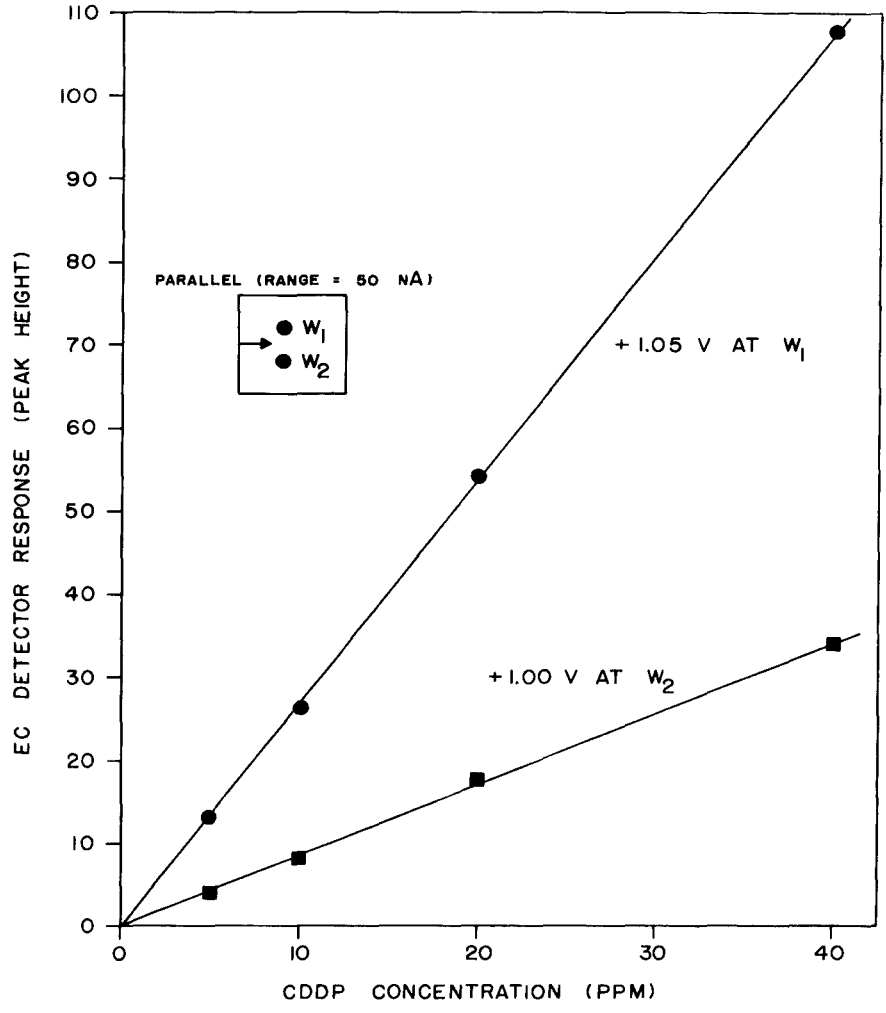

Figure 3. Plot of [CDDP] vs oxidative EC peak heights at two different working potentials with dual glassy carbon electrodes in parallel orientation to HPLC effluent.

TABLE 1. SUMMARY OF DUAL ELECTRODE RESPONSE RATIOS FOR CDDP, CBDCA, AND CHIP AT VARIOUS WORKING POTENTIALS

COMPOUND STUDIED	ELECTRODE SURFACE	WORKING POTENTIALS	DETECTOR RESPONSE RATIOS
CDDP	GLASSY CARBON	+1.05V/+1.00V	3.0
CDDP	GLASSY CARBON	-0.50V/+1.05V	2.6
CHIP	GLASSY CARBON	-0.50V/-0.45V	2.0
CBDCA	GLASSY CARBON	+1.24V/+1.18V	6.4
CDDP	GOLD/MERCURY	-0.01V/+0.01V	1.9
CHIP	GOLD/MERCURY	-0.01V/+0.01V	2.6

electrode detector, depending on the particular conditions used, would only detect one, another, or another. We have now been able to obtain just these desirable sets of operating conditions, as illustrated for one such set in Figure 4. The specific LCEC conditions are indicated in this Figure, with one glassy carbon electrode operated at +1.15V and the other at -0.40V. The top chromatogram illustrates the presence of both CBDCA and CDDP, while the bottom chromatogram indicates the presence of only CHIP, at these particular working potentials. By varying these potentials, or by holding one constant and varying the other, it is indeed possible to make one or more of these three LCEC peaks completely or partially disappear. Indeed, at these same concentration levels injected, by simply varying the potentials applied, any of the three peaks present can be made to increase, decrease, or completely disappear from the final chromatograms. This is indeed true analyte specificity in LCEC, and it now provides a new method of performing Pt compound speciation in the absence of an element selective detector, such as the GFAA (7, 8).

An alternative set of LCEC conditions for improved Pt analyte speciation via dual electrode approaches is indicated in Figure 5, with the specific conditions as indicated. Again, using parallel orientation of the two electrodes, it is possible to analyze for both CBDCA and CDDP present together using oxidative/reductive modes. In the oxidative mode, Figure 5 (top), both CBDCA and CDDP are apparent, but at different relative sensitivities. These relative sensitivities for these two Pt compounds, at +1.20V should be compared with the analogous responses obtained at a slightly lower working potential, viz., +1.15V, Figure 4 (top). In the reductive mode of detection, Figure 5 (bottom), only the CDDP is apparent at a working potential of -0.46V, together with the oxygen dissolved in the sample solution injected. The ratio of these two CDDP peak heights at this particular level injected with these two working potentials again becomes an identifying trait for this Pt derivative. There is an abnormal amount of apparent peak tailing for the CDDP peak in the reductive mode in Figure 5, but since this is an analytical standard injected here, it would appear not due to an interferent co-eluting with CDDP under these HPLC conditions. We prefer to believe that at this particular reductive potential, prolonged use of the glassy carbon electrode with HTAB present in the mobile phase causes some type of electrode fouling. This may be the cause of the apparent peak tailing observed here, but additional work would be needed to conclusively prove this point. At much lower reductive working potentials, -0.01V with a Au/Hg electrode, there is no apparent peak tailing, Figures 6-8.

Two other pertinent studies remain to be described here, especially with regard to the utilization of these methods for Pt drugs in human plasma samples. Indeed, Figure 6 illustrates the analysis of spiked plasma samples at two different concentration levels, as indicated. Specific conditions for the work-up and preparation of plasma samples for CDDP determinations has been

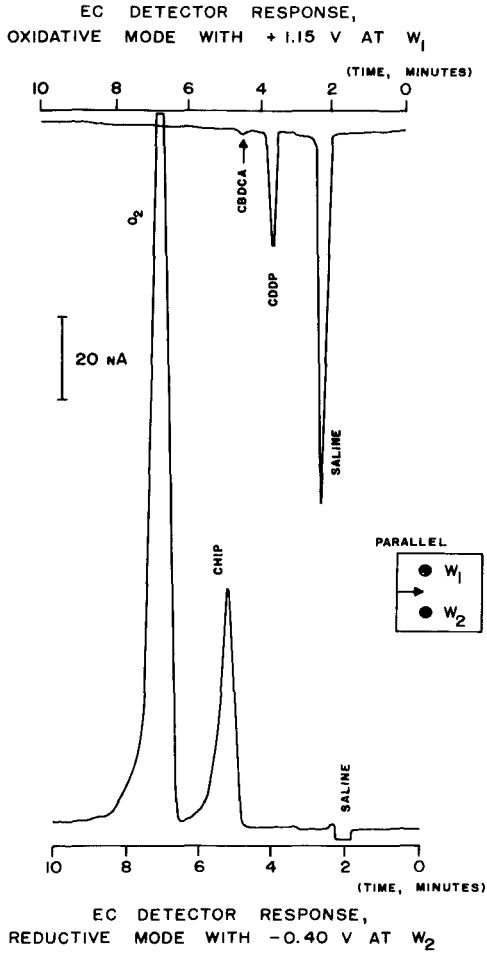

Figure 4. Dual electrode LCEC chromatograms of CDDP, CBDCA, and CHIP injected together onto a C_{18} RP column with a mobile phase of 95% 0.01M acetate buffer, pH 4.60, 0.15 mM HTAB, plus 5% MeOH, flow rate 1.0 ml/min. BAS dual glassy carbon electrodes in paralle orientation. CDDP (40 ppm), CBDCA (80 ppm), CHIP (80 ppm), all in 0.9% saline solution.

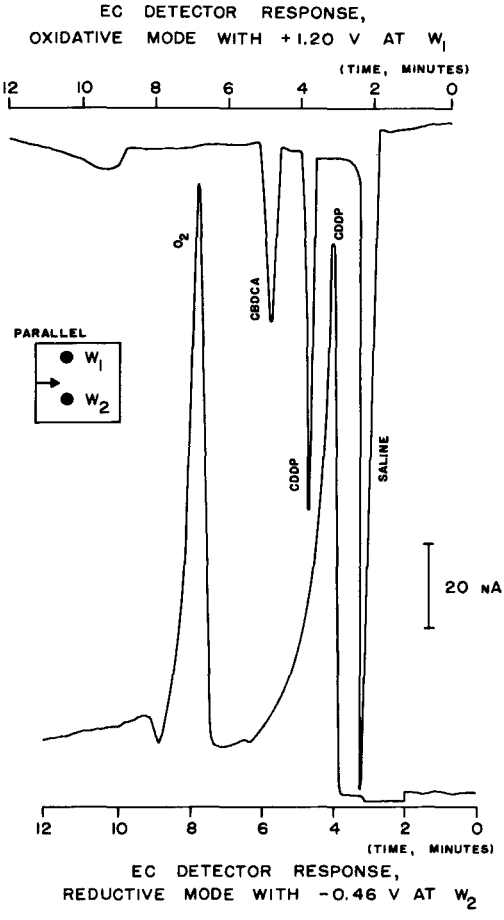

Figure 5. Dual electrode LCEC chromatograms of CDDP and CBDCA injected together onto a C_{18} RP column with a mobile phase of 0.01M acetate buffer, pH 4.60, 0.15 mM HTAB, flow rate of 1.0 ml/min. BAS dual glassy carbon electrodes operated in the parallel orientation. CDDP (20 ppm) and CBDCA (40 ppm) in 0.9% saline solution.

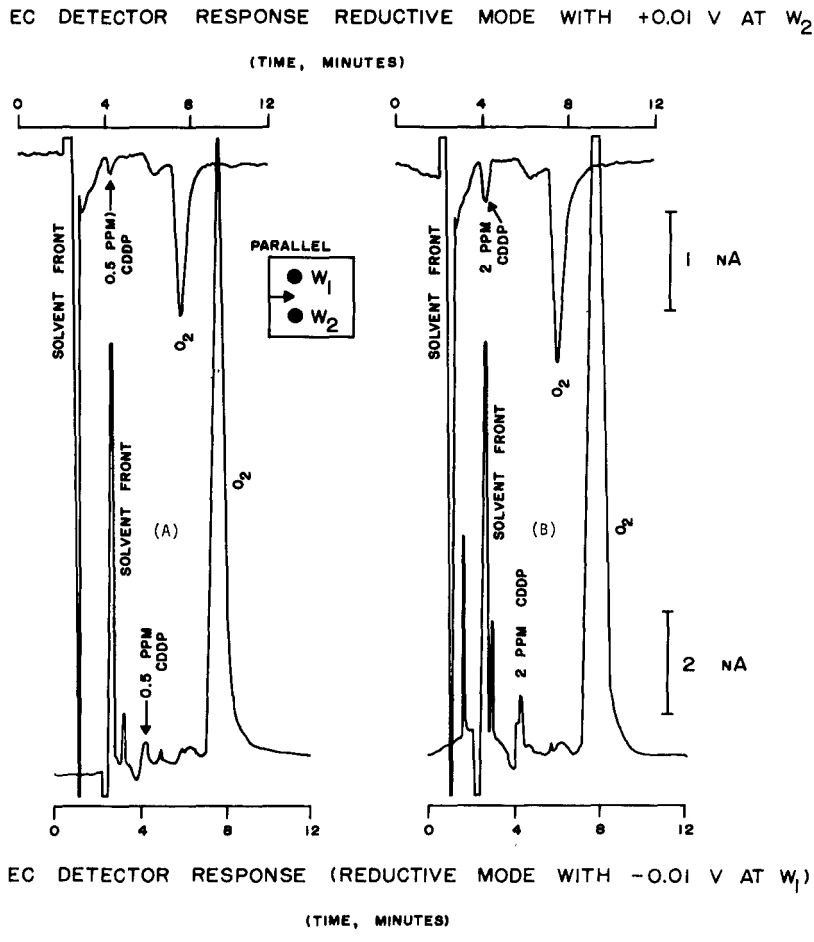

Figure 6. Parallel dual electrode (reductive/reductive) LCEC chromatograms of CDDP in human plasma: (A) 0.5 ppm; (B) 2.0 ppm. LCEC conditions used a C_{18} RP column with a mobile phase of 0.01M NaCl + 0.01M acetate buffer, pH 4.60, 0.15 mM HTAB, flow rate 1.0 ml/min, Au/Hg working electrodes operated in the parallel orientation (BAS).

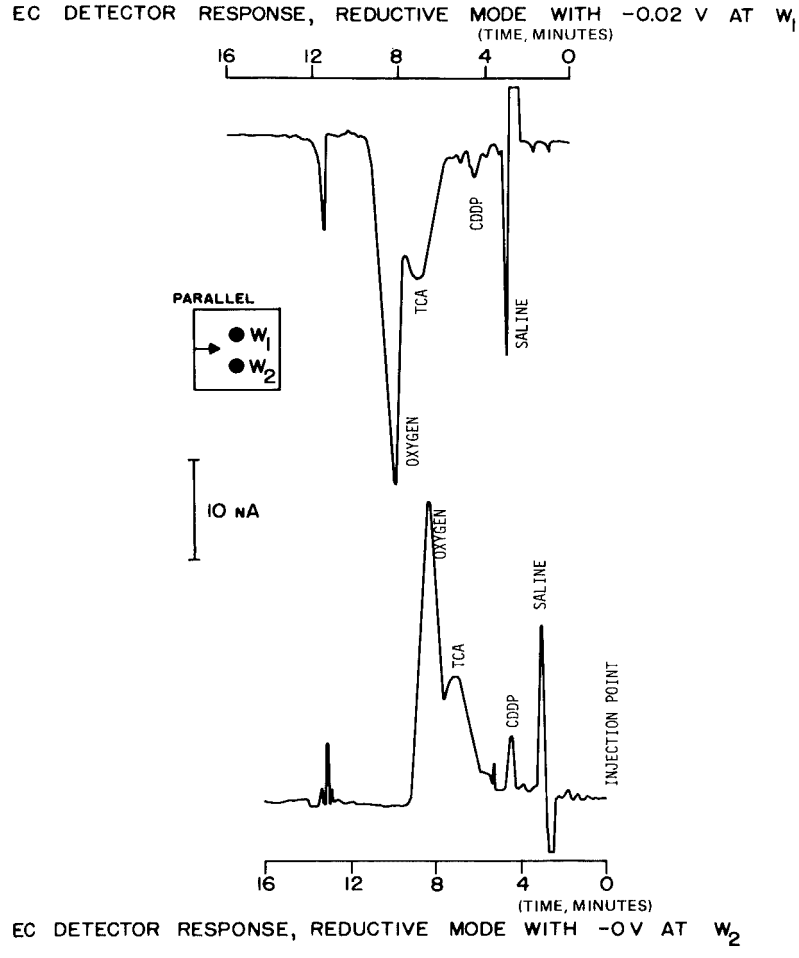

Figure 7. Dual electrode LCEC (reductive/reductive) chromatograms of cancer patient plasma sample after two hour infusion with CDDP, showing the presence of intact CDDP, work-up with TCA. HPLC used RP C_{18} column with mobile phase of 0.01M NaCl + 0.01M acetate buffer, pH 4.60, + 0.15 mM HTAB, 1.0 ml/min flow rate. BAS dual Au/Hg electrodes operated in the parallel orientation.

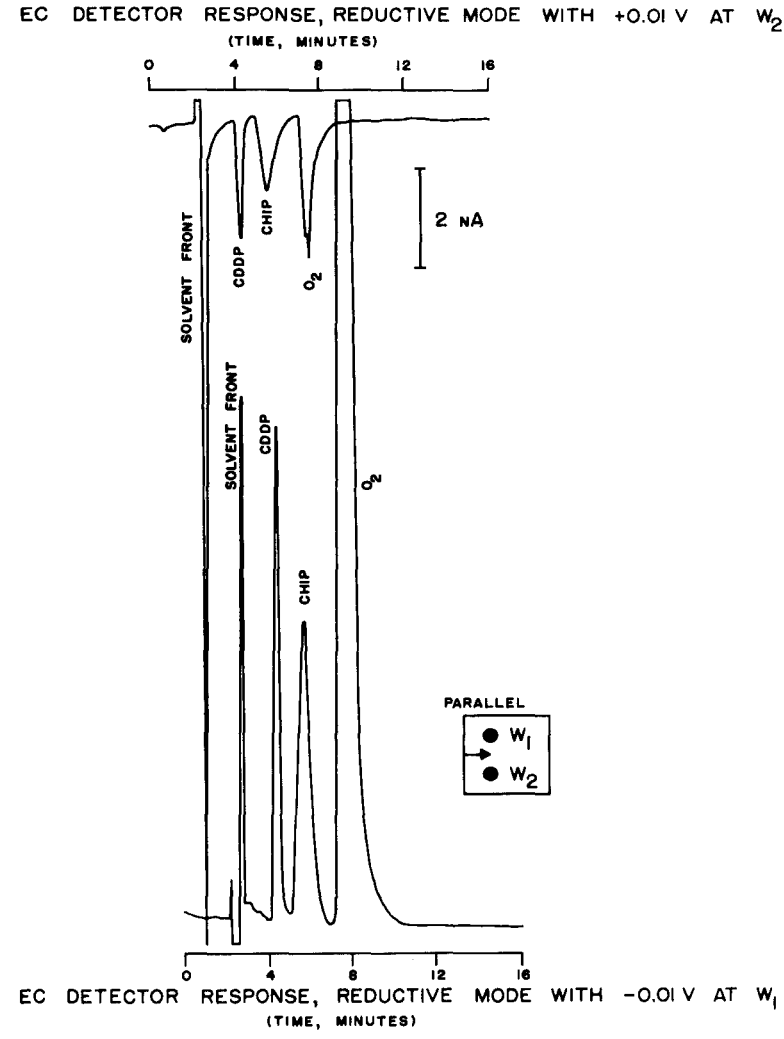

Figure 8. Parallel dual electrode (reductive/reductive) LCEC chromatograms of CDDP and CHIP at the 5.0 ppm levels. LCEC conditions used a RP C_{18} column with a mobile phase of 0.01M acetate buffer + 0.01M NaCl, pH 4.60, 0.15 mM HTAB, flow rate 1.0 ml/min. BAS dual Au/Hg working electrodes operated in the parallel orientation.

presented above (Experimental Section). In this particular study, two Au/Hg working electrodes were utilized, for both the oxidative and reductive EC detection of CDDP in plasma. Although Figure 6A suggests that 0.5 ppm (500 ppb) may be the detection limit for CDDP in plasma; in subsequent studies with actual cancer patient plasma samples, it has now been possible to detect as little as 0.1 to 0.2 ppm (100 to 200 ppb) of CDDP at the end of a 2 hr infusion period. These detection limits for CDDP in cancer patient plasma samples are more than adequate for determining actual levels of CDDP in such samples at the end of a conventional 2 hr infusion treatment, Table 2. Table 2 summarizes the levels of CDDP actually measured in patient infusion solutions, plasma just before infusion started, and plasma taken at the very end of the infusion (2 hrs). These particular patients were receiving the customary CDDP infusion levels at The Sidney Farber Cancer Center, Boston, Mass. Figure 7 is a typical dual electrode LCEC study of a cancer patient plasma sample taken at the very end of a two hour infusion period with CDDP, showing the presence of intact CDDP with specific conditions as indicated. In this case, sample work-up involved denaturation of the plasma sample with trichloroacetic acid (TCA), as discussed previously (Experimental Section). At the two reductive potentials used in this study, Figure 7, viz., -0.02V and -0.00V, the peak for CDDP represents a concentration of about 4.42 ppm in the original plasma itself.

Our earlier studies with single electrode LCEC for CDDP in plasma also suggested a detection limit of about 100 ppb or thereabouts. One would not expect parallel dual electrode LCEC to provide improved detection limits, as discussed already by others (10, 12). Clearly, the dual electrode approaches described here provide at least as useful detection limits for these Pt derivatives in human plasma, but now combined with greatly improved and enhanced analyte identification and specificity. We have indeed been able to successfully apply these dual electrode methods to actual cancer patient infusion and plasma samples containing unknown levels of intact CDDP, as above, Table 2. We have chosen in these patient studies to use the Au/Hg electrodes with relatively low operating potentials of -0.02V/-0.00V, although other suitable operating conditions would also be feasible. Our detection limits with these conditions have been more than adequate for the actual levels of CDDP present in real world patient samples, and thus there has been no need to utilize higher oxidative/reductive working potentials, as suggested by others. Indeed, the use of much higher working potentials for plasma samples might only lead to decreased analyte specificity because of matrix interferences, without providing us with significantly improved detection limits that are unnecessary in any case.

Finally, Figure 8 illustrates the use of dual Au/Hg electrodes with a mixture of CDDP and CHIP, both at the 5 ppm levels in saline solution, wherein both Pt derivatives can be detected simultaneously using two different

TABLE 2. QUANTITATIVE DETERMINATIONS FOR CDDP IN PATIENT INFUSION SOLUTIONS AND PLASMA SAMPLES

SAMPLE TYPE/NUMBER[1]	LEVELS CDDP DETERMINED BY LCEC[2] (AVERAGE ± STD. DEV.)	LEVEL CDDP AS PREPARED FOR[3] INFUSION TO PATIENT
INFUSION SOLN. #1	153 ± 2.0 ppm (n=4)	171 ppm
PATIENT PLASMA BEFORE INFUSION #1	ND[4]	----
PATIENT PLASMA AT END INFUSION #1	4.42 ± 0.9 ppm (n=4)	----
INFUSION SOLN. #2	72.8 ± 5.29 ppm (n=4)	75 ppm
PATIENT PLASMA BEFORE INFUSION #2	ND[4]	----
PATIENT PLASMA AT END INFUSION #2	0.748 ± 0.093 ppm (n=4)	----

1. These results represent chemotherapeutic treatments for two separate cancer patients on two separate days, using drug infusions over a 2 hr period, i.v., sample treatment and work-up conditions as indicated elsewhere (Experimental Section).
2. Dual electrode (reductive/reductive) LCEC approaches used for these quantitative analyses.
3. Infusion solutions prepared in hospital by qualified personnel using standard methods, levels of CDDP in initial infusion solutions as recorded at time of preparation.
4. ND = not detectible with the minimum detection limits inherent in LCEC approach (100 ppb). There should be no CDDP at all in these plasma samples before infusion began.

reductive potentials in LCEC. Again, it is clear that other EC working parameters would be feasible for such improved specificity of both analytes present in the same infusion or plasma solutions/samples.

SUMMARY

In the past, most practical methods of trace analysis and speciation for Pt derivatives utilized element selective detection via graphite furnace AA or related techniques (8). It may yet prove feasible to apply HPLC-inductively coupled plasma (ICP) emission spectroscopy or direct current plasma (DCP) emission spectroscopy for these and related Pt derivatives, but this will depend on final detection limits possible via such approaches (7). We have tried to demonstrate that the dual electrode LCEC approaches now possible with these Pt derivatives can indeed provide sensitivity and selectivity practical for real world sample analyses. Our ability to apply these methods to actual plasma samples spiked with Pt drugs or to actual cancer patient samples containing CDDP initially infused, clearly demonstrates that these newer methods of Pt analysis and speciation are indeed of practical utility and immediate applicability. Although it is very difficult to demonstrate specificity unequivocally, or to compare the LCEC specificity with the HPLC-GFAA specificity for these same compounds, it would at least appear as if these dual electrode LCEC methods will provide as much analyte specificity as any other existing method of metal speciation (8). At the same time, these newer methods of metal analysis and speciation can be readily applied with currently available instrumentation that costs considerably less, overall, than either GFAA, ICP, or DCP instruments. It is also the case that the LCEC interfacing is much easier to accomplish and maintain than almost any other metal speciation approach involving HPLC separations.

ACKNOWLEDGEMENTS

We are very grateful to Ron Shoup and Peter Kissinger of Bioanalytical Systems, Inc., for providing us with valuable information and guidance in the initial phases of this work. Karl Bratin, of Chas. Pfizer & Co., also provided valuable technical assistance and suggestions, which proved helpful in obtaining the final, successful results. Blood samples for the studies with *cis*-Pt drugs in human plasma, non-patient, were provided by The Massachusetts General Hospital via Fred Hochberg. Authentic samples of all three Pt derivatives were provided by Bristol Laboratories, Inc. and Johnson-Matthey, Inc. The sample of Platin, the commercial formulation of *cis*-Pt, was provided by The Massachusetts General Hospital, Boston, Mass. Samples of *cis*-Pt infusion solutions, as well as cancer patient blood/plasma samples taken before and after infusion, were provided by Dave Henner of The Sidney Farber Cancer Institute, The Children's Hospital, Boston, Mass.

This work was supported, in part, by a grant from the NIH Biomedical Sciences Research Support Grant, No. RRO7143, Department of Health and Human Resources, to Northeastern University. Mr. X-D. Ding was supported in these studies via a Visiting Chinese Scholar Fellowship from the Government of China (1982). We are indeed grateful for these various sources of financial assistance.

This is contribution number 157 from the Institute of Chemical Analysis at Northeastern University.

REFERENCES

1. Abbreviations used: HPLC = high performance liquid chromatography; EC = electrochemical detection; LCEC = liquid chromatography-electrochemical detection; MDL = minimum detection limits; ppb = parts-per-billion; ppm = parts-per-million; Au/Hg = gold/mercury amalgam; cis-Pt = CDDP = cis-dichloro diammine platinum (II); CBDCA = cis-diammine-1,1-cyclobutane dicarboxylate platinum (II); CHIP = cis-dichloro-trans-dihydroxy diisopropylamine platinum (VI); UV = ultraviolet detection; FL = fluorescence detection; GFAA = graphite furnace atomic absorption spectroscopy. MeOH = methanol; ACN = acetonitrile; TCA = trichloroacetic acid.
2. A.W. Prestakyo, S.T. Crooke, and S.K. Carter, eds., Cisplatin: Current Status and New Developments. Academic Press, New York, 1980.
3. I.S. Krull, X-D. Ding, S. Braverman, C. Selavka, F. Hochberg, and L.A. Sternson. Trace analysis for cis-platinum anti-cancer drugs via liquid chromatography-electrochemical detection (LCEC). J. Chromatogr. Sci., 21: 166-173 (1983).
4. S.T. Bannister, L.A. Sternson, and A.J. Repta. Evaluation of polarographic detection in the liquid chromatographic determination of anti-neoplastic Platinum complexes. Anal. Chim. Acta. In press (1983).
5. C.M. Riley, L.A. Sternson, and A.J. Repta. Assessment of cisplatin reactivity with peptides and proteins using reverse-phase high performance liquid chromatography and flameless atomic absorption spectroscopy. Anal. Biochem. 124: 167-179 (1982).
6. Y. Chang, L.A. Sternson, and A.J. Repta. Development of a specific analytical method for cis-dichlorodiammineplatinum (II) in plasma. Anal. Lett. B11(6): 449-459 (1978).
7. I.S. Krull and S. Jordan. Interfacing of GC and HPLC with plasma emission spectroscopy. Amer. Lab. 21-33 (October, 1980).
8. I.S. Krull, Trace Metal Analysis by High Performance Liquid Chromatography. In Liquid Chromatography in Environmental Analysis. J.F. Lawrence, ed., The Humana Press, Inc., Clifton, New Jersey. In press, 1983. Chapter 5.
9. LCEC Bibliography: Recent Reports in Liquid Chromatography/Electrochemistry. R.E. Shoup, ed. BAS Press, Inc., Bioanalytical Systems, Inc., West Lafayette, Indiana, 1982.

10. I.S. Krull, K. Bratin, R.E. Shoup, P.T. Kissinger, and C.L. Blank. Liquid chromatography/electrochemistry for trace analysis: Recent advances in instrumentation, methods, and applications. Amer. Lab. 57-65 (February, 1983).
11. K. Bratin and P.T. Kissinger. Reductive LCEC of organic compounds. J. Liquid Chromatogr. 4(Suppl. 2): 321-357 (1981).
12. D.A. Roston, R.E. Shoup, and P.T. Kissinger. Liquid chromatography/electrochemistry: thin-layer multiple electrode detection. Anal. Chem. 54: 1417A-1434A (1982).
13. R.W. Andrews, C. Schubert, J. Morrison, E.W. Zink, and W.R. Matson. Dual electrode cells for LCEC: recent developments. Amer. Lab. 140-151 (October, 1982).
14. I.S. Krull and X-D. Ding. Unpublished results (1983).

JOURNAL OF LIQUID CHROMATOGRAPHY, 6(12), 2195-2208 (1983)

A SIMULTANEOUS DETERMINATION OF TRAZODONE AND ITS METABOLITE 1-m-CHLOROPHENYLPIPERAZINE IN PLASMA BY LIQUID CHROMATOGRAPHY WITH ELECTROCHEMICAL DETECTION

Raymond F. Suckow

N.Y. State Psychiatric Institute
722 West 168th Street
New York, New York 10932

ABSTRACT

A liquid chromatographic method coupled with electrochemical detection was developed to measure plasma trazodone and its metabolite 1-m-chlorophenylpiperazine (m-CPP). Following extraction from 1 ml of alkaline plasma with methyl-t-butyl ether, the extracts were chromatographed on a reversed phase trimethylsilyl bonded column using a 0.05 M phosphate buffer and acetonitrile (90:10) with n-nonylamine and sodium heptane sulfonate added to the mobile phase. The compounds were detected via a thin layer electrochemical transducer with glassy carbon electrodes at a potential of +1.15V vs Ag/AgCl reference electrode. The recovery of trazodone ranged from 91-97% and the coefficient of variation was less than 5% for between run and within-run analyses. The recovery of m-CPP ranged from 82-86% and the coefficient of variation was less than 8% for between run and within-run analysis. Steady state plasma concentration data are presented from several patients.

INTRODUCTION

Trazodone is a triazolopyridine derivative with antidepressant activity that is chemically unrelated to other currently available antidepressant agents (Fig. 1a). In animals, trazodone exhibits

 0148-3919/83/0612-2195$3.50/0

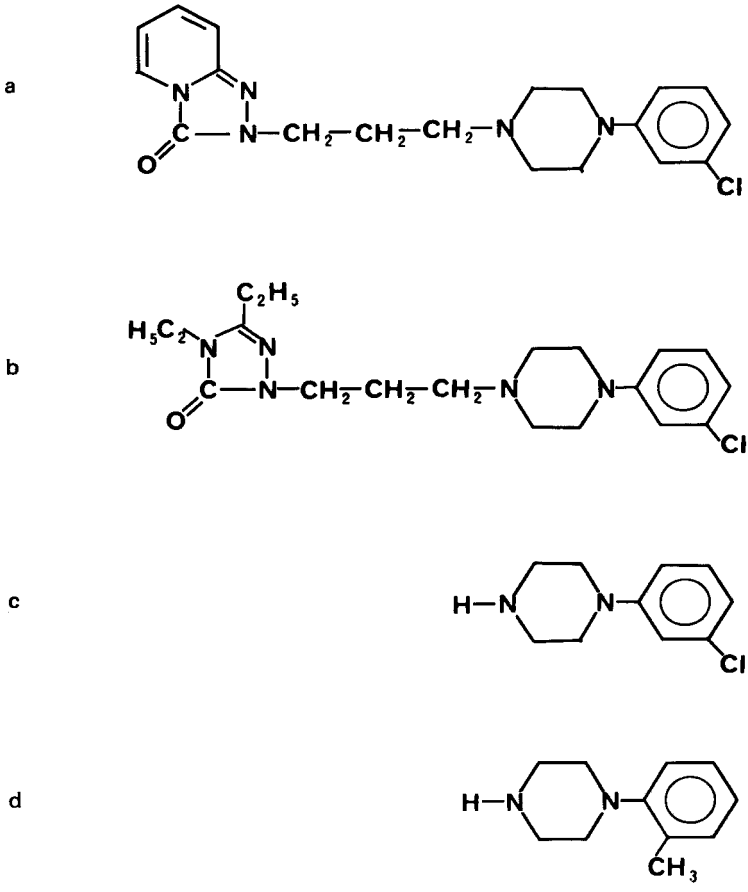

Figure 1: Chemical structures of (a) trazodone, (b) etoperidone, (c) m-chlorophenylpiperazine (m-CPP) and (d) 1-o-tolyl-piperazine (o-TP)

antiserotonin activity, but its mechanism of action in depressive illness in humans is not clear. Trazodone also possesses α-adrenergic blocking activity, but has very little anticholinergic effects as demonstrated in animal studies as well as in clinical trials in depressed patients. Several reviews of trazodone, its

pharmacology, chemistry, and therapeutic efficacy have been presented (1,2,3,4).

The biotransformation of trazodone can occur through oxidative and hydrolytic reactions causing the formation of hydroxy derivatives on both the pyridine and benzene nucleus and a diol derivative on the triazolopyridine ring. The hydrolytic reactions result in the formation of oxotriazolopyridinepropionic acid and its conjugate (5). The remaining fragment of the molecule resulting from hydrolytic cleavage is m-chlorophenylpiperazine (m-CPP) (Fig. 1c).

Recently, it has been suggested that m-CPP contributes to, or even accounts for the antidepressant action of the parent drug (6). Studies revealed that this metabolite acts as a direct serotonin receptor agonist (7). After oral administration of trazodone, m-CPP accumulates in the rat brain at a concentration comparable to that found after pharmacologically and biochemically effective doses of m-CPP (8). Maj et al. (9) reported that trazodone at low doses has antiserotonin properties while at higher doses, it acts as a central serotonin agonist. Furthermore, m-CPP was shown to be a pharmacologically active metabolite common to two structurally related psychotropic drugs etoperidone (Fig. 1b) and mepiprazole (10). In rats, the concentration of m-CPP in brain tissue reached several times that in body fluids (11).

To date, two methods have been reported for the determination of trazodone in plasma. Ankier et al. (12) used reversed-phase high-performance liquid chromatography with UV detection (254 nm) and achieved a lower limit of detection of 20 ng/ml for trazodone

only. Caccia et al. (11) quantitated both trazodone and its metabolite (mCPP) in plasma and brain tissue by gas-liquid chromatography. The latter method is complicated by the fact that after extraction the extracts were divided so that m-CPP could be derivatized and measured by electron capture while trazodone was quantitated by a nitrogen selective detector.

MATERIALS

Reagents

Acetonitrile (UV grade) and methyl-tert-butyl ether were obtained from Burdick and Jackson Laboratories (Muskegon, MI), sodium heptane sulfonate (Eastman Kodak Co., Rochester, NY) and n-nonylamine(Aldrich Chemical Co., Milwaukee, WI) were used without further purification. Reagent grade potassium phosphate monobasic and phosphoric acid were obtained from Fisher Scientific Co. (Fairlawn, NJ). Distilled water was passed through a water purification system before use (Milli-Q, Millipore Corp., Bedford, MA).

Trazodone HCl, etoperidone HCL, and m-chlorophenylpiperazine HCl (m-CPP) were kindly supplied by Dr. Keith Wheeler (Mead Johnson & Co., Evansville, IN). 1-(o-tolyl)piperazine (o-TP) 2 HCl was obtained from Aldrich Chemical Co. (Milwaukee, WI).

Standards

Stock solutions of 1 mg/ml of trazodone, etoperidone m-CPP and 1-(o-totylpiperazine) were prepared in 0.01N HCl and stored refrigerated. Working standards were prepared in 0.01N HCl in

concentrations of 10 ng/ul, for trazodone and etoperidone and and 1 ng/ul for m-CPP and 1-(o-tolyl)piperidone (o-TP).

Instrumentation

Chromatography was performed with a Model 6000A solvent delivery system and a Model U6K injector or WISP 710B automatic injector (Waters Associates, Milford, MA). The column was 4.6 mm i.d. x 25 cm packed with 5 μ particle size trimethylsilyl material (LC-1, Supelco, Bellafonte, PA). A Model LC-4B amperometric detector with a TL-5A (Bioanalytical Systems Inc., W. Lafayette, IN) thin layer transducer was used to monitor the compounds of interest. The current response was recorded by a dual pen Omniscribe Recorder (Houston Instruments, Austin, TX) at 1 V and 10 V inputs full scale preceded by a signal amplifier (gain = x1).

Cyclic voltammetry was carried out using a Model CV-1B cyclic voltammetry instrument (Bioanlytical Systems, W. Lafayette, IN) and a Model 7034A x-y recorder (Hewlett-Packard, Palo Alto, CA). The potential was scanned from 0.0V to + 1.3 V vs Ag/AgCl reference electrode at 180 mv/sec. Glassy carbon was used as the working electrode.

Sample Extraction

To 1 ml of plasma, 60 ul (600 ng) of internal standard etoperidone, 25 ul (25 ng) of the internal standard 1-(o-tolyl) piperazine, 1.0 ml carbonate buffer (0.6 M pH 9.5) and 8 mls of methyl-tert-butyl ether were added. The mixture was shaken for 10 minutes and centrifuged for 10 minutes. The organic layer was then transferred

to 15 ml tapered centrifuge tube containing 1.2 ml 0.1N HCl. After mixing and centrifuging for 10 minutes, the top layer was aspirated and the aqueous portion transferred to a 3 ml tapered glass-stoppered centrifuge tube. The contents were made alkaline with 0.5ml carbonate buffer (0.6 M pH 9.5) and extracted with 0.7 ml of methyl-tert-butyl ether. After mixing and centrifuging for 5 minutes, the lower layer was discarded and the ether layer transferred to small 1.0 ml vials or "low volume inserts" if automatic sampling was desired. After evaporation to dryness in a vacuum concentrator, Model SVC-100 M Speed Vac Concentrator, (Savant Instruments, Hicksville, NY), the residue was redissolved in 100 ul of mobile phase and injected on column.

Chromatographic Conditions

The mobile phase consisted of 90% phosphate buffer (0.05 M pH 3.0) and 10% acetonitrile with 0.005 M sodium heptane sulfonate and 0.005 M n-nonylamine added. The flow rate was 2.2 ml/min and temperature ambient. The effluent was monitored via a thin-layer flow through electrochemical transducer having a potential of +1.15 V vs Ag/AgCl reference electrode.

Quantitation

The peak-height ratios of trazodone to the internal standard etoperidone and m-CPP to the internal standard o-TP were plotted against concentration. A least squares linear regression analysis of these data were used to calculate the parameters slope, x-intercept, correlation coefficient and standard errors.

RESULTS AND DISCUSSION

Trazodone and its metabolite m-CPP were extracted from 1 ml of plasma, separated by reversed phase liquid chromatography, and quantitated by an electrochemical detector. The use of a divided signal from the controller and a dual recorder set at different attenuations permitted the simultaneous determination of trazodone and m-CPP without changing attenuation during each chromatogram. Thus, this procedure could be adapted to automatic sample processing.

In addition to the large difference in concentrations between plasma trazodone and m-CPP, other problems such as peak tailing and poor resolution due to possibly other as yet unidentified metabolites of trazodone were initially encountered. After testing several bonded reverse-plase columns (C_{18}-C_8) a trimethylsilyl bonded reverse phase column was found to adequately resolve the peaks of interest. The addition of n-nonylamine to the mobile phase and maintaining the pH at 3 improved peak symmetry and reduced overall retention times. Fig. 2 shows a dual chromatogram of a spiked plasma sample. The selection of two internal standards was obviously necessary because of the aforementioned concentration differences in plasma trazodone and m-CPP. Etoperidone (Fig. 1b) closely resembles trazodone chemically while o-tolylpiperazine (o-TP) (Fig. 1d) is chemically related to m-CPP. Because of the presence of the phenyl piperazine moiety, all of these compounds displayed similar cyclic voltammograms (Fig. 3). The scans indicate an irreversible oxidation reaction at ca +1.1V vs Ag/AgCl reference electrode.

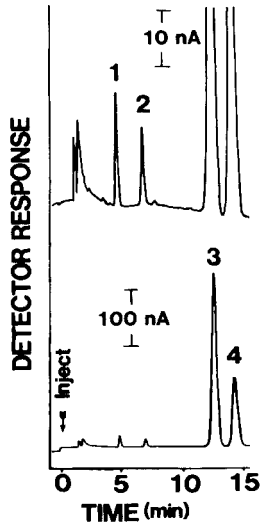

Figure 2: A dual chromatogram of a 1 ml spiked plasma sample containing 20 ng of m-CPP (2) and 1000 ng of trazodone (3). The entire reconstituted extract was injected. Etoperidone (4) and o-TP (1) are internal standards.

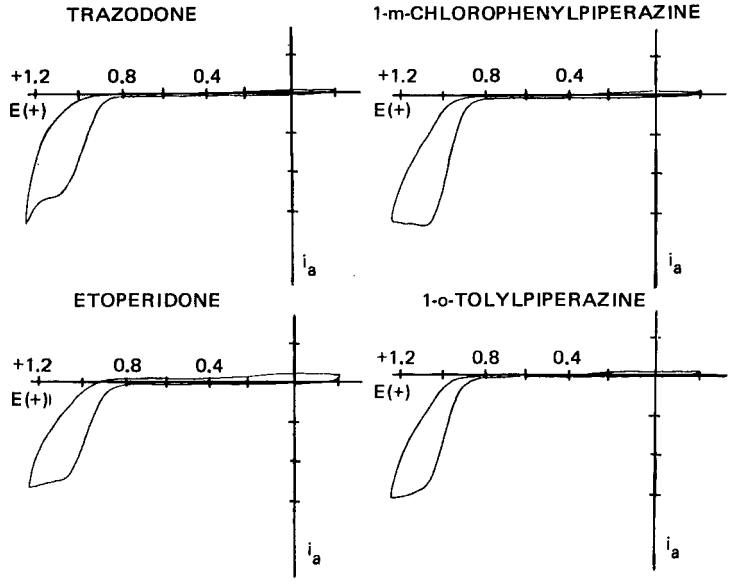

Figure 3: Cyclic voltammograms of trazodone, etoperidone, m-chlorophenylpiperazine (m-CPP) and 1-o-tolylpiperazine (o-TP). Concentrations for all compounds were 2 mg/10 ml of mobile phase.

Therefore, the detector was set at the the optimum potential +1.15 V vs Ag/AgCl reference electrode.

Even at this high potential, the chromatograms did not indicate any interfering endogenous peaks as shown by a plasma blank (Fig. 4). Therefore the minimum quantifiable level of detection was 5 ng/ml for m-CPP, while for trazodone 100 ng/ml was the lower limit because of the relatively high level of the internal standard etoperidone. If single dose studies were necessary then this limit would be reduced to ca 10 ng/ml by addition of 10% of the internal standard. With a signal to noise ratio = 3, 1 ng of m-CPP or trazodone injected directly can easily be detected. Fig. 5 shows a dual chromatogram of an actual patient plasma sample. The presence of "x" between peaks 1 and 2 is probably an induction of one or more as yet unidentified metabolites.

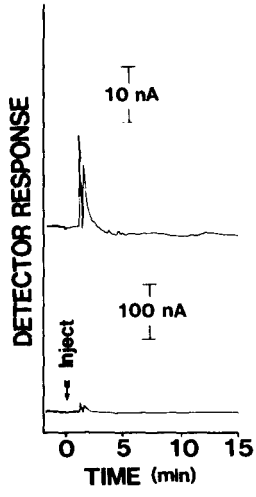

Figure 4: A dual chromatogram of a 1 ml blank plasma extract. Entire reconstituted extract was injected.

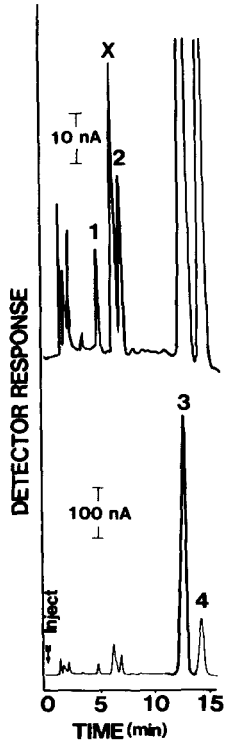

Figure 5: A dual chromatogram of a 1 ml plasma extract from a patient receiving trazodone daily for 3 weeks. Trazodone (3) levels were found to be 1797 ng and m-CPP (2) was at a concentration of 54 ng. The peak "x" probably represents other as of yet unidentified metabolites of trazodone.

The absolute recovery of trazodone and m-CPP was determined by spiking 1 ml of plasma with various concentrations of each compound. The extraction was carried out quantitatively. The internal standards were added after evaporation of the extract and again brought to dryness. The residue was reconstituted with mobile phase and injected. The same standards (non-processed and internal

standards) were also brought to dryness and reconstituted with mobile phase and injected directly on column.. The difference between the ratio of the standards and internal standard in the porcessed samples compared to the direct injection sample gave a measure of the overall recovery (Table 1).

The precision of the reported procedure was determined by spiking eight 1 ml aliquots of drug-free plasma with various concentrations of both trazodone and m-CPP. The samples were processed and chromatographed as described. The results appear in Table 2.

A measure of the stability of the assay is demonstrated by the variability in the slope of the linear regression curves on 6 different days (Table 3).

Steady-state plasma concentrations were analyzed for trazodone and m-CPP (Table 4).

TABLE 1

Recovery of Trazodone and m-CPP from Plasma (n=8).

Compound	Concentration (ng/ml)	Percent Recovery	C.V. %
Trazodone	2000	91	2.4
	500	97	2.8
m-CPP	50	82	4.2
	10	86	8.3

TABLE 2

Within-run Precision of Assay (n=8).

Compound	Concentration (ng/ml)	C.V. %
Trazodone	2000	1.5
	1000	1.5
	100	1.5
m-CPP	50	6.6
	20	2.3
	5	2.8

TABLE 3

Day-to-day Stability of Assay Based Upon Slope of the Linear Regression Curves (n=6)

	Slope (ng/ml)	+ S.D.	C.V.%
Trazodone	378.5	17.05	4.5
m-CPP	28.0	2.03	7.3

TABLE 4

Steady-State Plasma Concentrations in Five Depressed Patients

Patient	Trazodone (ng/ml)	m-CPP (ng/ml)
1	824	8
2	496	20
3	875	10
4	1212	28
5	618	22

The metabolite m-CPP ranged from 1 to 4% of the parent drug in plasma. In a single dose kinetic study (6), m-CPP reached 10 ng/ml at C_{max}, amounting to about 1% of the parent drug plasma concentrations. In another study (11), m-CPP was found to be present in significant quantities in rat brain after oral administration.

This method should facilitate the quantitation of trazodone and m-CPP in biological fluids and aid in the further eludication of the role of this metabolite in clinical efficacy and side effect relationships in man.

ACKNOWLEDGEMENTS

This work was supported in part by Health Research Council Grant 14-081 from the New York State Health Planning Commission. Dr. D.S. Robinson, Chairman, Department of Pharmacology, Marshall

University Medical School, Huntington, West Virginia generously supplied these patient samples to aid in the development of the assay procedure.

REFERENCES

1. Brogden, R.N., Heel, R.C., Speight, T.M. and Avery, G.S. Trazodone: A review of its pharmacological properties and therapeutic use in depression and anxiety. Drugs, 21, 401 (1981)

2. Al-Yassiri, M.M., Ankiers, S.I., and Bridges, P.K. Trazodone - A new antidepressant. Life Sci. 28, 2449 (1981)

3. Rawls, W.N., Trazodone, Drug Intell. and Clin. Pharm. 16, 7 (1982)

4. Silvestrini, B., Lisciani, R. and DeGregorio, M. Pharmacological and biochemical properties of drug substances. M.E. Goldberg, Ed. Vol. 3, American Pharmaceutical Association. Washington, D.C. (1981), p. 94

5. Barocchi, L., Frigerio, A., Giannangeli, M. and Palazzo, G. Basic metabolites of trazodone in humans. Arzneim. Forsch. 24 1966 (1974)

6. Caccia, S., Fong, M.M., Garattini, S., and Zanini, M.G. Plasma concentrations of trazodone and 1-(3-chlorophenyl)piperazine in man after a single oral dose of trazodone. J. Pharm. Pharmacol. 34, 605 (1982)

7. Fuller, R.W., Snodaly, M.D., Mason, N.R. and Oven, J.E. Disposition and pharmacological effects of m-chlorophenylpiperazine in rats. Neuropharmacology 20, 155 (1980)

8. Caccia, S., Ballabio, M., Samanin, R., Zanini, M.G. and Garattini, S. 1-m-chlorophenylpiperazine, a central 5-hydroxy tryptamine agonist, is a metabolite of trazodone. J. Pharm. Pharmacol. 33, 477 (1981)

9. Maj, J., Polinder, W., Rawlow, A. Trazodone, a central serotonin antagonist and agonist. J. Neural Transm. 44, 237 (1979)

10. Fong, M.H., Garattini, S., Caccia, S. 1-m-chlorophenylpiperazine is an active metabolite common to the psychotropic drugs trazodone, etoperidone and mepiprazole. J. Pharm. Pharmacol. 34, 674 (1982)

11. Caccia, S., Ballobio, M., Fanelli, R., Guiso, G. and Zanini, M.G. Determination of plasma and brain concentrations of trazodone and its metabolite 1-m-chlorophenylpiperazine, by gas-liquid chromatography. J. Chromatogr. 210, 311 (1981)

12. Ankier, S.I., Morton, B.K., Rogers, M.S., Carpenter, P.K., and Graham, C. Trazodone - A new assay procedure and some pharmacokinetic parameters. Br. J. Clin. Pharmacol. 11, 505 (1981)

JOURNAL OF LIQUID CHROMATOGRAPHY, 6(12), 2209-2230 (1983)

PRACTICAL ASPECTS OF LC/EC DETERMINATIONS OF PHARMACEUTICALS IN BIOLOGICAL MEDIA

D.J.Miner, M.J.Skibic, and R.J.Bopp

Analytical Development Division
Lilly Research Laboratories
307 E. McCarty Street
Indianapolis, Indiana 46285

ABSTRACT

Liquid chromatography with electrochemical detection (LC/EC) has proven itself to be a very useful technique for the determination of electrochemically oxidizable or reducible compounds in complex matrices. Practical aspects of the application of LC/EC to pharmaceuticals in biological samples are discussed. These have been gleaned from several years experience with the determination of over a dozen compounds. The aspects discussed are a comparison of EC and UV detection which facilitates a choice between the two, and common problems including electrode coating, late eluters, detector temperature dependence and baseline instability. Various possible solutions to these problems are considered.

INTRODUCTION

Since the invention of electrochemical detectors (EC) for liquid chromatography (LC) just over a decade ago, their use has grown exponentially, so that presently there are over one thousand literature reports of their use. For the liquid chromatographic determination of small, readily oxidized molecules, electrochemical detection is clearly established as being superior to the more generally

0148-3919/83/0612-2209$3.50/0

applicable and available ultraviolet (UV) detectors. For more than four years we have used EC detectors in the LC determination of a variety of pharmaceuticals in biological samples. These compounds have generally not been as ideally suited to EC detection as the catecholamines and related compounds for which EC was developed and for which it has been most frequently used. Nevertheless, LC/EC has proven to be a very useful technique. Several practical aspects of our experience with LC/EC are presented here.

MATERIALS AND METHODS

Reagents

Enviroxime, zinviroxime, hexestrol, enviradene and its cis-olefin isomer, frenazole, diethylstilbestrol, cis-diethyl-stilbestrol, and pergolide, were synthesized at the Lilly Research Laboratories. N-(4-hydroxyphenyl)-propionamide and N-(4-hydroxy-3-methylphenyl) acetamide were a gift from P.T.Kissinger, Purdue University. All other compounds were obtained commercially.

Distilled deionized water was used for preparation of mobile phases. Distilled-in-glass benzene, methanol and acetonitrile were obtained from Burdick and Jackson (Muskegon, MI), HPLC grade methanol from Tedia (Fairfield, OH) and analytical grade methanol from MCB Manufacturing Chemists (Cincinnati, OH). All other reagents were analytical reagent grade.

Equipment

The HPLC systems consisted of a solvent delivery pump and autoinjector (Models 6000A and WISP 710B, Waters Associates, Milford, MA), a guard column packed with pellicular packing material (CO:PELL ODS, Whatman, Clifton, NJ), a 250 x 4.6 mm reverse phase column, a column temperature controller and an electrochemical detector (Models LC-22/23

and LC-4 with a TL-5 or TL-5A glassy carbon detector cell, Bioanalytical Systems, W. Lafayette, IN). Detector potential was referenced to a Ag/AgCl/3 M NaCl reference electrode. A UV detector (Model 450, Waters Associates) was either substituted for the electrochemical detector or connected between the column and the electrochemical detector. The fluorescence detector used was a dual monochromator instrument (Model 650-10 S, Perkin Elmer, Norwalk, CT). Detector response was monitored by a chart recorder and a central chromatographic data acquisition computer system.

Column-switching was done as described previously (1), except that a silica column (Pre-SAT, Applied Science, State College, PA) was placed between the auxiliary pump and the 3cm reverse phase column, and a 250 x 4.6mm column was placed downstream from the 3 cm column, to provide a constant backpressure.

For the investigation of the temperature dependence of the electrochemical detector, the EC cell was thermostatted independently of the chromatographic column, as described previously (2).

Chromatography

Enviroxime and zinviroxime were chromatographed on an octylsilane column (Zorbax C8, Dupont Instruments, Wilmington, DE) with a mobile phase of 0.14 M sodium acetate and methanol (35:65), containing 3 mg of disodium EDTA per liter. The flow rate was 0.9 ml/min and the column temperature 28°C. The stilbestrols were chromatographed on an octadecylsilane column (Zorbax C18) with the same mobile phase as above. The flow rate was 1.5 ml/min and column temperature 30°C. Enviradene was also chromatographed on the Zorbax C18 column, but with a mobile phase of 0.2 M sodium acetate and methanol (25:75), containing 3mg EDTA/liter. The flow rate was 1.3 ml/min and column temperature was 28°C. For pergolide a nitrile column (Zorbax CN) was used, with a mobile phase of acetonitrile/methanol/0.1 M ammonium acetate (30:25:50). The flow rate was 2 ml/min. Acetaminophen and its analogs were chromatographed on an octadecyl column (Zorbax C8) with 0.1M citrate (pH 4.0) and methanol

(86:14) as the mobile phase. The flow rate was 1 ml/min and the column temperature was 28°C. The catecholamines were chromatographed with 1.4% monochloroacetate (pH 3.0) and methanol (95:5) as mobile phase. Sodium octyl sulfonate (25mg/l) and disodium EDTA (38mg/l) were also added to this solution. These amines also were run on a Zorbax C8 column at 28°C and a flow rate of 1 ml/min. The octadecylenol compound was assayed on a C18 column (Zorbax) with a mobile phase of 55% n-propanol. All mobile phases were filtered through a 0.2 μm pore filter (Rainin Inst. Co., Woburn, MA) and sonicated under vacuum prior to use.

RESULTS AND DISCUSSION

EC vs. UV Detection

The choice of an LC detector for an assay under development can involve a number of factors. Chief among these are signal-to-noise ratio (or detection limit), specificity and convenience. UV detection, which is the most universally used method, is the common alternative to EC detection. The relative merits of the two detectors, particularly in regard to the three factors listed above, were gleaned from consideration of assays developed for a number of compounds, including 1) two stilbestrols, 2) two pairs of antirhinovirals, 3) an octadecylenol, and 4) an ergot derivative. These assays are first discussed individually.

Diethylstilbestrol (DES) is a synthetic estrogen capable of producing all the pharmacologic and therapeutic responses attributed to natural estrogens. An assay was developed for DES (by definition the trans isomer) and its corresponding cis isomer involving a benzene extraction of the compound and an internal standard (benzestrol) from either plasma or urine. The plasma or urine was treated with a commercial glucuronidase/sulfatase preparation from H. pomatia prior to extraction if total drugs (free and conjugated) were to be determined. The organic extracts were evaporated and the residues reconstituted and injected. Detection parameters were chosen based upon electrochemical and spectral scans. Hydrodynamic voltammograms obtained for the three compounds are displayed in Figure 1. With two conjugated aromatic

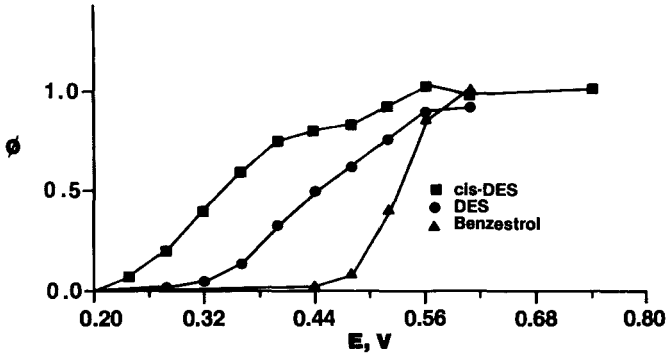

FIGURE 1. Hydrodynamic voltammograms of stilbestrols under the LC conditions described in the materials and methods section.

hydroxy groups, the stilbestrols are readily oxidized. Hydrodynamic $E_{\frac{1}{2}}$'s determined from the data in Figure 1 were +0.4 and 0.3 V for DES and cis-DES respectively. A detector potential of +0.70 V was used, although a somewhat lower potential would have sufficed to provide diffusion-limited oxidation. The ultraviolet absorption of DES and cis-DES was found to be moderate (ε_{262}=8635 for both isomers). Typical chromatograms of a plasma extract comparing UV and EC detection are depicted in Figure 2. EC detection can be seen to be clearly preferred in terms of freedom from interferences and signal-to-noise ratio (S/N). The detection limits realized were approximately 1 ng/ml of plasma for EC and 10 ng/ml for UV. Some increase in UV signal could be realized by operation at 210nm, but a concomitant increase in background noise would result in only a small increase in overall S/N.

Enviradene, whose structure is shown below, is the trans-methyl olefin analog of the antirhinoviral oxime enviroxime, whose determination in plasma has been previously reported (1). Zinviroxime is the cis-oxime

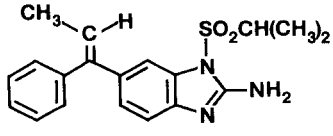

Enviradene

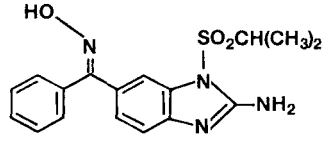

Enviroxime

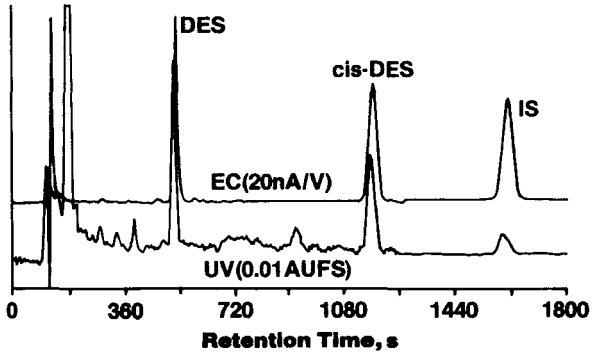

FIGURE 2. Serial UV and EC chromatograms of a 100ng per ml plasma extract.

isomer of enviroxime. The difference in the structures of these molecules is solely at the exocyclic double bond position. Plasma levels of enviradene may be determined by a procedure very similar to that reported for enviroxime, with the mobile phase altered slightly and the electrode potential increased to +0.90 V. The oxidations of enviroxime and zinviroxime were reasonably similar (hydrodynamic $E_{\frac{1}{2}}$=+0.72 and +0.81 V, respectively) and EC was clearly preferred over UV detection for plasma assays. Interestingly, and in contrast to the oximes, enviradene and its isomeric cis-olefin are more difficult to oxidize (Figure 3), with an $E_{\frac{1}{2}}$ of +0.8 and +0.94 V, respectively. Also, their oxidation potentials show a greater difference between each other. In addition, the methyl olefins have higher molar absorptivities (ε_{268}=17,800) than those of enviroxime and zinviroxime (ε_{272}=14,200). As as result, while EC S/N ratios are marginally better than UV for enviradene, S/N is better using UV detection for the cis-olefin. Figure 4 shows a plasma extract chromatographed on a system with EC and UV detectors set up in series. No significant interferences were observed in chromatograms with either detector. However, the use of UV detection was noted to have several advantages. The wavelength chosen was one at which the two isomers have identical molar absorptivities. Thus if peak areas are calculated, the two isomers can be quantitated from a single standard curve. The linearity of the UV detector extended to greater than 10μg on column,

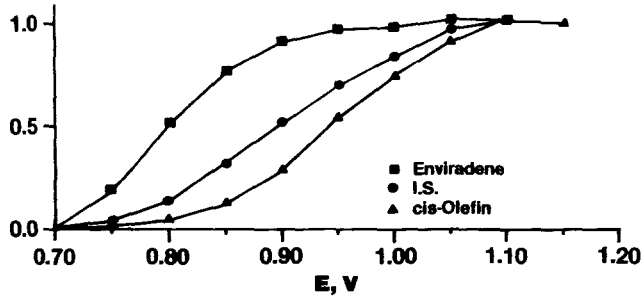

FIGURE 3. Hydrodynamic voltammograms of the methyl olefin antivirals under the LC conditions described in the materials and methods section.

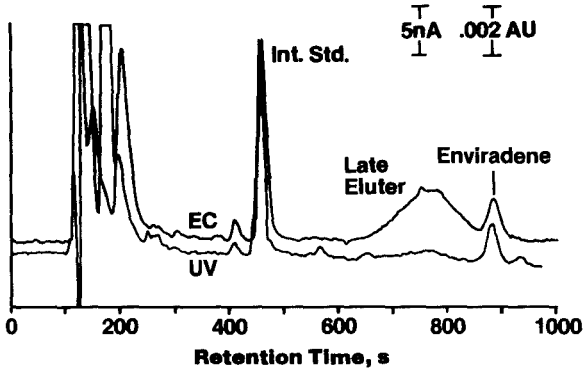

FIGURE 4. EC and UV chromatograms of an extract of a plasma sample spiked with 50 ng enviradene per milliliter

while the EC was limited to 400 ng. Also, the late eluters encountered with the EC detector (see Figure 4) were relatively much smaller on UV.

A third type of compound for which EC and UV detection were compared was an octadecylenol compound, CH_3-$(CH_2)_{17}$-OR. A hydrodynamic voltammogram for this compound is depicted in Figure 5. The oxidation of this molecule involves the enol oxygen, so that octadecylalcohol is probably liberated in the process. Although the half-wave potential for this oxidation is relatively low, the wave is far from reversible. The

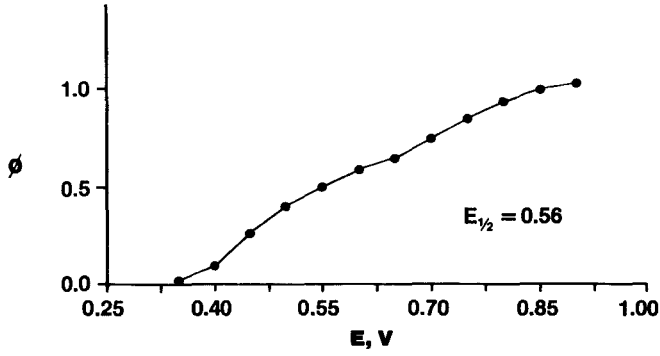

FIGURE 5. Hydrodynamic voltammogram of an octadecylenol compound obtained using the chromatographic conditions described in the materials and methods section.

UV absorption spectrum of this compound exhibited a maximum at 245 nm with an molar absorptivity of 9720. A procedure was developed for the determination of this compound in plasma at the 1 μg/ml level. The octadecylenol was isolated from plasma by precipitation of proteins with the addition of 1 volume of n-propanol, followed by 1 volume acetonitrile. This procedure gave chromatograms without EC or UV interferences. The minimum quantity which could be detected by EC (at a potential of +0.85 V) was 5 times lower than that by UV. However, a large EC response from non-retained components, severe coating problems (discussed further below) and the low solubility of salts in the mobile phase forced the abandonment of EC detection. Thus, UV detection was employed for this determination.

The fourth assay to be considered here is one developed for pergolide, the structure of which is shown below. Pergolide is an ergot

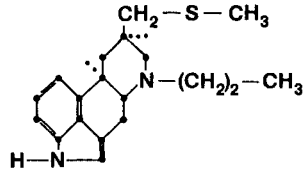

Pergolide

alkaloid derivative currently under study for the treatment of Parkinson's disease. It contains a single substituted aromatic amine group and is not easily oxidized (hydrodynamic $E_{1/2}$~+0.86 V at pH 7). Its molar absorptivity is relatively low (ε_{280}=5300) also. A procedure was developed for the determination of pergolide in feed samples in support of animal toxicology studies. The feed samples were dissolved in 10 volumes of 80:20 methanol/0.1M HCl. This solution was passed over alumina and an aliquot injected. The absolute detection limit using UV detection was 20ng on column, which was insufficient to allow detection of pergolide at the desired levels. The use of EC lowered the detection limit to 2ng on column, but a large t_o response was observed (see Figure 6) as were many large late eluters. Instead of either EC or UV detection, fluorescence detection was used, since it provided detection limits superior to EC and lacked interferences (Figure 7).

Several general observations relative to the choice between EC and UV detection for LC determination of drugs in biological matices may be drawn from the assays just discussed. First of all, the relative S/N of the two detectors is frequently an important consideration. For UV detection, the signal (peak area or height) obtained for different analytes (assuming comparable retention times) is proportional to their extinction coefficient at an accessible ultraviolet or visible wavelength. Signal to noise with EC detection is more complex. The

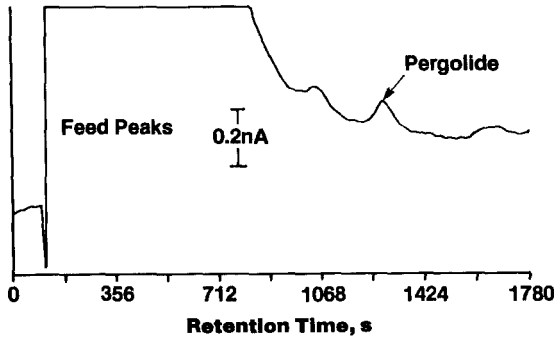

FIGURE 6. LC/EC chromatogram of an extract of feed spiked with 2 ppm of pergolide.

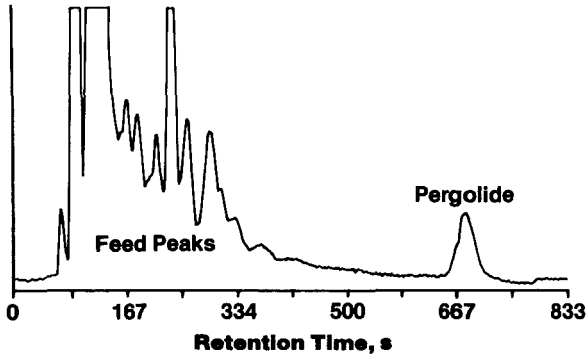

FIGURE 7. LC/Fluorescence chromatogram of an extract of feed that was spiked with 2 ppm of pergolide. The excitation wavelength was 285 nm (slit 10nm) and the emission wavelength was 345 nm (slit 5nm).

signal for conventional amperometric detectors is a function of their configuration, the working electrode potential of the detector, and the diffusion coefficient, half-wave potential and reversiblity of the analyte under the chromatographic conditions. The noise of a conventional solid electrode detector is a function of many factors, but it is generally relatively constant from 0.0 volts out to the potential at which solvent oxidation (or reduction) begins to occur. From there on, background current and noise increase exponentially. Thus as the half-wave potential of a theoretical analyte approaches the oxidation potential of the the solvent, the maximum realizable S/N decreases.

For readily oxidized molecules, such as catecholamines or the stilbestrols discussed above, the S/N of EC detection is clearly better than that of UV detection. As analytes of increasing oxidation potential are investigated, S/N will decrease for EC detection. As analytes with larger extinction coefficients are investigated, S/N for UV detection will increase. Thus with increasing $E_{1/2}$ or ε or both, a point will be reached at which S/N for the two detectors is equivalent. Analytes with even higher $E_{1/2}$ or ε will exhibit a better S/N by UV detection. The results of the four assays just described confirm this hypothesis. Figure 8 includes a point for each compound, and the line represents the points at which S/N is equal for EC and UV. The regions in which EC or

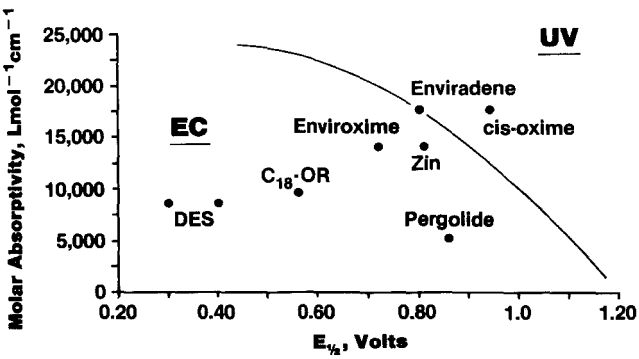

FIGURE 8. EC versus UV detection for LC-Dependence on molecular parameters. The compounds to the left of the line have lower absolute detection limits by EC detection than by UV detection. The opposite is true for compounds to the right of the line.

UV detection are preferred are clear. Data for additional analytes, particularly some with high $E_{\frac{1}{2}}$/low ε and high ε/low $E_{\frac{1}{2}}$, will allow a better definition of the location of this line. Nonetheless, it is apparent that a guideline can be established for making a choice between EC and UV detection when signal-to-noise ratio is an important consideration.

A number of additional factors influence the choice of detector for a given determination. The advantages of EC and UV detection relative to each other are summarized in Table 1. Many of the factors listed there were encountered in assays described above. The particular advantages of the EC detector are its sensitivity and specificity. For electrochemically active analytes, EC detection has a superior absolute sensitivity to UV. For an electrochemically active compound, the specificity of EC detection can make assay development much easier. UV detection on the other hand is useful for more analytes. UV detection is more convenient, since the condition of electrodes is not a consideration, as is the case with EC detection. An isobestic point may be chosen so that more than one compound can be quantitated from a single standard curve. For an internal standard to be maximally effective, its chemical properties should closely approximate those of the analyte. In

TABLE 1

	EC	UV
Advantages	**Sensitivity**	**Ease of Use**
	Specificity	**Universality**
		Isobestic Points
		Choice of Int. Stds.
Disadvantages	**Coating**	**Drug Interferences**
	Ref. Electrode Stability	**Temperature Sensitivity**
	Temperature Sensitivity	
	Late Eluters	

this regard UV detection has an advantage since internal standards are more readily found which approximate the UV properties of an analyte, than those which have similar electrochemical properties.

The disadvantages of the two detectors relative to each other are also summarized in Table 1. Some of the potential problems with EC detection, including electrode coating, temperature sensitivity and late eluters are discussed in detail below. UV detectors are subject to fluctuations in response with room temperature also. The more universal nature of UV detection also means that more of the components of the sample matrix will be detected and so are potential interferences. Thus background can be more of a problem with UV detection than with EC detection.

Common Problems-Electrode Coating

Electrode inactivation, or coating, is common in conventional voltammetric work. The occurrence of coating in LC/EC has been previously noted (3,4), but it is a much less frequent problem. This is a function both of the relatively low amounts of compounds chromatographed (picograms to a few micrograms) and the relatively high velocity of the mobile phase over the working electrode surface. In our work we have encountered a number of examples of compounds which exhibit

coating problems, however. The details of these problems, as well as a series of possible solutions which were investigated, are discussed below.

When injecting samples containing high concentrations of enviroxime and zinviroxime (0.4 to 1.5 μg/ml) it was noted that the peak height of the internal standard hexestrol decreased considerably during the chromatography of a single set of samples. Further investigation revealed that the sensitivity of the detector to enviroxime and zinviroxime decreased also. A series of experiments were performed to determine the source of the problem. Various combinations of the three compounds, all at 1 μg per injection, were repeatedly injected. Between experiments the glassy carbon working electrode was repolished. These experiments are summarized in Table 2. The compound(s) injected are listed on the left and % decreases in peak height per injection are listed to the right. Since the loss of sensitivity of hexestrol and enviroxime are similar in the first two experiments, it is clear from the last two experiments that hexestrol (a diphenol) is the primary source of the electrode inactivation. This is not surprising since phenols are well known to polymerize at electrode surfaces (5). It should also be noted from the data in Table 2 that enviroxime is capable of coating the electrode, albeit at a much slower rate.

The concentration dependence of the action of hexestrol is depicted in Figure 9. Here again, each data point represents one experiment, and the electrode was repolished in between each experiment. A roughly linear dependence is observed. The rate of coating was quite variable

TABLE 2

Compounds Injected (1 μg each)	% Decrease in Peak Height per Injection	
Enviroxime/Zinviroxime/Hexestrol	Enviroxime	14.3
	Hexestrol	14.4
Enviroxime/Hexestrol	Enviroxime	14.1
	Hexestrol	13.7
Hexestrol	Hexestrol	14.4
Enviroxime	Enviroxime	0.4

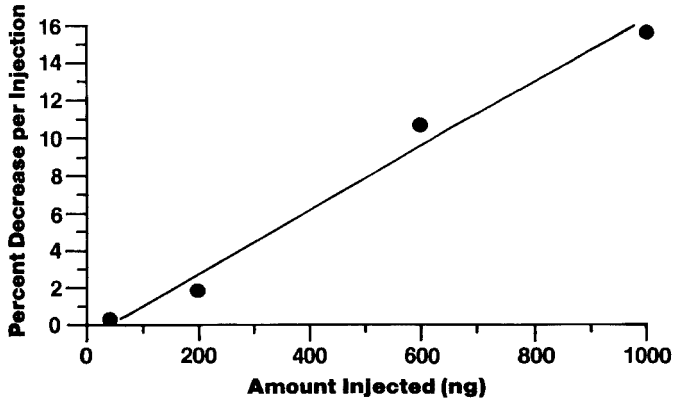

FIGURE 9. Concentration dependence of electrode coating by hexestrol. Coating determined by electrode response to zinviroxime.

(relative standard deviation = 27%) at the 200 ng level but reproducible at the 1 μg level. In order to minimize the coating of the electrode surface by hexestrol, or to regenerate coated electrodes, a variety of experimental approaches were tried. These are summarized in Table 3. The only approach found to be of signigicant value was to keep the amount of hexestrol injected low. It was possible in this case to do this without significantly degrading S/N. In addition, the similar electrochemical properties of hexestrol, zinviroxime, and enviroxime mean that hexestrol will reduce the effect on the analytes to sensitivity losses due to electrode coating. See for example Figure 10.

Studies of another benzimidazole structurally related to enviroxime manifested electrode coating in an additional way. When chromatographed under conditions similar to those for enviroxime, coating was seen at the rate of 0.4% per 300 ng injected. In addition, a dip in the baseline immediately after elution of the compound was observed (see Figure 11). The background current eventually returned to its initial level. The size of the dip is proportional to the amount of this compound injected. It was therefore attributed to reversible coating of the surface which strongly affected the background oxidation current. Such an effect has previously been observed (6). The reason for this reversibility was

TABLE 3

Experimental Approaches	Effective?
Switch E to −0.4 V for 10 min.	No
Let mobile phase "wash" surface overnight	No
Wash off-line with $CHCl_3$/acetone/CH_3OH	Partially
Switch from NaOAc to citrate/phosphate	Slightly
Add octyl sulfonate to mobile phase	No
Lower the amount injected	Yes

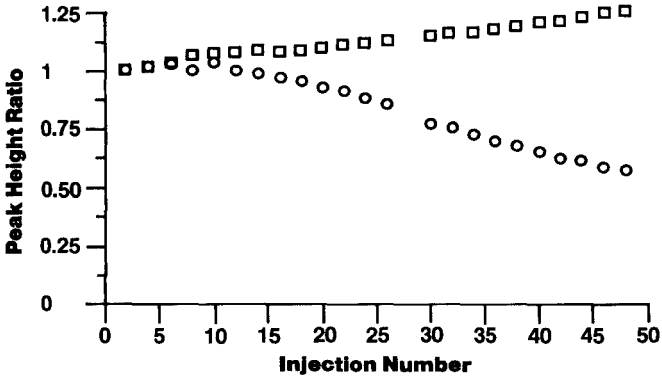

FIGURE 10. Peak height ratio for enviroxime upon repeated injection of a mixture of enviroxime and hexestrol. Key: 0 ratio to initial peak height, □ ratio to peak height of hexestrol.

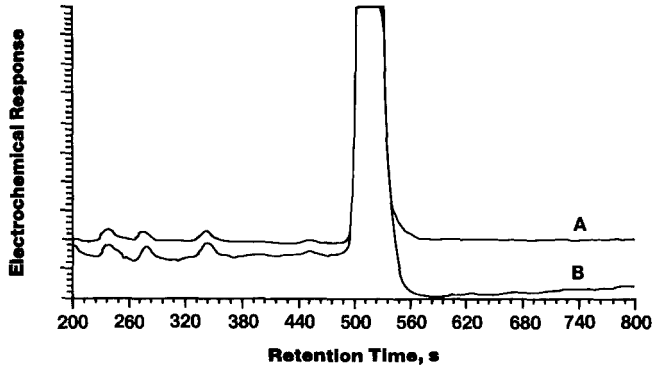

FIGURE 11. EC chromatograms of a benzimidazole. Chromatogram A was obtained at +0.86 V; The relative peak height was 64%. B was obtained at +0.90 V.

not known, and it is in contrast to the other example of coating encountered. The dip could be eliminated by lowering the oxidation potential (from +0.90 to +0.86 V).

The coating problems encountered with an octadecylenol analyte were noted above. It was presumed from the electrochemistry that octadecylalcohol is liberated during the oxidation of this molecule. Thus an attempt was made to reverse the loss of sensitivity by making large injections of wash solvent. This was unsuccessful, as were all other approaches tried for this compound (see Table 4).

In general we have been able to minimize electrode coating problems by lowering the amount of the compound injected, decreasing the detector potential or including an internal standard with electrochemical properties very similar to those of the analyte. These approaches have not always proven to be possible and successful. Greater success can probably be achieved though the use of pulsed EC detection for LC (7,8).

Late Eluters

Late-eluting peaks are strongly retained components from one injection, which elute during subsequent chromatograms. When samples are injected manually, the time between injections varies and the source and effect of late eluters is not always obvious. When an autosampler is used, the position of late eluters becomes reproducible and thus are more readily identified.

Late eluters will be observed at times with all types of LC detectors. Perhaps because of the superior sensitivity of EC detection,

TABLE 4

Experimental Approaches	Effective?
Lower detector potential	No
Change from glassy carbon to graphite/polymer	No
Inject slugs of wash solvent	No
Switch E to −0.65 between injections	No

we have more commonly observed late eluters with EC detection than with UV detection (see for example Figure 4). During the determination of enviroxime and zinviroxime in dog and rabbit liver homogenates and rabbit lung homogenates, many troublesome late eluters were observed. In the case of enviradene, late eluting peaks were observed in all physiological fluid extracts. Late eluters were a severe problem in the LC/EC determination of pergolide in feed discussed above.

In some simple cases it is possible to adjust the timing of injection such that late eluters elute in a non-critical portion of subsequent chromatogram. Waiting for the elution of all late eluters prior to making another injection is frequently not practical, even if elution is speeded by an increase in the organic modifier content of the mobile phase.

A very practical approach to removing late-eluting components is to use the well known technique of column-switching. For enviroxime and enviradene, a 3 cm column, mounted in a switching valve, was interposed between the pump and the 25 cm analytical column. The samples are injected onto the short column. After a time sufficient to allow the analytes and internal standard to elute from the 3 cm column onto the analytical column, the valve is automatically switched. The strongly retained components are then washed to waste using mobile phase and an auxiliary pump. Since the 3 cm column is washed with mobile phase there is very little reequilibration time when it is switched back into line. This type of system is ideal for running automated assays on large numbers of samples. Column switching produced cleaner chromatograms (compare Figure 12A and B), and compared with the other approaches mentioned above, increased sample throughput.

Interestingly, when column-switching was used during the determination of enviroxime in relatively clean biological extracts, fewer trace level interferences were seen. This resulted in an unexpected improvement in detection limits. The late eluters removed were small enough that their origin had not been determined.

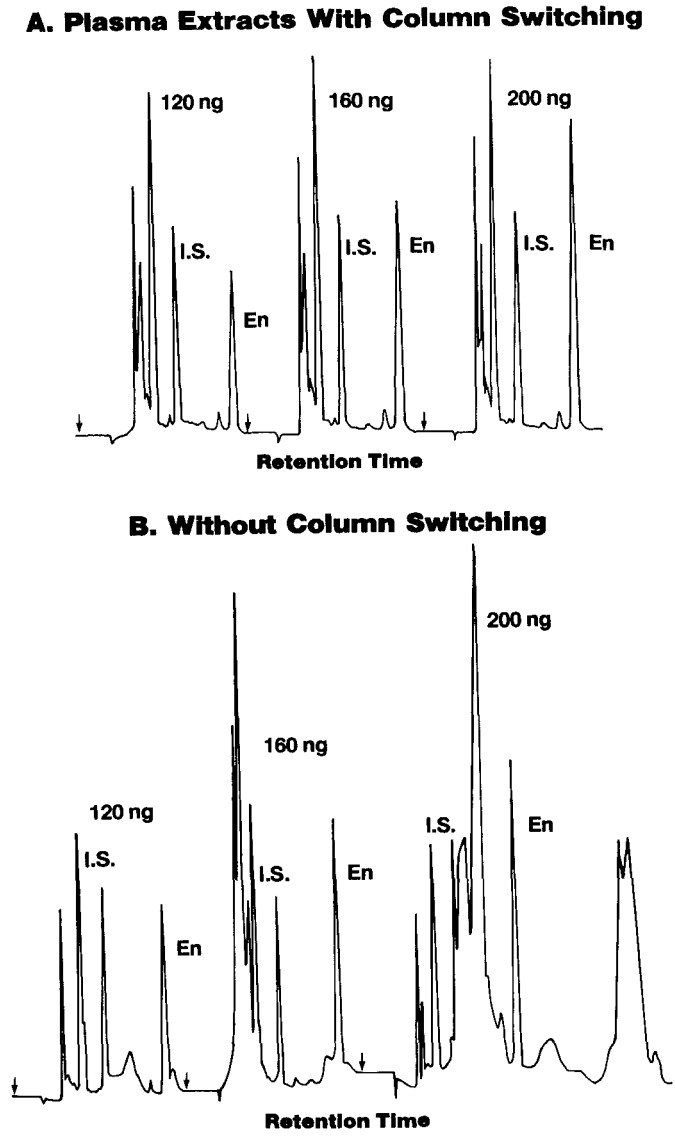

FIGURE 12. Chromatograms of extracts of plasma spiked with enviradene.

Temperature Dependence

A third common problem that can be encountered with the use of EC detection is the temperature dependence of amperometric detectors. This problem was originally recognized in our laboratory during lengthy unattended chromatography of enviroxime and zinviroxime-containing biological extracts (1). The EC responses to standards decreased dramatically when the ambient temperature decreased.

A detailed study was made in which several types of compounds, commonly determined by LC/EC, were chromatographed repeatedly with the detector temperature controlled over the range 0 to 50°C (2). Enviroxime and zinviroxime, the stilbestrols mentioned above, acetaminophen and some of its analogs, and several catecholamines were examined under typical assay conditions. Chromatographic response (peak height or area) of these compounds was observed to vary linearly as a function of temperature in some cases, and showed some upward curvature in others. The slope of these curves (taken at 22°C) ranged from a 1.5 to 2% change in EC response per °C for the catecholamines to greater than 8% per °C for zinviroxime.

The temperature dependence of amperometric EC detectors is due to the temperature dependence of 1) the diffusion coefficients of the analytes and 2) their rate of reaction at the electrode surface. Thus the changes in temperature influence both the number of molecules reaching the electrode surface and the fraction which are oxidized or reduced there. The contribution of diffusion was estimated by obtaining dependences with the working electrode potential high enough to assure diffusion-limited oxidation. Dependence of about 2% per °C or below were observed for the stilbestrols and acetaminophen and its analogs under such conditions. The contribution of changes in the rate of the electrode reaction to the overall temperature dependence increased exponentially as the detector potential was decreased, beginning about +75 mV above the hydrodynamic $E_{\frac{1}{2}}$ of the analytes.

A number of approaches are available which when used separately or in combination can decrease temperature dependences to insignificant levels. These are summarized in Table 5. The first is to thermostat the

TABLE 5

1. Thermostat detector
2. Thermostat column/increase flow rate
3. Operate well past $E_{1/2}$
4. Choose a good internal standard

EC detector, but this is not ordinarily convenient. The second is to thermostat the chromatographic column. Because of the dynamics of heat transfer in the EC detector cell block, thermostatting the column decreased the observed temperature dependences of acetaminophen and its analogs by a factor of 4. A third approach to minimizing EC temperature dependence is, whenever possible, to operate well past the $E_{1/2}$ of the analyte, so that diffusion alone contributes to temperature dependence. Finally, the use of an internal standard with similar diffusional and electrochemical properties will largely compensate for temperature induced changes in response.

Baseline Instabilities

During initial assay development for DES and enviroxime, the background current of the glassy carbon working electrode oscillated erratically and gradually but continuously increased. Repolishing the electrode reduced the background to its initial level. Since EDTA was commonly added to mobile phases used in determination of penicillamine and catecholamines, it was added to mobile phases used for DES and enviroxime. With this addition the background current was much more stable, both in terms of long-term drift and medium-term oscillations. Metal ions leached from the steel LC components or from the silica backbone of the column are presumably reponsible for the baseline instabilities, but the mechanism of the phenomenon is not known. Use of phosphate/citrate buffers in the mobile phase have some of the same effect as EDTA.

A second contributor to long-term drift is electrode coating by constituents of the mobile phase. Analagous to the coating by analytes discussed above, this is most frequently a problem at high oxidation

potentials. During the determination of enviroxime, it was found that the use of a reagent grade methanol in the mobile phase caused a 50% loss of sensitivity after only a few days of continuous use. Two manufacturers' distilled-in-glass methanols gave better results, but one (Burdick and Jackson) was clearly superior to the other. This assay is probably particularly sensitive to coating effects, since the oxidations are not at diffusion-limited conditions. Nevertheless, the benefits to be gained from use of the best available reagents for a given determination should be carefully considered.

CONCLUSION

The versatility of EC detection for LC has been demonstrated in our laboratory by its application to the determination of over a dozen compounds in biological matrices. Its durability has been proven by the successful assay of over 15,000 samples. Several problems which were encountered during routine use of the electrochemical detector have been investigated. A number of practical ways of overcoming these difficulties were evaluated, and in most cases the problems were surmountable.

REFERENCES

1. Bopp,R.J. and Miner,D.J., Determination of Enviroxime in a Variety of Biological Matrixes by Liquid Chromatography with Electrochemical Detection, J. Pharm. Sci., 71, 1402, 1982.

2. Miner,D.J., Temperature Dependence of Electrochemical Detection for Liquid Chromatography, Anal. Chim. Acta, 134, 101, 1982.

3. Koile,R.C. and Johnson,D.C., Electochemical Removal of Phenolic Films from a Platinum Anode, Anal. Chem., 51, 741, 1979.

4. King,W.P. and Kissinger,P.T., Liquid Chromatography with Amperometric Reaction Detection Involving Electrogenenrated Reagents: Applications with in-Situ Generated Bromine, Clin. Chem., 26, 1484, 1980.

5. Taylor,W.I. and Battersby,A.R., Oxidative Coupling of Phenols, Marcel Dekker, New York, 1967.

6. MacCrehan, W.A., Differential Pulse Detection in Liquid Chromatography and its Application to the Measurement of Organometal Cations, Anal. Chem., 53, 74, 1981.

7. VanRooijen,H.W. and Poppe,H., An Electrochemical Reactivation Method for Solid Electrodes used in Electrochemical Detectors for High-Performance Liquid Chromatography and Flow Injection Analysis, Anal. Chim. Acta, 130, 9, 1981.

8. Hughes,S., Meschi,P.L. and Johnson,D.C., Amperometric Detection of Simple Alcohols in Aqueous Solutions by Application of a Triple-Pulse Potential Waveform at Platinum Electrodes, Anal. Chim. Acta, 132, 1, 1981.

JOURNAL OF LIQUID CHROMATOGRAPHY, 6(12), 2231-2254 (1983)

NOISE AND DRIFT PHENOMENA IN AMPEROMETRIC AND COULOMETRIC DETECTORS FOR HPLC AND FIA

H.W.van Rooijen and H.Poppe

Laboratory for Analytical Chemistry
University of Amsterdam
Nieuwe Achtergracht 166
1018 WV Amsterdam
The Netherlands

ABSTRACT

Noise and drift phenomena in electrochemical detectors with solid electrodes are discussed.A relationship between the capacity of the working electrode and the noise of the detector is demonstrated in three different ways,using direct correlation of noise with capacity,time correlation functions and electrical simulation of the cell properties.Conclusions are drawn with respect to the prospects of various measures to improve the detection limit.

INTRODUCTION

As small electrical currents,down to picoamperes,corresponding to picocoulombs during a time constant of 1 second,can be readily measured electronically,the detection limit of electrochemical devices could be expected,from that point of view,to be in the range of 10^{-17} mole (1). However,detection limits in or below the picogram range,roughly 10^{-14} mole,still form an exception in routine analysis.As many analytical investigations nowadays aim at the quantita-

 0148-3919/83/0612-2231$3.50/0

tive determination of analytes at extremely low concentrations it is worthwhile to improve the performance of detectors in this respect.

As a first step the investigation of the various sources of noise and drift may be helpful,in order to indicate those measures which could lead to substantial improvement.An inventory of these sources is as follows.

Causes of drift may be:

1. The stabilisation processes taking place at the working electrode (2-5),
2. Gradual fluctuations in temperature (6) and air humidity,
3. Electrode contamination (7),
4. Gradual changes in the composition of the background electrolyte (carrier,mobile phase), e.g. due to the dissolution of oxygen or metals somewhere in the system (2,8,9).

Noise may originate from various sources:

1. The detector cell and the electronic equipment,
2. Power frequency pick up,
3. Electrical pulses,produced by other instruments,received via the power cord or otherwise,
4. Electrostatic influences often exerted by the operator.

In this paper some work on the characterisation of some of these phenomena is reported.Special attention is given to the generally observed proportionality of base line noise with electrode area.Such a dependence is not probable under all circumstances.An electrode may be considered as consisting of several parts;e.g. two parallel electrodes in the same liquid layer are in principle not different from one wide electrode of the same total area.The noise component in the total current of the two separate electrodes is $\sqrt{2}$ times larger than that of a single electrode,when the two behave independently,i.e. when there is no correlation between the two signals. Rather than addition of standard deviations an addition of variances has to be applied in such a case.

On the other hand,with full correlation between the two electrodes a summation of amplitudes,that is of standard deviations,has to be expected.In that case a two times larger noise for the two

times larger area is found in the given example.Thus,depending on conditions a proportionality of noise with area or with the square root of the area may be found.

Some kinds of noise may lead to correlation between the various parts of an electrode surface.Examples are the contributions due to fluctuations in the concentration of an electroactive substance in the carrier stream,temperature fluctuations,etc..However,when detection limits are approached and proper operating conditions are chosen so as to avoid large background signals and thermal instability,the noise contribution of the electrode itself is likely to be the predominant contribution.On first consideration an independent behaviour,uncorrelated noise,would be expected for distinct electrode sections.This would lead to a square root dependence of noise on area.Nevertheless,in general a direct proportionality is observed.An important objective of this work is to clarify these matters,with the idea that a good understanding of the origin of noise may indicate ways to further improvement.

THEORETICAL

It is assumed that it is possible to exclude all external effects by sufficient isolation of the whole system from electrical,thermal and other influences.When also the working electrode has stabilised sufficiently,we can restrict ourselves only to the voltage and current noise sources present in the system itself.What follows is an analysis of the effect of various noise sources on the output voltage,which is a representation of the current flowing through the working electrode.A schematic circuit,as given in fig.1,allows such calculations,which are carried out with the usual electric circuit laws, e.g. using complex alternating current formalism.

The following assumptions are made:

1. The various noise sources are independent;the variances caused by them are additive.
2. No current flows through the reference electrode so the impedance of the latter can be neglected.The potential applied by the

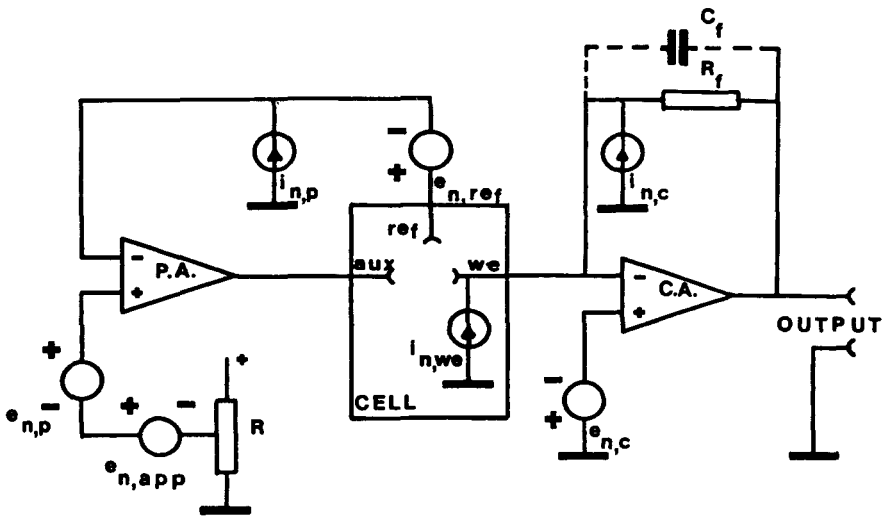

FIGURE 1 Simplified representation of the cell and the electronic circuits of the potentiostat and current amplifier.Cell: we: working electrode; ref:reference electrode; aux:auxiliary electrode.Potentiostat amplifier circuit: P.A.:potentiostat amplifier; R:potentiometer for adjustment of cell potential.Current amplifier circuit: C.A.: current amplifier; R_f:feedback resistor; C_f: feedback capacitor for low pass filtering. Current noise sources:$i_{n,p}$, $i_{n,we}$ and $i_{n,c}$ generated by the potentiostat amplifier,the working electrode and the current amplifier respectively.Voltage noise sources: $e_{n,app}$, $e_{n,p}$, $e_{n,ref}$ and $e_{n,c}$ generated by the potential source,the potentiostat amplifier ,the reference electrode and the current amplifier respectively.

potentiostat ,which is the potential difference between reference and working electrode,therefore accurately represents the potential difference between working electrode and liquid.

3. No large potential differences occur in the liquid.
4. For small voltage and current fluctuations for which the system can be considered as linear,the impedances are located at or quite near to the electrodes.This assumption is based on the observation (see Results and Discussion) that measured cell resistances are much larger than those calculated from the specific resistance of the carrier.

5. The linear system behaves ideally in the sense that deviations due to finite open loop gain of the amplifiers can be neglected at the frequencies of interest.

The current and voltage noise generated by each part of the system are accounted for by insertion of parallel or series sources in the system respectively, as is shown in fig. 1. This is a standard method in the noise analysis of electronic circuits. The sources will be described alternatively as a function of time or frequency: $i_{n,k}(t)$ and $e_{n,k}(t)$ or $i_{n,k}(\omega)$ and $e_{n,k}(\omega)$ in which i is currrent, e is voltage, n refers to the noise component, k identifies the element generating the noise (electrode or amplifier), t is time and ω is angular frequency. The various noise sources given in fig. 1 will now be discussed.

a) The potentiostat amplifier and the current amplifier

These contribute voltage noise, $e_{n,p}$ and $e_{n,c}$, respectively and current noise $i_{n,p}$ and $i_{n,c}$ respectively. However, the reference electrode was assumed to have a low impedance and $i_{n,p}$ can be neglected because it is short-circuited.

b) The working electrode

Its voltage noise will be neglected, because it cannot be distinguished from the current noise in potentiostatic operation. The working electrode contributes current noise, $i_{n,we}$, e.g. due to chemical processes taking place at its surface.

c) The reference electrode

This contributes voltage noise, $e_{n,ref}$, e.g. due to fluctuations in the temperature, the chemical equilibrium of the half raction $AgCl + e^- \rightleftarrows Ag\downarrow + Cl^-$, etc.. The current noise of this element will be neglected as the impedance of the electrode was assumed to be very low.

d) The auxiliary electrode

Both voltage and current noise of this electrode will be neglected because these effects are eliminated by the potentiostat amplifier.

The potential difference between the working electrode and the liquid is:

$$\Delta E = E_{app} + e_{n,p} + e_{n,ref} + e_{n,c} \quad (1)$$

where ΔE is the potential difference and E_{app} is the applied potential. As E_{app} may also display noise of magnitude $e_{n,app}$, due to insufficient stabilisation of E_{app}, the fluctuations in E will amount to :

$$e_{n,tot} = e_{n,p} + e_{n,ref} + e_{n,c} + e_{n,app} \quad (2)$$

The varying potential difference between the working electrode and the liquid leads to fluctuations in the current through the working electrode, the magnitude of which depends on the impedance of this electrode.

Baseline noise is especially important when very low concentrations are to be measured. When also sufficient precautions are taken to prevent the presence of electroactive contaminations in the carrier the current is small; the slope in the voltammogram is also small and the resistive part of the conduction can be neglected. Under these conditions the electrode behaves as a pure capacitor, which is of the order (see Experimental) of a few hundreds $\mu F/cm^2$. This means that a capacitive current, i_C , results:

$$i_C = C_{we} \frac{d}{dt} (e_{n,tot}) \quad (3)$$

The output voltage of the current amplifier will contain a noise component , $e_{n,out}$, which can be calculated to be:

$$e_{n,out} = R_f\{C_{we} \frac{d}{dt}(e_{n,tot}(t) + i_{n,we}(t) + i_{n,c}(t) \} + e_{n,c}(t) \quad (4)$$

where R_f is the value of the feedback resistor in the current amplifier circuit.

The last term in eqn (4) can be made negligible by choosing a large value for R_f. Insertion of a value of 100-400 $\mu F/cm^2$ for the capacity and a few μV for $e_{n,tot}$ suggests that the first term of eqn (4) may be responsible for a substantial part of the noise observed at the detector output. High frequency noise contained in $e_{n,tot}$ is especially amplified because of the derivative in eqn (4). In all electrochemical detectors this effect is diminished by the

application of low pass filtering with a feedback capacitor C_f (see fig.1),or by means of filtering in subsequent amplifier stages.

The effect of such measures is more easily represented in the frequency domain.For filtering with C_f it follows:

$$e_{n,out}(\omega) = \left(\frac{1}{R_f} + j\omega C_f\right)^{-1}\{j\omega C_{we} e_{n,tot}(\omega) + i_{n,we}(\omega) + i_{n,c}(\omega)\} \quad (5)$$

where $j^2 = -1$. The total variance in the output voltage, $\sigma^2_{V,out}$, which is the mean square value of $e_{n,out}$ can be found from equations such as (5) by applying Parseval's theorem (10).This leads to an integration in the frequency domain and the noise power spectra of the contributions in eqn (5) should be known.However, without performing this task in all detail we can derive in this way that:

$$\sigma^2_{V,out} = c_1 C_{we}^2 \overline{e^2_{n,tot}} + c_2 \overline{i^2_{n,we}} + c_3 \overline{i^2_{n,c}} \quad (6)$$

where c_1 , c_2 and c_3 depend on the spectral characteristics of noises and filters and the upper bars refer to mean (square) values.

It can be seen from eqn (6) that the capacity of the electrochemical double layer of the working electrode,C_{we}, which we shall indicate as "cell capacity" ,is at least partly determining the noise at the detector output.By mounting various electrodes having different values for the cell capacity and measuring the resulting noise at the output,relation (6) can be verified experimentally. The cell capacity can be estimated e.g. by measuring the charging current resulting from a small potential step E' applied via the potentiostat.The capacity is:

$$C_{we} = \frac{1}{E'} \int_0^t i(t)\, dt \quad (7)$$

Our interpretation of the cell capacity obtained in this way is that it resides mainly in the interface between solution and working electrode.It may be partly associated with redox and adsorption desorption phenomena,and its interpretation as the capacity of the double layer may therefore be questioned.However,for the present discussion this is not of great concern provided the cell response

is the same,on the time scale used,as that of a real capacitor of a suitable value (which might be bigger than the capacity of the interface due to the phenomena referred to).The effect on the output noise would be still described by eqns (5) and (6),with insertion of the effective value for C_{we},measured by the experiment indicated.As is reported under Results and Discussion,the current response in this experiment was as fast as could be observable under the experimental conditions.We therefore believe that the modelling of a probably complicated set of phenomena by one capacitor is adequate for our purpose as a first approximation .

From eqn (4),it can be seen that a relationship should exist between the instantaneous values of the noise voltage at the output,$e_{n,out}$, and the potentials of working and reference electrodes. Such relationships can be studied (11) by measuring the auto- and crosscovariance functions between the potentials at the electrode terminals on the one hand and the output signal on the other hand.

The expression for a autocovariance function ϕ_{xx} of a signal x is :

$$\phi_{xx}(\tau) = \lim_{T\to\infty} \frac{1}{T} \int_0^T x(t)\, x(t+\tau)\, dt \qquad (8)$$

in which T is the measuring time and τ is the time delay.For $\tau = 0$ the autocovariance function is equal to the variance (12).

The expression for the crosscovariance function ϕ_{xy} of two signals x and y is:

$$\phi_{xy}(\tau) = \lim_{T\to\infty} \frac{1}{T} \int_0^T x(t)\, y(t+\tau)\, dt \qquad (9)$$

A correlation coefficient,$\rho(\tau)$, can be defined:

$$\rho(\tau) = \phi_{xy} \{ \phi_{xx}(0)\ \phi_{yy}(0) \}^{-\frac{1}{2}} = \phi_{xy} / \sigma_x \sigma_y \qquad (10)$$

For all τ it holds:

$$\rho(\tau) \leq 1 \qquad (11)$$

If the equality applies, $\rho(\tau) = \pm 1$ for some value of τ, both signals x and y are completely correlated;the one is a time shifted

version of the other. If $\rho(\tau) = 0$ for all τ both signals are completely uncorrelated. This means that there is either no relationship at all, or such relation is strongly non-linear. Intermediate values indicate a partial correlation, in combination with other, uncorrelated influences.

EXPERIMENTAL

A coulometric detector (775 LP, Kipp Analytica, Emmen, Holland) and an amperometric detector (LC-4A, Bioanalytical Systems, West Lafayette, Indiana, USA) were used. Both electrochemical cells were operated with the supplied potentiostat and amplifier electronics. The smallest time constants were used, 0.1 and 0.5 seconds for the coulometric and amperometric detector respectively. The design of the cells and the electronic circuits have been described elsewhere (2,13), although some alterations in both systems have been applied since then.

In order to minimize power frequency pick up as much as possible, the systems were built up step by step. After the addition of each successive component, the output signal was examined with an oscilloscope, paying special attention to power frequency, 50 Hz in our case. First the electronics were examined, next the cell was connected, and then the solvent delivery system was connected to the cell. The last step, especially the connection of the metal parts, appeared to be the most important cause of power frequency pick up. Solvent was delivered by a hydrostatic syphoning system consisting of two glass solvent containers, connected via 1/16'' teflon^{R} tubing, 0.5 mm i.d. A stainless steel stopcock, two low dead volume unions positioned directly at the inlet and outlet of the cell and a restrictor, 10 m teflon^{R} tubing, 0.25 mm i.d., connected with a union at the outlet of the cell completed the system.

The solvent delivery system was completely shielded electrically by means of metal tubing and aluminium foil. The cell with the unions and the stopcock were placed under a dewar vessel, serving the dual purpose of faradaic cage and thermal insulation. Sudden fluctuations

in air humidity could also be avoided in this way.All metal shielding parts were connected to a single grounding point at the grounding strip of the power connection.These precautions reduced the 50 Hz component in the output significantly.Additional reduction was obtained by connecting the unions near the cells via a capacitor of 500 μF to ground.This of course can only be applied in the case of potentiostatic operation.

After the system proper had been installed in this way,measuring instruments needed for this work were connected,avoiding ground loops as much as possible and carefully observing the effect of each addition on the signal.Residual power frequency pick up could be eliminated by using passive custom made 5o Hz filters.

For the analysis of signal fluctuations at various points in the system the following instruments were used:
Correlator:Hewlett Packard,model 3721 A,West Lothian,U.K.
Oscilloscopes:Advance Instruments,model OS 1000 and OS 1000A, Hinault,U.K.
Preamplifier:Princeton Applied Research,model 113,Princeton,N.J., USA.
DC Amplifiers:Knick,model A3,Berlin,G.F.R. and Philips,model PM 5170 Eindhoven,Holland.
Recorder:Siemens,model Kompensograph III,Karlsruhe,G.F.R.
Precision voltage source:Knick,model S 16,Berlin,G.F.R.
The time integral of charging currents could be measured with an integrator,Autolab System I,Spectra Physics,Santa Clara,Cal,USA.
Cell impedances were measured with a conductivity bridge,Philips , model RR 9500,Eindhoven,Holland.

Potassium chloride (Suprapure^{R},Merck,Darmstadt,G.F.R.) and glacial acetic acid (Baker Chemicals b.v.,Deventer,Holland) were used to prepare the solvent, 0.1 M in acetic acid and 0.01 M in potassium chloride.The pH was 2.75.The solutions were prepared in double distilled water and filtered through 0.8 μm Millipore^{R} filters before use.

RESULTS AND DISCUSSION

Drift due to environmental influences

During our work we confirmed the observation by Fenn (6) that temperature changes near the cell induce drift.In electrochemical detectors both silver-silver chloride (2,3,6,13,14) and calomel electrodes (6,8,15,16) are used as a reference electrode.The temperature coefficients of their potentials are -1 mV/^{o}C (17) and -0.3 mV/^{o}C (18) respectively.Apart from the direct effect via the working electrode,the reference electrode may therefore also be involved in the temperature sensitivity.With the coulometric detector,we found that air humidity changes also cause drift.We could trace this to conduction between the electrodes at the outside of the cell.The long term stability was improved when the cell was placed underneath the dewar vessel.

Stabilisation drift

Stabilisation drift was observed after applying the potential to the cell and after potential changes.It was already reported by Kissinger et al. that especially for a freshly mounted working electrode the stabilisation process takes several hours (3-5). Accepting a drift of 1 % full scale per minute we found that at a full scale sensitivity of 100 nA for the coulometric detector and of 0.5 nA for the amperometric detector this process took three hours.An electrode which has been in use for some days stabilises faster after switching on the potential and eventually one half hour is sufficient.The procedure of injecting a standard a few times as suggested in the Bioanalytical Systems operations and service manual did not influence the stabilisation time noticeably.This problem has not yet been solved.

Drift due to electrode deactivation

In a previous paper (7) we discussed the decrease of the response of the working electrode after deactivation.This time-dependent be-

haviour also applies to the electrochemical reactions of the background electrolyte which are responsible for the background current. We observed that repeated injection of a deactivating agent or the addition of the latter (7) to the background electrolyte resulted in a continuous decrease of the background current.The electrochemical method for restoring the electrode activity proposed in ref.(7) can partially abate deactivation problems.

Power frequency pick up

With the precautions as described under Experimental power frequency pick up usually was not a problem as long as the signals were displayed on a strip chart recorder.This is in accordance with the strong rejection of mains frequency signals by most recorders of good quality.In a few cases we observed that the amperometric detector was in an overload mode at sensitivities of 5 nA/V or lower,while the absolute value of the background current certainly could not be out of range.In such cases overload was caused by power frequency signals.For the experiments to be described it was essential to reduce these interferences further,because very high total amplification were needed and overload of later stages otherwise would occur.The amplitudes at 5o Hz measured at the output with the precautions described ranged from 1.3×10^{-1} to 10^{-2} nA for the amperometric detector and from 20 to 1.5 nA for the coulometric detector.In some case it was necessary to insert the 50 Hz filters.

Capacity and output noise

The cell capacity was measured as described under Theoretical.Potential steps between 5 and 50 mV were applied after stabilisation at 400 mV.Usually the integrator terminated integration after 2-5 seconds.With the same electrode the peak-to-peak noise was measured from the trace on the recorder.

In fig.2 these values are plotted.The following electrode materials have been used:

Au I and Au II: polished gold electrodes

Pt I and Pt II: polished platinum electrodes

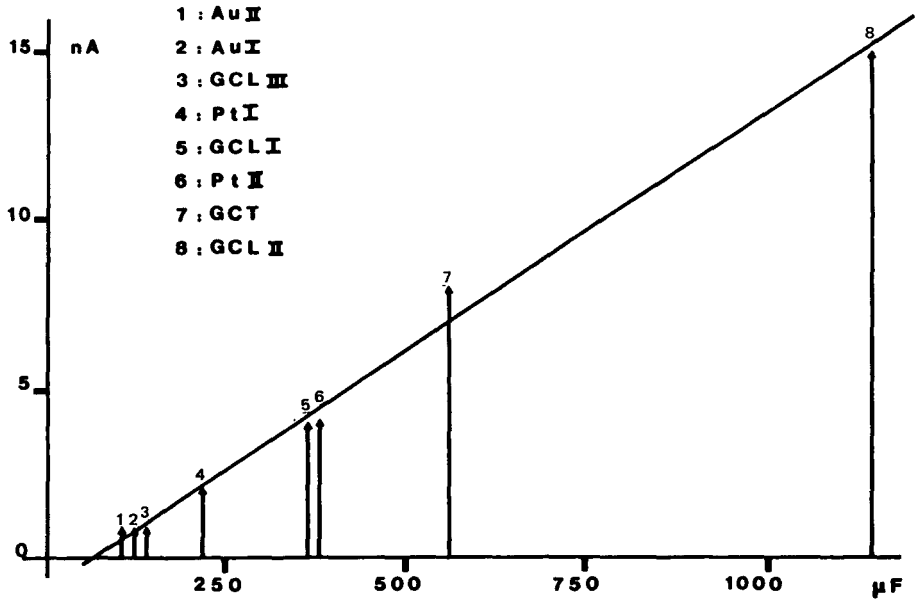

FIGURE 2 Relationship between the peak-to-peak noise and the cell capacity for different electrode materials. Coulometric detector equipment; surface area of the electrodes 3 cm^2.

GCL I and GCL II: polished glassy carbon electrodes, material from Le Carbone Lorraine, grade V 25 (ref.17)

GCT : polished glassy carbon electrode, material from Tokay Man.Co., grade GC 10 (ref.17)

GCL II: scoured glassy carbon electrode, material from Le carbone Lorraine, grade GC 25 (ref.17)

The relationship between the output noise and the capacity appears to be linear. It should be noted that in this experiment the surface areas of the electrodes were the same, equal to 3 cm^2. The differences in capacity are therefore related to differences in geometrical or chemical structures of the surfaces. Therefore we believe that the increase of noise levels observed for the high capacities in fig.2 is intrinsically related to the high capacity, also because a nearly perfect linear relation is observed. Also, an alternative

explanation,assuming that the noise is predominantly of faradaic nature would require to assume that the activity of the electrode or the noise generation in a faradaic process would be proportional to capacity.

As can be seen from fig.2,the rougher surface of the GCL II electrode leads to a considerably higher capacity and noise level,indicating the importance of proper electrode preparation procedures. Microscopically it can be observed that the surface of glassy carbon contains many pores,leading to enlargement of the electrode surface exposed to the liquid.This may explain why this material in general yields higher noise levels than do gold and platinum, which have a smoother surface.Although carbon paste was not included in this study we generally observe smaller noise levels with this material as well.

The relationship between the geometric surface area,cell capacity and noise level was studied also by using spacers of varying slit areas.This yielded the result that these three parameters are in proportion for a given electrode material.Contrary to the experiment of fig.2 this does not allow to distinguish between capacitive and faradaic sources of noise.

Auto- and crosscorrelation measurements

In order to corroborate further the results obtained,auto- and crosscorrelation functions were measured.In our opinion this would give more direct evidence of the contribution of voltage noise via the cell capacity ,because such measurements show the correlation between two parameters in the most direct way.

As the correlator needs relatively high input levels,each voltage to be studied was amplified by two amplifiers in series.The signal was also visualised on an oscilloscope in order to ascertain that random noise was predominant.

For the coulometric detector the results for the autocorrelation functions are presented in fig.3.For $\tau = 0$ the characteristic values are:

σ_V = 1.6 μV for the working electrode connection,

σ_V = 7.0 μV for the auxiliary electrode connection,

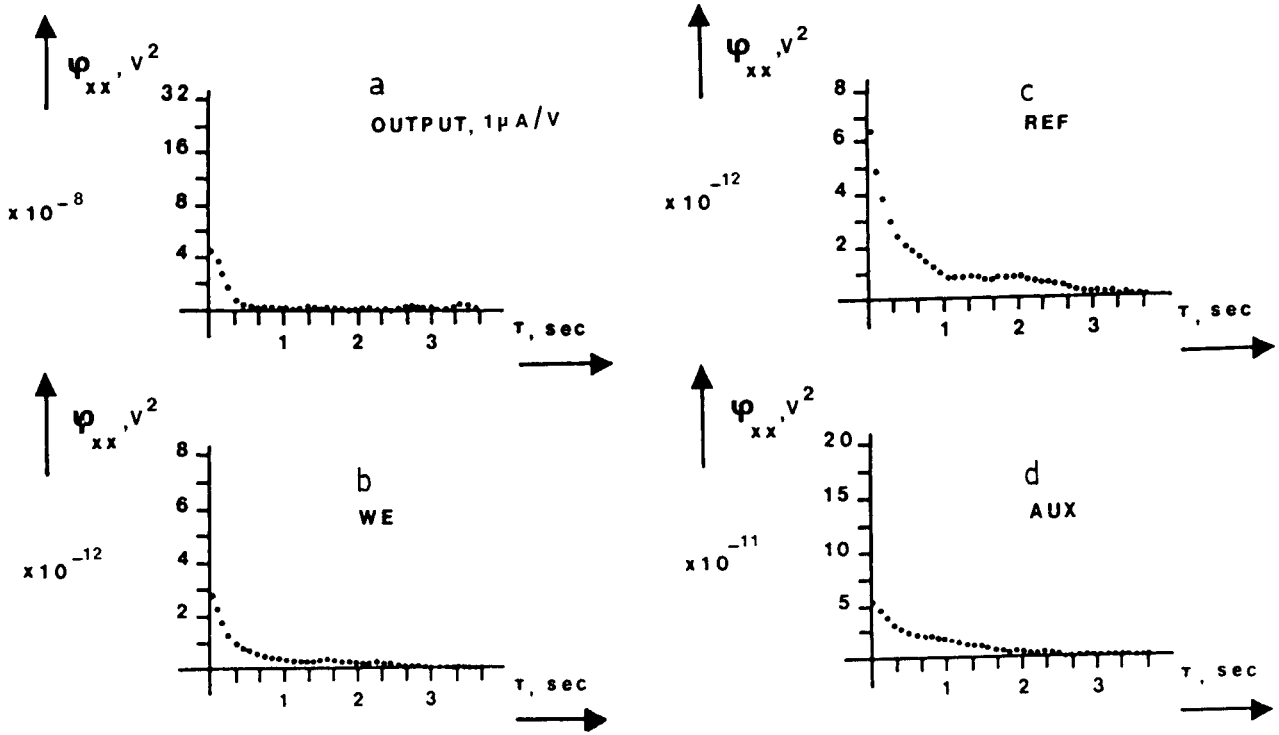

FIGURE 3 a,b,c,d Autocovariance functions measured on various terminals of the coulometric detector: a at the detector output,b at the working electrode,c at the reference electrode and d at the auxiliary electrode.

σ_V = 2.3 μV for the reference electrode connection and

σ_i = 0.2 nA for the detector output.

Note that,contrary to what has been done in eqns(4-6) , the detector output parameter is expressed in current units.This was done in order to avoid confusion due to varying attenuator settings.

The crosscovariance functions of the signals measured at the same connections of the electrodes,with the output of the detector are shown in fig.4.These curves have the shape of a peak,rather than that of the first derivative of a peak,with positive and negative excursions,as would be expected from the derivative operator in eqn (4). However,this operator cancels with integrating operations on the signal in the subsequent parts of the measuring chain,such as the low pass filters in the detector electronics and in the additional amplifiers used in our experiments.In the maximum of the crosscovariance functions we found the following values for ϕ and ρ:

working electrode-output $\phi_{max} = 2\times10^{-16}$ VA ; $\rho_{max} = 0.63$

auxil.electrode - output $\phi_{max} = 1\times10^{-15}$ VA ; $\rho_{max} = 0.07$

refer. electrode -output $\phi_{max} = 2.7\times10^{-16}$ VA; $\rho_{max} = 0.59$

These values indicate that the voltage noise at the electrode connections contributes significantly to the current noise observed at the output.The contribution from the auxiliary electrode appears to be an order of magnitude smaller than that of the other ones,which is not surprising because the circuit point is within a electronic feedback loop.

Similar measurements were carried out with the amperometric detector.With the amplifiers available it was impossible to measure the autocovariance functions at the working and auxiliary electrode connections;the fluctuations were too small compared to the noise of the best amplifier available (PAR 113).For $\tau = 0$ the standard deviations were less than 0.1 μV. The noise of the current amplifier (measurable with disconnected working electrode), $\overline{i^2}_{n,c}$, (see eqn(6)) and that of the potential source, $\overline{e^2}_{app}$, were also small compared with the other signals.From the autocovariance functions measured

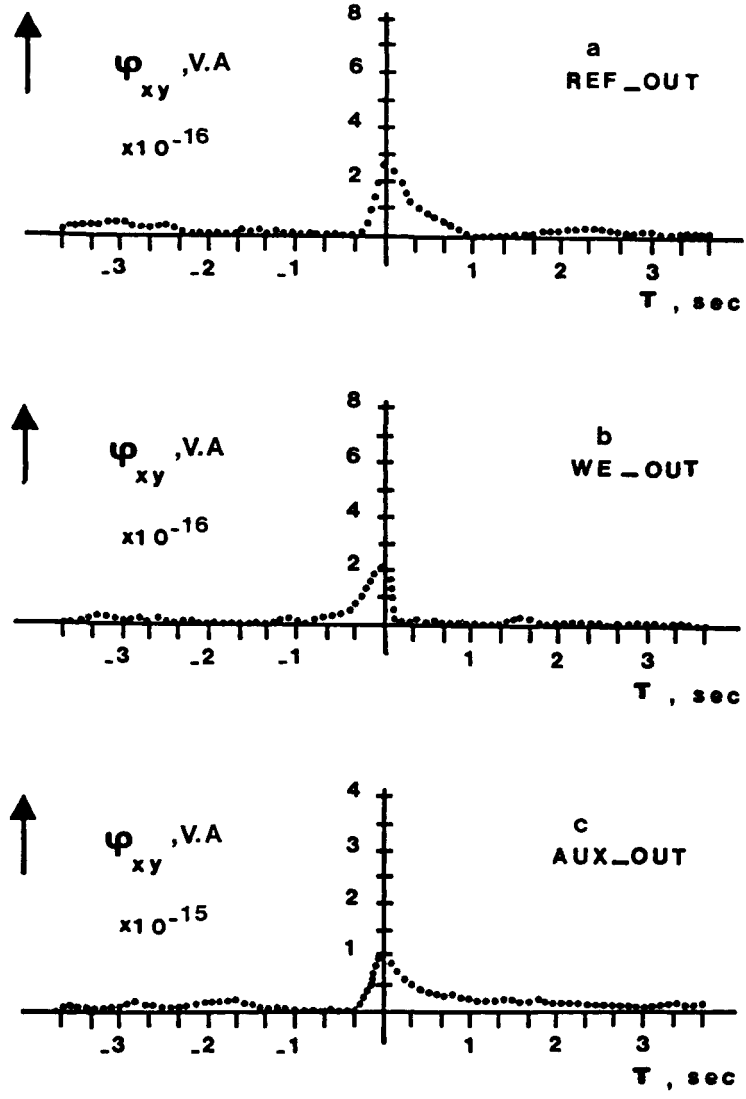

FIGURE 4 a,b,c Crosscovariance functions measured between the detector output of the coulometric detector and the signals present at a the reference electrode,b the working electrode and c the auxiliary electrode.At the right hand side of the curves the detector output signal is delayed.

at the reference electrode connection and the detector output we found, for $\tau = 0$, that $\sigma_V = 9\ \mu V$ and $\sigma_i = 2.2\times10^{-11}$ A respectively. The crosscovariance function of these two signals had a maximum value of 2.3×10^{-16} VA. Therefore the correlation coefficient according to eqn(10), ρ, is close to unity. This indicates that the voltage noise present at the reference electrode connection has a significant effect on the noise in the output signal. A correlation coefficient unity means that the reference elctrode signal is virtually completely responsible for the noise.

According to these results eqn(6) may be considerably simplified for the amperometric detector. The voltage noise factor $\overline{e^2_{n,tot}}$ is virtually equal to the contribution of the reference electrode, $\overline{e^2_{n,ref}}$, because the other contributions were too small to be measured, and the current contributions in eqn(6) can also be neglected; the amplifier noise, $\overline{i^2_{n,c}}$, was measured to be small and the working electrode contribution, $\overline{i^2_{n,we}}$, is probably also small because the nearly complete correlation found in the crosscorrelation experiment. Therefore eqn(6) becomes:

$$\sigma^2_{V,out} = c_1 C^2_{we} \overline{e^2_{n,ref}} \qquad (12)$$

or in current units and taking the square root:

$$\sigma_{i,out} = c_1' C_{we} (\overline{e^2_{n,ref}})^{\frac{1}{2}} = c_1' (\overline{e^2_{n,ref}})^{\frac{1}{2}} C_{we}' A_{el} \qquad (13)$$

$$= \beta A_{el}$$

in which c_1' replaces c_1 when the output is expressed in current units, C_{we}' is the capacity per unit area of the working electrode material under the chosen conditions, A_{el} is the electrode area and β summarizes the proportionality between electrode area and noise and is a constant for a particular combination of electrode material, voltage noise level and filter settings.

Equation (13) is also useful for more complicated cases, such as that of the coulometric detector used in this work, be it that other voltage noise sources may also contribute to β.

Electrical simulation of the cell properties

As an additional check on the validity of the approach taken in this work we wanted to ascertain that a system which accurately conforms to the adopted model for the cell and amplifiers would respond as can be expected on the basis of this model.We therefore simulated the electrical properties of the cell,incorporating the observed values of the cell capacity and the cell resistances in the simulation (19).With this some of the experiments described above were repeated.

The cell resistances were measured on the real cells using a frequency of 1000 Hz on the conductivity bridge.We assumed that at this frequency the cell capacity will not give a significant contribution to the observed impedances.The results are given in table 1. In a simulation these values can be duplicated by means of a network consisting of resistors,for which we took a triangular one. The cell capacity was introduced in the simulation by insertion of a capacitor in series at the working electrode terminal.

We first checked whether the the method for estimation of the cell capacity was correct.The method was performed in the same way as was done with the real cells,with capacitors of 50 and 166 μF. The experiment yielded the right values for these capacities.

The noise at the detector output was also measured as was done before, with the 166 μF capacitor.The value obtained fits nicely into

TABLE 1

Cell Impedances of the Electrochemical Cells,Measured at a Frequency of 1000 Hz

Coulometric Cell		Amperometric Cell	
WE - REF	13 k	WE - REF	300 k
REF- AUX	12 k	REF - AUX	18 k
AUX- WE	4.5 k	AUX - WE	300 k

WE: working electrode; AUX: auxiliary electrode; REF: reference electrode

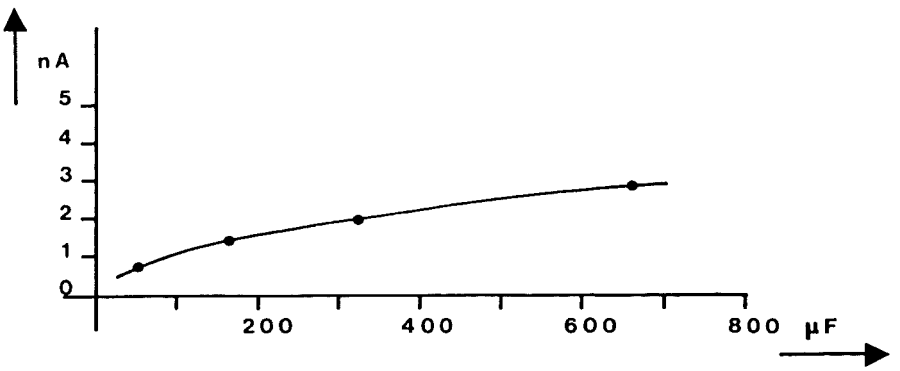

FIGURE 5 Relationship between the peak-to-peak noise at the detector output of the electronical circuit of the coulometric detector when connected to the simulated cell and the value of the capacitor in the simulated cell.

the plot of fig.2 ; i.e. it is in accordance with the value of the noise observed with the real cell having the same cell capacity. Next,additional capacitors were introduced in the simulation network,and the output noise was measured.The results are plotted in fig.5. As can be seen the noise level increases as expected with the capacity.However,the relation between noise and capacity departs slightly from linearity,which indicates that the model described by eqns(12-13) is a bit too crude.Nevertheless we believe that this experiment further corroborates the importance of capacity for the noise level.

CONCLUSION

It is useful to draw some conclusions with respect to the choice of electrode material,electronic equipment and electrode area.This discussion focusses on thin layer cell,but similar arguments apply to other cases,such as the wall jet geometry.

Eqn(13) summarized the proportionality between noise and area.A first approach for obtaining better detection limits of course

would consist in an attempt to decrease the factor β . As this is proportional to the capacity per unit area of the electrode in the carrier solution,careful selection of electrode material,while retaining the activity in electrochemical conversions of analytes, may lead to improvements.In the screening and development of electrode materials more attention should be given to the capacity these materials have per unit area.

The factor β is also proportional to the voltage noise,introduced via the reference electrode or otherwise (the term $\overline{e^2_{n,tot}}$ or $\overline{e^2_{n,ref}}$ in eqns (6) and (13) respectively).A thorough examination of reference electrodes and amplifiers with respect to their contribution to voltage noise appears to be important.

A next approach is of course the optimisation of the signal, while keeping the electrode area as small as possible.The signal can be expressed as:

$$i_s = F_c \, n \, F \, c_i \, Y \qquad (14)$$

where F_c is the flow rate,n is the number of electrons,F is the Faraday,c_i is the concentration of analyte i and Y is the electrochemical conversion yield.

As all factors in eqn(14) can be considered as constants except Y,the expression for Y as a function of cell geometry in the laminar flow region (the case of interest for analytical work) should be considered.The most general expression is given by Lankelma and Poppe (13,20) as:

$$Y = 1 - \exp(-Sh \, D \, A_{el} \, / \, 2 \, F_c \, d \,) \qquad (15)$$

where D is the diffusion coefficient and d is the layer thickness. Sh is the (dimensionless) Sherwood number,which describes the mass transfer.For not too low values of the argument in eqn(15) this is equal to 4.86;for lower values the graphs given by Stephan (20) for infinite Schmidt number can be used.These then give results which are virtually equal to those obtained with the Levêque expression, (21,22) and which involve a proportionality of Y with the length

to the two third power,which is equivalent to $A_{el}^{2/3}$ when the electrode width is constant.

The minimum detectable concentration c_i of the analyte is obtained by division of the eqns (14) and (13).Leaving out the factor $\beta/n\ F$,which is now considered to be constant,and inserting a factor 3 for statistical confidence leads to:

$$c_i \propto 3\ A_{el}/Y\ F_c \qquad (16)$$

For a value of the diffusion coefficient of 10^{-9} $m^2 s^{-1}$ and a flow rate of 1 ml/minute,this expression was calculated.The results are given in fig.6 . At high values of A_{el} ,the coulometric region, the detection limit increases with area.In that range the additional area generates more noise,but adds nothing to the signal because the

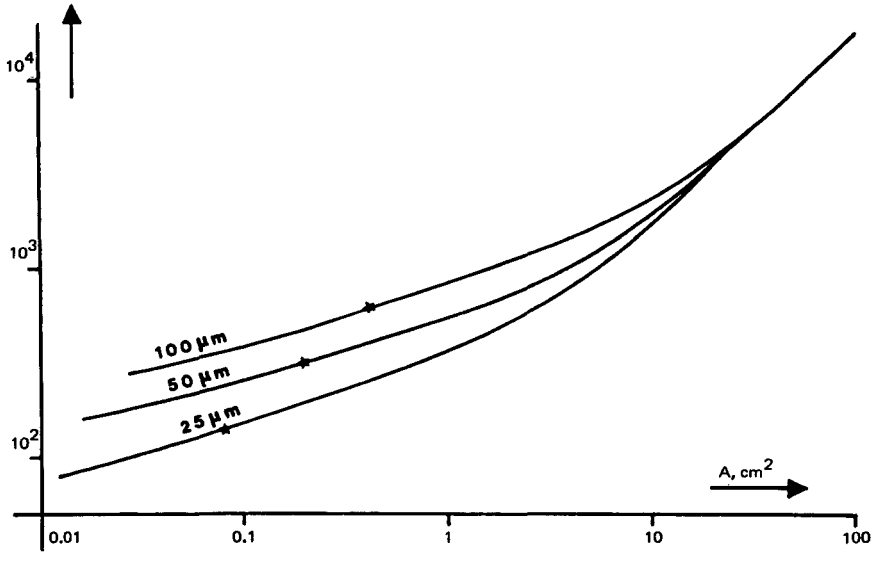

FIGURE 6 The geometry-dependent factor in the expression for the detection limit, $3A_{el}/F_cY$ (eqn(16)) as a function of the area of the electrode for liquid film thicknesses of 25,50 and 100 µm. Electrode width is assumed to be equal to channel width.The parts of the curves at the left hand side of the stars are based on extrapolated Sherwood numbers (ref.20).

solution is already fully depleted.The curves move smoothly into the range where signal is proportional to $A_{el}^{2/3}$ .This is the amperometric region.

It is tempting to look for conditions where Sh is large,as was done by Weber and Purdy (23) and Hanekamp and Nieuwkerk (24) , which occurs for small areas and small film thicknesses.In both papers it was pointed out that a decrease of the area should be accomplished via the electrode length ,not the width.However,drastic changes in A_{el} , and thus of absolute current levels,would be needed for a moderate reduction in $\underline{c_i}$,as the latter decreases with a one third power of A_{el}.We therefore believe such an attempt would not be very succesful.Amplifier current noise soon would predominate.

A more substantial (power 2/3) improvement can be obtained by the use of smaller film thicknesses.,because the absolute value of the current may remain sufficiently large to avoid electronic measurement noise problems.The improvement when going from 100 to 25 μm thickness is illustrated in fig.6.The most important obstacle while going into this direction appears to involve the mechanical problem of avoiding leakages and short-circuiting as a result of machining imperfections and increased pressure build up in the cell.

ACKNOWLEDGEMENT

This work was supported skillfully by Mrs K.Camstra and J.Kuysten who took care of many mechanical and electronic aspects.Mr M.Groeneveld polished the electrodes.Dr.Ir.H.C.Smit is acknowledged for a discussion on the correlation functions.Prof.Dr.G.den Boef was so kind to discuss the manuscript with us.

REFERENCES

1) H.Poppe in J.F.K.Huber (Ed),Instrumentation for H.P.L.C.,Elsevier, Amsterdam,1978.

2) P.T.Kissinger,Anal.Chem.,49 (1977) 447A.

3) P.T.Kissinger,Anal.Chem.,48 (1976) 17R.

4) W.E.van der Linden and J.W.Dieker,Anal.Chim.Acta,119 (1980) 1

5) R.N.Adams,Electrochemistry at Solid Electrodes,M.Dekker,New York, 1969

6) R.Fenn,A Liquid Chromatography Detector Employing Thin Layer Twin Electrode Steady State Amperometry,Thesis,University of Massachusetts,1977

7) H.W.van Rooijen and H.Poppe,Anal.Chim.Acta,130 (1981) 9.

8) K.Brunt and C.H.P.Bruins,J.Chromatog., 16 (1978) 310.

9) D.G.Swartzfager,Anal.Chem., 48 (1969) 2189.

10) R.Deutsch, System Analysis Techniques,Prentice Hall EE Series, Prentice Hall Inc.,Englewood Cliffs.N.J., 1969.

11) R.P.Duursma,H.C.Smit and F.J.M.J.Maessen,Anal.Chim.Acta,133 (1981) 393.

12) G.M.Jenkins and D.G.Watts,Spectral Analysis and its Application, Holden Day,San Francisco,1969.

13) J.Lankelma and H.Poppe,J.Chromatog.,125 (1976) 375.

14) R.E.Shoup and P.T.Kissinger,Chemical Instrumentation,7 (1976) 171.

15) C.L.Blank, J.Chromatog., 117 (1976) 35.

16) R.M.Wightman,E.C.Paik and M.A.Dayton,Anal.Chem., 50 (1978) 1410.

17) G.Milazzo and S.Caroli,Tables of Standard Electrode Potentials, Wiley,New York,1978.

18) D.J.G.Ives and G.J.Janz,Reference Electrodes,Theory and Practice, Academic Press,New York,London,1961.

19) A.J.Bard and L.R.Faulkner,Electrochemical Methods,Fundamentals and Applications,Wiley,New York,1980.

20) K.Stephan,Chemie Ing.Techn. 32 (1960) 401.

21) J.Newman in A.J.Bard (Ed),Electroanalytical Chemistry,Vol.6, Marcel Dekker,New York,1973.

22) E.M.Roosendaal and H.Poppe,to be published.

23) S.G.Weber and W.C.Purdy,Anal.Chim.Acta, 100 (1978) 531.

24) H.B.Hanekamp and H.J.Nieuwkerk,Anal Chim.Acta 121 (1980) 13.

JOURNAL OF LIQUID CHROMATOGRAPHY, 6(12), 2255-2274 (1983)

GRADIENT ELUTION OF BIOGENIC AMINES AND DERIVATIVES IN REVERSED PHASE ION-PAIR PARTITION CHROMATOGRAPHY WITH ELECTROCHEMICAL AND FLUOROMETRIC DETECTION

U.R. TJADEN and J. de JONG

Department of Analytical Chemistry and Pharmaceutical Analysis, Subfaculty of Pharmacy, Gorlaeus Laboratories, University of Leiden, P.O. Box 9502, 2300 RA Leiden, The Netherlands

and C.F.M. van VALKENBURG

Department of Pharmacology, Sylvius Laboratories, University of Leiden, The Netherlands

SUMMARY

The compatibility of gradient elution and reversed phase ion-pair partition systems combined with electrochemical and fluorometric detection has been investigated. The phase system consisting of buffers with perchlorate counter-ions as mobile phases and tri-n-butylphosphate as stationary phase allows the use of pH and counter-ion gradients. It appeared that (i) use of gradients is time saving and favourable with respect to detection limits and (ii) dual electrode detection may offer a solution to the problem of gradient-induced baseline shifting in electrochemical

0148-3919/83/0612-2255$3.50/0

detection. Native fluorometric detection allows the monitoring on nanogram level in gradient runs. The method described is applied to biological samples, i.e. rat brain tissue (striatum).

INTRODUCTION

The determination of biogenic amines, precursors and metabolites with HPLC techniques combined with electrochemical detection has become increasingly important, since the selectivity and the sensitivity of this combination allows the separation and detection of a number of such compounds in the subnanogram level (1-3).The compounds of interest often have diverse characteristics in the now commonly used reversed phase systems. Dependent on the solutes studied, run times may be lengthy, which hampers the application for routine analysis requiring short run times and a high throughput of samples. Besides, high values of the capacity ratios results in unfavourable detection limits, as can be concluded from equation (1).

$$(1) \quad c^{m}_{i,max} = \frac{m_i \sqrt{N_i}}{\sqrt{2\pi}\,(1+k')V_m}$$

where $c^{m}_{i,max}$ is the maximum outlet concentration of compound i, m_i is the injected amount, N_i is the theoretical plate number, k' is the capacity ratio and V_m is the volume of the mobile phase in the column.

There are several ways to speed up analysis. Application of the so-called High Speed systems using smaller particle sizes resulting in highly efficient columns allows the use of shorter columns with smaller void volumes V_m, which in practice is partly counteracted by the commonly increased inner diameters, necessary for a reasonable loading capacity of the column. However, introduction of larger sample volumes is limited, especially in isocratic runs (4,5).

Another way to speed up analysis is to make use of gradients during the chromatographic run. The effect of gradients on the detection limit is twofold: (i) improvement of the

maximum outlet concentration, caused by peak compression during the run, which is favourable and (ii) increase of the baseline shortterm noise and longterm noise (shift), which is unfavourable for the detection limits. Besides, with respect to analysis time one should realize that gradient elution demands a regeneration time for the column, which must be taken into account for the total analysis time.

Increase of the baseline noise is a severe drawback of the use of gradients with electrochemical detection, which is caused by the high sensitivity of electrochemical detectors towards changes in the composition of the mobile phase especially with respect to pH and ionic strength and only to a slight extent (6-8) with respect to the modifier content.For the reasons mentioned above, most workers prefer isocratic conditions for their analyses, especially if trace level analysis is required.However, there are some interesting possibilities to correct for this baseline shift in gradient HPLC: (i) correction by means of the method of background subtraction, which has some drawbacks, since it demands a highly reproducible gradient system and a system to store blank runs, while increasing the effective runtime, because of the need for blank runs, (ii) the use of a dummy system with identical characteristics as the measuring system (9) and (iii) the use of dual detection systems in which the two working electrodes are placed in series towards the flow direction (6).

We studied the applicability of the latter mode of correction. Changes of current occurring during the chromatographic runs can be caused by several processes :

$$(2)\quad \Delta i_{tot} = \Delta i_{f,analyte} + \Delta i_{c+f,grad}$$

with i_{tot} is the total current, $i_{f,analyte}$ is the faradaic component caused by the analyte and $i_{c+f,grad}$ is the component caused by the gradient, which component can include both faradaic and charging currents. The problem is to distinguish between $i_{f,analyte}$ and $i_{c+f,grad}$. This can be achieved by applying the same potential to both working

electrodes (6,10) and subtracting the signal of the downstream detector from the signal of the upstream detector. In this way the downstream electrode or so-called shift-detector, is used to follow changes in the mobile phase.

Two types of electrochemical detectors can be taken into account, viz. the coulometric and amperometric detectors. Supposing that Δi_{grad} is only caused by charging current and that both cells have similar electrochemical characteristics, this contribution to the total current i_{tot} is the same for the upstream and downstream detector, and the differential signal is therefore corrected for gradient effects. In practice Δi_{grad} also includes a faradaic current resulting in only a partial correction for dual coulometric cells but in principle complete correction for amperometric types (6,8). However, in dual coulometric detection systems $i_{f,analyte}$ at the downstream detector is negligible and so in the differential signal information concerning the analyte is not attenuated.

It is also possible to apply different potentials to the working electrodes whereby the shift detector has a potential lower than the half-wave potential of the compounds of interest assuming that the shift characteristics are similar at different potentials.

EXPERIMENTAL

Apparatus

The liquid chromatograph consisted of a high-pressure gradient system (SP 3500B, Spectra Physics, Santa Clara, CA, U.S.A.) equipped with thermostatted eluent reservoirs, a thermostatted stainless steel column (100 x 3 mm I.D.) and different detection systems. The amperometric detection system consisted of a so-called wall-jet detector cell-unit (E.D.T., London, U.K.) coupled with a potentiostat (E-230, Bruker, Karlsruhe, G.F.R.). The detector cell was modified

by replacement of the Ag/AgCl reference electrode by a home-made saturated calomel electrode. The (dual) coulometric detection system including a guard cell, placed between the dynamic mixer of the gradient system and the injector, consisted of a dual detector cell-unit coupled with a dual potentiostat (Coulochem, Model 5100A, ESA, Bedford, MA, U.S.A.). The fluorometric detector was a double monochromator type with 150 Watt Xe-source (SFM 23 LC, Kontron, Zurich, Switzerland). Chromatograms were registered with flat-bed recorders (BD-8, Kipp & Zn., Delft, The Netherlands).

Chemicals and Materials

The compounds used as chromatographic reference substances are listed in Table I. All other chemicals and solvents were of analytical or reagent grade and were used without further purification except for water which was purified by a Milli-Q Water Purification System (Millipore, Bedford, MA, U.S.A.). The chromatographic support material was Nucleosil C-8, 5 µm (Macherey-Nagel, Duren, G.F.R.). Columns were packed by means of a slurry technique described elsewhere (11).

The constituents of the mobile phase were saturated with tri-n-butylphosphate (Aldrich, Milwaukee, WI, U.S.A.) before use.

Columns were loaded with tri-n-butylphosphate (TBP) in situ as described elsewhere (4,5). Thus a liquid-liquid reversed phase system was built up with TBP saturated buffers as mobile phases and TBP as stationary phase.

Chromatography

The capacity ratio k' was determined from its retention time t_{Ri} and the retention time of an unretained compound t_{RO}, for which potassium iodide was used.

TABLE I STRUCTURAL TYPES OF INTEREST

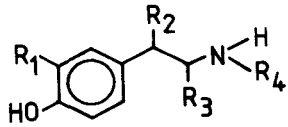

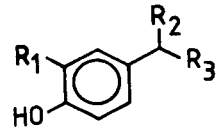

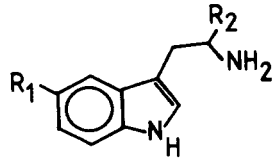

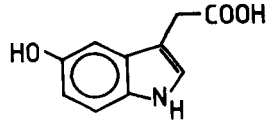

THEORETICAL

The compounds of interest can be divided in amines, acids, amino acids and neutral compounds (see Table I). Each group has its own distribution characteristics between the two liquid phases. Taking into account a possible ion-pair dissociation in the organic phase (S), the distribution of a protonated amine (BH^+) with perchlorate (X^-) as counter-ion can be described as follows (4,5) :

$$(3) \quad BH^+_{aq} + X^-_{aq} + n\ S_{org} \overset{K_{ex}}{\rightleftharpoons} BHXS_{n,org}$$

$$(4)\quad BHXS_{n,org} \rightleftharpoons^{K_{diss}} BHS^{+}_{n,org} + X^{-}_{org}$$

From these equations an expression can be derived describing the distribution of amines :

$$(5)\quad D_{amine} = K_{ex} \cdot [X^{-}]_{aq} \cdot [S]^{n}_{org} \left(1 + \frac{K_{diss}}{[X^{-}]_{org}} \right)$$

Equation (6) gives the distribution for un acid HA :

$$(6)\quad D_{acid} = \frac{K_{HA}}{1 + \frac{K_a}{[H^+]}}$$

where K_{HA} is the partition coefficient of the undissociated acid and K_a the acid dissociation constant. Combining equations (5) and (6) an expression for the distribution of an amino acid ion-pair can be derived :

$$(7)\quad D_{amino\ acid} = K_{ex}[X^{-}][S]^{n}_{org}\left(1 + \frac{K_{diss}}{[X^{-}]_{org}}\right)\left(1 + \frac{K_a}{[H^{+}]}\right)^{-1}$$

where K is the acid dissociation constant of the carboxylic group of the amino acid.

From equations (5), (6) and (7) it can be concluded that, depending on the physico-chemical properties, the capacity ratios can be influenced by the counter-ion concentration and/or the pH of the mobile phase. The retention of neutral compounds can be influenced only by adding an organic modifier to the mobile phase.

RESULTS AND DISCUSSION

Chromatography

In figure 1 a typical chromatogram of a test mixture of the 13 reference substances under isocratic conditions is given. Although the compounds are well separated, it will be clear that this type of chromatography is rather time-consuming and that for the more retained compounds the dilution during the chromatographic process is considerable. The analysis time can be shortened by increasing the flow-rate. However,

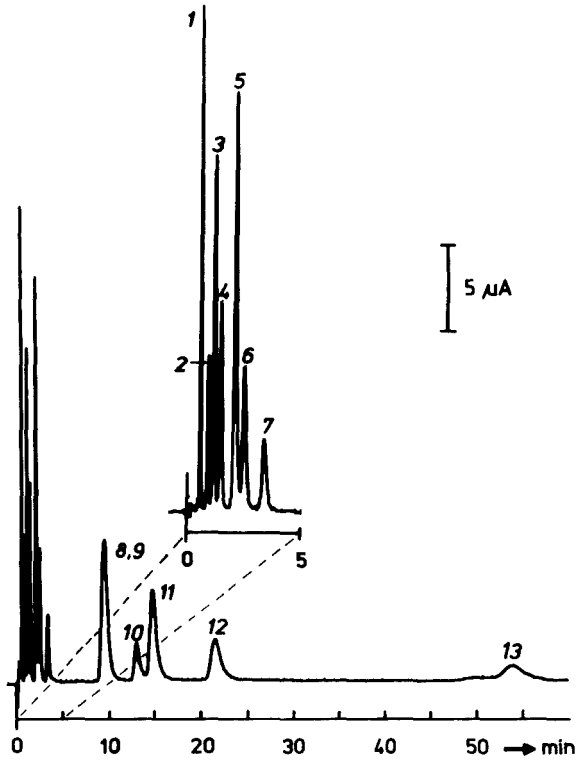

Fig. 1. Separation of the test mixture under isocratic conditions. Perchlorate concentration 0.2 m, pH 2.15, temperature 300 K, coulometric detection +700 mV.
Compounds: 1. MOPEG; 2. A; 3. NA; 4. DOPA; 5. VMA; 6. DA; 7. TYR; 8. 5-HTP; 9. HVA; 10. DOPAC; 11. 5-HT; 12.TRP; 13. 5-HIAA.
Injected amounts: 150 - 520 pmole, except for 5-HIAA: 1270 pmole.

because of pressure limitations, this can only be done to a certain extent and even leads to less favourable detection limits (see eq.(1)).

Application of gradients is a better way to solve this problem, although a regeneration time for the column is necessary. In principle there are three basic parameters to influence the retention, i.e. the pH, the counter-ion

concentration and the modifier content of the mobile phase (12,13). Obviously the use of modifier gradients can give raise to stability problems because the stationary phase can be stripped off. Therefore, we studied only the pH and counter-ion gradients.

In order to get insight into the retention behaviour of the compounds under gradient conditions and to optimize the gradient, the influence of the counter-ion concentration and the pH of the mobile phase was investigated separately.

In figure 2 the dependence of the capacity ratios on the pH is given. According to equations (6) and (7) the slope of the log k' vs. pH plot amounts to about -1 for pH values above the pK value of the acids and amino acids.

In figure 3a,b the relation between the capacity ratios and the perchlorate concentration in the mobile phase is given for pH 2.25 and 6.00. As can be derived from equations (5) and (7) the capacity ratios of the amines and the amino acids should be proportional to the counter-ion concentration, which is confirmed by the experimental data. It should be noted thar for amines the same value for the capacity ratio is expected for the same counter-ion concentration at both pH 2.25 and 6.00. However, as is demonstrated by the plots in figure 3, the capacity ratios of the amines slightly increase with raising pH of the mobile phase, a phenomenon that has been observed before (4,5). This indicates that the net effect of decreasing the perchlorate concentration is less than expected, if the pH is raised simultaneously during the gradient. The dashed lines represent the linear interpolation between the initial and final conditions of the optimal gradient used in our experiments. From the slope of these lines it can be concluded that the pH is more effective than the counter-ion gradient. In figure 4, which shows the chromatogram of a 9 minutes linear gradient, this effect declares itself obviously (see peaks 12 and 13). Notice that the concentration of 5-HIAA (peak 12) in the test mixture for the gradient is decreased three-fold with respect to the mixture used in the isocratic run. The time, needed for

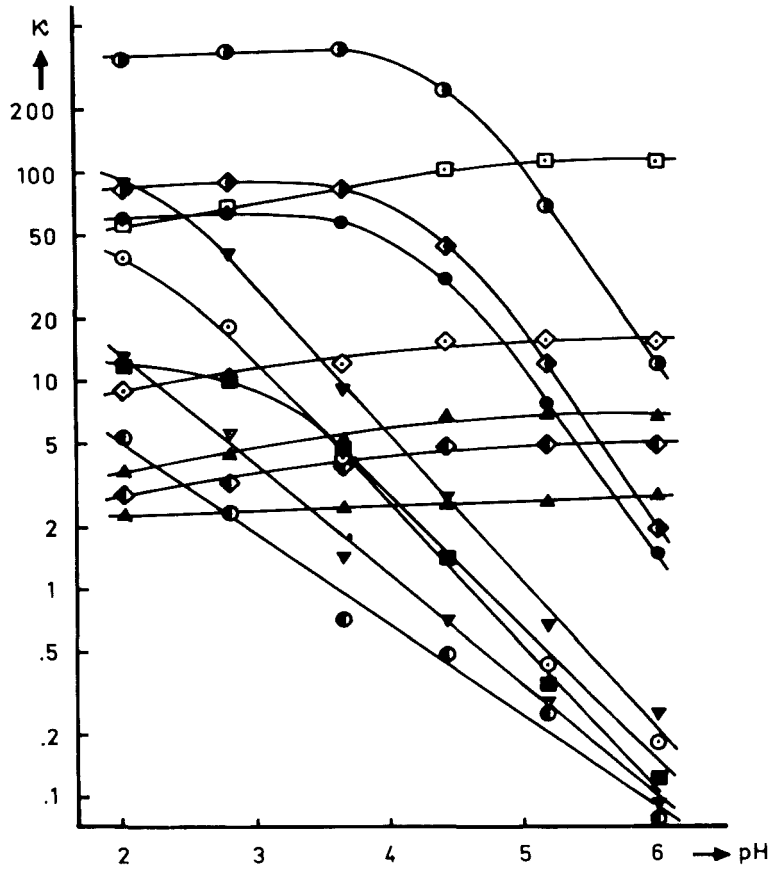

Fig. 2. Influence of the pH of the mobile phase on the capacity ratios.
Perchlorate concentration: 0.10 M, temperature 298 K.
Compounds: ⊡ 5-HT; ◇ DA; ◑ 5-HIAA; △ NA; ◆ A; △ MOPEG; ◆ DOPAC; ● HVA; ▼ TRP; ⊙ 5-HTP; ■ VMA; ▽ TYR; ◐ DOPA.

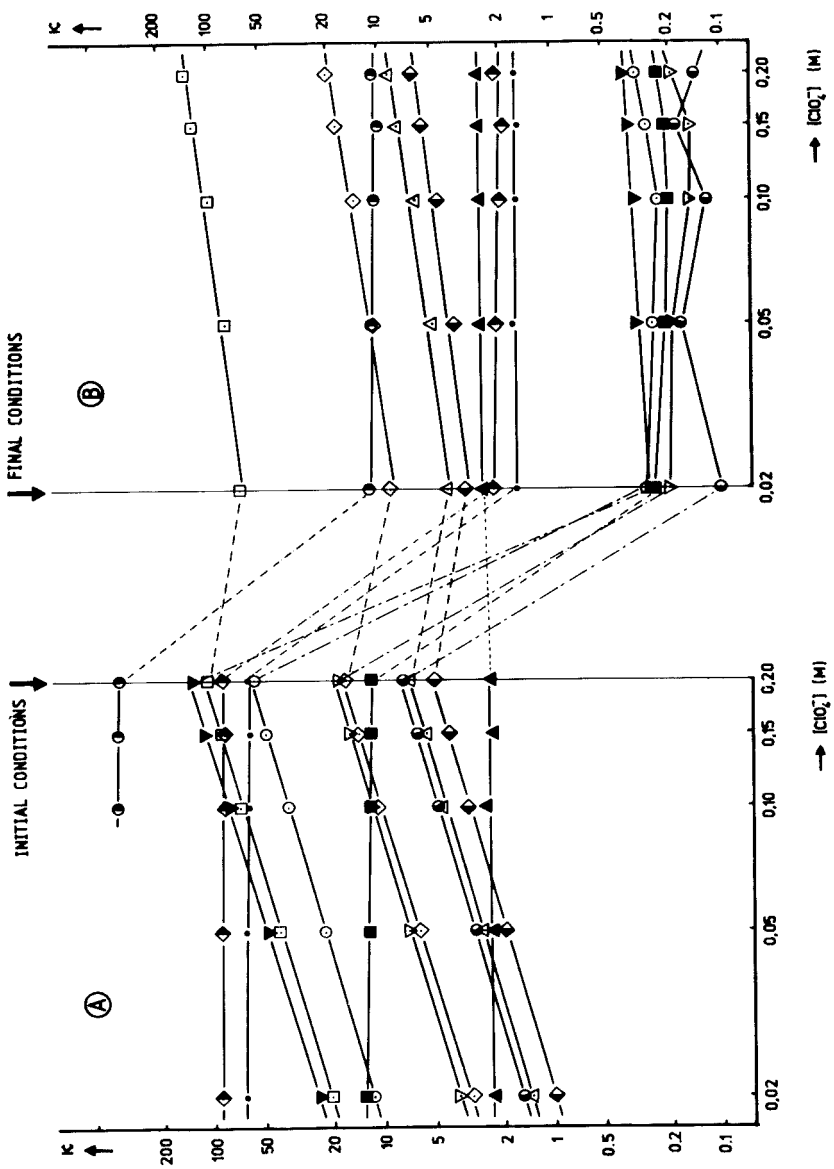

Fig. 3. Influence of the perchlorate concentration in the mobile phase on the capacity ratios at pH 2.25 (A) and pH 6.00 (B). Temperature 298 K, compounds: see Fig. 2.

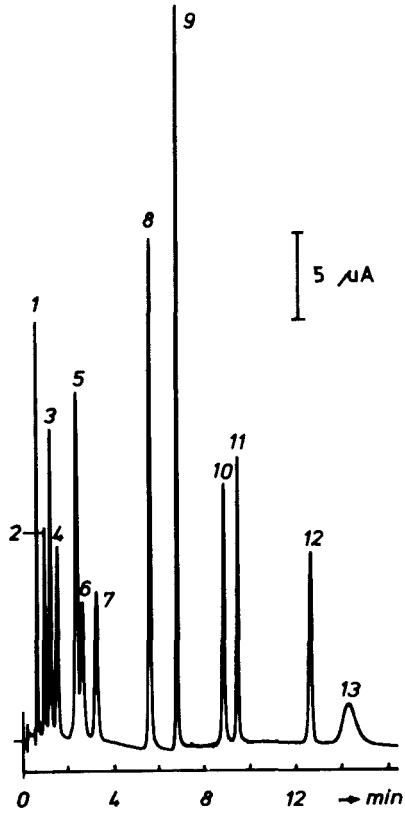

Fig. 4. Gradient elution of the test mixture. Eluent A: perchlorate 0.20 M, pH 2.15. Eluent B: perchlorate 0.02 M, pH 6.00.
Gradient: 9 minutes linear from 0 to 99% B. Temperature 300 K, flow-rate 1.5 ml/min. Coulometric detection +700 mV.
Compounds: 1 - 8 as in Fig. 1; 9. TRP; 10. HVA; 11. DOPAC; 12. 5-HIAA; 13. 5-HT. Injected amounts: 180 - 520 pmole per compound.

re-equilibration, the so-called regeneration time, appeared to be less than 5 minutes resulting in a total analysis time of about 20 minutes.

Influence of the gradient on the detection system

Electrochemical detectors are very sensitive towards changes in the composition of the mobile phase. This effect is clearly demonstrated in figure 5, which shows the chromatogram of a test mixture of the 13 compounds of interest under gradient conditions. Detection was performed by means of an amperometric detection system. It is obvious that the full scale deflection (i.e. 50 nA) can hardly be increased, due to the baseline shift during the run. It is observed that use of a new or recently polished working

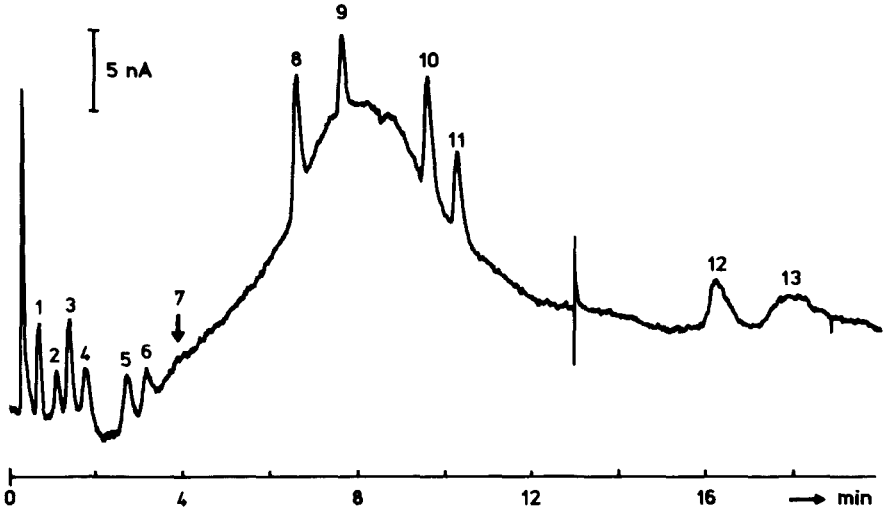

Fig. 5. Amperometric detection of the test mixture after gradient elution.
Applied potential +800 mV vs. SCE, time constant 1 s, flow-rate 1.3 ml/min., temperature 300 K. Compounds: see Fig. 4. Injected amounts: 7.2 - 20.7 pmole per compound. Gradient: see Fig. 4.

electrode resulted in a less prominent shift. However, as a function of time the shift increased.

Next to electrochemical activity the compounds of this study have a native fluorescence, which can be used for detection on subnanogram level (14). Due to the small difference between the excitation and emission wavelength (248 and 318 nm respectively) one should apply a double monochromator system. In figure 6 the chromatogram of the same test mixture with fluorometric detection is given. This kind of

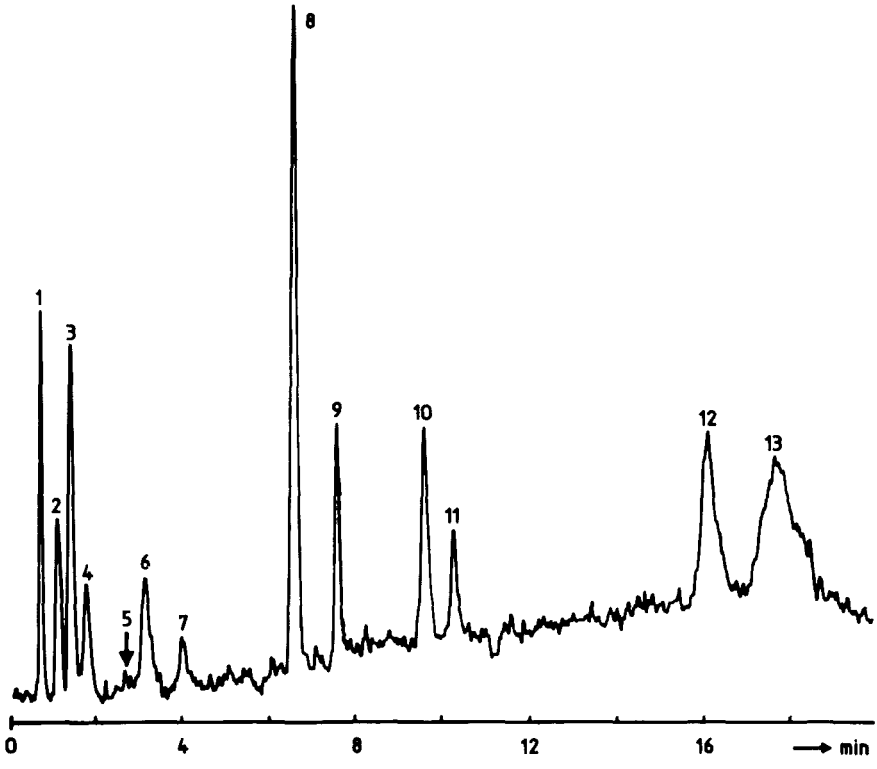

Fig. 6. Fluorometric detection of the test mixture after gradient elution. Excitation wavelength 284 nm, emission wavelength 318 nm.
Conditions: see Fig. 4. Injected amounts: 7.2 - 20.7 pmole per compound.

detection appears to be less sensitive towards changes in the mobile phase. Besides, the sensitivity for TRP and derivatives is more favourable than with electrochemical detection, which corresponds with data from literature (14). Nevertheless, with fluorometric detection it is not possible to detect all the compounds at lower levels without derivatization (e.g. see VMA). Therefore, we studied the possibilities of a dual electrochemical detector to overcome the gradient induced shift problem.

Figure 7 shows the principle of baseline detection with dual coulometric detection. From trace B (downstream detector) it can be seen that at +700 mV most compounds are converted coulometrically in the upstream detector (trace A). However, the shape of the gradient induced baseline shift is more or less the same for both detectors, which slightly indicates that $\Delta i_{gradient}$ (see eqn. 2) is mainly caused by charging current contributions ($\Delta i_{c,gradient}$), or alternatively that as far as faradaic contributions ($\Delta i_{f,gradient}$) are involved the upstream detector does not work coulometrically. A further indication that $\Delta i_{f,gradient}$ is negligible relative to $\Delta i_{c,gradient}$ comes from the fact that although traces A and B (Fig. 7) have the same shape, the absolute differences are more pronounced for the downstream detector and therefore before subtraction its signal is reduced to 60%. The difference in sensitivity of both cells are caused by differences in activity. It was observed that the yield of conversion for a number of compounds amounts to more than 100% (e.g. MOPEG 260%), which explains the differences in activity for both cells. The peak in trace B which coincides with adrenaline (peak 2) is caused by injection. The differential signal is also corrected for this phenomenon.

The results as shown in figure 7 demonstrate the possibilities of baseline correction by means of the downstream shift detector. However, subtraction leads to an increase of noise (see Fig. 7c) and consequently in the flat parts of trace A subtraction does not improve detectability. It should be emphasized that until now no attempts were made to reduce the noise of the differential signal, which should

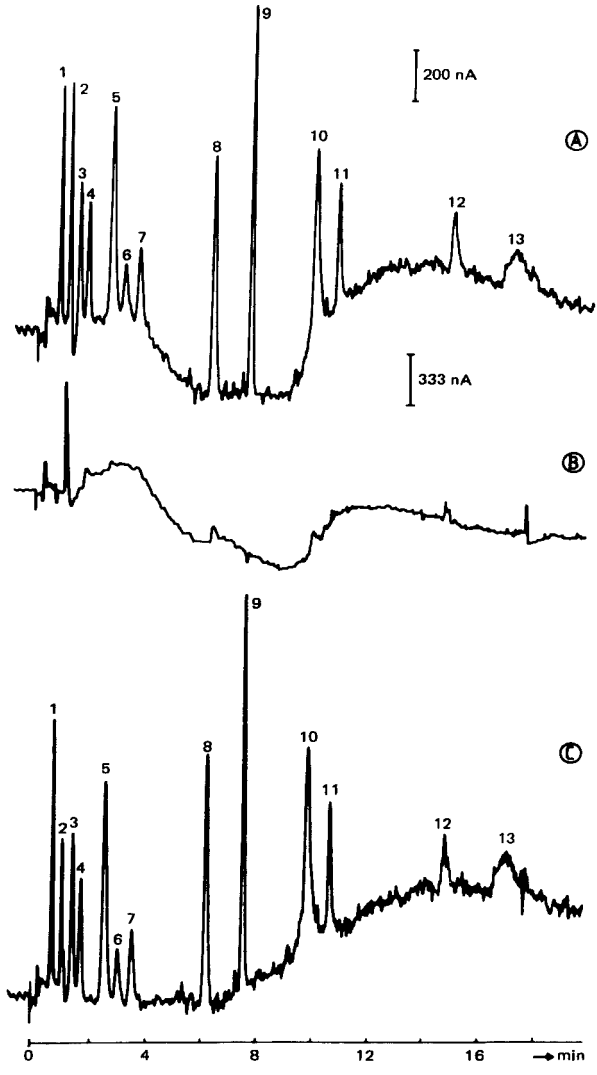

Fig. 7a,b,c Dual coulometric detection of the test mixture after gradient elution. Applied potentials: 700/700 mV. Conditions: see Fig. 4. Injected amounts: 7.2 - 20.7 pmole per compound.
(A) Signal of the upstream detector (2 μA FS)
(B) signal of the downstream detector (3.33 μA FS)
(c) Differential signal (see text).

be possible, for example by means of "time-delayed subtraction".

The power of the dual coulometric detection system is more clearly shown in figure 8, which shows the chromatogram of a homogenate of rat brain tissue. The sample is pretreated as described elsewhere (15). The quantitative results are summarized in Table II.

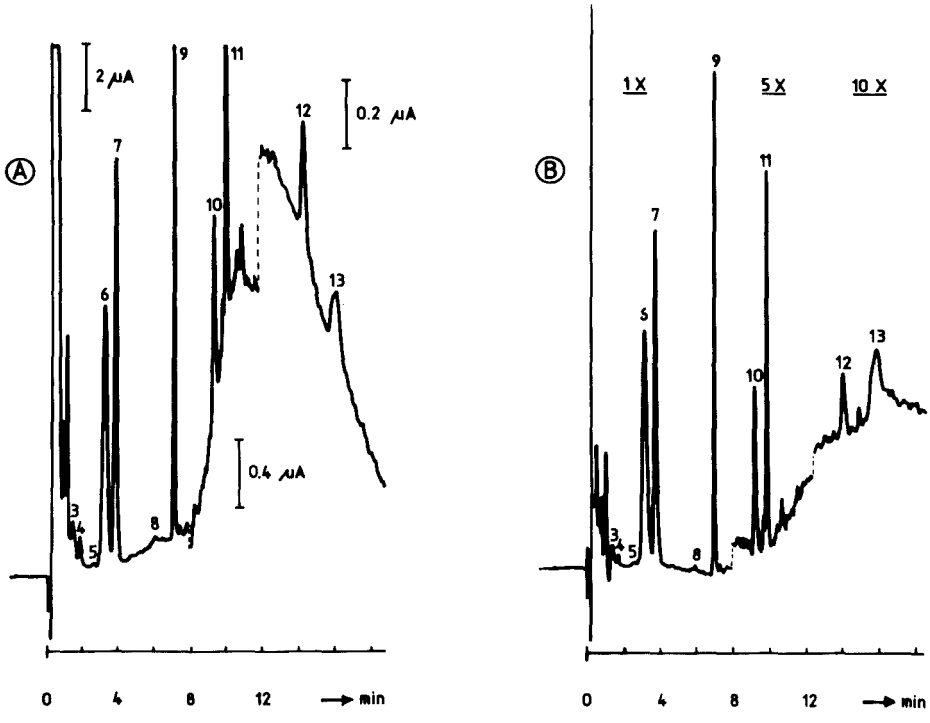

Fig. 8a,b . Analysis of a rat striatum homogenate. Dual coulometric detection: 800/800 mV. Conditions: see Fig. 4, except for flow rate: 1.4 ml/min.
(A) Signal of the upstream detector
(B) Differential signal (see text)
Injection volume: 100 l corresponding to 4 mg striatal tissue.

TABLE II

Compound	amount injected (pmole)	tissue content (ng/g)
MOPEG	n.d.[1]	n.d.[1]
A	n.d.[1]	n.d.[1]
NA	15.3	650
DOPA	11.4	560
VMA	4.5	220
DA	514	19670
TYR	484	21950
5-HTP	1.9	100
TRP	171	8720
HVA	34.6	1575
DOPAC	124	5190
5-HIAA	15.2	724
5-HT	17.2	750

[1] not detectable

CONCLUSIONS

Compared to isocratic chromatography the advantage of gradient elution of biogenic amines and their main precursors and metabolites is two-fold: speeding up analysis and lowering detection limits of especially the more retained compounds.

Fluorometric detection is relatively insensitive towards changes of the pH and the ionic strength of the mobile phase and offers detection limits comparable with electrochemical detection.

Electrochemical detectors are rather sensitive towards changes in the mobile phase. Applying the differential coulometric detection principle the gradient induced baseline shift is reduced and consequently the quantification of a number of compounds is facilitated, although noise levels are slightly increased.
Future research will be devoted to noise investigations in order to minimize detection limits.

ACKNOWLEDGEMENTS

The authors wish to thank Kipp & Zn., Delft, The Netherlands, for the loan of the coulometric detection system, and Kontron Nederland, Maarssen, The Netherlands for the loan of the fluorometric detector.
The discussions with Dr. W.P. van Bennekom and Drs. J.C. Hoogvliet were highly appreciated.

REFERENCES

1. P.T. Kissinger, C.S. Bruntlett and R.E.Shoup, Life Sci. 28(1981)455
2. A.M. Krstulovic, J. Chromatogr. 229(1982)1
3. I.N. Mefford, J. Neurosci. Methods 3(1981)207
4. H.J.L. Janssen, Ph.D. Thesis, University of Leiden (1981)
5. H.J.L. Janssen, U.R. Tjaden, H.J. de Jong and K.-G. Wahlund, J. Chromatogr. 202(1980)223
6. R.E. Shoup, Abstract No. 15, Symposium on LCEC and Voltammetry, Indianapolis, IN, U.S.A., May 1982
7. D.A. Roston, R.E. Shoup and P.T. Kissinger, Anal. Chem. 54(1982)1417A
8. R.E. Shoup, personal communication
9. K Brunt and C.H.P. Bruins, J. Chromatogr. 172(1979)87
10. J.C. Hoogvliet and W.P. van Bennekom, in preparation

11. U.R. Tjaden, M.T.H.A. Meeles, C.P. Thys, J. Chromatogr. 181(1980)227

12. K.-G. Wahlund and B. Edlen, J. Liq. Chromatogr. 4(1981)309

13. J. de Jong, U.R. Tjaden, W. van 't Hoff and C.F.M. van Valkenburg, submitted for publication

14. G.M. Anderson and J,G, Young, Life Sci. 28(1981)507

15. C.F.M. van Valkenburg, U.R. Tjaden, J. van der Krogt and B. van der Leden, J. Neurochem. 39(1982)990

JOURNAL OF LIQUID CHROMATOGRAPHY, 6(12), 2275-2310 (1983)

USE OF A DUAL COULOMETRIC-AMPEROMETRIC DETECTION CELL APPROACH IN THYROID HORMONE ASSAY

Bradford R. Hepler and William C. Purdy

Department of Chemistry
McGill University
801 Sherbrooke Street West
Montreal, Quebec, Canada H3A 2K6

ABSTRACT

The development and application of a dual (in series) coulometric-amperometric thin-layer electrochemical detection cell system to the assay of thyroid hormones following reversed-phase chromatography is described. Using this approach the system was characterized by empirically determined electrolysis efficiencies, demonstrating adherence to the diffusion-layer approximation theory. When academic mixtures of the thyroid hormones were studied, the precision of both response and relative retention data was to within 4%. With the dual-cell approach, improvements by a factor of two in the limit of detection were noted over the same system using only amperometric detection. The electrochemical behavior of these analytes in the dual-cell system was also studied. These latter experiments demonstrated that, in principle, it is possible to assay the thyroid hormones with both cells set at a potential where mass transport control obtains, analyzing the oxidation products of the first cell at the amperometric cell.

INTRODUCTION

The use of two electrodes in series, or two thin-layer electrochemical (TLED) cells in sequence has previously been

 0148-3919/83/0612-2275$3.50/0

applied in several areas. Gerischer and coworkers (1) first introduced and discussed the arrangement of two closely spaced electrodes in a configuration where laminar flow obtained. The first electrode served as a "generator" electrode and the latter as the detection or "collector" electrode. This type of configuration would have similar advantages to that of the ring-disc system (2) for applications to electrode-kinetic studies, and in spite of theoretical rigor from several groups (3-5), the ring-disc system remains the more popular application.

In 1976 Blank (6) noted that with closely spaced channel electrodes placed in series within one cell body, it was possible to conveniently monitor a chromatographic effluent at two separate potentials. Using this approach, if coelution of electroactive components occurred, it was possible to determine the presence or absence of a given component by independently evaluating peak responses as a function of applied potential. More recently, studies involving dual channel electrodes in series have been carried out by several groups (7-12). Increased selectivity (7,10,12), on-line blank correction (8,9), electrochemical analysis of electrolysis products (10,12), removal of oxygen interferences (10,11) and increased sensitivity (10,12) have both suggested and further demonstrated the potential utility of this configuration in application to specific problems.

Other examples of the application of dual electrode systems of varying geometry and configuration have appeared in the literature. Both Fenn et al. (13) and Weber (14,15) have demonstrated the use of parallel opposed electrodes in a TLED cell configuration for purposes of improved detection limits, while Roston and Kissinger (16) have utilized this approach to evaluate phenolic constituents in commercial beverages. Schieffer (17) has demonstrated the use of a minimum volume packed bed coulometric detection cell placed on-line in front of an amperometric TLED cell for purposes of improving selectivity in this latter cell. Most recently Matson and co-workers (18) utilized two porous graphite coulometric electrodes in series to detect electroactive components at two different potentials, improving both qualitative and quantitative data and providing the ability to screen out unwanted signals from specific chromatographic systems.

In the current work on the thyroid hormones, discrimination against electroactive background was felt to be desirable in order to improve detection limits. In this approach, as opposed to the single-cell method previously reported (19), two cells were connected in series following the chromatographic column. The first served as a "scavenger" cell to remove electroactive background unimportant to the analysis, while the second cell was an amperometric cell the purpose of which was to detect and

assay the analytes of interest. The more efficient the first cell (i.e., approaching coulometric yields) the better the clean-up. Using low temperature isotropic carbon, LTIC (20), as a working electrode material in a thin-layer "sandwich cell" (21) geometry, it was hoped to accomplish this goal with a minimum of cell volume.

Applying the above approach to the assay of the thyroid hormones it was possible to characterize the dual-cell system through empirically determined electrolysis efficiencies. These data were, in turn, utilized to document the adherence of these cell types to the diffusion-layer approximation theory (15,22). Improvements in the limit of detection of the thyroid hormones in a dual-cell system were demonstrated and the electrochemical behavior of these analytes studied.

EXPERIMENTAL

Apparatus

The liquid chromatographic system used in this work was the same as that previously described (19). Detection was carried out with (i) a Waters Model 440 absorbance detector at 254 nm connected in series with a laboratory designed TLED cell, (ii) a single TLED cell following the chromatographic column or (iii) two TLED cells in series. The PAR 174A Polarographic Analyzer previously noted (19) and/or a Bioanalytical Systems Inc. Model DCV-4 voltammetry control unit were used as potentiostats in the

amperometric work. Heath-Schlumberger Model SR-204 strip-chart recorders were employed to record chromatograms at chart speeds of 0.1 in. min^{-1}. Electrode resistance measurements were made with a Fluke Model 8030A multimeter. An Orion Model 701A pH meter was used for pH measurements.

Construction of LTIC Cells

1. Amperometric cell: external TLED cell geometry - The cell design used in this work is the same as that previously described (19).

2. Coulometric cell - The coulometric cell designed for use in this work is shown in Figure 1. The design follows the precedent set in previous designs by employing the hemi-cylindrical-yoke approach (19). The difference in this cell lies with the replacement of the platinum and/or silver-hoop electrode imbedded in the upper Kel-F half by a second LTIC plate electrode, M. Two holes, 0.1 cm in size, were drilled approximately 2.0 cm apart centrally in this plate using a diamond-tipped drill bit. The location of the two holes was such that when the plate was overlaid on the upper cell half, they were aligned with the entry, C, and the exit, L, ports previously drilled through the cell block (Figure 1). This plate was fixed in place using EPD-TEK 353 ND epoxy (Epoxy Technology Inc., Billerica, MA 01821). Contact to this second plate was made by means of the banana plug-stainless steel

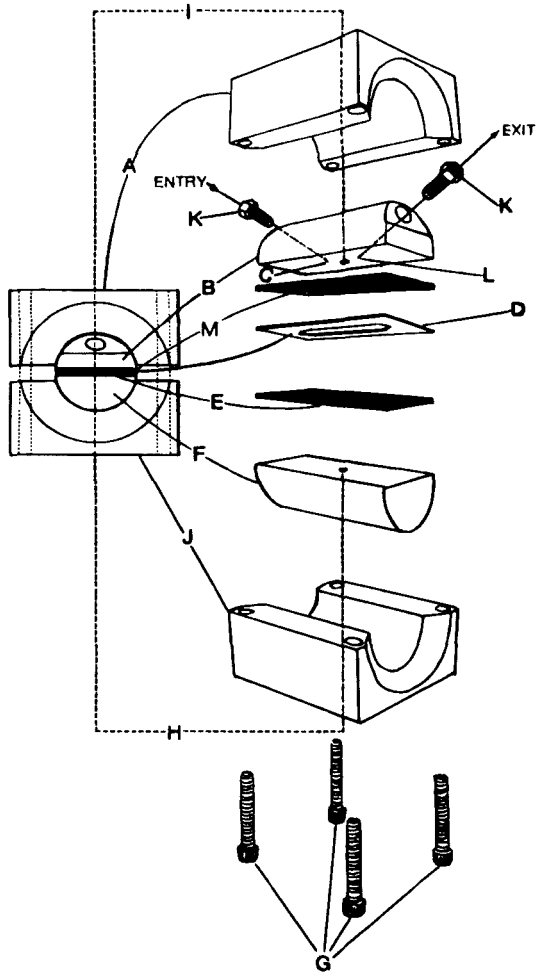

FIGURE 1. Hemicylindrical coulometric TLED cell, end view at left, exploded view at right, (A) and (J) upper and lower yokes machined from polyvinyl chloride for holding together hemicylindrical cell, (B) and (F) upper and lower cell halves machined from Kel-F, (C) entry port into cell's inner channel, (D) PTFE spacer, (E) LTIC plate working electrode, (G) stainless steel screws for holding yokes together, (H) electrical contact to LTIC plate working electrode, (I) electrical contact to combined reference-auxiliary LTIC plate electrode, (K) Altex 1/16 inch fittings, (L) exit from cell's inner channel, (M) LTIC plate combined reference-auxiliary electrode.

spring combination described elsewhere (19). Spacers were cut from 0.0025 cm PTFE material and the channel in the spacer provided a working electrode area of about 3.0 cm^2. This resulted in cell volumes of 7-8 μL. The cell was utilized in both a two-electrode and three-electrode short-circuited geometry mode (19). In the former configuration the upper LTIC plate served as a "reference" electrode to which the auxiliary electrode lead from the PAR 174A (or Bioanalytical Systems DCV-4 analyzer) had been shorted. In the three-electrode short-circuited configuration the upper LTIC plate was shorted to the external Ag/AgCl reference electrode. The stainless steel capillary served as both an exit conduit and auxiliary electrode.

Reagents

The structures of the various tyrosine and thyronine analogs used in this study are shown in Figure 2. The sodium salts of triiodothyronine (T_3) and tetraiodothyronine (T_4) as well as the compounds diiodothyronine (T_2), monoiodotyrosine (MIT), diiodotyrosine (DIT) and thyronine (T_o) were obtained from the Sigma Chemical Co. (St. Louis, MO 63178). The reverse triiodothyronine (rT_3) used was from the same lot of material provided earlier by Dr. Russel Saunders of the Nuclear Medical Laboratories. Stock standards were prepared at 1.00 mg mL^{-1} in 3% (v/v) concentrated NH_4OH in methanol (Fisher Scientific, Montreal, PQ). These materials were stored tightly capped at

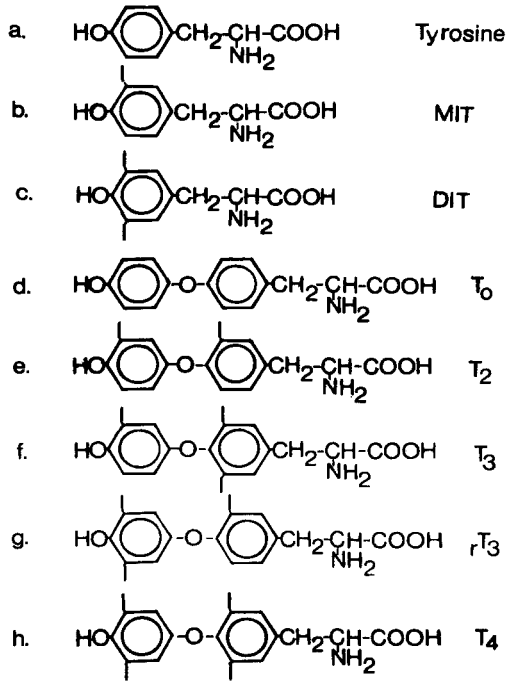

FIGURE 2. Structures of the various tyrosine and thyronine analogs. a. Tyrosine, b. Monoiodotyrosine, c. Diiodotyrosine, d. Thyronine, e. Diodothyronine, f. Triiodothyronine, g. "Reversed" triiodothyronine, h. Tetraiodothyronine.

-20°C. Fresh standards were prepared every six weeks. Working standards were prepared as needed in the appropriate chromatographic mobile phase.

Procedures

All glassware used was first washed with Fisher-brand (Sparkleen) detergent, followed by rinsing first in tap water

and finally in distilled water. These washed items were soaked overnight in 6 $\underline{M}$ HNO_3, rinsed again in tap water followed by distilled water, oven dried, cooled and silylated with 10% (v/v) chlorotrimethylsilane in toluene. This reagent was prepared from toluene which had been dried and stored over molecular sieves (American Chemicals Ltd., grade 564, type 3A, 8-12 mesh). The combined silane-toluene reagent was also stored over these same molecular sieves and reused up to ten times. All silylations were carried out by total immersion in the silylation bath for 15-30 min, followed by toluene, then methanol rinsing and finally overnight oven drying at 120°C. Glassware prepared in this manner was then stored dessicated at room temperature until used.

Duplicate hydrodynamic voltammograms were run on chromatographic peaks following 20-μL injections of mixtures containing 25 ng each of T_2, T_3 and rT_3 and 50 ng of T_4; duplicate voltammograms were taken after independent 20-μL injections of 25 ng each of MIT, DIT and T_o. Voltammograms were run from a positive potential setting in the region of the hydrodynamic plateau (i.e., the potential invariant peak height) to a negative value where the signal was indistinguishable from the background. These voltammograms were plotted from averaged peak current values as a function of potential applied. Injection and retention precision data were obtained from 10 replicate injections of 25 ng each (50 ng in the case of T_4) of the mixtures noted

above. Relative retention data were determined using rT_3 as an internal standard.

Dual-cell, diffusion-layer approximation verification and coulometric-yield (electrolysis-efficiency) experiments were carried out with the amperometric-cell (or "following" TLED cell) potential set at 1.500 V and the coulometric (guard) TLED cell potential varied as necessary. MIT and DIT (at concentrations of 25 ng/20μL) were used as model compounds in electrolysis-recovery (efficiency) experiments. In these recovery experiments the applied potential of the guard cell was set on the experimentally determined hydrodynamic plateau for the particular analyte and the change in recovery for the compound was monitored by the amperometric cell as the guard cell was turned on and then off during separate runs. Recovery was then determined by taking the ratio of the peak current obtained at the following amperometric cell with the guard cell turned on, to that obtained with the guard cell turned off. When this ratio is multiplied by a factor of 100 percent recovery is obtained. If this percentage is subtracted from 100, the percent electrolysis efficiency for a given analyte under defined conditions at a given cell can be determined.

In dual cell experiments on the electrochemistry of the thyroid hormones, the guard cell potential was varied until the hydrodynamic plateau for a specific thyroid hormone was determined. The electrolysis products obtained from this oxida-

tion process were then monitored at the following amperometric cell at a potential of 1.500 V, as a function of analyte recovery (guard cell off, then on) and transport time between the guard and amperometric cell. By variation of the flow rate both analyte recovery of the cells studied and the transport time between cells could be varied. Flow rates used in these studies were 0.20, 0.50, 0.70, 1.00 and 1.50 ($\pm$0.02) mL min^{-1}. In these latter experiments all recoveries obtained as a function of the electrolytic removal of analyte by the guard cell, were normalized by the averaged recovery obtained from the model compounds MIT and DIT evaluated under the same conditions.

For all of these experiments the chromatographic columns were thermostatted at 60°C.

RESULTS AND DISCUSSION

Precision Studies

Representative precision data for the dual-cell TLED system were obtained from the chromatographic analysis of academic test mixtures of the thyroid hormones. These data are presented in Tables 1-3 and in Figure 3. Within-day and between-day retention data can be compared from Tables 2 and 3. As might be expected for both cases retention precision is best when based upon an internal standard (rT_3).

TABLE 1

Tabulated Peak Height Data from 20-μL Injections of a Mixture of T_2, T_3, rT_3 and T_4 Containing 25, 25, 25 and 50 ng, Respectively. Conditions of the chromatographic experiment were: applied potential of analytical cell, 1.500 V (short-circuited geometry); applied potential of guard cell 0.600 V (51% electrolysis efficiency); flow rate 1.00 mL min^{-1}; 50:50 aqueous 0.015 M phosphate buffer, pH 2:methanol; temperature of LC column, 60°C. Peak heights were measured in nA.

	T_2	T_3	rT_3	T_4
Mean	59.91	33.21	26.01	32.63
SD	0.728	0.413	0.402	0.449
RSD	0.0122	0.0124	0.0155	0.0138
n	10	10	10	10

TABLE 2

Within-Day Retention Time (RT) and Relative Retention Time (RRT) Data for a Mixture of T_2, T_3, rT_3 and T_4. Chromatographic conditions are the same as those in Table 1.

	RT, min				RRT[a]		
	T_2	T_3	rT_3	T_4	T_2	T_3	T_4
Mean	4.14	5.91	8.11	9.46	0.510	0.728	1.166
SD	0.0852	0.105	0.127	0.120	0.00864	0.0115	0.00989
RSD	0.0206	0.0178	0.0157	0.0127	0.0169	0.0159	0.00849
n	12	12	12	12	12	12	12

[a] Relative to rT_3

Evaluation of the Coulometric TLED Cell for Application in Dual-Cell Experiments

As mentioned previously, the coulometric TLED cell has many uses in liquid chromatography. One of these is to selectively serve as an on-line clean-up (or guard) device to

TABLE 3

Between-Day[a] Retention Time (RT) and Relative Retention Time (RRT) Data for a Mixture of T_2, T_3, rT_3 and T_4. Chromatographic conditions are the same as those in Table 1.

	RT, min				RRT[b]		
	T_2	T_3	rT_3	T_4	T_2	T_3	T_4
Mean	4.22	6.26	8.58	9.97	0.492	0.730	1.162
SD	0.126	0.321	0.434	0.523	0.0184	0.0132	0.0210
RSD	0.0300	0.0512	0.0505	0.0524	0.0374	0.0181	0.0181
n	11	11	11	11	11	11	11

[a] Collected over a two-week period
[b] Relative to rT_3.

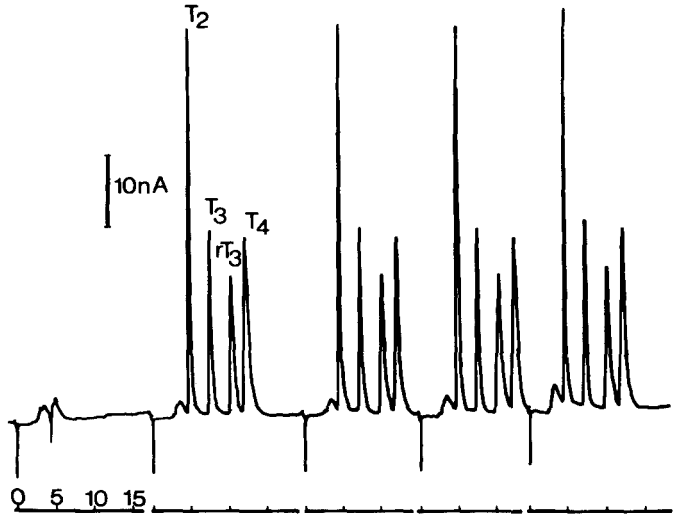

FIGURE 3. Representative chromatograms from repetitive 20-μL injections of an academic mixture of T_2, T_3, rT_3 (25 ng each) and T_4 (50 ng) into the chromatographic system containing the dual-cell detector. The guard cell potential was set at 0.600 V and the amperometric detection cell potential at 1.500 V. Chromatographic conditions are given in Table 1.

remove unwanted electroactive background either contained in the mobile phase or introduced into it during the chromatographic process. Conceptually, the principle of this use is straightforward; however, in the present context its implementation was of limited success. The inherent advantage of a coulometric cell is the complete conversion of the total amount of material available for the electrolysis process, as opposed to the rather small portions converted in amperometric cells. The practical disadvantage of the coulometric cell lies in the cell geometry required to achieve total conversion of an electroactive analyte. Historically this has meant using packed beds of conduction fibers or particles (17,23), larger surface area channel electrodes (13,15,24) or a metal-gauze or carbon-cloth electrode (25). It has been noted (21,23,24) that under these conditions the larger electrode surfaces resulted in proportionally larger background currents and hence similar signal-to-noise ratios. Additionally the argument can be made that with the increased electrode areas necessary to achieve total conversion come increased cell volumes which are potentially detrimental to chromatographic processes. These problems are due to larger extra-column dead volumes which facilitate band broadening.

By using LTIC plate electrodes and the cell design shown in Figure 1 it was hoped to obviate both problems mentioned above. Using the diffusion-layer approximation theory (15,22) and an

assumed flow rate of 1.00 mL min^{-1}, the cell efficiency was plotted against the working electrode area at the various PTFE template thicknesses available (see Figure 4). A close inspection of this figure demonstrates the dynamic aspect of varying the template thickness. For example, if a cell of 90% coulometric efficiency is required, a working electrode area of 1.7 cm^2 is needed with a 0.00064-cm spacer or an electrode area of 5.0 cm^2 with a 0.0025-cm spacer. This translates into cell volumes of 11 and 130 µL, respectively. Snyder and Kirkland (7) have previously observed that it is desirable to keep extra-column dead volumes to less than 100 µL and ideally less than 30 µL. With the advent of microbore chromatography (26) keeping

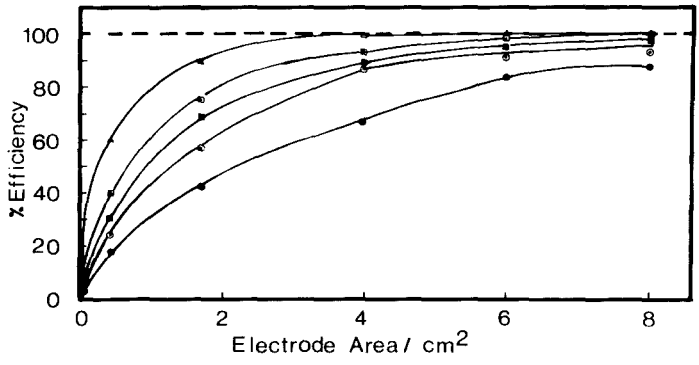

FIGURE 4. Plot of electrolysis efficiency vs. working electrode area as a function of spacer thickness. These data were obtained for a constant flow rate of 1.00 mL min^{-1} and with the working electrode width equal to the channel width. Calculations were based on the diffusion-layer approximation theory. Thicknesses are: Δ 0.00064, □ 0.0013, ■ 0.0019, O 0.0025, ● 0.0051 cm.

this parameter small becomes even more crucial. Examination of Figure 4 reveals that the easiest way to achieve the goal of smaller cell volumes is to decrease template thickness. The use of LTIC electrode material helped to realize this goal.

Preliminary experiments with two strips of plastic, 0.4 cm x 5.0 cm x 0.0006 cm thick placed along the edge between two LTIC plates, demonstrated that when these plates were squeezed together between the PTFE-insulated jaws of a vise, contact between the plates did not occur. Thus, in principle, any commercially available PTFE material of this or greater thickness could serve as a spacer in TLED cells.

Two plates which exhibited no contact under the above conditions were chosen as electrodes in the TLED cell. When constructed, however, it was quickly apparent that irrespective of the thickness of spacer material (0.00064-0.0051 cm), no TLED cell could be assembled that possessed an efficiency greater than 50% at a flow rate of 1.00 ± 0.01 mL min^{-1}. This was due to electrode contact problems and was independent of template thickness. More efficient electrolysis could be achieved at slow flow rates (maximum 86% at 0.20 ± 0.02 mL min^{-1}), the trade-off being greatly extended analysis times. No further studies on electrode material were undertaken.

The inability to fully achieve the promise offered by the LTIC materials was a disappointment. However it was felt that the failure was not with the material itself but rather with its

bonding to the Kel-F. In affixing the LTIC plates to the Kel-F hemicylindrical cell half with the EPO-TEK 353 ND epoxy, a curing temperature of 60°C was used (27). Although both the Kel-F (28) and the LTIC (29) materials are stable at this temperature, some expansion and contraction does occur due to the different thermal properties of the two materials. When this occurs, even the slightest "warping" of one or both surfaces can be expected which leads to contact problems such as those observed above. One might speculate that allowing these materials to cure gradually at room temperature might obviate this problem. Cells constructed recently (30) with a 3-5 day curing may yet fulfill the promise initially suggested for the LTIC product. In the present work it was decided to accept the electrolysis efficiencies that the "coulometric" cell would give at a flow rate of 1.00 mL min^{-1}.

The 8-μL volume added by the "coulometric" cell had a negligible influence on chromatographic parameters. In contrast, although Schieffer (17) also found negligible effects with the addition of a packed-bed coulometric cell to a chromatographic system in one application, in related work (31) using a technically much less complicated packed-bed cell an overall 12% loss in chromatographic efficiency was observed. The use of plate electrodes and thinner spacers ultimately offers not only the advantages of decreased cell volumes, but the possibility of applying "super-coulometric" techniques (14,15,32) in analyses

where the potential of one plate is controlled at an oxidizing potential and that of the facing plate at a reducing potential. This is not possible with packed-bed cells.

Finally the dual-cell approach was used to reduce background current. Employing the dual LTIC plate electrolysis guard cell with an electrolysis efficiency of 50.0 $\pm$ 2.0% (determined over a two-week period) the potential of the working electrode was set at 0.600 V, the foot of the wave for the most readily oxidized thyroid hormone (rT_3). Background currents were measured. Background currents recorded at the amperometric (8.6 $\pm$ 0.1% efficient) analysis cell (potential of the working electrode set at 1.500 V) ranged from 75-200 nA with the guard cell off. When the guard cell was operating, the reduction in background currents at the amperometric cell ranged from 25-50 nA. For the dual-cell approach this translates to a reduction of 25-33%. Since this reduction reflects losses in the faradaic component of the background current, the range in values is due to the quality variation of the mobile phase which was prepared on a daily basis. More important, when detection limits for a given day were compared for the dual-cell approach and the single amperometric TLED cell (19), lower detection limits were seen with the dual cell (see Table 4). These results, using the same cells, templates, chromatographic conditions and calibration techniques, suggest that if faradaic components of the background are minimized by their electrolytic removal from the

TABLE 4

Limit of Detection[a] Determined as the Amount of Analyte[b] Necessary Under Chromatographic Conditions[c] to Generate a Signal Twice the Size of the Peak-to-Peak Noise for Both the Single Amperometric Cell and Dual-Cell Systems.

	Single cell[d], ng	Dual cell[e], ng	Ratio single/dual
T_3	0.12	0.047	2.6
rT_3	0.096	0.061	1.6
T_4	0.18	0.096	1.9

[a] Determined as sensitivities in nA ng^{-1} and twice the p-p noise value in nA from amperometric cell data.
[b] Using academic standards of T_3, rT_3 and T_4.
[c] 1.00 mL min^{-1}; 50:50 (v/v) aqueous 0.015 M phosphate buffer, pH 2:methanol; column temperature, 60°C.
[d] Amperometric TLED cell (8.6 ± 0.1% efficient) short-circuited geometry, applied potential 1.00 V.
[e] TLED guard cell, 0.600 V applied potential, 50.0 ± 1% efficient, amperometric TLED cell as in (d).

mobile phase, flow-dependent noise will in turn be minimized with appropriate improvements in the limits of detection. Except for T_3, the improvement seen in the ratio of dual-cell: single-cell response reflects a similar improvement in the limit of detection for similar electrode processes. The deviation of the T_3 value from the other values seen in Table 4 is probably artifactual and due to chromatographic factors involving bands eluting close to the void volume and extra column band broadening.

Determination of TLED Cell Efficiencies

The dual-cell approach was used to empirically determine specific TLED cell efficiencies. The cell of interest served as

the first in a two-cell sequence and its effect on the removal of a test analyte (MIT and DIT) from the flow stream was determined. In these experiments the first cell was utilized in the "two-electrode" mode, with either the platinum disc (19) or the upper LTIC plate (Figure 1) serving as a combined auxiliary-reference electrode. With the second cell functioning as the analytical cell, the ratio of peak heights for repetitive injections of the model compounds as a function of the first cell being turned off or on, would represent the electrolysis efficiency of the first cell. In these studies, 3 to 5 injections of each compound were generally made and the average of results for MIT and DIT were compared. The precision of these measurements for both peak height and retention were consistent with the data in Tables 1-3; agreement between the averaged MIT and DIT values was within 2%. Typical hydrodynamic tracings as a function of the potential applied to the first cell (or cell being tested) are in Figure 5. The response of the test and the analytical cell are shown in 5a and 5b, respectively. These plots are both determined as averaged peak currents vs. the potential applied to the guard cell. It was noted that with the analysis cell held essentially at infinite potential, the hydrodynamic voltammograms obtained are qualitatively the mirror image of those generated at the test cell. Plateaus are achieved both prior to and following the electrolysis process occurring in the test cell. The relative magnitude of current

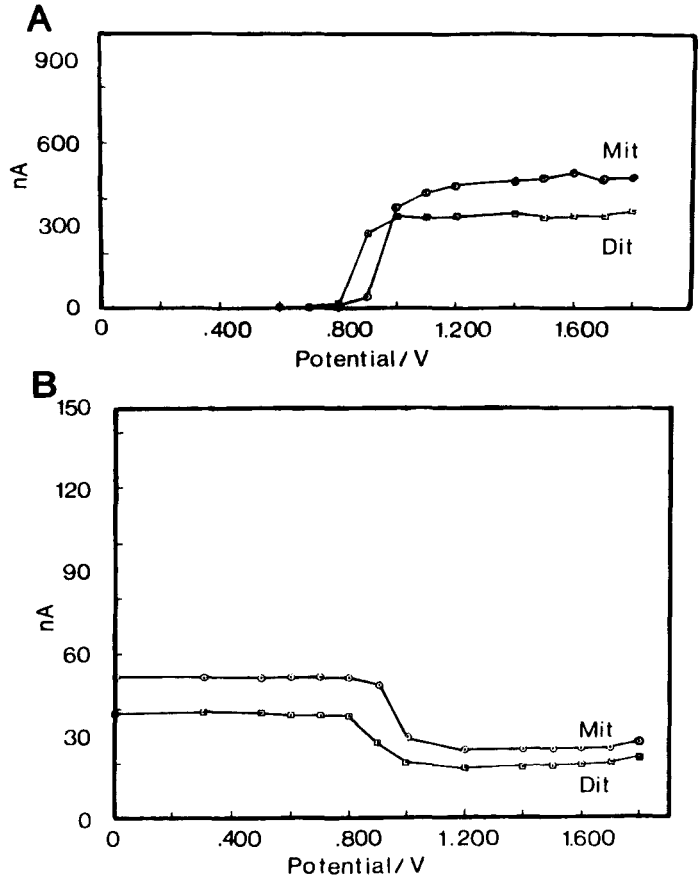

FIGURE 5. Hydrodynamic voltammograms for MIT and DIT as a function of the guard cell potential in the dual-cell system. A. Voltammogram from the guard cell. B. Voltammogram from the amperometric TLED cell. Applied potential of the amperometric cell was set at 1.500 V, using short-circuited geometry. Guard cell was in two-electrode mode. Each point is the average of duplicate determinations. Chromatographic conditions are given in Table 1.

seen at each cell in series is a reflection of the approximate factor of 5 difference in the electrode areas between the two cells, the cell geometries and potential applied to the guard cell. The relative difference in the magnitude of current between MIT and DIT for a similar electron transfer process is due to the fact that all voltammograms in this work were obtained under chromatographic conditions and MIT elutes before DIT. If voltammograms such as these are generated, the plateau currents observed in the amperometric analysis-cell tracing (Figure 5b) can be used directly to determine electrolysis efficiency.

Demonstration of Adherence to the Diffusion-Layer Approximation Theory

It is graphically possible to display a logarithmic electrolysis efficiency parameter for channel electrodes as a function of a logarithmic cell geometry parameter (15,22). This latter parameter, r_L, is a combination of volume flow rate, cell thickness, cell width, channel width, length of electrode and diffusion coefficient for the analyte of interest. The relationship is:

$$r_L = \frac{DLW_c}{\bar{u}b}$$

where D is the diffusion coefficient of the analyte in cm^2 sec^{-1}, L is the electrode length in cm, W_c is the channel width in cm, $\bar{u}$ is the volume flow rate in cm^3 sec^{-1} and b is the cell

thickness in cm. W_c is equal to the electrode width, W_e, with r_L being expressed as a function of the normalized (by cell thickness, b) diffusion layer, $\bar{\delta}_L$, determined at the end of the electrode in the direction of flow (15,22).

It has been shown previously (15) that r_L is the ratio of analyte residence time within the cell to the time necessary for the analyte to diffuse to the electrode surface prior to the electron-transfer process. The shorter the cell residence time relative to the diffusion time, the less efficient the cell. This is seen in Figure 6 by observing the decrease in cell efficiency as r_L becomes smaller.

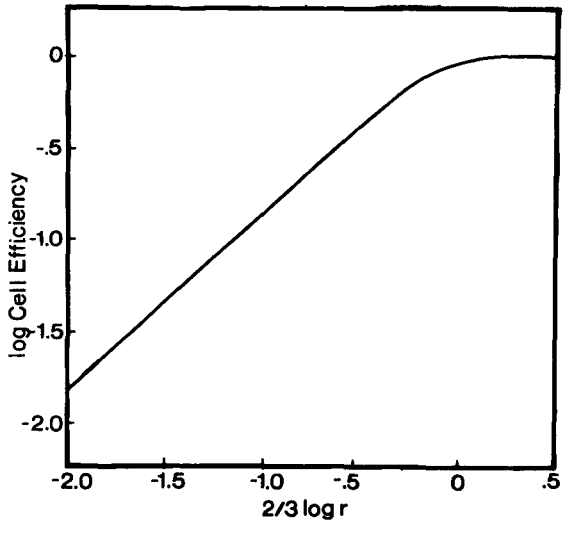

FIGURE 6. Plot of the logarithm of cell efficiency vs. a logarithmic function of 4, the dimensionless ratio of intercell analyte residence time to the time required for the analyte to diffuse to the working electrode surface prior to electron transfer (15,22).

Adherence to this relationship can be demonstrated by determining steady-state currents obtained at infinite potential for given analytes at specific concentrations and comparing the experimentally obtained values to those predicted for TLED cells of known geometries. This was essentially the approach used in the original verification of the diffusion-layer approximation theory applied to channel electrodes in a flowing stream (15,22). In the present work however, by using empirically determined cell efficiency values (obtained as discussed above) and the graphic relationship of Figure 6, it is possible to empirically determine a specific cell geometry constant based upon the fixed geometrical parameters for a given cell and upon knowledge of the diffusion coefficient of the analyte of interest and the flow rate. The value of this cell geometry constant is readily obtained from the above equation.

In principle, for a given analyte, TLED cell and PTFE template, this value should remain constant. In practice, exact knowledge of the diffusion coefficient is unnecessary for conditions of constant temperature, mobile-phase composition and analyte composition as this value will also be constant and become part of the "cell constant" for a given system. Once this "cell constant" value has been determined, r_L can be varied as a function of flow rate and the predicted cell efficiency (expressed as percent recovery) may be compared to the empirically determined cell efficiency (expressed in a like

manner). A plot of this relationship should ideally be a straight line at a 45° angle through the origin. For the TLED cell used in the present work this relationship is plotted in Figure 7 (values to within 1%). As is readily seen adherence occurs up through a flow rate of 1.00 mL min^{-1}. Above this flow rate deviation from the diffusion-layer approximation theory is observed. Since it is known that the diffusion-layer approximation theory has been validated at flow rates up to 3.0 mL min^{-1} (15,22) and the flow rates utilized were measured to within $\pm$ 0.02 mL min^{-1}, the deviation is within the cell constant parameter. Because the same temperature (to within $\pm$ 0.1°C), mobile phase and standard solution were used in this determination, the variance would be expected to be in the geometric parameters of this constant. This deviation may, in fact, be due to the expansion of the PTFE template at increased

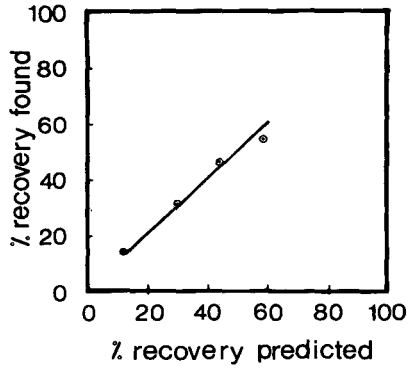

FIGURE 7. Plot of percent model compound found (recovered) vs. percentage expected for TLED cells from the diffusion-layer approximation theory (15,22).

flow rates and/or a change in the flow pattern within the cell which influences the transport of analyte to the electrode surface. In either event, all experiments were carried out at a flow rate of 1.00 ± 0.01 mL min^{-1} or less assuring a region in which adherence to the diffusion-layer approximation theory obtained for the cell utilized. Use of the dual-cell approach provides a way in which experimental data can be generated for cells in which laminar flow does not obtain prior to crossing the surface of the working channel electrode. Although not applied in the present work, it would follow that with knowledge of specific "cell constant" values (obtained from data using analytes of known diffusion coefficients under defined conditions) in regions where the diffusion-layer approximation theory applied, steady-state currents could be predicted and/or diffusion coefficients for other analytes empirically determined.

Dual-Cell Electrochemistry of the Thyroid Hormones

The electrochemical oxidation of the thyroid hormones in all probability emulates the model compound chosen for this group, thyronine, T_o. T_o is initially oxidized in a two-electron step with increasing positive potential; subsequently a homogeneous hydrolysis step occurs in which a quinone and tyrosine residue are produced (see Figure 8). Tyrosine upon further increase in potential is itself oxidized in an overall two-electron step. It has been suggested that the thyroid hormones

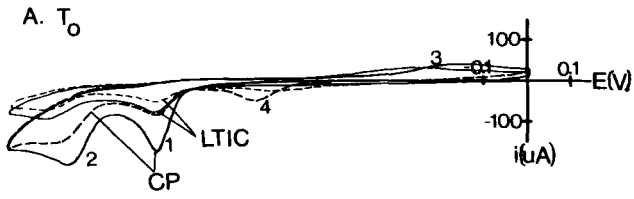

FIGURE 8. Cyclic voltammograms of T_o determined on carbon paste (CP) and LTIC stationary electrodes (20). Concentration of T_o is 2.0×10^{-4} g mL^{-1} in 1.0 M H_2SO_4. 1: 2-electron oxidation of T_o, 2: 2-electron oxidation of the hydrolytically generated tyrosine, 3: 2-electron reduction of the generated p-quinone, 4: subsequent 2-electron oxidation of p-hydroquinone.

follow a similar path (33); this is not refuted by the present work. A cursory search of the literature has not yielded information of the rate of hydrolysis to form quinone and tyrosine; however it has been suggested that the determination of these constants would be difficult (33). The dual-cell approach as described above would seem to provide a useful way in which to explore these constants in a qualitative if not a quantitative fashion.

In the current work using the dual-cell system, the guard cell was set such that the most difficult to oxidize analyte MIT and DIT were electrolyzed essentially at infinite potential (i.e., 1.500 V, Figure 5). Likewise, the following amperometric cell was set to a potential of 1.500 V. In principle at this potential setting any MIT or DIT residue generated as a function of hydrolysis of a given thyroid hormone would be available for oxidation at the following amperometric cell. Hence, the

electrochemical reaction products focused on in this evaluation were the iododinated residues MIT and DIT.

In studying the dual-cell electrochemical behavior of the thyroid hormones under these conditions, it was felt that if the rates of hydrolysis of these materials were fast compared to the intercell residence time within the guard cell ($\sim$ 0.5 sec for an 8-μL cell volume), then the electrolysis recoveries obtained would correspond to those of the iodinated tyrosine residues (MIT and DIT) used as model compounds in the present work. However, when the experiment was performed, the recoveries found were quite different from those for the model compounds (see Table 5).

TABLE 5

TLED Percent Recovery Using the Dual-Cell System.[a] Each value in the table represents the average of at least two determinations[b] of the thyroid hormones obtained on three separate days.

	Day 1 % recovery	Day 2 % recovery	Day 3 % recovery
T_o	74.6	76.8	76.5
T_2	64.4	68.7	64.4
T_3	68.8	73.3	74.4
rT_3	80.6	81.4	83.3
T_4	80.1	83.4	86.4
MIT	51.4	49.8	48.8
DIT	49.1	49.7	49.6

[a] Guard cell potential set at 1.500 V using two-electrode mode, amperometric TLED cell potential set at 1.500 V using short-circuited geometry.

[b] Determined chromatographically (chromatographic conditions as in Table 4) with the guard cell off, then turned on.

The size of the recoveries demonstrate that under the conditions noted, either thyroid hormones are not being removed at the guard cell in an overall process to the same extent as the model compounds, the interceding homogeneous electrolysis step is indeed not instantaneous, or most likely, the interceding homogeneous and heterogeneous chemical processes following the initial 2e oxidation of the thyroid hormones in this system are more complex than expected. In the first instance, if electrolytic removal of the various analytes were preceding to a smaller extent one might reasonably expect that at the potential applied the hydrodynamic waves of the thyroid hormones at the guard cell had not been achieved. Inspection of the voltammograms on Figure 9 however, demonstrates that at 1.500 V mass transport control in every case does obtain and that hydrodynamic plateaus are well established, hence, the potential applied is essentially "infinite". As before, superimposed upon the system, other relative differences in current magnitudes at the two electrochemical cells for similar overall electrode processes include those of electrode area and the determination of the voltammograms under chromatographic conditions (elution order MIT, DIT, T_2, T_3, rT_3 and T_4).

The second and third explanations for the observed differences in recovery are interrelated and a result of the complexities of the specific system studied. One might expect however, that if the hydrolysis rate of the interceding reaction was slow

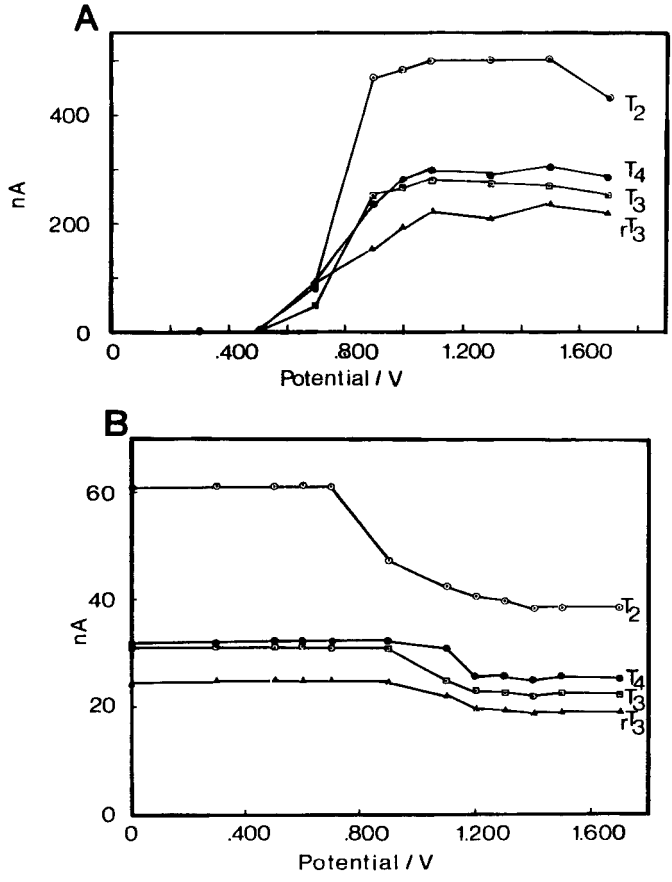

FIGURE 9. Hydrodynamic voltammograms as a function of guard cell potential for the electrolysis of T_2, T_3, rT_3 and T_4 (25 ng of each analyte, respectively, except for T_4 which was 50 ng, in a 20-μL injection). Points are the average of duplicate values. A. Voltammogram from guard cell using two-electrode model. B. Voltammogram from amperometric TLED cell using short-circuited geometry and a constant applied potential of 1.500 V.

(i.e., > 0.5s), its measurement would be readily made by existing electroanalytical methods (28). In the context of the current work with a parallel opposed two electrode circuit in the guard cell present the possibility for additional heterogeneous reductive electrochemical reactions does exist further complicating interpretation of these results.

Further experiments were undertaken to determine the influence of increasing the time it takes the analyte to flow from the first to the second cell. If electroactive material is being generated as a function of time, an increase in the time between cells would be expected to result in an increased recovery relative to the model compounds MIT and DIT. This experiment was performed and the results are presented in Figure 10, where normalized recovery (normalized to the averaged MIT-DIT recovery) is plotted as a function of the transit time between the guard and amperometric TLED cells. As can be seen, the recovery relative to the averaged model compounds does increase as a function of time. Interestingly, when these results are extrapolated back to zero time, it is seen that the efficiencies for the electrolysis of the thyroid hormones equal those of the model compounds. This infers that within the residence time of the first cell an overall electrochemical process does occur that is as efficient (i.e., equal recovery) as that for the model compounds. Subsequent to this initial oxidation process the product(s) that have formed interact

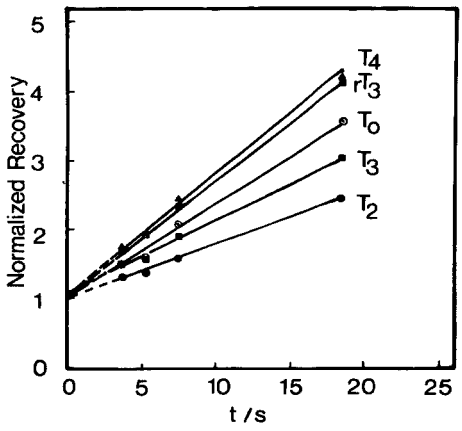

FIGURE 10. Plot of the normalized (to the averaged MIT, DIT recovery values) electrolysis recovery of T_0, T_2, T_3, rT_3 and T_4 as a function of transport time (in sec) between the guard cell (potential setting 1.500 V) and the amperometric TLED cell (potential setting 1.500 V) in a dual-cell experiment.

further through heterogeneous interactions and/or homogeneous interactions to produce additional electroactive analytes that are readily oxidized at the following amperometric cell. As can be seen from the relative slopes in Figure 10, the overall rates of these processes are not uniform. The greatest similarity seems to occur between rT_3 and T_4, molecules in which the outer ring (see Figure 2) is doubly iodinated. By contrast, molecules with a single iodinated outer ring (T_2 and T_3) seem to demonstrate this influence at a slower rate.

The importance of these findings in the current system lie in the utility of being able to set the guard cell at a higher potential allowing for greater removal of faradaic background

from the mobile phase, while still generating electroactive products derived from the thyroid hormones under investigation. Better understanding of the nature of the process of production of these derivatives awaits further study.

CONCLUSIONS

The use of the dual-cell approach, although not totally successful in demonstrating coulometric yields, did show that reductions in background were possible. In addition, improvement was observed over previously evaluated amperometric methods in the limit of detection for thyroid hormones. The failure to achieve coulometric yield with the dual LTIC electrode cell design is due to manufacturing problems and not with the design or materials.

Using the dual-cell approach it is possible to study both the electrolysis of the thyroid hormones and the nature of the hydrolysis constant associated with the electrochemical mechanism. Additional work in this area may permit quantitative evaluation of the constants involved. Also, the use of the dual-cell approach in validating adherence to the diffusion-layer approximation theory for thin-layer cells and in empirically evaluating specific cell electrolysis efficiencies has been demonstrated. These are reliable tools which can be applied in a predictable fashion.

The ultimate utility of the dual-cell approach may yet be with coulometric and supercoulometric cell configurations. A

system can be envisioned which has a guard cell set at "infinite potential" for the electrolysis of the thyroid hormones, removing other faradaic background present in the mobile phase subject to electrolysis at these potentials. After sufficient time delay the effluent stream would then proceed to a super coulometric cell which would be set to electrochemically recycle an electrochemically reversible couple (i.e., the iodinated quinone-hydroquinone couple), amplifying the signal accordingly. In theory (15,22,32), sufficient signal could be generated to analyze levels of free circulating T_3 and T_4, which indeed may be the ultimate avenue for thyroid function evaluation by laboratory methods (34,35).

ACKNOWLEDGEMENTS

We are grateful to William Bastian and Alfred Klück for construction of the TLED cells used in this work and to the Natural Sciences and Engineering Research Council of Canada for financial support.

The present address of Dr. Hepler is: Coroner's Office, County of Cuyahoga, 2121 Adelbert Road, Cleveland, OH 44106.

REFERENCES

1. H. Gerischer, I. Mattes and R. Barum, J. Electroanal. Chem., 10, 553 (1965).

2. W.J. Albery and M.L. Hitdman, "Ring-Disc Electrodes", Oxford University Press, London, 1971.

3. H. Matsuda, J. Electroanal. Chem., 16, 153 (1968).

4. R. Braun, J. Electroanal. Chem., 19, 23 (1968).

5. K. Tokuda and H. Matsuda, J. Electroanal. Chem., 52, 421 (1974).

6. C.L. Blank, J. Chromatog., 117, 35 (1978).

7. S.G. Weber and W.C. Purdy, Anal. Lett., 12, 1 (1979).

8. K. Brunt and C.H.P. Bruins, J. Chromatog., 161, 310 (1978).

9. K. Brunt and C.H.P. Bruins, J. Chromatog., 172, 37 (1979).

10. W.A. MacCrehan and R.A. Durst, Anal. Chem., 53, 1700 (1981).

11. K.B. Bratin and P.T. Kissinger, J. Liq. Chromatog., 4, 321 (1981).

12. D.A. Roston and P.T. Kissinger, Anal. Chem., 54, 429 (1982).

13. R.J. Fenn, S. Siggia and D.J. Curran, Anal. Chem., 50, 1067 (1978).

14. S.G. Weber, Ph.D. Thesis, McGill University, Montreal, 1979.

15. S.G. Weber and W.C. Purdy, Anal. Chem., 54, 1757 (1982).

16. D.A. Roston and P.T. Kissinger, Anal. Chem., 53, 1695 (1981).

17. G.W. Schieffer, Anal. Chem., 52, 1994 (1980).

18. W.R. Matson, R.W. Anderson, J. Ball, D. Skinner, R. Vitukevich and E.W. Zuck, "A new electrochemical HPLC detector", Paper 565, Pittsburgh Conference on Analytical Chemistry and Applied Spectroscopy, Atlantic City, N.J., 1981.

19. B.R. Hepler, S.G. Weber and W.C. Purdy, Anal. Chim. Acta, 113, 269 (1980).

20. B.R. Hepler, S.G. Weber and W.C. Purdy, Anal. Chim. Acta, 102, 41 (1978).

21. P.T. Kissinger, Anal. Chem., 49, 447A (1977).

22. S.G. Weber and W.C. Purdy, Anal. Chim. Acta, 100, 531 (1978).

23. D.C. Johnson and J. Larochelle, Talanta, 20, 959 (1973).

24. J. Lankelma and H. Poppe, J. Chromatog., 125, 375 (1976).

25. Y. Takata and G. Muto, Anal. Chem., 45, 1864 (1973).

26. R.P.W. Scott and P. Kucera, J. Chromatog., 169, 51 (1979).

27. EPO-TEK 349 High Temperature Epoxy Bulletin, Epoxy Technology Inc., Billerica, MA 01821, 1979.

28. D.T. Sawyer and J.L. Roberts, "Experimental Electrochemistry for Chemists", John Wiley and Sons, New York, 1974.

29. J.C. Bokros, R.J. Akins, H.S. Shim, A.D. Haubold and N.K. Agarwar, Chem. Techn., 7, 40 (1977).

30. S.A. McClintock, McGill University, Personal Communication.

31. G.W. Schieffer, Anal. Chem., 53, 126 (1981).

32. S.G. Weber and W.C. Purdy, Paper 102, Pittsburgh Conference on Analytical Chemistry and Applied Spectroscopy, Atlantic City, NJ, 1980.

33. S.V. Tatwawadi, S. Piekarski, M.D. Hawley and R.N. Adams, Chem. Listy, 61, 624 (1967).

34. L.J. McDonald, N.I. Robin and L. Siegel, Clin. Chem., 24, 652 (1978).

35. L. Siegel, L.J. McDonald and N.I. Robin, Clin. Chem., 24, 1891 (1978).

JOURNAL OF LIQUID CHROMATOGRAPHY, 6(12), 2311-2335 (1983)

DETERMINATION OF COMMON ANALGESICS IN SERUM AND URINE BY LIQUID CHROMATOGRAPHY/ELECTROCHEMISTRY

D. A. Meinsma, D. M. Radzik, and P. T. Kissinger

Department of Chemistry
Purdue University
West Lafayette, Indiana 47907

ABSTRACT

A reverse phase LC method with amperometric electrochemical detection is described for determination of several common analgesics in blood serum and urine. The retention properties as a function of organic mobile phase modifier and pH are graphically illustrated and discussed. Electrochemical properties of the analgesics and possible internal standards are also presented. Step-gradient elution was used to facilitate simultaneous determination of analgesics with a wide range of hydrophobicities. Parallel dual-electrode detection with two glassy carbon working electrodes enables acetaminophen to be selectively determined in the same chromatographic run at +0.75 V while several other analgesics are determined at +1.15 V.

INTRODUCTION

Analgesics are a group of readily available and widely consumed pharmaceutical products. Acetaminophen (APAP), salicylate (SAc), salicylamide (SAm), phenacetin (Phen), methyl salicylate (MeS), naproxen (NPX), and codeine (Cod) (see Figure 1) are among the most common. They may be self-administered and/or clinically prescribed

 0148-3919/83/0612-2311$3.50/0

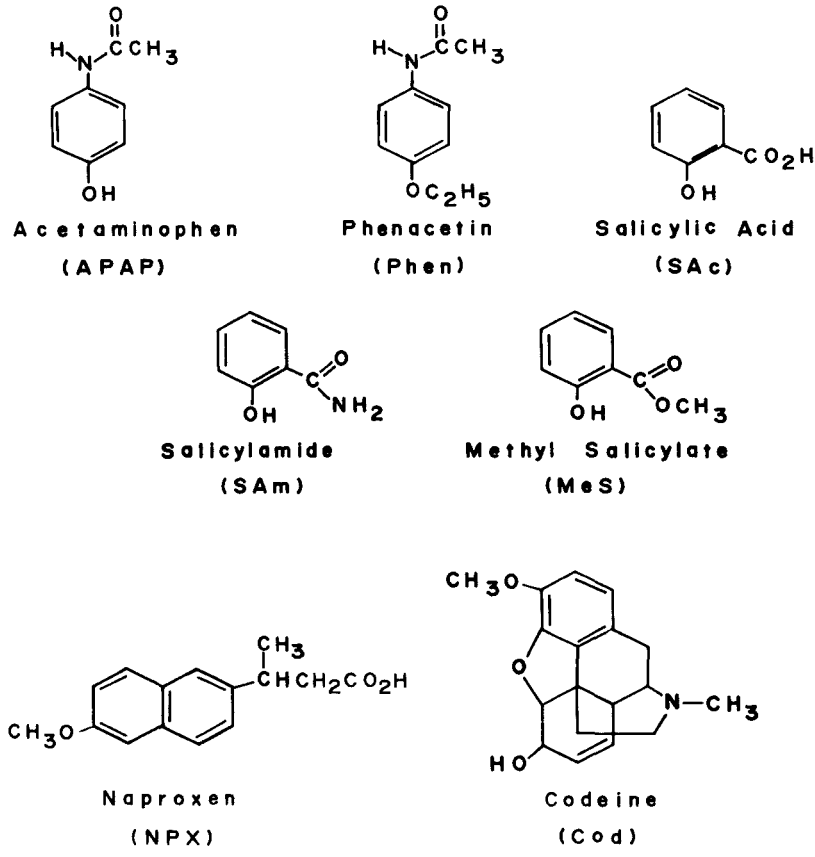

FIGURE 1. Structural formulas of the common analgesics investigated.

in a variety of combinations and dosage levels (1,2). Their determination in biological fluids is important for toxicological, clinical, drug interaction, and pharmacokinetic studies.

Liquid chromatographic procedures have been described for determining many of these compounds in blood serum or plasma (3-10) and in dosage formulations (11). Simultaneous deter-

mination of several common analgesics has seldom been presented and determinations in urine have been largely ignored. The majority of LC separations reported employ UV detection and are thus subject to interference by many other common drugs. Fluorescence detection has also been reported (12,13) but lacks general applicability. Unlike some other drugs, the common analgesics shown in Figure 1 are electrochemically active at analytically useful potentials and are therefore amenable to the selectivity and sensitivity of electrochemical (EC) detection. Determination of acetaminophen in serum by LCEC has previously been demonstrated (14).

Investigations were undertaken to evaluate the electrochemical and chromatographic properties of these analgesic compounds and of several possible internal standards. Step-gradient elution was evaluated to determine its usefulness and compatibility with EC detection. Dual electrode detection is shown to provide increased versatility by allowing simultaneous determination of early eluting APAP at a significatly lower and thus more selective detector potential.

Simple, rapid sample preparation was employed to provide methods which would facilitate routine use of LCEC in these determinations.

EXPERIMENTAL

Reagents

Acetaminophen, salicylic acid, and salicylamide were obtained from Sigma Chemical Co. (St. Louis, MO); codeine and methyl salicylate from Mallinckrodt (Paris, KY); naproxen was a generous gift from Syntex (Palo Alto, CA); phenacetin (4'-ethoxy-acetanilide), 2-acetamidophenol, and 3-methylsalicylic acid from Aldrich (Milwaukee, WI); and p-hydroxyphenylpropionic acid and p-methoxy-acetanilide from Pfaltz and Bauer (Stamford, CT). N-propionyl-p-aminophenol (PrPAP) was synthesized by conventional methods

(15). Water was double distilled and methanol was single distilled technical grade. All other chemicals were reagent grade.

Apparatus

Cyclic voltammetry was performed with a CV-1A cyclic voltammetry instrument from Bioanalytical Systems, Inc. (BAS) (West Lafayette, IN).

The liquid chromatograph consisted of a Milton Roy single-piston pump, a Rheodyne model 70-10 injector with a 20 µL loop, and a Biophase 5 µm C_{18} column (25 cm x 4.6 mm) (BAS). Electrochemical detection was performed with a dual-electrode system in the "parallel-adjacent" mode by use of two modified BAS LC-4A controllers and a BAS dual-electrode thin-layer cell with glassy carbon working electrodes and a Ag/AgCl reference electrode. A Rheodyne low pressure 4-way rotary valve was placed upstream of the pump to allow alternate selection of two mobile phases. Column temperature was controlled with a BAS LC-23 column heater and LC-22 temperature controller.

Cyclic Voltammetry

Cyclic voltammetric data for APAP, SAc, SAm, Phen and MeS were obtained at concentrations of 1 mM in 25% methanol with pH 4.0 acetate (0.1 M) and 0.1 M KNO_3 as buffered electrolyte. Naproxen was scanned at 2 mM in 40% methanol: 60% (v:v) pH 5.0 acetate (0.1 M). Codeine was evaluated at 5 mM in 50% methanol: 50% pH 4.5 acetate buffer (0.05 M) containing 0.1 M $NaClO_4$. The scan rate was 150-200 mV/sec.

Standard and Recovery Solutions

Stock analgesic solutions were prepared containing 1 mg/mL of each compound in 70% methanol with ethyl paraben (EtP) and PrPAP included as internal standards. Aliquots of pooled serum and urine were spiked with the appropriate volume of stock

solution to achieve the desired concentration levels. Working standards were prepared by addition of stock solution to an equivalent aliquot of water and processed identically.

Sample Preparation

Serum samples were prepared by mixing 500 µL of spiked serum with 500 µL of acetonitrile in 1.5 mL Eppendorf capped centrifuge tubes, followed by centrifugation in an Eppendorf centrifuge (Brinkmann Instruments, Westbury, N.Y.) for five minutes. To 500 µL of the supernatant was added 500 µL of 0.1 M (pH 3.2) monochloroacetate (MCA) buffer and 100 µL of 1.0 M phosphoric acid. For samples in which codeine was to be determined, the supernatant was diluted with 0.1 M (pH 7.0) phosphate buffer. The samples were then filtered through 0.2 µm Nylon-66 filter membranes with a Swinnex syringe filter assembly (Millipore Corp., Bedford, MA).

Urine samples were prepared in a similar manner, but were not filtered. At higher concentrations, some additional dilution with mobile phase was employed to remain in a more desirable detector sensitivity range. For acetaminophen determinations, 500 µL samples were mixed with 500 µL of 1 M (pH 7.0) phosphate in a small test tube and extracted with 1.0 mL of ethyl acetate by vortex mixing. A 500 µL portion of the organic extract was evaporated under nitrogen and the residue reconstituted in 500 µL mobile phase.

Liquid Chromatography

The retention properties of several compounds were evaluated versus organic modifier strength by varying the percentage methanol (v/v) in a mobile phase containing 0.1 M acetate buffer at pH 5.0. Retention versus pH was determined for NPX, SAc, and Cod by using MCA, acetate, and phosphate buffers to vary the pH of a 50% methanol mobile phase.

Serum samples were initially evaluated under isocratic conditions with a mobile phase containing 0.05 M ammonium MCA (pH 3.2) and 0.1 M $NaClO_4$ in 50% methanol:50% water (v:v). For step changes in eluent strength, eluents A and B contained 40 and 60 percent methanol, respectively, with the same molar concentrations of buffer and electrolyte. The stepwise gradient change was effected by manual switching from eluent A to B at a consistent time (5 min.). Serum recovery samples were run via gradient elution with dual-electrode detection at +0.75 and +1.15 V and at room temperature to simultaneously determine all analgesics except codeine. Codeine was determined isocratically with 50% methanol:50% pH 7.0, 0.2 M phosphate buffer, a column temperature of 30°C, and an applied potential of +1.12 V. A flow rate of 1.5 mL/min. was used for all studies.

Urine recovery samples were run with gradient elution for determination of SAm, SAc, Phen, MeS, and NPX. APAP was determined with eluent A and an applied detector potential of +750 mV following the quick extractive cleanup described above. Codeine in urine was determined with a mobile phase containing pH 5.8 phosphate (0.1 M) in methanol:water (45:55, v/v) and a column temperature of 45°C.

Analyte and internal standard responses were quantitated by measuring peak height. Relative recovery values were calculated by comparing analyte/internal standard response ratios of spiked samples against aqueous standards of similar concentrations. Samples were usually bracketed by standards for every 3 to 5 injections.

RESULTS AND DISCUSSION

Electrochemical Properties

Half-wave potentials from chromatographically assisted hydrodynamic voltammograms (HDV's) of the analgesic compounds (see Figure 1) and several possible internal standards are

TABLE 1

Hydrodynamic Voltammogram (HDV) Half-wave Potentials ($E_{1/2}$) for Common Analgesics and Possible Internal Standards*

ANALGESICS	$E_{1/2}$ (VOLTS)
Acetaminophen	0.62
Phenacetin	1.08
Salicylamide	1.03
Salicylic Acid	1.09
Methyl Salicylate	1.10
Naproxen	0.86
Codeine	1.12
INTERNAL STANDARDS	
N-Propionyl-p-aminophenol	0.62
2-Acetamidophenol	0.65
p-Methoxyacetanilide	1.08
Ethyl Paraben	1.09
p-Hydroxyphenylpropionic Acid	0.92
3-Methylsalicylic Acid	1.09

* LC mobile phase conditions: pH 4.5 acetate (0.1 M) with variable percent methanol, except for codeine which was evaluated in pH 7.0 phosphate (0.1 M) with 50% methanol.

listed in Table 1. Normalized HDV's of the analgesics are illustrated in Figure 2 and representative cyclic voltammograms (CV's) are shown in Figure 3.

Acetaminophen and phenacetin are substituted aminophenols whose electrochemical properties have been previously investigated (15). APAP is oxidized at modest potentials, whereas Phen is shifted to somewhat higher potentials due to ethyl substitution of the phenol. Although SAc, SAm, MeS, and EtP (I.S.) represent ring-substituted phenols and require even greater anodic potentials, they are well within the analytically useful range. Naproxen, a substituted naphthol, is oxidized at a lower potential

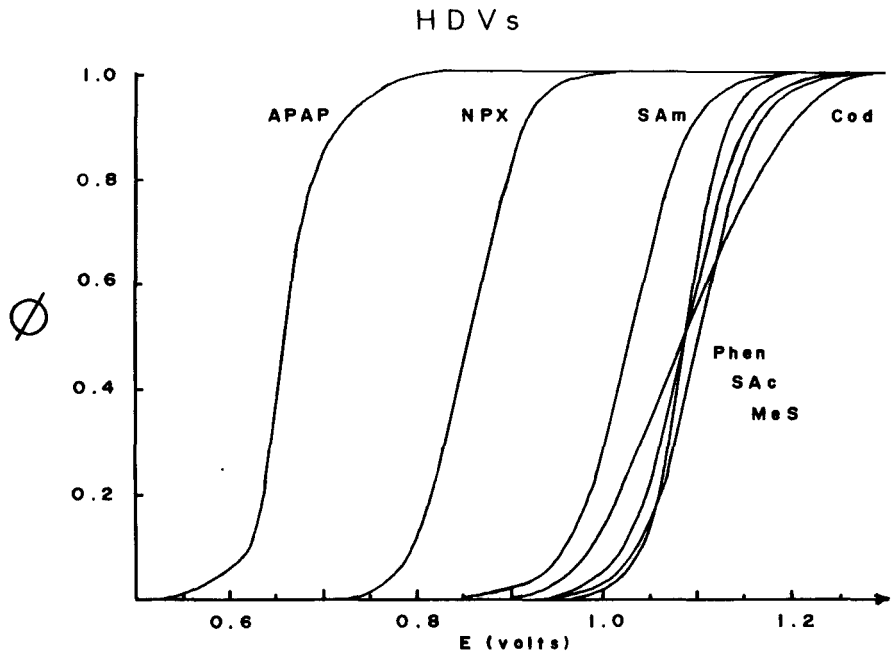

FIGURE 2. Normalized hydrodynamic voltammograms (HDV's) of analgesic compounds. LC mobile phase conditions same as Table 1.

than free phenols. The extensive ring conjugation is apparently responsible for this unexpected behavior.

Codeine is more difficult to oxidize but still may be determined at an advantageous potential. There is some evidence to support oxidation at the tertiary nitrogen (17,18) but the presence of a disubstituted catechol group suggests possible participation of this site. The appearance of two anodic waves in its CV indicates that both sites may be involved at adjacent potentials.

Chromatographic Properties

As shown in Figure 4, the desired analytes tend to elute with a wide range of retention times. APAP and its correspond-

ing internal standard (PrPAP) which elute early, can be detected with greater selectivity due to their significantly lower oxidation potentials.

The retention of SAc, NPX, and Cod is strongly pH dependent as shown in Figure 5. In order to sufficiently increase the retention of SAc relative to SAm and endogenous components, it was necessary to use a mobile phase of pH 3.2. At this pH, SAc (ca. pK_a = 3.0) is partly undissociated and thus more strongly retained. NPX, however, is predominately unionized and exhibits strong lipophilic behavior. Codeine is almost completely cationic at this pH and elutes with the endogenous milieu of biological samples. At values near pH 6 and above, the retention of Cod is sufficiently increased to provide separation from most endogenous compounds. Endogenous electroactive urine components tend to be predominately anionic near neutral pH, and a general reversal of retention properties therefore occurs. The anionic nature of such urine components was demonstrated by observing their strong retention on an anion-exchange minicolumn.

Simultaneous determination of all the analgesics does not appear readily feasible due mainly to the disparate properties of codeine. However, the remainder can be determined in a single chromatographic run. Employment of gradient elution to alleviate the problem of diverse retention times is illustrated and discussed below.

Internal Standards

The use of appropriate internal standards facilitates accurate quantitation while eliminating stringent volumetric transfers during sample preparation. Compensation is also made for slight changes in injection volume and chromatographic parameters. Several compounds were evaluated for suitable electrochemical and chromatographic properties. EtP and PrPAP were chosen as most appropriate for these investigations. The additional com-

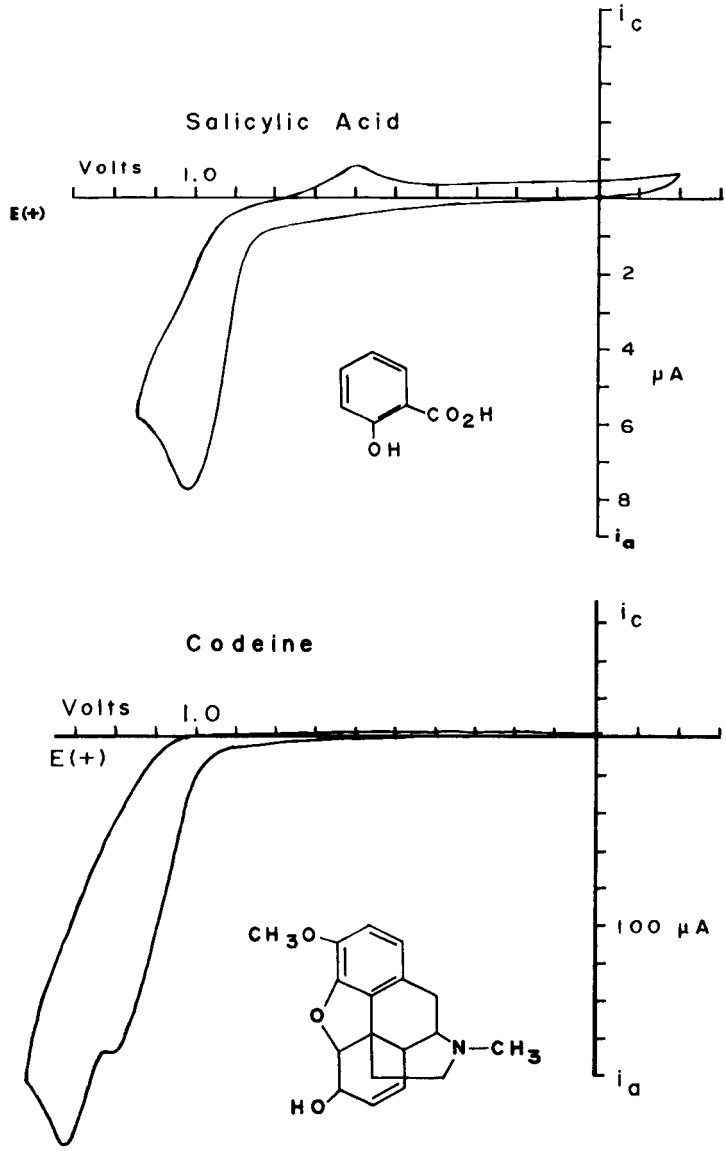

FIGURE 3. Cyclic voltammograms of acetaminophen, salicylic acid, naproxen, and codeine. See text for conditions.

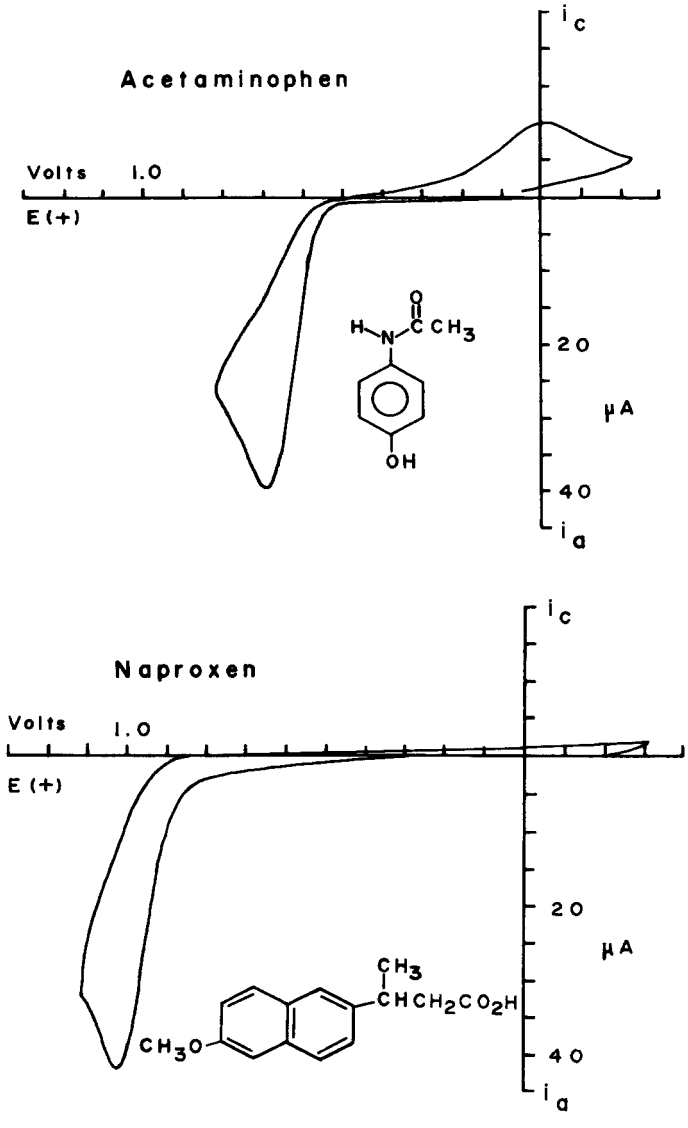

FIGURE 3 (continued)

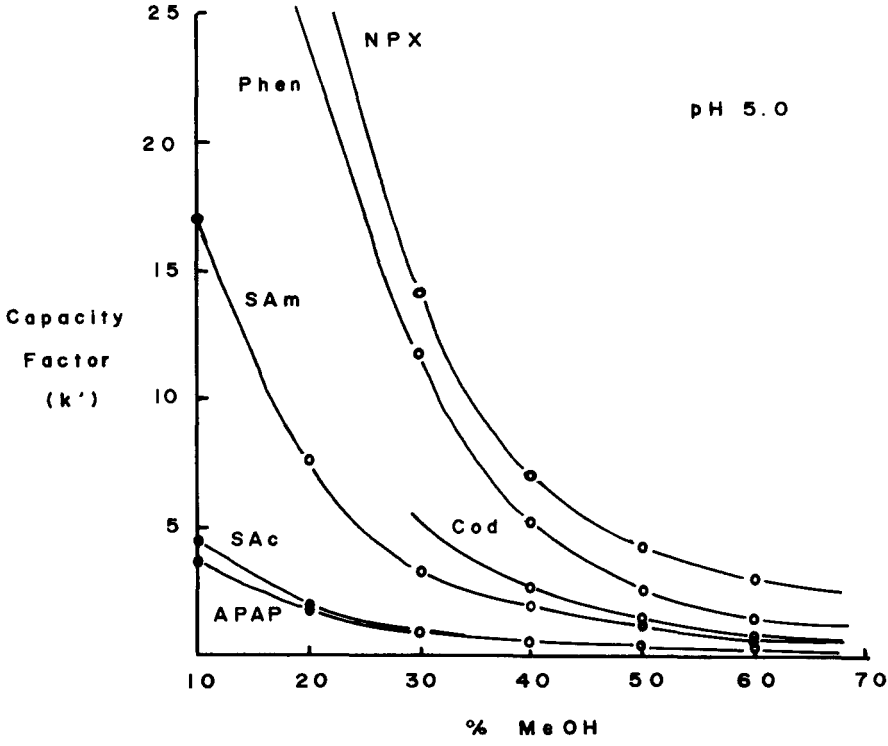

FIGURE 4. Plot of LC capacity factor (k') versus % methanol for several analgesics at pH 5.0.

pounds in Table 1 are listed as useful candidates for additional or alternate internal standards to promote flexibility in applying LCEC to other specific applications. For controlled studies, the electroactive analgesics not under investigation also represent possibile internal standards.

Serum and Urine Determinations

Serum samples run isocratically as shown in Figure 6 provide reasonable determinations at levels above about 5 μg/mL. NPX and

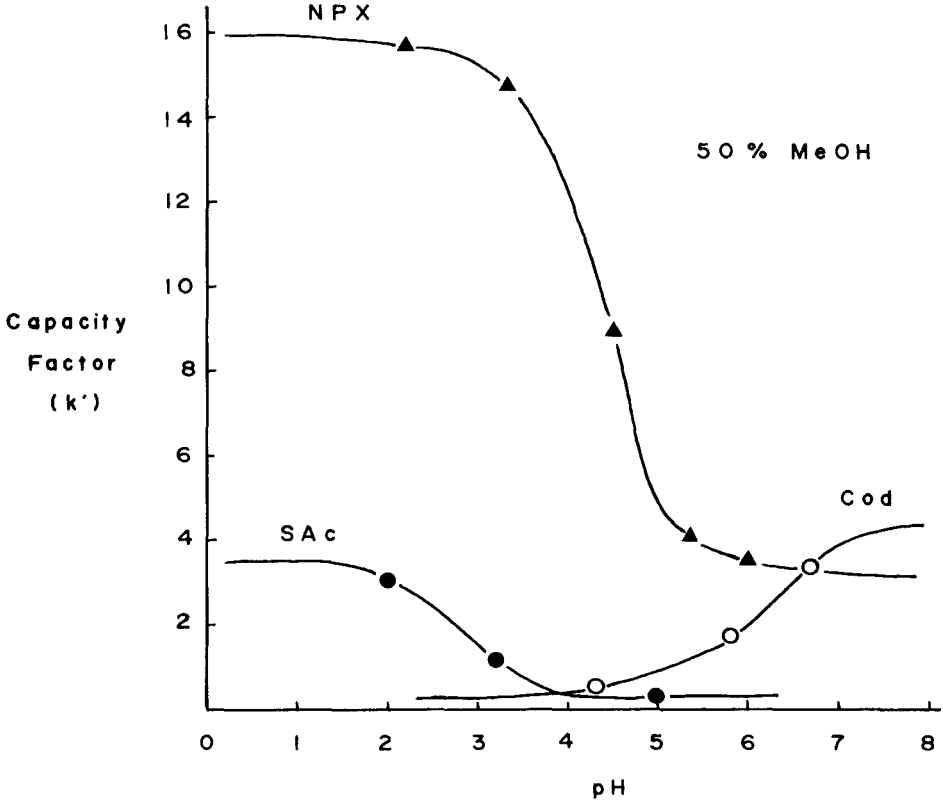

FIGURE 5. Plot of LC capacity factor (k') versus pH for SAc, NPX, and Cod in 50% methanol as mobile phase.

MeS, however, elute rather late as fairly broad peaks, and the interference of endogenous peaks with APAP, SAm, and SAc becomes significant at lower concentration levels. A simple step-gradien elution was evaluated in an attempt to improve resolution of early eluting components and sharpen the peaks of later eluting ones. Inclusion of dual-electrode detection in the "parallel-adjacent" mode enabled simultaneous determination of all analgesics except codeine. Representative chromatograms illustra-

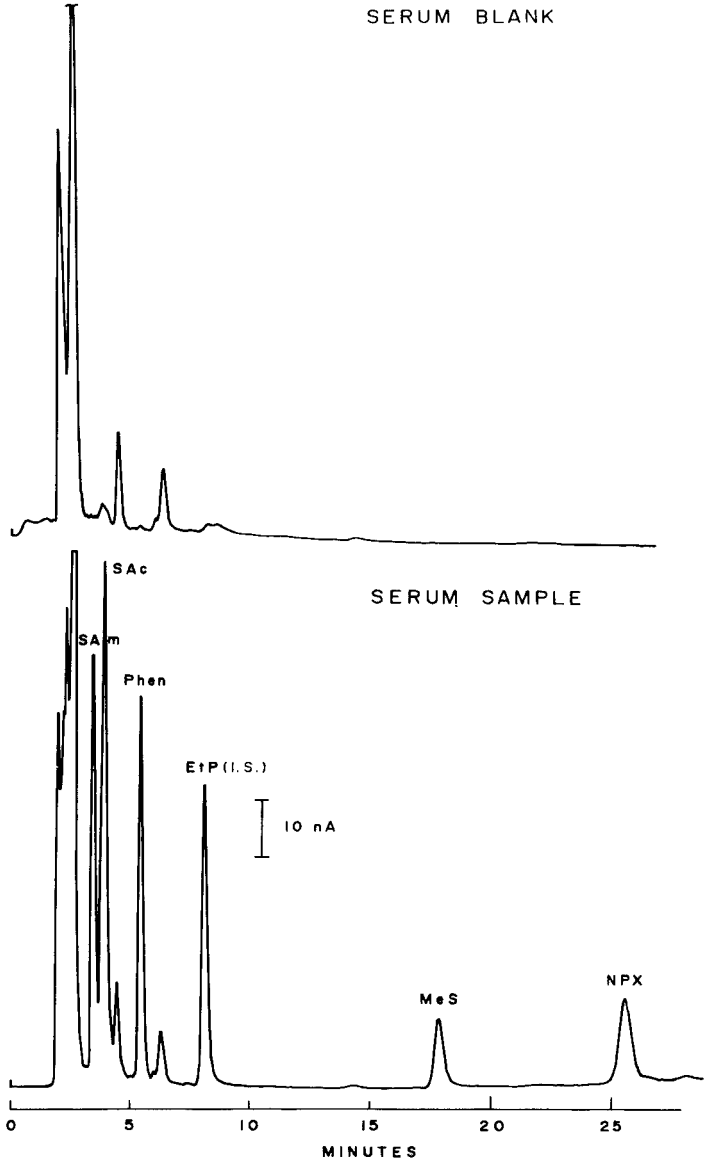

FIGURE 6. Isocratic LC separation of several analgesics in a spiked serum sample. Mobile phase = 0.05 M ammonium MCA (pH 3.2), 0.1 M $NaClO_4$ in MeOH:H_2O (50:50). Detector potential = +1.15 V. Approx. 40 ng of each injected.

ting gradient elution with parallel dual-electrode detection are shown in Figures 7 and 8.

Codeine in serum was determined separately with the 50:50 (v/v) pH 7.0 phosphate:methanol mobile phase. At this pH, Cod is well retained and the retention time of NPX is reduced from 26 to 6 minutes to elute just before Cod. SAm, Phen, NPX, and MeS can be conveniently determined with Cod under these conditions. APAP can often be included in the higher concentration range with adequate selectivity by setting one electrode potential at about +600 mV.

Serum recovery samples at analgesic levels of 2-50 µg/mL were run via step-gradient elution at pH 3.2 and isocratic elution at pH 7.0. Results are listed in Table 2.

One molar phosphoric acid and MCA buffer were added to the injection solution to improve recovery values for SAc and NPX. Initial injections of the supernatant from 50:50 (serum:CH_3CN) protein precipitation yielded low recoveries versus aqueous standards. The problem was traced to inadequate pH control in the sample injection solution. Low pH maximizes retention at the head of the column and increases the sharpness of the "plug" injection.

Urine samples contain a fairly high concentration of early eluting endogenous compounds and moderately polar metabolites which generate greater interference in APAP determinations. A simple ethyl acetate extraction proved sufficient to eliminate interferences at the levels evaluated. Note that the working standard must be processed through the extraction step since the analyte and internal standard distribution coefficients are not identical. Although the other analgesics can be readily extracted, SAc and MeS are sufficiently volatile to be partially lost in the evaporation step. The gradient-elution approach proved adequate for determining SAm, SAc, Phen, NPX, and MeS by direct injection as shown in Figure 7. APAP was determined with

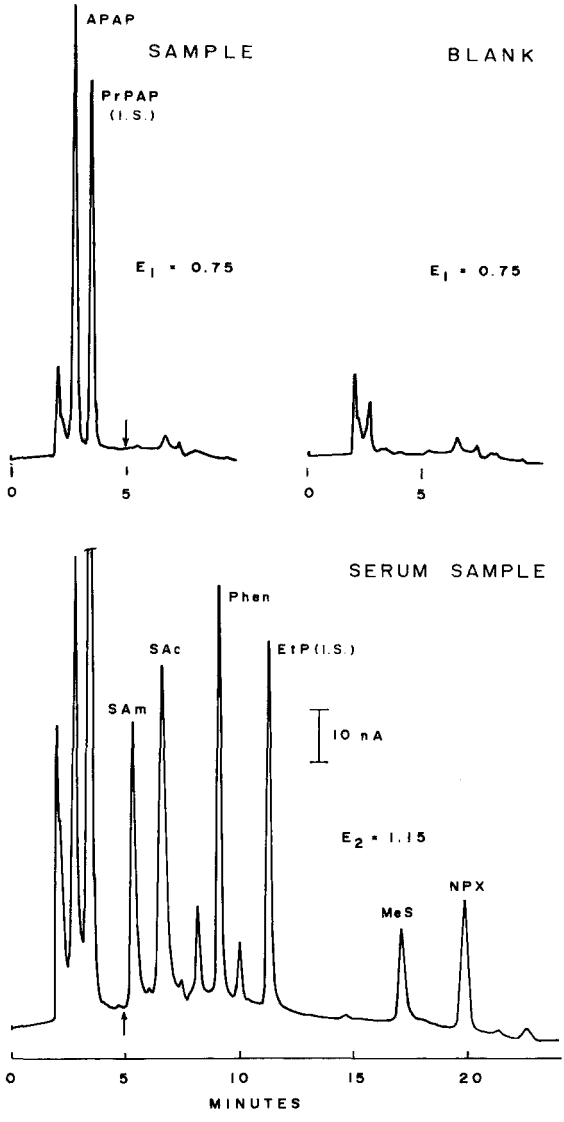

FIGURE 7. Simultaneous determination of several analgesics via step-gradient elution with parallel dual-electrode detection. Mobile phase change from A to B at 5 min. Approx. 40 ng of each injected.

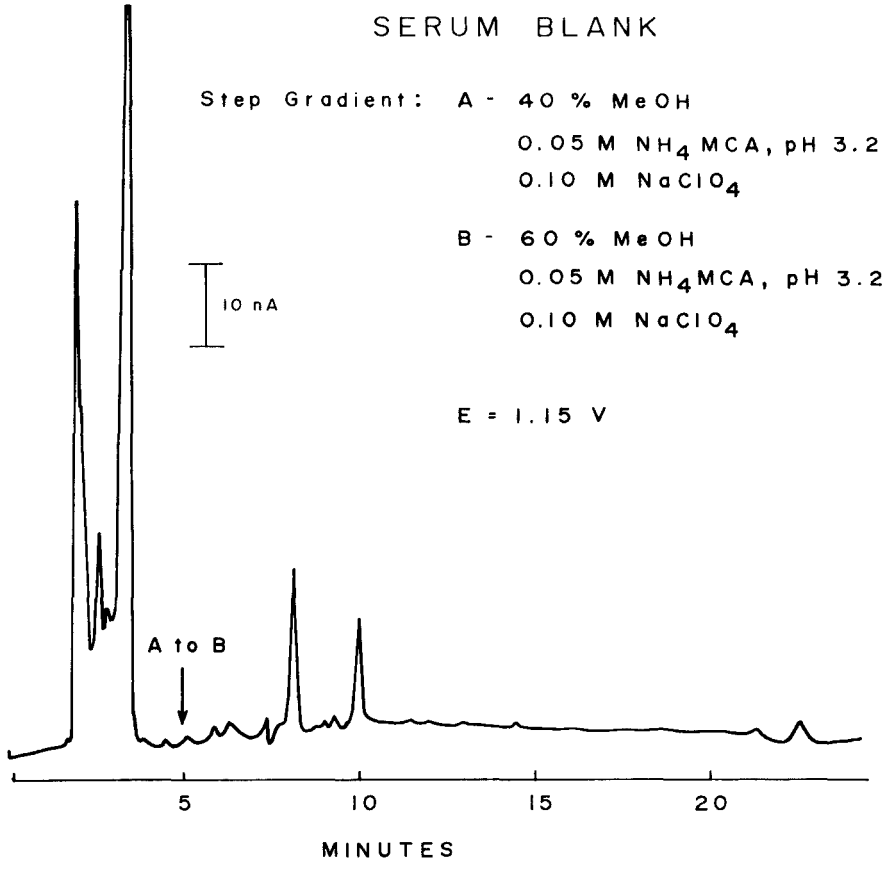

FIGURE 8. Serum blank response for step-gradient elution (A to B) as illustrated in Figure 7.

mobile phase A. Phen, Cod, and NPX could be determined together under isocratic conditions. Urinary recovery results are listed in Tables 3 and 4.

A fabricated C_{18} minicolumn (1.5 cm x 4 mm i.d., 30 µm packing) was evaluated as an alternate sample cleanup tool. After loading a 500 µL urine sample, the column was washed with four

TABLE 2

Serum Recovery Values

Analgesic	Conc.(μg/mL)[a]	% Rec'y[b]	C.V.
APAP	2	100.2	1.0
	10	97.3	2.4
	50	98.1	0.3
SAm	2	101.7	2.0
	10	98.3	3.6
	50	102.0	3.2
SAc	2	101.7	1.4
	10	96.7	2.5
	50	99.8	5.4
Phen	2	97.3	2.4
	10	99.2	2.9
	50	98.5	1.7
MeS	2	99.0	7.4
	10	98.9	1.5
	50	100.6	1.1
NPX	2	99.0	8.9
	10	83.3	10.8
	50	87.9	9.9
Cod[c]	2	105.0	6.3
	10	103.2	2.6
	50	104.0	7.4

a) initial serum concentration
b) n = 4
c) pH 7.0 phosphate, 50% MeOH mobile phase

column volumes (ca. 1.0 mL) of 5% methanol in pH 7.0, 0.1 M phosphate. Four column volumes of 100% methanol were then used to elute and collect the analytes. Endogenous interferences were greatly diminished by this simple procedure to suggest potential value for urinary and other analgesic determinations, especially for analyte pre-concentration where lower level determinations are desired. Unfortunately, the cleanup step did not eliminate an endogenous component which tends to coelute with APAP and exhibit a slightly lower oxidation potential.

TABLE 3

Urine Recovery Values with Step-Gradient Elution

Analgesic	Conc.(μg/mL)[a]	% Rec'y[b]	C.V.
SAm	10	106.6	3.3
	50	100.0	1.8
SAc	10	99.8	10.0
	50	97.2	1.4
Phen	10	112.0	2.1
	50	103.8	3.5
MeS	10	98.6	9.7
	50	102.6	1.0
NPX	10	104.4	3.4
	50	110.0	4.3

a) initial urine concentration
b) n = 4

TABLE 4

Urine Recovery Values with Isocratic Elution

Analgesic	Conc.(μg/mL)[a]	% Rec'y[b]	C.V.
APAP[c]	5	101.7	3.1
	10	101.2	1.6
	50	95.1	0.3
Phen[d]	5	96.9	2.8
	10	96.6	0.8
	50	100.2	0.4
Cod	5	97.9	1.3
	10	93.0	2.9
	50	97.2	2.7
NPX	5	96.7	1.9
	10	95.0	1.9
	50	99.5	0.4

a) initial urine concentration
b) n = 4
c) mobile phase A, E = +600 mV
d) mobile phase = 45% methanol/50% 0.2 M phosphate at pH 5.8

Codeine exhibited extensive tailing and peak broadening even on a relatively new column. Lowering the eluent pH to 5.8 and increasing the column temperature to 45°C improved the peak shape somewhat. A representative urine sample under these conditions is shown in Figure 9. The problem of peak integrity proves to be by far the limiting factor in detectability. Codeine exhibits low molar absorptivity at wavelengths of 254 nm and above (19), therefore, work is currently in progress to circumvent this problem and exploit the sensitivity advantage of electrochemical detection.

Gradient Elution

Employment of a stepwise gradient change from 40 to 60 percent methanol was quite successful. Inspection of Figure 7 shows a small "derivative" type baseline disturbance about 2 minutes after the mobile phase change. This is followed by a very slight rise in baseline. Frequently, the baseline disturbance was more pronounced with the baseline rising asymptotically about 10 nA within two minutes to a new plateau. Parameters involved appear to include dielectric constant, pH, temperature, purity of mobile phase and electrode sensitivity. The mobile phase electrolyte concentration was held constant with 0.05 M buffer and 0.10 M $NaClO_4$ to minimize ionic strength changes. A stepwise mobile phase change from pH 3.0 to 4.0 with 0.05 M MCA buffer and 0.1 M $NaClO_4$ in 40% methanol created a baseline shift of similar shape and magnitude. A less abrupt or smooth eluent change with regard to organic modifier and/or pH may provide a quite acceptable baseline transition. Other workers have recently described notable success with linear gradient elution and discussed some of the parameters involved (20-22). At lower electrode potentials the magnitude of gradient-induced baseline shift decreases with the magnitude of the background current. Gradient elution

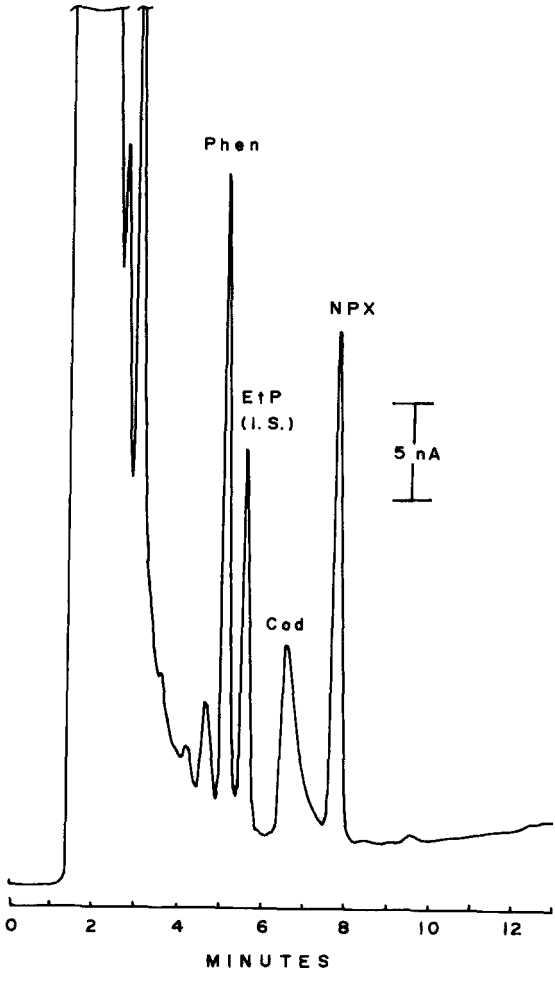

FIGURE 9. Isocratic LC separation of Phen, Cod, and NPX in a spiked urine sample (5 µg/mL). Mobile phase = 0.1 M ammonium phosphate (pH 5.8) in MeOH:H_2O (45:55). Column temp. = 45° C. Detector potential = +1.12 V. Approx. 25 ng of each analyte injected.

is therefore even more amenable to LCEC at lower detector potentials.

It is well known that the mobile phase viscosity changes with methanol content, yielding corresponding changes in frictional heating while eluent is traversing the column. Since background current is temperature dependent, temperature changes will cause observable baseline shifts. The column eluent was thus passed through a section of stainless steel tubing looped in a room temperature water bath to stabilize its temperature. This setup also noticeably decreased random baseline fluctuations, presumably attributed to variable air cooling of the friction-heated eluent. When elevated column temperatures are employed, eluent cooling is extremely effective in reducing total background current.

When the mobile phase is merely altered by organic modifier strength, the EC baseline disturbance has often been observed to be much less than for a 254 nm detector operating at similar sensitivity. Given certain constraints, the application of electrochemical detection to gradient elution separations may frequently equal or surpass the performance of UV detection.

SUMMARY

LCEC has been shown to provide sensitive determination of several analgesics in complex biological samples with minimal sample preparation. Pertinent chromatographic and detection parameters have beem compiled and discussed to facilitate future applications.

Due to the inherent sensitivity of EC detection for these compounds, practical detection limits depend mostly on the degree of interference from endogenous components. Simple extraction or mini-column cleanup procedures can conveniently eliminate the majority of these interferences to extend useful detection limits.

Baseline stability is another important factor in attaining low detection limits. This can be improved by using isocratic elution or continuous gradients, adequate temperature control, electrochemically pure mobile phases, and uniform mobile phase delivery. The results shown here represent determinations achievable with relatively lowcost equipment.

The analgesics evaluated yield diverse UV absorbance and fluorescence response sensitivities but rather consistent amperometric responses. The detector electrode response appears to be predominately diffusion dependent and hence of very similar magnitude for each analyte.

Parallel dual-electrode detection proved convenient for simultaneous determination of APAP along with compounds of higher oxidation potential. Others have demonstrated the additional utility of this electrode configuration in affirming peak identity by comparing detector response ratios for electrodes at adjacent potentials between sample and standard (23,24). This provides an additional parameter of identification comparable to absorbance ratioing with UV detection.

REFERENCES

1. American Drug Index, Billups. N.F., 26 ed., J.B. Lippincott Co. Philadelphia, 1982.

2. Stacher, G., Bauer, P., Schneider, C., Winklehnen, S., and Schmierer, G., Effect of a Combination of Oral Naproxen Sodium and Codeine on Experimentally Induced Pain, Eur. J. Clin. Pharmacol., 21(6), 485 (1982).

3. Ching-Nan, O., and Frawley, V.L., Theophylline, Dyphilline, Caffeine, Acetaminophen, Salicylate, Acetylsalicylate, Procainamide, and N-Acetyl-procainamide Determined in Serum with a Single Liquid-Chromatographic Assay, Clin. Chem., 28,(10), 2157 (1982).

4. Uges, D.R.A., Bloemhoff, H., Christensen, E.K.J., An HPLC Method for the Determination of Salicylic Acid, Phenacetin,

and Paracetamol in Serum, with indications; Two Case-reports of Intoxication, Pharm. Weekbl., 3, 205 (1983).

5. Nielsen-Kudsk, F., HPLC Determination of Some Antiinflammatory, Weak Analgesic and Uricosuric Drugs in Human Blood Plasma and its Application to Pharmacokinetics, Acta. Pharmacol. Toxicol, 47(4), 267 (1980).

6. Broquaire, M., Rovei V., and Braithwaite, R., Quantitative Determination of Naproxen in Plasma by a Simple High-Performance Liquid Chromatographic Method, J. Chromatogr. 224, 43 (1981).

7. Ferrell, W. and Goyette, G., Analysis of Acetaminophen and Salicylate by Reverse Phase HPLC, J. Liq. Chromatogr., 5 (1), 93L (1982).

8. Kinberger, B. and Holmen, A., Simultaneous Determination of Acetaminophen, Theophylline and Salicylate in Serum by High Performance Liquid Chromatography, J. Chromatogr., 229, 492 (1982).

9. Morrell, G., Adusumalli, S. Borden, R.W., and Manthuruthil, S., Simultaneous Determination of Acetaminophen, Salicylic Acid, Dyphylline, and Theophylline by Automated High-Performance Liquid Chromatography, Clin. Chem., 26(7), 964 (1980).

10. Micelli, J.N., Aravind, M.K., Cohen, S.N., and Done, A.K., Simultaneous Measurements of Acetaminophen and Salicylate in Plasma by Liquid Chromatography, Clin. Chem. 25(6), 1002 (1979).

11. Gupta, V.D., Simultaneous Quantitation of Acetaminophen, Aspirin, Caffeine, Codeine Phosphate, Phenacetin, and Salicylamide by High-Pressure Liquid Chromatography. J. Pharm. Sci., 69, 110 (1980).

12. Burgoyne, R.F., Brown, P.R., and Kaplan, S.R., The Simultaneous Assay of Naproxen and Salicylic Acid in Serum using High Pressure Liquid Chromatography, J. Liq. Chromatogr., 3(1), 101 (1980).

13. Gautam, S.R., Chungi, V., Hussain, A., Babhair, S., and Papdimitrou, D., A Direct and Simple Method for the Determination of Salicylamide in Microplasma Samples by High-Performance Liquid Chromatography using Flourescence Detection, Anal. Lett., 14(B8), 577 (1981).

14. Miner, D.J., and Kissinger, P.T., Trace Determination of Acetaminophen in Serum, J. Pharm. Sci., 68, 96 (1979).

15. Miner, D.J., Rice, J.R., Riggin, R.M., and Kissinger, P.T., Voltammetry of Acetaminophen and Its Metabolites, Anal. Chem., 53, 2258 (1981).

16. Fieser, L.R. and Fieser, M., Advanced Organic Chemistry, Reinhold, New York, 1961, p. 758.

17. Surman, P., Voltammetrische Untersuchungen an Opiumalkaloiden, Arch. Pharm., 312, 734 (1979)

18. Korpi, E.R., Phelps, B.H., Granger, H., Chang, W., Linnoila, M., Meek, J.L., and Wyatt, R.J., Simultaneous Determination of Haloperidol and Its Reduced Metabolite in Serum and Plasma by Isocratic Liquid Chromatography with Electrochemical Detection, Clin. Chem., 29(4), 624 (1983).

19. Muhtadi, F.J., and Hassan, M.M.A., Analytical Profiles of Drug Substances, 10, Klaus Florey, ed., Academic Press, New York, 1981, p. 104.

20. St. Claire, R.R. III, Ausari, G.A.S. and Abell, C.W., Determination of Tetrahydroisoquinolines by Reversed-Phase Liquid Chromatography with Gradient Elution and Amperometric Detection, Anal. Chem. 54, 186 (1982).

21. Hadj-Mohammali, M.R., Ward, J.L., and Dorsey, J.G., Rapid Separation and Determination of Thyromimetic Iodoamino Acids by Gradient Elution Reverse Phase Liquid Chromatography with Electrochemical Detection, J. Liq. Chromatogr., 6(3), 511 (1983).

22. Shoup, R.E., Allison, L.A., Mayer, G.S., Anal. Chem., manuscript in preparation.

23. Shoup, R.E. and Mayer, G.S., Determination of Environmental Phenols by Liquid Chromatography/Electrochemistry, Anal. Chem., 54(7), 1164 (1982).

24. Roston, D.A. and Kissinger, P.T., Isolation and Identification of Benzene Metabolites in Vitro with Liquid Chromatography/Electrochemistry, Anal. Chem., 54(11), 1793 (1982).

JOURNAL OF LIQUID CHROMATOGRAPHY, 6(12), 2337-2351 (1983)

ANALYSIS OF TRACE AMOUNTS OF CATECHOLAMINES AND RELATED COMPOUNDS IN BRAIN TISSUE: A STUDY NEAR THE DETECTION LIMIT OF LIQUID CHROMATOGRAPHY WITH ELECTROCHEMICAL DETECTION

Ben H.C. Westerink

Pharmaceutical Laboratories, Department of Medicinal Chemistry, University of Groningen, A. Deusinglaan 2, 9713 AW Groningen The Netherlands

ABSTRACT

Analysis of catecholamines and related metabolites is often based on direct injection on the HPLC column of supernatants of centrifuged brain homogenates. In this study we have investigated to what extent direct injection techniques are also useful for analysis in the picogram-range. The use of Sephadex G 10 (which allows a rapid sample purification for 11 compounds) appeared an attractive alternative when direct injection techniques cannot be applied. Various aspects of the routine use of the electrochemical detector at a sensitive setting are discussed. Finally the identity of small peaks in the chromatogram is addressed.

INTRODUCTION

An increasing number of methods based on liquid chromatography and electrochemical detection (LC-ED) have been described for analysis of monoamines and related metabolites in brain tissue (1,2). These methods were mainly concerned with the assay of the neurotransmitters dopamine (DA), noradrenaline (NA), 5-hydroxytryptamine (5-HT) and their metabolites 3,4-dihydroxyphe-

 0148-3919/83/0612-2337$3.50/0

nylacetic acid (DOPAC), homovanillic acid (HVA) and 5-hydroxyindolacetic acid (5-HIAA) in various brain regions. Concentrations of these compounds are in the nanogram to microgram-range (0.2 - 12 µg/g; amounts of tissue available usually less than 50 mg). However, various other metabolites of DA and NA such as 3-methoxytyramine (3-MT), 3,4-dihydroxyphenylethyleneglycol (DOPEG), 3-methoxy-4-hydroxyphenylethyleneglycol (MOPEG), 3,4-dihydroxyphenylalanine (DOPA) and normetanephrine (NM) are found in the brain in the picogram-range (3-30 ng/g). In the same order of magnitude are the levels of DA, DOPAC and HVA in the so-called non-dopaminergic areas (brain regions with a relatively small dopaminergic innervation such as the frontal cortex, stem, hippocampus and cerebellum). Quantification of these amounts, which are two orders of magnitude less than the usually studied contents, require a careful analytical approach as these assays reach the detection limits of the routinely performed LC-ED techniques.

Various authors have described attractive methods based on direct injection on the HPLC column of the supernatant of centrifuged brain homogenates (3,4,5). These methods combine an easy sample handling with a high analytical recovery, and allow quantification of a large series of compounds (4-6) in a single chromatographic run. However, when this analytical approach is applicated to the analysis in the pg-range, interfering peaks in the chromatograms are to be expected. Purification of the brain samples is the classical answer to this analytical problem, and a number of purification procedures for monoamines and related metabolites are found in the literature (6,7,8).

In this study we have investigated to what extent direct injection techniques are also useful for analysis in the pg-range. When these techniques could not be used, pretreatment of samples on Sephadex G 10 was performed. This paper is also concerned with two aspects which require special care when the assay is in the pg-range: the routine use of an electrochemical detector at the highest sensitive setting, and the identity of small peaks in the chromatogram.

METHODS

Reagents

Materials and their sources were as follows: dopamine.HCl, noradrenaline bitartrate, 3,4-dihydroxyphenylalanine, 3,4-dihydroxyphenylethyleneglycol, normetanephrine (Sigma), 3,4-dihydroxyphenylacetic acid, homovanillic acid, and 5-hydroxyindolacetic acid (Fluka). All other chemicals were of analytical reagent grade and were purchased from E. Merck. All aqueous solutions were prepared from deionized water distilled in glass. Stock solutions of

the various compounds consisted of 100 µg/ml in 0.01 M formic acid and 0.1 mM EDTA and were stored in portions of approx. 1 ml in the freezer (-80°). Standard solutions were prepared every 2 weeks from a portion of the stock solutions after appropriate dilution in 0.01 M formic acid and 0.1 mM EDTA. Ascorbic acid (final concentration 0.01 mM) was added to the stock solution of 5-HIAA. The mobile phases used for the various assays are summarized in Table 1. The solutions were filtered before use (0.5 µm Millipore filter).

Animals, drug treatment and dissection

Male albino rats of 175-200 g weight (Wistar, C.D.L., Groningen, The Netherlands) were used. Pargyline.HCl was administered intraperitoneally. The animals were killed by decapitation. The brain structures dissected included the frontal cortex, striatum, hypothalamus, hippocampus, brain stem and cerebellum. The tissue samples were frozen on solid CO_2. Samples were kept at -80°C until assayed.

Isolation procedure on Sephadex G 10

Several columns (at least 40) can be handled in one run with the help of automated pipettes. Before use the columns were washed with 3.0 ml 0.02 M ammonia and 3.0 ml 0.01 M formic acid. Tissue samples (up to 150 mg) were homogenised in 1.0 ml 0.1 M perchloric acid. Following centrifugation (4000 g; 4°C) the supernatants were put on Sephadex G 10 columns (5 x 70 mm) prepared in long-size Pasteur pipettes. Two different routes of purification are possible (route I and route II).

Route I: After tissue extracts have passed through the columns, 1.0 ml 0.01 M formic acid and 1.5 ml 0.02 M ammonia (containing 0.01 mM ascorbic acid and 0.1 mM EDTA) were added. NA, DA, 3-MT, DOPAC, HVA and 5-HIAA are then eluted with 1.5 ml 0.02 M ammonia (containing 0.01 mM ascorbic acid and 0.1 mM EDTA). Because of instability of catecholamines in ammonia this fraction is collected in a vial to which 50 µl concentrated formic acid was added.

Route II: After tissue extracts have passed through the columns, 2.0 ml of a solution of 0.01 M formic acid and 0.1 mM EDTA was added. Tyrosine (TYR), DOPA, DA, NA, NM, 3-MT, DOPEG and MOPEG were then eluted with 1.0 ml of the formic acid solution followed by 1.5 ml of a phosphate solution (5 mM $Na_2HPO_4.2H_2O$ and 0.1 mM EDTA). DOPAC, HVA and 5-HIAA were subsequently eluted with 2.0 ml of a solution containing 0.02 M ammonia, 0.1 mM EDTA and 0.01 mM ascorbic acid. This fraction was collected in a vial to which 50 µl concentrated formic acid was added.

The columns are stored in 0.02 M ammonia. The isolation procedure is summarized in Fig. 1. The columns do not need regeneration; they are refilled after 6 months use.

Table 1.

Optimised chromatographic conditions for the various assays.

Compound	% methanol	type eluent	pH	potential setting (mV)
TYR	0	acetate/phosphate	5.8-6.0	850
DOPA	0	0.1 M TCA	3.1	550
DA, NA, DOPAC, 5-HIAA	15-20%	0.1 M TCA	3.9	550
HVA, 3-MT	15-20%	0.1 M TCA	3.9	700
free DOPEG, total DOPEG	0	citrate/phosphate or acetate/phosphate	4.8-5.9 4.6-5.0	550
free MOPEG, total MOPEG	0-3%	acetate/phosphate	4.6-5.0	750
NM	5	0.1 M TCA	3.4	850

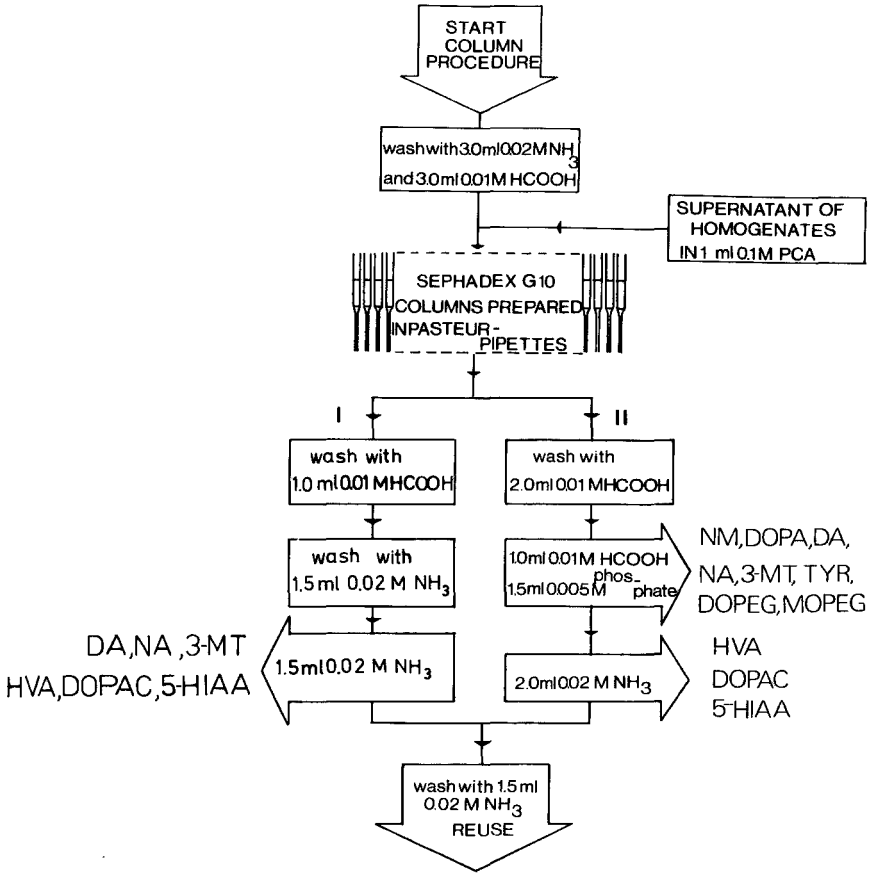

Fig. 1. Flow chart of the isolation procedures.

Chromatography

A Waters (model 6000A) liquid chromatograph was employed in conjunction with an electrochemical detector. A detector based on a rotating disc electrode was used (9). A potentiostat from Bioanalytical Systems, type LC-2A, has been used. The detector potentials for the various assays are summarized in Table 1. The column (150 x 4.6 mm i.d.) was packed with a slurry of Nucleosil 5 C 18 (Mackerey-Nagel, Düren, F.G.R.) reverse-phase material in methanol/carbon tetrachloride (20/80, v/v). The slur-

ry (10% w/v), degassed in an ultrasonic generator, was pumped into the chromatographic column at the highest possible flow rate. Columns were washed by passing 200 ml of methanol and further equilibrated with the mobile phase. Columns were refilled after 5-6 months of use. To maintain the integrity of the microparticulate column a precolumn (70 x 4.6 mm i.d.; filled with Nucleosil 5 C 18) was placed between the pump and the injection valve. The precolumn was packed according to the same procedure as the analytical column. Analyses were performed at a flow rate of 60 ml/h at room temperature. When supernatants of brain homogenates were directly injected into the chromatograph, a guard column filled with reverse phase material (Chrompack; 75 x 2.1 mm i.d.) was placed between the injection valve and the analytical column. Material was injected with a high-pressure injection valve (Rheodyne) fitted with a 50-500 µl sample loop. Concentrations in brain samples were calculated with the aid of (linear) calibration curves obtained after the injection of pure standards. Recoveries of the various compounds were determined by analysing spiked brain tissue. If the Sephadex eluates had to be preserved till the next day, they were stored at 4°C. The chromatographic conditions for the various assays have been described earlier (9,10,11,12) and are summarized in Table 1.

RESULTS AND DISCUSSION

The necessity of Sephadex G 10 as purification step

HPLC of catecholamines and related compounds is usually carried out with alkylsulphonate-containing mobile phases and a reverse phase column (1,2,3,4,5). Alkylsulphonates give the reverse phase material cation-exchanging properties ("soap"-chromatography) and for this protonated catecholamines are strongly retarded on the HPLC column. Asmus and Freed (13) have described the use of trichloracetic acid (TCA) containing eluents as alternative to the alkylsulphonates. TCA is thought to form ion-pair complexes with protonated catecholamines and these ion-pairs are retarded on the reverse phase material. It is our experience that the use of TCA-solutions results in a somewhat better chromatographic separation of the studied compounds when compared with eluents based on alkylsulphonates. Moreover the noise level of the detector signal was more favourable in the case of TCA-solutions. During this study we have developed a TCA-containing eluent which could be used for simultaneous assay of 6 compounds. When the pH of the eluent was 3.9 ± 0.1, separation was achieved between NA, DOPAC, DA, 5-HIAA, HVA and 3-MT (Fig. 2). In Fig. 2[a] a chromatogram obtained after direct-injection of a homogenate of striatal tissue is depicted.

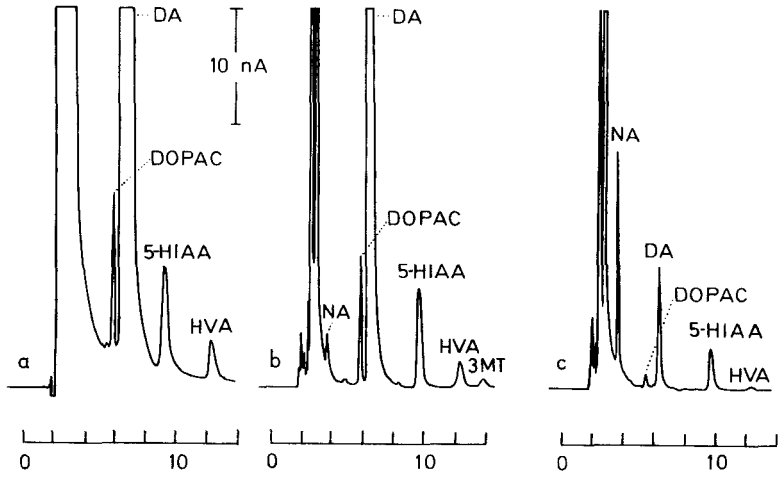

Fig. 2. (a) Chromatogram of 40 mg striatal tissue after direct injection of centrifuged homogenate. (b) Chromatogram of 48 mg striatal tissue after isolation on Sephadex G 10 (route I). (c) Chromatogram of 42 mg hypothalamic tissue after isolation on Sephadex G 10. Chromatographic conditions: mobile phase: 78% 0.1 M TCA, pH 3.9, 22% methanol; flow 1.0 ml/min; 100 µl sample loop; potential setting 750 mV.

It is clear from this figure that in case of striatal tissue the direct-injection method is acceptable for quantification of DOPAC, DA, 5-HIAA and 5-HT; but not for NA. The 5-HT and 5-HIAA content is in the same order of magnitude throughout the brain (Table 2), which means that for these compounds the direct injection technique is always the method of choice. However, in several areas of the brain the concentrations of DA, DOPAC and HVA are 20-100 times lower than in the striatum (Table 2). When these amounts are to be determined attenuation of the detector signal to 20-100 times that of Fig. 2 is necessary. Fig. 2 indicates that at such a sensitive detector setting the broad and tailing front of the chromatogram will seriously disturb the quantitation of DA, DOPAC and (to a less extent) HVA. The quality of the chromatogram was much improved when the brain samples were pretreated on Sephadex G 10 columns (Fig. 2b,c). Note that quantification of NA is now also possible. Only 5-HT cannot be determined as this compound is strongly bound to the Sephadex resin. The assays of the NA metabolites DOPEG and MOPEG are other examples of assays in which direct injections of homogenates cannot be used. Retardation on a reverse-phase column with TCA or alkylsulphonate is

Table 2.

Concentrations of the various compounds in 6 brain areas of decapitated rats. The values are given in ng/g ± S.E.M. (n: 4-6), except for TYR which is given in µg/g.

Compound	Striatum	Hypothalamus	Frontal Cortex	Hippocampus	Stem	Cerebellum
TYR	12.1± 0.3	11.8± 0.5	10.8± 1.3	n.d.	n.d.	11.8± 0.9
DOPA	7.3± 0.4	7.7± 0.6	4.3± 0.2	n.d.	n.d.	3.6± 0.2
DA	9856 ±92	246 ±92	52 ± 3.1	4.6± 0.3	51 ±6	2.8± 0.2
DOPAC	873 ±42	35 ± 2.5	52 ± 3.3	3.0± 0.3	11.8±0.3	2.2± 0.2
HVA	1044 ±27	34 ± 4.5	67 ± 9.1	5.6± 0.3	20.0±1.8	8.0± 1.4
3-MT*	20.5± 0.9	< 1	< 1	< 1	< 1	< 1
NA	136 ±18	1450 ±58	237 ±58	352 ±61	n.d.	258 ±31
NM	4.3± 1.0	13.8± 2.6	8.0± 1.0	12.9± 1.3	7.9±1.0	12.6± 1.3
free DOPEG	7.2± 0.5	16.2± 3.5	n.d.	11.9± 1.1	10.7±1.3	15.0± 3.2
total DOPEG	25 ± 0.5	170 ± 2.8	n.d.	39 ± 2.5	55 ±5.4	49 ± 6.7
free MOPEG	11.3± 1.8	19.5± 3.8	n.d.	15.7± 2.1	38.7±4.0	45.9± 4.0
total MOPEG	61 ± 6.5	117 ±12.0	n.d.	78 ± 6.9	122 ±4.3	66 ± 1.4
5-HIAA	282 ±23	462 ±35	152 ±23	272 ±23	n.d.	42 ± 4

*: rats killed by micro-wave.

n.d. = not determined.

not possible with alcoholic derivatives such as DOPEG or MOPEG. That pretreatment of samples on Sephadex G 10 is required for quantification of DOPEG is illustrated in Fig. 3[a] and 3[b]. Determination of free DOPEG was achieved with a phosphate-acetate buffer (Table 1; manuscript in preparation). The need of sample purification was also established for the determination of DOPEG sulphate, free MOPEG, MOPEG sulphate, DOPA and NM (results not shown).

The procedure of purification of samples on Sephadex G 10 columns is depicted in Fig. 1. Two different routes are possible. Route I, which was developed during this study, concentrates DA, NA, 3-MT, tyrosine (TYR), DOPAC, HVA and 5-HIAA in a relatively small fraction of 1.5 ml. DOPEG and MOPEG are not quantitatively recovered in this fraction, whereas chromatographic separation of NM, DOPA and interfering compounds was not complete. Route II has been described in an earlier study (9). Purification via this route is more complete, as the method affords two fractions. The first fraction contains the catecholamines, DOPEG and MOPEG. Endogenous levels of DOPA and NM can also be quantified from this fraction according to the appropriate chromatographic conditions (Table 1). The acidic metabolites are now found in a second

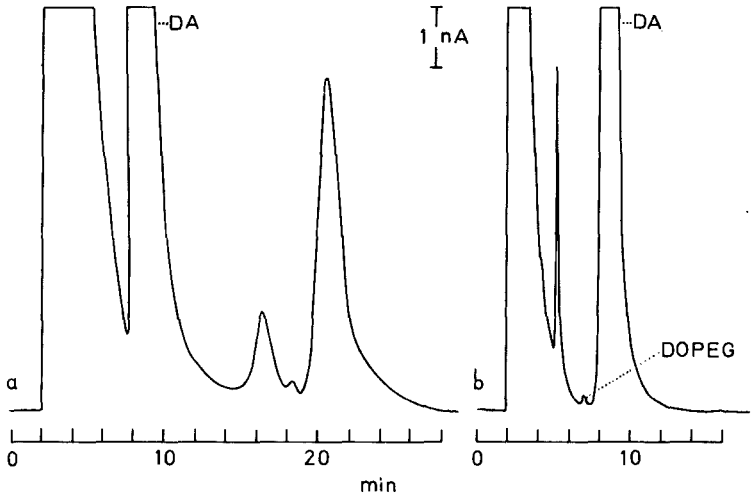

Fig. 3. (a) Chromatogram of 55 mg striatal tissue after direct injection of centrifuged homogenate. (b) Chromatogram of 60 mg striatal tissue after isolation on Sephadex G 10 (route II). Chromatographic conditions: mobile phase citrate/phosphate buffer 0.35 M, pH 5.8; 50 µl sample loop; flow 1.0 ml/min; potential setting 550 mV.

fraction. Route II, which is somewhat more time-consuming than route I, results in a better purification of brain samples. The analytical recoveries of both routes were between 80 and 90%. Internal standards were not used. From 18 rat brains we have analyzed the bilateral striatal structures with the direct injection method (left striatum) and with the method including Sephadex G 10 (route I)(right striatum). The results (µg/g ± S.E.M., n = 18), were, DA: 9.7 ± 0.4 (left) and 9.7 ± 0.3 (right); DOPAC: 0.57 ± 0.03 (left) and 0.55 ± 0.02 (right); HVA: 0.73 ± 0.03 (left) and 0.68 ± 0.03 (right). From these data it is concluded that both methods yield similar recoveries.

In summary, there are several conditions when direct injection techniques cannot be used. The use of small Sephadex G 10 columns is then an attractive alternative. The eluates of the Sephadex procedure consist of relatively clean solutions and allow the detection of small amounts of compounds with minimal interference of other biological substances. Purification on Sephadex G 10 is possible for a total number of 11 compounds. This versatile application is an advantage to currently used purification methods such as alumina pretreatment, ion-exchange chromatography, or solvent-solvent extraction (6,7,8), as the latter methods are restricted to catechol-containing compounds. As the columns can be used during many months and for a variety of assays, they are very suitable for routine determinations. Handling of the columns with the help of automated pipettes takes only some seconds per column. New Sephadex G 10 material may contain some compounds that interfere with the chromatographic separation. These compounds disappear after excessive washing of the resin or during routine use of the columns.

Routine use of the electrochemical detector

In our laboratory the HPLC is carried out with a rotating-disk electrochemical detector. The rotating-disk detector prosesses some advantages over the widely used thin-layer cells that are of importance for determination of compounds in the pg-range (9). The rotation of the electrode results in an increased sensitivity of the detection (by 250-600%, depending of the compound). The sensitivity of the detector is in the range of 3-6 nA/ng for the compounds in this study (50-200 µl sample loop; retention time less than 10 min). The most sensitive setting during routine use was 2 nA/V. If we assume 1% of the full scale value as detection limit, it means that 0.01 x 2 nA = 20 pA can be detected. 20 pA corresponds to 3-7 pg per injection. When a 200 µl sample loop is used and assuming that the compounds are eluted in 1.5 ml, it can be calculated that $\frac{1.5}{0.2}$ x (3-7) = about 25-50 pg/sample is the detection limit of the method during routine use. The di-

lution of the sample during the Sephadex G 10 procedure is a limitation of the method. However, several assays (HVA, 5-HIAA, 3-MT) permit the use of a 500 µl sample loop with virtually no peak broadening.

When pg amounts are to be detected, special attention should be given to the following aspects:

--When various mobile phases were compared, the signal-to-noise levels varied as follows: phosphate/citrate buffer = phosphate/acetate buffer > trichloracetic acid containing eluent > alkylsulphonate containing eluent. In general the noise level increased with a decreasing pH value. It was often noticed that a mobile phase of pH < 4 resulted in an unstable baseline. These baseline fluctuations (in which the pump-pulsation was sometimes recognized) could be overcome by the addition of EDTA to the mobile phase (final concentration: 10^{-4} M). This indicates formation of Fe^{2+} in the HPLC equipment, probably caused by the relatively low pH of the buffer.

--External sources of electrical noise can seriously disturb the baseline of the detector, especially at a sensitive setting. This problem is usually overcome by placing electronic filters between the HPLC equipment and the mains supply.

--The various parts of the HPLC and detector equipment should be earthed properly. A Faraday cage around the detector should be used when the analysis is in the pg-range.

--An unfavourable signal-to-noise level is not always solved by repacking the carbon paste electrode. A carbon electrode can be used during several weeks/months. A high residual current and an instable baseline are indications that the electrode needs repacking (when other sources of baseline noise are excluded).

It should be noted that these precautions do not prevent the fact that often an inexplicable day-to-day fluctuation in the amount of electrical noise was noticed.

Identification of small amounts in chromatograms

Determination of compounds near the detection limit usually means quantification of one of the smallest peaks in the chromatogram. It is therefore of utmost importance to have sufficient certainty about the identity of the peak to be calculated. Apart from the typical chromatographic behaviour, there are in general three possible ways to confirm the identity of these compounds.

a) Determinations of a voltammogram. Chromatograms of both a purified brain extract and a standard solution are recorded at various oxidation potentials. The studied compound and the authentic one should have similar electrochemical behaviour. In Fig. 4 the electrochemical behaviour of endogenous DOPA,

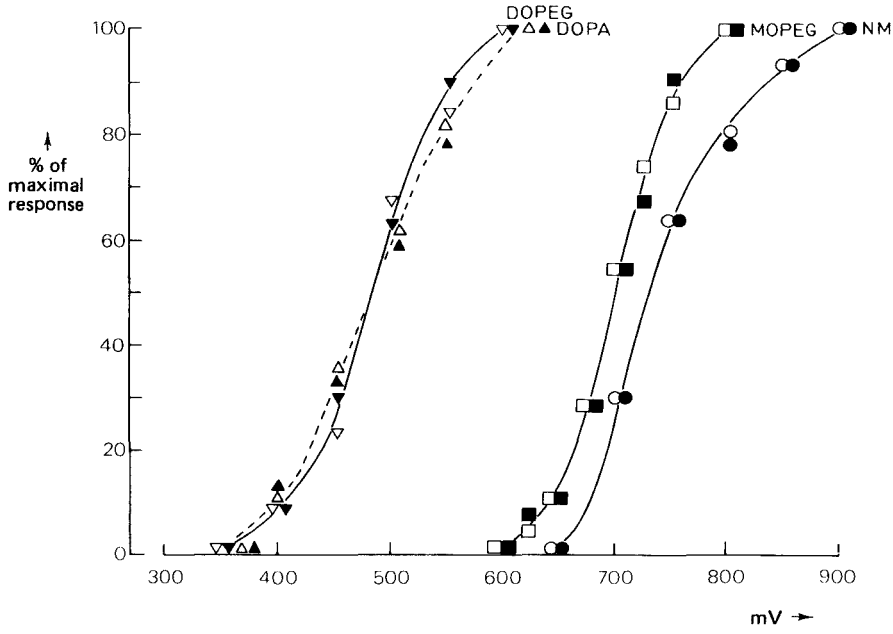

Fig. 4. Influence of the electrode potential setting on the response of authentic DOPA, DOPEG, MOPEG and NM (open symbols) and on the compounds isolated from brain tissue (closed symbols).

free DOPEG, free MOPEG and NM isolated from the brain tissue, is compared with corresponding standard solutions. The similarity of the voltammograms supports the specificity of the assay.

b) Catecholamines and related amino acids are retarded on Sephadex G 10 columns as ion-pair complexes with perchlorate (9). If brain samples are homogenised in 0.1 M HCl instead of perchloric acid, the former compounds do not bind to the Sephadex resin and disappear from the chromatograms (acids such as HVA, 5-HIAA and DOPAC do not require perchlorate and these compounds remain in the chromatogram). This method has been used in our laboratory to support the identity of endogenous DOPA, NM and 3-MT in brain samples.

c) The most elegant way to contribute to the identity of a compound is the use of selective enzyme inhibitors. Inhibition of the enzymatic reaction can remove certain metabolites from the brain (and subsequently from the chromatograms). Concentrations of oxidative deaminated metabolites such as DOPEG, MOPEG,

Table 3.

Effect of monoamine oxidase inhibition (75 mg/kg pargyline, i.p.) on the levels of the oxidative desaminated metabolites of DA and NA in the striatum of rats. Values are given in ng/g ± S.E.M. (n).

Compound	time of pre-treatment with pargyline (h)	controls	pargyline treated
DOPAC	1	873 ±42 (5)	22 ± 5.9 (3)
HVA	1	1044 ±27 (5)	141 ±14.6 (3)
free DOPEG	3	7.2± 0.5 (6)	< 5
total DOPEG	3	25.0± 0.5 (4)	< 5
free MOPEG	3	11.3± 1.8 (4)	< 5
total MOPEG	3	61 ± 6.5 (6)	23.8± 4.2 (3)

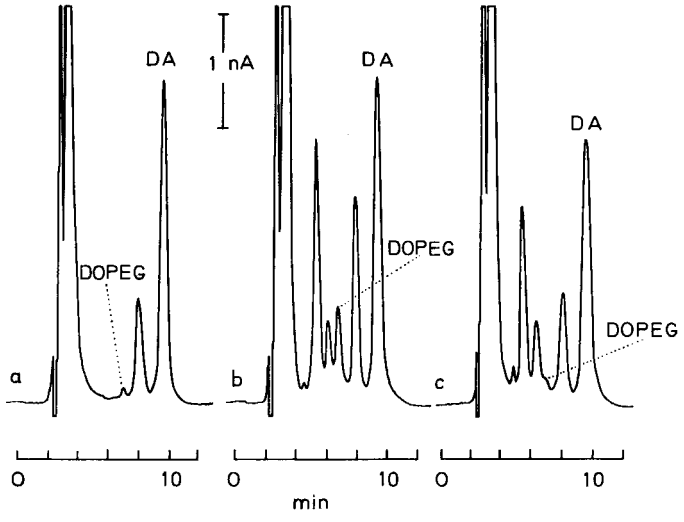

Fig. 5. (a) Chromatogram of 64 mg hypothalamic tissue (50% of the sample). (b) Chromatogram of the remaining 50% of the same sample after thermic hydrolysis (10', 100°C). (c) Chromatogram of 40 mg hypothalamic tissue after thermic hydrolysis (10', 100°C). The rat was pretreated with pargyline.HCl (100 mg/kg) for 3 hours. Chromatographic conditions: isolation on Sephadex G 10 (route II), HPLC conditions see legend to Fig. 3.

DOPAC; HVA and 5-HIAA are considerably reduced after monoamine oxidase inhibition (Table 3). Fig. 5[b] shows the chromatogram of a brain extract after thermic hydrolysis. The hydrolysis induced a pronounced rise in the "DOPEG" peak (probably caused by hydrolysis of DOPEG-sulphate), but the chromatogram does not seem very reliable as various compounds eluted with retention times near that of DOPEG. Pretreatment of the rat with a monoamine oxidase inhibitor (pargyline.HCl; 100 mg/kg), virtually removed "DOPEG" from the chromatogram, thereby confirming its identity (Fig. 5[c]).

Other pharmacological tools which can be used for identification of compounds are tropolone and reserpine. The catechol-O-methyl transferase inhibitor tropolone induces a selective and pronounced decrease (> 90%) in brain concentrations of methylated metabolites such as 3-MT and HVA. Reserpine is known to deplete (> 90%) catecholamine stores in nervous tissue.

ACKNOWLEDGEMETS

The author wishes to thank Mrs. Aaf Westerbrink for valuable technical assistance, and Mrs. Nelly Teeuwen for help in preparing the manuscript.

REFERENCES

1. Felice, L.J., Felice, J.D. and Kissinger, P.T., Determination of catecholamines in rat brain parts by reverse-phase ion-pair liquid chromatography, J. Neurochem. 31, 1461, 1978.

2. Sasa, S. and Blank, C.L., Determination of serotonin and dopamine in mouse brain tissue by high performance liquid chromatography with electrochemical detection, Anal. Chem. 49, 354, 1977.

3. Magnusson, O., Nilsson, L.B. and Westerlund, D., Simultaneous determination of dopamine, DOPAC and homovanillic acid, J. Chromatogr. 221, 237, 1980.

4. Kilts, C.D., Breese, G.R. and Mailman, R.B., Simultaneous quantification of dopamine, 5-hydroxytryptamine and four metabolically related compounds by means of reversed-phase high-performance liquid chromatography with electrochemical detection, J. Chromatogr. 255, 347, 1981.

5. Wagner, J., Palferyman, M., Zraika, M., Determination of DOPA, DOPAC, Epinephrine, Norepinephrine, α-Monofluoromethyl dopa and

α-Difluoromethyl dopa in various tissues of mice and rats using reversal-phase ion-pair liquid chromatography with electrochemical detection, J. Chromatogr. 164, 41, 1979.

6. Morier, E. and Rips, R., A new technique for simultaneous assay of biogenic amines and their metabolites in unpurified mouse brain, J. Liquid Chromatogr. 5, 151, 1982.

7. Saraswat, L.D., Holdiness, M.R., Justice, J.B. et al., Determination of dopamine, homovanillic acid, and 3,4-dihydroxyphenylacetic acid in rat striatum by high performance liquid chromatography with electrochemical detection, J. Chromatogr. 222, 353, 1981.

8. Smedes, F., Kraak, J.C. and Poppe, H., Simple and fast solvent extraction system for selective and quantitative isolation of adrenaline, noradrenaline and dopamine from plasma and urine, J. Chromatogr. 231, 25, 1982.

9. Westerink, B.H.C., Mulder, T.B.A., Determination of picomole amounts of dopamine, noradrenaline, 3,4-dihydroxyphenylalanine, 3,4-dihydroxyphenylacetic acid, homovanillic acid, and 5-hydroxyindolacetic acid in nervous tissue after one step purification on Sephadex G-10, using high performance liquid chromatography with a novel type of electrochemical detection, J. Neurochem. 36, 1449, 1981.

10. Westerink, B.H.C. and Spaan, S.J., Estimation of the turnover of 3-methoxytyramine in the rat striatum by HPLC with electrochemical detection: implications for the sequence in the cerebral metabolism of dopamine, J. Neurochem. 38, 342, 1982.

11. Westerink, B.H.C., van Es, T.P. and Spaan, S.J., Effects of drugs interfering with dopamine and noradrenaline biosynthesis on the endogenous 3,4-dihydroxyphenylalanine levels in rat brain, J. Neurochem. 39, 44, 1982.

12. Westerink, B.H.C. and Wirix, E., On the significance of tyrosine for the synthesis and catabolism of dopamine in rat brain: evaluation by HPLC with electrochemical detection, J. Neurochem. 40, 758, 1982.

13. Asmus, P.A. and Freed, C.R., Reversed-phase high-performance chromatography of catecholamines and their congeners with simple acids as ion-pairing reagents, J. Chromatogr. 169, 303, 1979.

JOURNAL OF LIQUID CHROMATOGRAPHY, 6(12), 2353-2373 (1983)

HIGH-SPEED LC ANALYSIS USING ELECTROCHEMICAL DETECTION

J.M. Di Bussolo, M.W. Dong and J.R. Gant

The Perkin-Elmer Corporation
Norwalk, Connecticut 06855

ABSTRACT

The chromatographic performance of an electrochemical detector incorporating a flowcell with improved dispersive characteristics has been evaluated for use in high-speed liquid chromatography. High-speed C18/3 μm columns, 100 x 4.6 mm, i.d. were found to be well matched to this detector with respect to extra-column contributions to band broadening. The capabilities of this high-speed LC-EC system are demonstrated by a 3-minute separation of phenols and a 4-minute separation of catecholamines and acetominophen.

INTRODUCTION

In 1981, several publications by DiCesare et al. provided an introduction to practical high-speed liquid chromatography (LC) (1,2). The importance of considering all components of the LC system, in order to optimize system performance, was clearly demonstrated in studies carried out examining the relationship between column geometry and the extra-column contributions to

 0148-3919/83/0612-2353$3.50/0

peak dispersion, the so-called instrumental bandwidth (IBW). As a result of this effort, the first commercial LC system designed for high-speed analysis became available (1).

Important features of this system include a low dispersion injector, low volume (2.4 µL originally, now 1.4 µL) detector flowcell, fast detector response time (135 milliseconds originally, now 20 milliseconds) and short, 0.007 inch i.d. connecting tubes. This system is compatible with short columns (e.g. 100 or 33 mm long by 4.6 mm i.d.) packed with 3 µm particles. Reduction in particle size from 10 µm or 5 µm to 3 µm provides two main advantages. As particle size decreases, the column length required to achieve a given efficiency decreases proportionally. Also as particle size decreases, the optimum mobile phase velocity increases. Therefore, shorter columns at higher flow rates achieve similar separations in reduced times as discussed below.

The intervening years have seen rapid growth (3-10) in the acceptance of high-speed LC and significant improvements over initial systems in several respects. Specifically, further reductions in instrumental bandwidth contributions of connecting tubing (11), detectors (12), and injectors (13) are responsible for these advances.

All of these early developments occurred using the most commonly encountered variable wavelength UV detector. A similar path of development is being traversed by fluorometric (14) and RI detection (15) where IBW values of 40 and 55 µL, respectively, have been reported. To-date, little has been reported with respect

to high-speed liquid chromatography with electrochemical (EC) detection (16). However, many practical applications (e.g. 17-20) and several good discussions of basic detection principles (21, 22) have been published using EC detection. The purpose of this communication is to report the results of preliminary investigations of the high-speed capabilities of LC-EC.

EXPERIMENTAL

All chromatographic equipment used in this study is available from The Perkin-Elmer Corporation (Norwalk, CT). Peak dispersion studies and high-speed LC of catecholamines were performed with a SERIES 10 pump. Other high-speed analyses were performed with the SERIES 4 Liquid Chromatograph. Injections were made through a Model 7125S injector equipped with either a 6 µL or a 20 µL sample loop. Samples were chromatographed on HS-3 C18 (100 x 4.6 mm i.d. - part number 0254-1501) and 3x3 C18 (33 x 4.6 mm i.d. - part number 0258-0160) columns containing 3 µm C18 bonded phase particles. Short lengths of 0.007" i.d. stainless steel tubing were used for injector-to-column connections. An LC-85B variable wavelength UV detector equipped with a 1.4 µL flowcell was used for peak dispersion studies.

Amperometric detection was accomplished with the LC-4B electrochemical detector equipped with TL-5 glassy carbon electrode cell block and an Ag/AgCl reference electrode. For high-speed LC-EC, the plastic top half of the TL-5 cell block was stainless steel and also served as the auxiliary electrode. In other cases, the metal outlet

tube of the reference compartment served as the auxiliary electrode (Figure 2). Column-to-detector cell connections were made with either 0.011" i.d. Tefzel tubing (Zeus Industrial Products, Raritan, NJ) or 0.031" i.d. Teflon tubing.

Phenols and catecholamines were purchased from Sigma Chemical Company, St. Louis, MO or Aldrich Chemical Company, Milwaukee, WI. Mobile phases consisted of HPLC grade organic modifiers and deionized, distilled water. Other mobile phase additives were analytical-reagent grade. Mobile phase compositions are listed in Figure legends.

Instrumental bandwidths of the EC detector were estimated by analyzing peaks produced by 6 μL injections of phenol solution (100 ng/μL) through the chromatographic system in which the EC cell was connected directly to the injector (Figure 1). Phenol was then

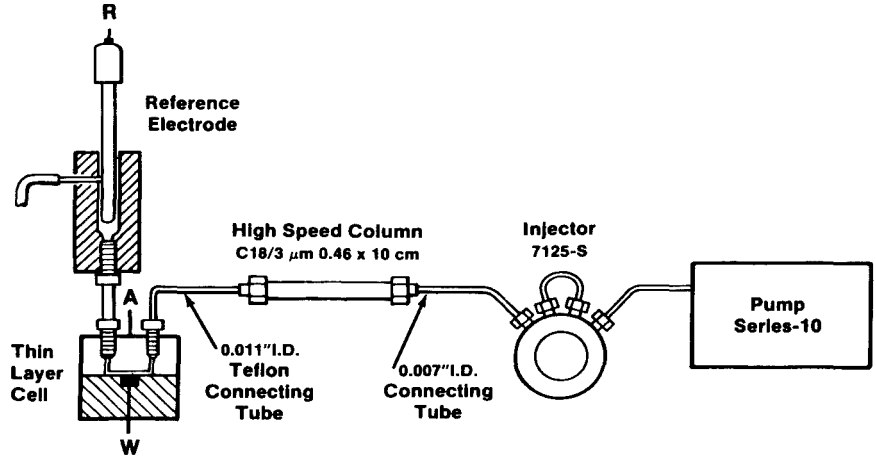

FIGURE 1
High-Speed LC-EC System.

detected at an applied potential of +1.0 V with a mobile phase of 50% acetonitrile in 0.2 M $NaClO_4$, 5 mM sodium citrate, pH 5.4. A 1-meter coil of 0.007" stainless steel tubing was placed between the injector and pump in order to produce sufficient backpressure to allow proper operation of the pulse dampener. In order to determine the upper limit of the cell volume contribution to peak dispersion, the outlet of the cell was connected to the LC-85B UV detector via a short length of 0.007" i.d. stainless steel tubing (Figure 2) with a specially made low-volume end fitting. Phenol peaks were then detected at 280 nm. By connecting the LC-85B directly to the injector, dispersion due to the system without the EC cell was estimated. Bandwidths (4 sigma) were calculated

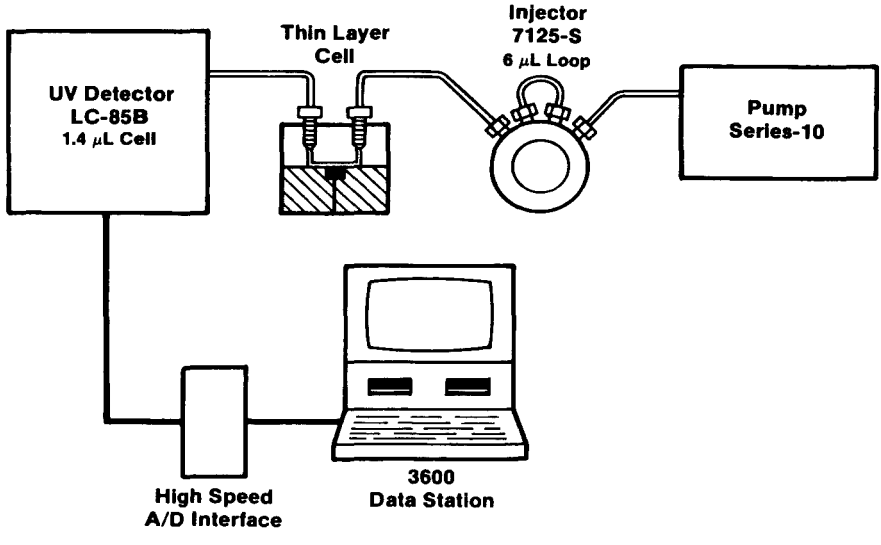

FIGURE 2

System for estimating EC flowcell hydraulics' contribution to dispersion.

by width at half-heights as measured on recorder paper and by computer determination of central moments.

Detector output signals were acquired by a Model 3600 Data Station via the Chromatography Interface (Figure 2) which is a high-speed analog to digital converter. Data acquisition and storage were controlled by software written in BASIC. Central moments of peaks were then determined as discussed by Grushka, et al. (23) using a second BASIC program. An abbreviated algorithm of this program is shown in Figure 3.

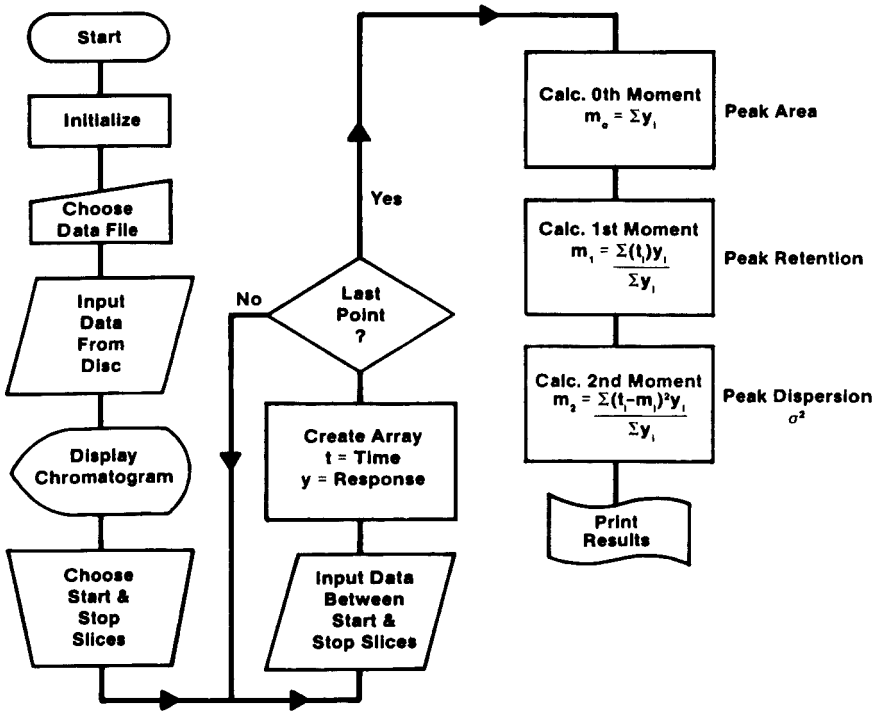

FIGURE 3

Flow chart for computerized Central Moments Determination.

RESULTS AND DISCUSSION

Instrumental Bandwidth

IBW can be defined as the band broadening of a solute zone passing through the LC system caused by all the system components except the column. IBW is determined by injecting a solute into the chromatograph with the column replaced by a zero dead volume connection (or appropriate capillary tubing directly connecting the injector and detector) and measuring the volume of the resultant eluted peak. Replacing the column with a zero-dead volume union in Figure 1 illustrates such a system. IBW is equal to four times the standard deviation (σ) of the eluting peak.

The value of σ can be estimated in many ways, analogous to the many methods of determining theoretical plate number N. The quality of the value obtained in σ estimation (or N estimation) depends on the shape of the peak and the measurement technique used. In this study we have estimated IBW using two procedures:

1. Peak width at half-height
2. Statistical moments

The half-height method allows estimation of σ and, therefore, 4 σ according to:

$$\sigma = \frac{W_h}{2.354} \qquad (1)$$

where W_h is the peak width at half-height.

This method assumes gaussian peak shape and any deviation results in an underestimation of dispersion and, therefore, an overestimation of resolving power. This method is a practical alternative since many practicing chromatographers do not have

ready access to the instrumentation and software required to apply statistical moments analysis to the general problem of estimating dispersion.

Application of the moments method provides good estimation of peak variance as illustrated by Kirkland, et al. (24) even for very asymmetrical peaks. Peak variance σ^2, the second central moment, can be expressed as (23)

$$\sigma^2 = \frac{\Sigma(t_i - m_1)^2 y_i}{\Sigma y_i} \qquad (2)$$

Where t_i = time

m_1 = the first moment

y_i = response

Figure 3 schematically illustrates the computer program for moments determination (25) using chromatographic data stored on disc. The data file is selected from disc and displayed graphically on the CRT. The beginning and end of the peak of interest is determined (either manually or automatically) and a time versus response array is created. The zeroeth, first and second moments are calculated and the results printed.

In this study, our specific aim was to estimate IBW for the high-speed LC-EC system illustrated in Figure 1 so that we could estimate the proper instrument-column match, assess the impact of improved cell design and compare the state of high-speed LC-EC with high-speed LC using UV detection.

The improvement in performance resulting from cell design modifications is very apparent by comparing Figure 4a with 4b. The

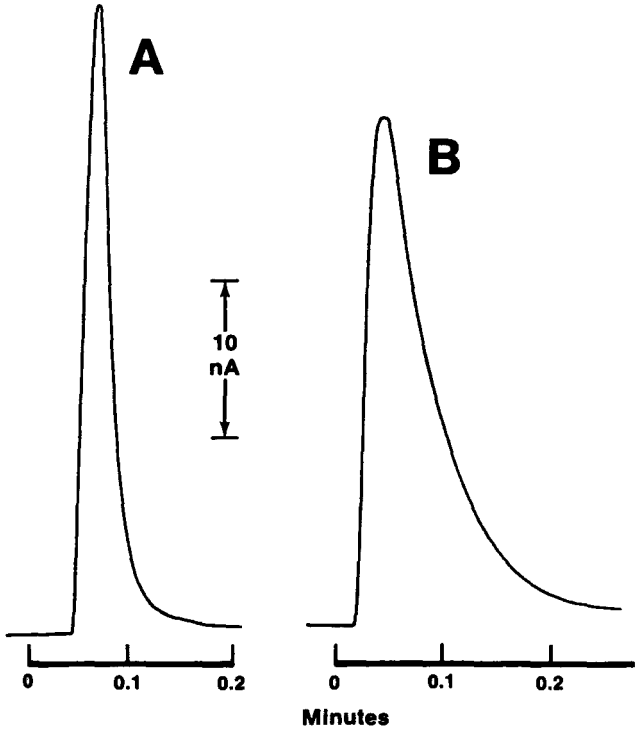

FIGURE 4

Dispersion of new versus old cell design. (A) High-speed cell 4 σ = 47 µL by W_h, 4 σ = 64 µL by moments. (B) Conventional cell, 4 σ = 113 µL by W_h, 4 σ = 164 µL by moments.

estimation of IBW by half-height decreases from 113 µL to 47 µL and by moments from 164 µL to 64 µL. For a 15,000 theoretical plate column at k' = 3, this corresponds to changes in observed N of 11257 to 14184 and 8821 to 13554 using the half-height and moments estimations of IBW, respectively. The resultant decrease in bandwidth is obvious just by looking at the width and tailing of the two peaks. It's interesting that this improvement in high-speed

LC-EC is roughly equivalent to the improvement reported for the first high-speed LC systems using UV detection relative to 'conventional' systems of the time (1-3). The practical conclusion is columns of about 100 x 4.6 mm packed with 3 µm particles are compatible with high-speed LC-EC.

This compatibility is best illustrated by the example of Table 1.

The observed efficiency ($N_{observed}$) of a 15,000 theoretical plate column (N_{col}) is compared to N_{col} with respect to % loss of N defined as

$$\% \text{ loss } N = \frac{N_{col} - N_{observed}}{N_{col}} \times 100 \qquad (3)$$

and % loss of resolution (R_s) defined as

$$\% \text{ loss } R_s = \frac{R_{s\,col} - R_{s\,observed}}{R_{s\,observed}} \times 100 \qquad (4)$$

TABLE 1

Influence of IBW on Observed Efficiency and Resolution (a)

k'	N_{col}	$N_{observed}$	% loss N	% loss R_s
0	15000	4491	70	-
1	15000	9464	37	21.0%
3	15000	13086	13	6.6%
5	15000	14085	6	3.1%
10	15000	14715	2	1.0%

(a) IBW = 50 µL, initial R_S = 1.25, 100 x 4.6 mm 3 µm column with V_o = 1 mL.

where $R_{s\ col}$ is 1.25 and

$$R_{s\ observed} = \frac{\sqrt{N_{observed}}}{\sqrt{N_{col}}} \times R_{s\ col} \qquad (5)$$

The example of Table 1 assumes IBW = 50 μL and V_o = 1.0 mL (V_o = column void volume) for a 100 x 4.6 mm column packed with 3 μm particles. At low k' (k' = capacity factor) (26), 0 to 1, 40% to 70% of the column efficiency is lost due to IBW. At k' = 3.0, only about 10% of the efficiency is lost. Of greater practical consequence is the resultant loss in R_s. Even at k' = 1, only 20% of the R_s is lost. At k' = 3, the loss in R_s is quite small, only about 6%.

It is of interest to attempt to differentiate the various instrumental contributions to band broadening. We have attempted to isolate the influence of the cell flow path (σ^2_{FP}) by placing the cell between an injector and detector of known dispersion as illustrated in Figure 2. The total EC detector variance (σ^2_{DET}) can be described as

$$\sigma^2_{DET} = \sigma^2_{FP} + \sigma^2_{ELEC} + \sigma^2_{ECP} \qquad (6)$$

where σ^2_{ELEC} = apparent dispersion resulting from the detector electronics and σ^2_{ECP} = apparent dispersion resulting from electrochemical processes (22). The σ_{FP} contribution of flow through the cell is about 5 μL by this procedure. The variance due to the flow path is estimated by subtracting the variance of the system composed of injector, connecting tubes and LC-85B from this system illustrated in Figure 2. The actual contribution of the flow path is from the detector inlet to the working electrode. σ^2_{FP} was used to estimate

the upper limit of the cell flow path volume contribution to σ^2_{DET} since the IBW data of Figure 4 led us to suspect a significant contribution from something other than flow path volume. By combining this result with the IBW of the system in Figure 1, an estimate of IBW of 'total electronic factors' 4 σ_{ELEC} = 60 μL, can be achieved. This confirms our suspicion and indicates one direction for future developments in high-speed compatible EC detectors, i.e. reduction in 'electronic factors' related dispersion. Further, more detailed studies are necessary to support this observation and should be designed to differentiate between σ^2_{ELEC} and σ^2_{ECP}.

Another experiment performed during this study further illustrates the importance of 'electronic factors' in IBW of EC cells. It is well known that positioning of the auxiliary electrode relative to the working electrode is very influential regarding detector response (22). Generally, the closer the auxiliary electrode is to the working electrode, the greater the linear range, all other factors being equal. With the new cell design, there are two convenient auxiliary electrode positions - the top half of the cell block and the outlet tube from the reference electrode (see Figure 1). Figure 5 compares IBW as determined using the two different auxiliary electrode configurations. Clearly, using the top half of the cell as the auxiliary electrode is vastly superior, presumably by minimizing the resistance and concomitantly sharpening the potential gradient.

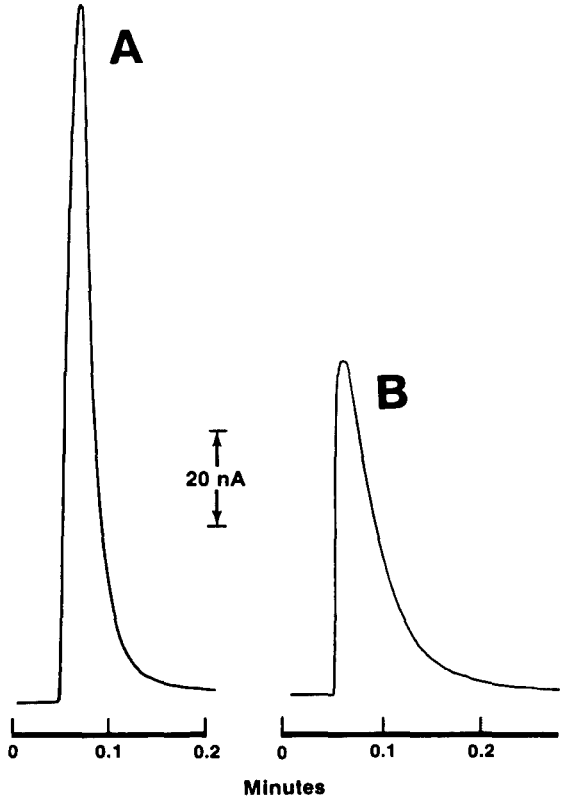

FIGURE 5

Effect of auxiliary electrode position on dispersion. (A) top half of cell as auxiliary electrode : 4 σ = 47 µL by W_h, 4 σ = 64 µL by moments. (B) Outlet tube as auxiliary electrode: 4 σ = 74 µL by W_h, 4 σ = 109 µL by moments.

Another important consideration in high-speed LC-EC is the dependence of IBW on flow rate. Over the flow rate range examined, IBW increases linear with flow rate (Figure 6). This is distinctly different from results reported for a high-speed UV detector where

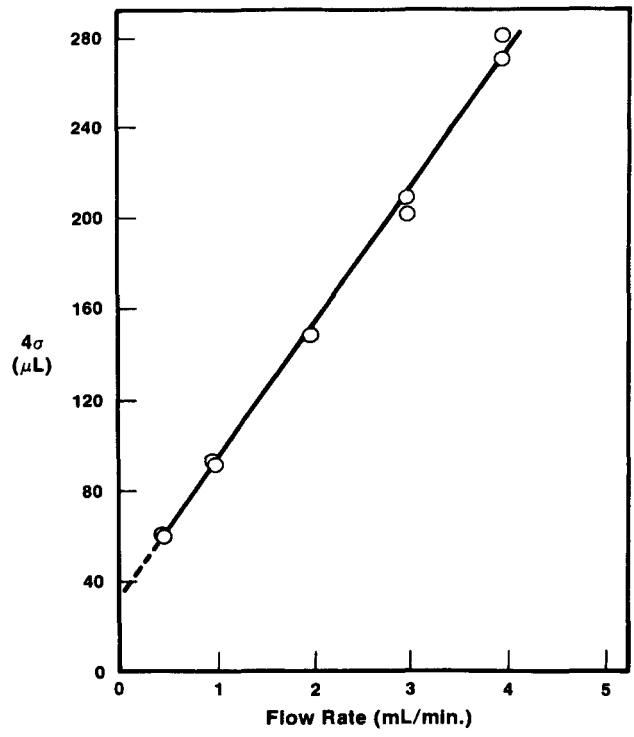

FIGURE 6

The influence of flow rate on dispersion in the high-speed EC cell.

IBW does not increase, but actually decreases slightly over the flow rate range of the present study (2). At the present time, the reasons for the different relationships between IBW and flow rate for the two different detector types are unknown. An understanding of this phenomena would be quite useful in further improving the high-speed characteristics of the EC cell.

Applications of High-Speed LC-EC

The benefits of high-speed LC-EC are best illustrated by comparison of high-speed chromatograms with 'conventional' LC-EC chromato-

grams. The separation of two important sample types, phenols and catecholamines will be used for this purpose.

The determination of phenols in environmental samples is important due to their toxicity and widespread use. Recently, Dong and DiCesare (16) have reported high-speed LC-EC separations of phenols, and Shoup and Mayer (27) have reported the determination of phenols in environmental samples. High-speed isocratic and gradient separations of phenols are demonstrated in Figures 7 and 8. A high-speed C18 column using 3 μm particles, 100 x 4.6 mm i.d. was used to achieve 3-minute isocratic and 6-minute gradient chromatograms. Similar conventional separations required over 20 minutes (28, 29).

The physiological importance and diagnostic value of catecholamine assays necessitate their optimization in terms of both speed of analysis and sensitivity. LC-EC has great potential in this respect, as evidenced by recent reviews of various protocols for the quantitation of subnanogram levels of catecholamines (30-32).

Using a mobile phase of 0.1 M formic acid containing 4% (V/V) acetonitrile, 1 M EDTA and 0.2 mM sodium octyl sulfate at a pH of 3.2 (adjusted with solid KOH) and a flow rate of 3 mL/min, the isocratic separation of DOPA, norepinephrine, epinephrine, acetaminophen and dopamine was accomplished within four minutes on a 100 x 4.6 mm i.d. high-speed 3 μm C18 column (Figure 9). This chromatogram was detected using the optimized system in which the metal cell block served as the auxiliary electrode and was connected to the column via a 10 cm length of 0.011" i.d. tubing. The suitability of this system for plasma samples will be the subject of a forthcoming paper.

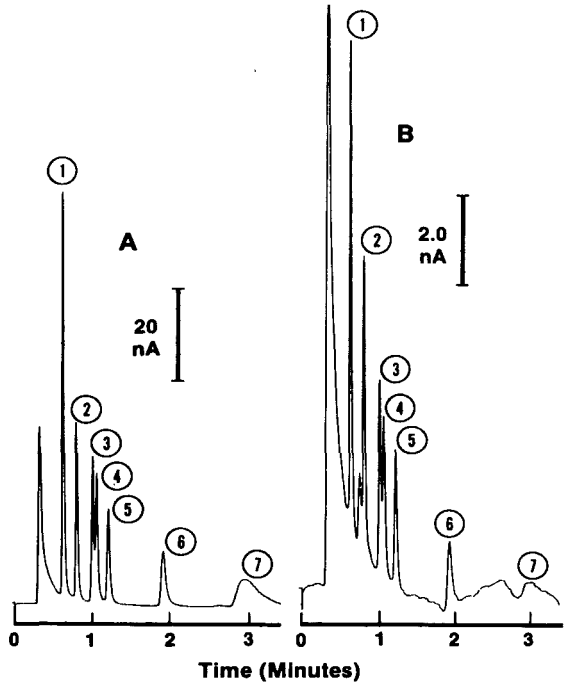

FIGURE 7

Isocratic high-speed LC-EC separation of phenols. Column: C18 - 3 μm. Pump: SERIES 4. Detector: LC-4B (+0.9 V). Flow rate: 2.5 mL/min. Mobile phase: 50% acetonitrile/50% aqueous solution of 0.2 M $NaClO_4$, 0.005 M sodium citrate (pH 5.4). Peak identification: (1) phenol, (2) o-chlorophenol, (3) 2,4-dimethylphenol, (4) 4-chloro-m-cresol, (5) 2,4 dichlorophenol, (6) 2,4,6-trichlorophenol, (7) pentachlorophenol. Amount injected in A: (1) 800 pg, (2) 700 pg, (3) 300 pg, (4) 1300 pg, (5) 800 pg, (6) 1150 pg and (7) 14000 pg. Amount injected in B is 10 times less than A.

Using the same mobile phase at a flow rate of 4 mL/min, this same separation was accomplished in one-minute with the 33 x 4.6 mm column (Figure 10). The use of the shorter column at one-fourth the analysis time of the 10 cm column resulted in a small loss of

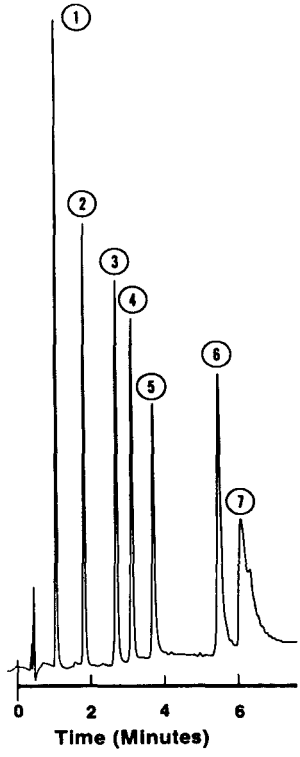

FIGURE 8

Gradient high-speed LC-EC separation of phenols. Conditions as in Figure 8 except mobile phase. Mobile phase: linear gradient 0% to 60%A in 6 minutes. A = acetonitrile, B = 30% acetonitrile/70% aqueous solution of 0.2 M $NaClO_4$, 0.005 M sodium citrate (pH 5.4).

resolution which could be compensated for by adjustment of mobile phase components (33). However, increased baseline noise observed with the short column prevented acceptable detection below 300 pg. This phenomenon is currently under investigation. It is apparent that further improvements in EC detector design, including flow

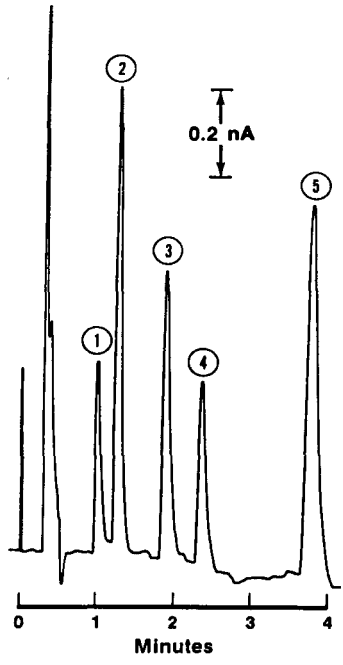

FIGURE 9

High-speed LC-EC separation of catecholamines and acetaminophen. Column: C18-3 μm, 0.46 x 10 cm. Pump: SERIES 10. Detector: LC-4B, + 600 mV. Flow rate: 3 mL/min. Mobile phase: aqueous solution of 0.1 M formic acid, 4% (V/V) acetonitrile, 0.001 M EDTA, 0.0002 M sodium octyl sulfate, adjusted to pH 3.2 with KOH. Peak identification: 300 picograms each of (1) L-dopa, (2) norepinephrine, (3) epinephrine, (4) acetaminophen, (5) dopamine.

geometry of the cell as well as electronics, are needed in order to match the performance of the shorter column.

CONCLUSIONS

The IBW of a conventional LC-EC system has been estimated at approximately 160 μL by a computerized central moments procedure. An

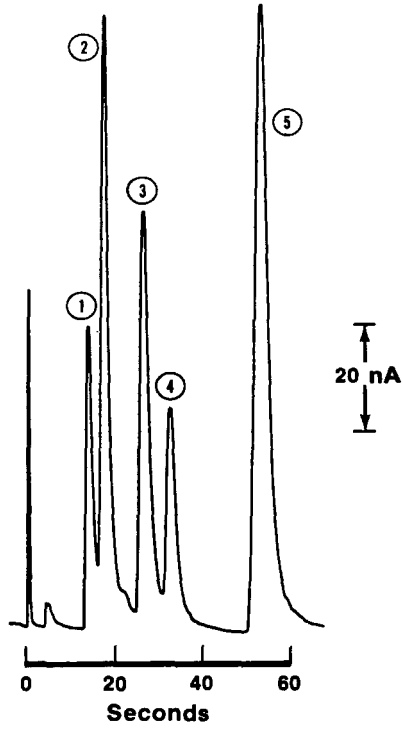

FIGURE 10

High-speed LC-EC separation of catecholamines and acetaminophen using a 3.3 cm column. Conditions as in Figure 10 except column length is 3.3 cm and flow rate is 4.0 mL/min. Peak identification: 60 ng each of (1) L-dopa, (2) norepinephrine, (3) epinephrine, (4) acetaminophen, (5) dopamine.

improved high-speed LC-EC system has an IBW of approximately 60 μL. The metal block EC cell design permitting use of 0.011" connecting tubing and proper location of the auxiliary electrode is responsible for the improved IBW characteristics. This system is compatible with high-speed 3 μm particle columns, 100 x 4.6 mm and is roughly compa-

rable to reported fluorescence and refractive index detector-based systems with respect to IBW. High-speed LC-EC has not achieved the IBW performance reported for systems using UV detection (i.e. IBW = 15 μL) (12), but may well be capable of evolving to that performance level.

REFERENCES

1. DiCesare, J.L., Dong, M.W. and Ettre, L.S., Chromatographia, 14, 257, 1981.

2. DiCesare, J.L., Dong, M.W. and Atwood, J.G., J. Chromatogr., 217, 369, 1981.

3. DiCesare, J.L., Dong, M.W. and Ettre, L.S., Introduction to High-Speed Liquid Chromatography, Perkin-Elmer, Norwalk, CT, 1981.

4. Cooke, N.H.C., Sivorinovsky, G., Archer, B.G., Paper No. 773 presented at the Pittsburgh Conference, 1982, Atlantic City, NJ.

5. Dong, M.W. and DiCesare, J.L., J. Chromatogr., 253, 159, 1982.

7. DiCesare, J.L., Dong, M.W. and Vandemark, F.L., Amer. Lab., 13, 52, 1981.

8. Dong, M.W. and DiCesare, J.L., J. Chromatogr. Sci., 20, 330, 1982.

9. Dong, M.W. and DiCesare, J.L., J. Chromatogr. Sci., 20 517, 1982.

10. Dong, M.W. and DiCesare, J.L., Food Technol., 36, 58, 1983.

11. Katz, E. and Scott, R.P.W., Submitted to J. Chromatogr.

12. DiCesare, J.L., Ind. Res. and Devel., 110, April, 1983.

13. Katz, E. and Scott, R.P.W., J. Chromatogr., 246, 191, 1982.

14. DiCesare, J.L., Personal Communication.

15. Miller, R.L., Paper No. 954 presented at the 1983 Pittsburgh Conference, Atlantic City, NJ.

16. Dong, M.E. and DiCesare, J.L., Current Separations, in press.

17. Recent Reports on Liquid Chromatography/Electrochemistry, Shoup, R.E., editor, BAS, West Lafayette, IN, 1982.

18. King, W.P. and Kissinger, P.T., Clin. Chem., 26, 1484, 1980.

19. Jacobs, W.A. and Kissinger, P.T., J. Liquid Chromatogr., 5, 881, 1982.

20. Riggin, R.M. and Howard, C.C., Anal. Chem., 51, 210, 1979.

21. Kissinger, P.T., Anal. Chem., 49, 447A, 1979.

22. Weber, S.G. and Purdy, W.C., Ind. Eng. Chem. Prod. Res. Dev., 20, 593, 1981.

23. Grushka, E., Myers, M.N., Schettler, P.D. and Giddings, J.C., Anal. Chem., 41, 889, 1969.

24. Kirkland, J.J., You, W.W., Stoklosa, H.J. and Dilks, C.H., Jr., J. Chromatogr. Sci., 15, 303, 1977.

25. DiBussolo, J.M., Unpublished Results.

26. Karger, B.L., Snyder, L.R. and Horvath, C., An Introduction to Separation Science, John Wiley and Sons, New York, 30, 1973.

27. Shoup, R.E. and Mayer, G.S., Anal. Chem., 54, 1164, 1982.

28. Realini, R.A., J. Chromatogr. Sci., 19, 124, 1981.

29. Ogan, K. and Katz, E., Anal. Chem., 53, 160, 1981.

30. Allenmark, S., J. Liquid Chromatogr., 5, 1, 1982.

31. Krstulovic, A.M., J. Chromatogr., 229, 1, 1982.

32. Holly, J.M.P. and Makin, H.L.J., Anal. Biochem., 128, 257, 1983.

33. Lammers, N., Zeeman, J. and deJong, G.J., J. HRC & C, 4, 444, 1981.

JOURNAL OF LIQUID CHROMATOGRAPHY, 6(12), 2375-2377 (1983)

LC NEWS

REACTIVATION SOLUTION RESTORES SILICA COLUMNS following water-deactivation during normal phase LC. The three-component solution provides a cost-saving treatment which avoids a lengthy series of multiple solvent washes and reduces down time. Burdick & Jackson Labs., JLC/83/12, 1953 S. Harvey Street, Muekegon, MI, 49442, USA.

DIGITAL MICROPIPETTOR is a positive displacement device with a digital display, is easily set and secured at a precise volume. Sample volumes are unaffected by surface tension, viscosity, vapor pressure or density. No calibration for each reagent is necessary. Labindustries, JLC/83/12, 620 Hearst Avenue, Berkeley, CA, 94710, USA.

REVERSED-PHASE ODS COLUMNS are constructed of stainless steel with a highly polished interior surface. They are packed with Spherisorb ODS-II, a spherical silica of very narrow particle size distribution. It is coated with a C18 function and is fully end capped. Columns are guaranteed to deliver 50,000 to 80,000 plates per meter. HPLC Specialties, JLC/83/12, P. O. Box 484, Edmond, OK, 73083, USA.

THE MOLECULAR BIOLOGY CATALOG contains information on DNA/RNA-modifying enzymes, restriction nuclease enzymes, DNA sequencing products, nucleic acids, cloning vectors, oligodeoxynucleotides and other nucleosides and nucleotides of special interest. Included are technique information, references, cloning procedures, cloning vector maps, restriction nuclease assay conditions, and more. Pharmacia P-L Biochemicals, JLC/83/12, 1037 W. McKinley Ave., Milwaukee, WI, 53205, USA.

PHENOLS IN WATER are determined by isocratic mode LC. A large volume of water is injected onto a reversed-phase column, and eluted with a 40:60 acetonitrile/water mobile phase. Detection is at 200 nm down to less than 0.001 ppm. Pye Unicam Ltd., JLC/83/12, York Street, Cambridge CB1 2PX, England.

ULTRA-RESOLUTION IN GPC ANALYSIS is offered by a new generation of GPC columns for polymer analysis and testing. They are available in 500, 1,000, 10,000, and 100,000 angstroms exclusion limits as

well as a mixed-bed column that provides ultra-resolution from less than 100 to well over 20 million Daltons. They are available packed in any of several commonly used GPC solvents and in many polymer solvents not generally available with GPC columns. Jordi Associates, Inc., JLC/83/12, 397 Village Street, Millis, MA, 02054, USA.

VARIABLE WAVELENGTH ABSORBANCE DETECTOR is compatible with analytical and microbore scale LC and operates from 190 to 800 nm. A membrane touch panel provides all setup and operation parameter control. The unit is completely automatable. For microbore chromatography, it can be equipped with a 0.5 mucroliter flowcell that provides for direct column to flowcell hookup to minimize dead volume. Kratos Analytical Instruments, JLC/83/12, 170 Williams Dr., Ramsey, NJ, 07446, USA.

HPLC GRADIENT CONTROLLER is a microprocessor-based module designed to provide maximum flexibility for binary and ternary programs. It helps minimize errors by constantly showing run status, all system parameters, and the file name during the run. Tracor, Inc., JLC/83/12, 6500 Tracor Lane, Austin, TX, 78721, USa.

HPLC-GRADE WATER is produced on demand by a system it employs an organic scavenger resin cartridge combined with absolute 0.45 micron low-extractable membrane filtration to give consistenly pure water from average-quality distilled or deionized feed water. Up to 15 liters of organic-free water is produced by a single cartridge. Millipore Corp., JLC/83/12, Bedford, MA, 01730, USA.

DEDICATED SUGAR ANALYSIS LC is custom-tailored for use by producers and large-scale users of sugar products. It is optimized for rapid analysis of corn, beet, and cane sugars and processing liquors. Waters Associates, Inc., JLC/83/12, 34 Maple Street, Milford, MA, 01757, USA.

SULFITE IN FOODS is determined without interferences using electrochemical detection at ppm levels. Samples need only be homogenized, diluted, and filtered prior to injection. Dionex Corp., JLC/83/12, 1228 Titan Way, Sunnyvale, CA, 94086, USA.

PROTEIN ANALYSIS LC is described in a recent brochure. Four separation mechanisms are used--ion exchange, gel filtration, reverse phase, and hydroxyapatite fractionation. The methods allow identification and quantitation of components that might not be amenable to any single mechanism. Bio-Rad Labs, JLC/83/12, 2200 Wright Avenue, Richmond, CA, 94804, USA.

AUTOMATED TLC SAMPLE APPLICATOR consists of a control unit and the actual applicator. The control unit is a Z-80 microprocessor-based device that holds 8 sample application modes, five of which are user programmable. Sample volumes from 100 nL to 20 microL may be applied. Applied Analytical Industries, JLC/83/12, Route 6, Box 55, New Hanover Air Park, Wilmington, NC, 28405, USA.

THIN-LAYER CELL FOR ELECTROCHEMICAL DETECTION allows placement of the auxilliary electrode both downstream and across from the working electrode. A highly polished stainless steel top extends cell life, permits compatibility with new "high speed" columns, and allows for connection of low dead volume fittings for use with micro columns. Bioanalytical Systems, Inc., JLC/83/12, 1205 Kent Avenue, Purdue Research Park, West Lafayette, IN, 47906, USA.

LIQUID PROCESSING UNIT can be used to feed most analytical instruments. It performs all of the crucial sample pickup, mixing and dispensing operations. A pair of syringes whose plungers are driven by a stepper motor and precision ball lead screws, a mixing chamber, and a hand-held control unit are the principal working parts. A computer program directs all operations. Processing parameters such as time, volume, ratios, and increments are entered thru the control unit and become a part of an individual routine program. Hamilton Company, JLC/83/12, P. O. Box 10030, Reno, NV, 89510, USA.

JOURNAL OF LIQUID CHROMATOGRAPHY, 6(12), 2379-2381 (1983)

LC CALENDAR

1983

OCTOBER 12-13: 8th Annual Baton Rouge Anal. Instrum Discussion Group Symposium, Baton Rouge, LA. Contact: G. Lash, P. O. Box 14233, Baton Rouge, LA, USA

OCTOBER 12-14: Analyticaon'83 - Conference for Analytical Science, sponsored by the Royal Society of Chemistry and the Scientific Instrument Manufacturers Ass'n of Grereat Britain, Barbican Centre, London. Contact:G. C. Young, SIMA, Leicester House, 8 Leicester Street, London, WC2H 7BN, England.

NOVEMBER 3-4 ACS 18th Midwest Regional Meeting, Lawrence, Kansas. Contact: W. Grindstaff, SW Missouri State Univ., Springfield, MO, 65802, USA.

NOVEMBER 9-11: ACS 34th SE Regional Meeting, Charlotte, NC. Contact: J. M. Fredericksen, Chem. Dept., Davidson College, Davidson, NC, 28036, USA.

NOVEMBER 10-11: Electrofocusing and Electrophoresis Workshop, Birmingham, AL, USA. Contact: Workshop Registrar, LKB Instruments, Inc., 9319 Gaither Rd., Gaithersburg, MD, 20877, USA.

NOVEMBER 14-16: 3rd Int'l. Sympos. on HPLC of Proteins, Peptides and Polynucleotides, Monte Carlo, Monaco. Contact: S. E. Schlessinger, 400 East Randolph, Chicago, IL, 60601, USA.

NOVEMBER 16-18: Eastern Analytical Symposium, New York Statler Hotel, New York City. Contact: S. David Klein, Merck & Co., P. O. Box 2000, Rahway, NJ, 07065, USA.

NOVEMBER 22-23: Short Course: "Sample Handling in Liquid Chromatography," sponsored by the Int'l. Assoc. of Environmental and Biological Samples in Chromatography, Palais de Beaulieu, Lausanne, Switzerland. Contact: Dr. A. Donzel, Workshop Office, Case Postale 130, CH-1000 Lausanne 20, Switzerland.

NOVEMBER 24-25: Workshop: "Handling of Environmental and Biological Samples in Chromatography," sponsored by the Int'l. Assoc. of Environmental Anal. Chem., Palais de Beaulieu, Lausanne, Switzerland. Contact: Dr. A. Donzel, Workshop Office, Case Postale 130, CH-1000 Lausanne 20, Switzerland.

NOVEMBER 29-30: Electrofocusing and Electrophoresis Workshop, San Francisco, CA, USA. Contact: Workshop Registrar, LKB Instruments, Inc., 9319 Gaither Road, Gaithersburg, MD, 20877, USA.

DECEMBER 6-7 and 8-9: Electrofocusing and Electrophoresis Workshop, Los Angeles, CA, USA. Contact: Workshop Registrar, LKB Instruments, Inc., 9319 Gaither Road, Gaithersburg, MD, 20877, USA.

1984

FEBRUARY 12-16: 14th Australian Polymer Symposium, Old Ballarat Travel Inn, Ballarat, Australia, sponsored by the Polymer Div., Royal Australian Chemical Inst. Contact: Dr. G. B. Guise, RACI Polymer Div., P. O. Box 224, Belmont, Victoria 3216, Australia.

FEBRUARY 20-22: International Symposium on HPLC in the Biological Sciences, Regent Hotel, Melbourne, Australia. Contact: The Secretary, Int'l Symposium on HPLC in the Biological Sciences, St. Vincent's School of Medical Research, 41 Victoria Parade, Fitzroy 3065, Victoria, Australia.

APRIL 8-13: National ACS Meeting, St. Louis, MO. Contact: Meetings, ACS, 1155 16th Street, NW, Washington, DC, 20036, USA.

MAY 20 - 26: 8th Intl. Symposium on Column Liquid Chromatography, New York Statler Hotel, New York City. Contact: Prof. Cs. Horvath, Yale University, Dept. of Chem. Eng., P. O. Box 2159, Yale Stn., New Haven, CT, 06520, USA.

JUNE 18-21: Symposium on Liquid Chromatography in the Biological Sciences, Ronneby, Sweden, sponsored by The Swedish Academy of Pharmaceutical Sciences. Contact: Swedish Academy of Pharmaceutical Sciences, P. O. Box 1136, S-111 81 Stockholm, Sweden.

AUGUST 26-31: National ACS Meeting, Philadelphia, PA. Contact: Meetings, ACS, 1155 16th Street, NW, Washington, DC, 20036, USA.

OCTOBER 1-5: 15th Int'l. Sympos. on Chromatography, Nurenberg, West Germany. Contact: K. Begitt, Ges. Deutscher Chemiker, Postfach 90 04 40, D-6000 Frankfurt Main, West Germany.

DECEMBER 16-21: International Chemical Congress of Pacific Basin Societies, Honolulu, Hawaii, sponsored by the Chemical Inst. of

Canada, Chemical Soc. of Japan, and the American Chem. Soc. Contact: PAC CHEM '84, International Activities Office, American Chem. Soc., 1155 Sixteenth St., NW, Washington, DC, 20036, USA.

1985

FEBRUARY 11-14: Polymer 85, Int'l Symposium on Characterization and Analysis of Polymers, Monash University, Melbourne, Australia, sponsored by the Polymer Div., Royal Australian Chemical Inst. Contact: Polymer 85, RACI, 191 Royal Parade, Parkville Victoria 3052, Australia.

APRIL 28 - MAY 3: 189th National ACS Meeting, Miami Beach. Contact: A. T. Winstead, ACS, 1155 16th Street, NW, Washington, DC, 20036, USA.

SEPTEMBER 8-13: 190th National ACS Meeting, Chicago. Contact: A. T. Winstead, ACS, 1155 16th Street, NW, Washington, DC, 20036, USA

1986

APRIL 6-11: 191st National Am. Chem. Soc. Mtng., Atlantic City, NJ. Contact: A. T. Winstead, ACS, 1155 16th Streeet, NW, Washington, DC, 20036, USA.

SEPTEMBER 7-12: 192nd National Am. Chem. Soc. Mtng., Anaheim, Calif. Contact: A. T. Winstead, ACS, 1155 16th Street, NW, Washington, DC, 20036, USA

1987

APRIL 5-10: 193rd National Am. Chem. Soc. Mtng., Denver, Colo. Contact: A. T. Winstead, ACS, 1155 16th Street, NW, Washington, DC, 20036, USA.

AUGUST 30 - SEPTEMBER 4: 194th National Am. Chem. Soc. Mtng., New Orleans, LA. Contact: A. T. Winstead, ACS, 1155 16th Street, NW, Washington, DC, 20036, USA.

The Journal of Liquid Chromatography will publish announcements of interest to liquid chromatographers in every issue of the Journal. To be listed in the LC Calendar, we will need to know: Name of the meeting or symposium, sponsoring organization, when and where it will be held, and whom to contact for additional details. You are invited to send announcements to Dr. Jack Cazes, Editor, Journal of Liquid Chromatography, P. O. Box 1440-SMS, Fairfield, CT, 06430, USA.

keep in touch with the latest . . .

ADVANCES IN chromatography

edited by **J. CALVIN GIDDINGS**, *University of Utah, Salt Lake City*
ELI GRUŠHKA, *The Hebrew University of Jerusalem, Israel*
JACK CAZES, *Fairfield, Connecticut*
PHYLLIS R. BROWN, *University of Rhode Island, Kingston*

VOLUME 21

March, 1983 360 pages, illustrated

VOLUME 21

CONTENTS

MARCEL DEKKER, INC.
270 MADISON AVENUE, NEW YORK, N.Y. 100
(212) 696-9000

ADVANCES IN chromatography

THE EXPLOSIVE GROWTH of chromatography has made it difficult for any single person to maintain a coherent view of progress in the field. Individual investigators trying to preserve even a moderate awareness of advances must rely upon responsible surveys, rather than attempting to read the avalanche of original research papers.

This continuing series presents critical, current reviews, written by noted authorities, of the most important developments of chromatographic science. The wealth of literature, even in specialized areas of chromatography, is so great that in these superb volumes recognized experts separate hard-core advances from the overwhelming mass of supporting evidence and data. The authors summarize and develop self-contained evaluations of various facets and trends in research, putting their subject matter into perspective.

Volume 21, like its predecessors, provides up-to-the-minute coverage of topics of contemporary interest, including

- **quantitation in trace analysis by GC, by the renowned expert, Josef Novák**
- **HPLC/MS instrumentation and applications, one of the fastest growing chromatographic techniques**
- **the use of capillary columns in LC, an approach that lowers costs, speeds analyses, and affords ultra high resolution**
- **droplet counter-current chromatography, a newly developed partition chromatography method**
- **chromatographic determination of copolymer composition, expanding the range of chromatographic applications**

These volumes are of utmost interest to all researchers who need to use separation techniques effectively—especially analytical, organic, and physical chemists; biochemists; biomedical researchers; clinical chemists; polymer scientists; environmental scientists; as well as scientists in academia, government, hospitals, and industry, both in research and quality control.

INSTRUCTIONS FOR PREPARATION OF MANUSCRIPTS FOR DIRECT REPRODUCTION

Journal of Liquid Chromatography is a bimonthly publication in the English language for the rapid communication of liquid chromatographic research.

Directions for Submission

One typewritten manuscript suitable for direct reproduction, carefully inserted in a folder, and two (2) copies of the manuscript must be submitted. Since all contributions are reproduced by direct photography of the manuscripts, the typing and format instructions must be strictly adhered to. Noncompliance will result in return of the manuscript to the authors and delay its publication. To avoid creasing, manuscripts should be placed between heavy cardboards and securely bound before mailing.

Manuscripts should be mailed to the Editor:

Dr. Jack Cazes
Journal of Liquid Chromatography
P. O. Box 1440-SMS
Fairfield, Connecticut 06430

Reprints

Owing to the short production time for articles in this journal, it is essential to indicate the number of reprints required upon notification of acceptance of the manuscript. Reprints are available in quantities of 100 and multiples thereof. For orders of 100 or more reprints, twenty (20) free copies are provided. A reprint order form and price list will be sent to the author with the notification of acceptance of the manuscript.

Format of Manuscript

1. The general format of the manuscript should be as follows: title of article; names and addresses of authors; abstract; and text discussion.

2. Title and Authors: The entire title should be in capital letters and centered on the width of the typing area at least 2 inches (5.1 cm) from the top of the page. This should be followed by three lines of space and then by the names and addresses of the authors in the following way (also centered):

A SEMI-AUTOMATIC TECHNIQUE FOR THE SEPARATION AND DETERMINATION OF BARIUM AND STRONTIUM IN SURFACE WATERS BY ION EXCHANGE CHROMATOGRAPHY AND ATOMIC EMISSION SPECTROMETRY

F. D. Pierce and H. R. Brown
Utah Biomedical Test Laboratory
520 Wakra Way
Salt Lake City, Utah 84108

3. Abstract: Three lines below the addresses, the title ABSTRACT should be typed (capitalized and centered on the page). This should be followed by a single-spaced, concise, abstract comprising less than 10% of the length of the text of the article. Allow three lines of space below the abstract before beginning the article itself.

4. Text Discussion: Whenever possible, the text discussion should be divided into such major sections as INTRODUCTION, MATERIALS, METHODS, RESULTS, DISCUSSION, ACKNOWLEDGMENTS, and REFERENCES. These major headings should be separated from the text by two lines of space above and one line of space below. Each heading should be in capital letters, centered, and underlined. Secondary headings, if any, should be flush with the left margin, underscored, and have the first letter of all main words capitalized. Leave two lines of space above and one line of space below secondary headings.

5. Paragraphs should be indented five (5) typewriter spaces.

6. Acknowledgment of collaboration, sources of research funds, and address changes for an author should be listed in a separate section at the end of the paper.

7. References (including footnotes) in the text will be numbered consecutively by numbers in parentheses. All references (and footnotes) should then be aggregated in sequence at the end of the communication. No footnotes should be shown at the bottom of pages. The reference list follows immediately after the text. The word REFERENCES should be capitalized and centered above the reference list. It should be noted that all reference lists should contain initials and names of all authors; *et al.* will not be used in reference lists. Abbreviations of journal titles and styles of reference lists will follow the American Chemical Society's Chemical Abstracts List of Periodicals. References should be typed single-spaced with one line space between each reference.

8. Each page of manuscript should be numbered lightly at the bottom of the sheet with a light blue pencil.

9. Only standard symbols and nomenclature approved by the International Union of Pure and Applied Chemistry should be used.

10. Any material that cannot be typed, such as Greek letters, script letters, and structural formulae, should be drawn carefully in black India ink (do not use blue ink).

Typing Instructions

1. The manuscript must be typewritten on good quality white bond paper measuring approximately 8½ x 11 inches (21.6 cm x 27.9 cm). Do not use Corrasible bond or its equivalent. The typing area of the article opening page, including the title, should be 5½ inches wide by 7 inches deep (14 cm x 18 cm). The typing area of all other pages should be no more than 5½ inches wide by 8½ inches deep (14 cm x 21.6 cm).

2. In general, the chapter title and the abstract, as well as the tables and references, are typed single-spaced. All other text discussion should be typed 1½-line spaced, if available, or double-spaced. Prestige elite characters (12 per inch) are recommended, if available.

3. It is essential to use black typewriter ribbon (carbon film is preferred) in good condition so that a clean, clear impression of the letters is obtained. Erasure marks, smudges, creases, etc., may result in return of the manuscript to the authors for retyping.

4. Tables should be typed as part of the text but in such a way as to separate them from the text by a three-line space at both top and bottom of each table. Tables should be inserted in the text as close to the point of reference as possible, but authors must make sure that one table does not run over to the next page, that is, no table may exceed one page. The word TABLE (capitalized and followed by an Arabic number) should precede the table and be centered on the page. The table title should have the first letters of all main words in capitals. Titles should be typed single-spaced. Use the full width of the type page for the table title.

5. Drawings, graphs, and other numbered figures should be professionally drawn in black India ink (do not use blue ink) on separate sheets of white paper and placed at the end of text. Figures should not be placed within the body of the text. They should be sized to fit within the width and/or height of the type page, including any legend, label, or number associated with them. Photographs should be glossy prints. A typewriter or lettering set should be used for all labels on the figures or photographs; they may not be hand drawn. Captions for the pictures should be typed single-spaced on a separate sheet, along the full width of the type page, and preceded by the word FIGURE and a number in arabic numerals. All figures and lettering must be of a size to remain legible after a 20% reduction from original size. Figure numbers, name of senior author, and arrow indicating "top" should be written in light blue pencil on the back or typed on a gummed label, which should be attached to the back of the illustration. Indicate approximate placement of the illustrations in the text by a marginal note in light blue pencil.

6. The reference list should be typed single-spaced although separated from one another by an extra line of space. Use Chemical Abstract abbreviations for journal titles. References to journal articles should include (1) the last name of all author(s) to any one paper, followed by their initials, (2) article title, (3) journal, (4) volume number (underlined), (5) first page, and (6) year, in that order. Books should be cited similarly and include (1) author, surname, first and middle initials, (2) title of book, (3) editor of book (if applicable), (4) edition of book (if any), (5) publisher, (6) city of publication, (7) year of publication, and (8) page reference (if applicable). E.g., Journals: Craig, L. C. and Konigsber, W., Use of Catechol Oxygenase and Determination of Catechol, Chromatogr., 10, 421, 1963. Books: Albertsson, P. A., Partition of Cell Particles and Macromolecules, Wiley, New York, 1960. Article in a Book: Walter, H., Proceedings of the Protides of Biological Fluids, XVth Colloquim, Pteeters., H., eds., Elsevier, Amsterdam, 1968, p. 367.